

UC Berkeley

UC Berkeley Electronic Theses and Dissertations

Title

Extending and Characterizing Fuel Flexibility in Small-Scale Power Systems

Permalink

<https://escholarship.org/uc/item/8kh1q035>

Author

McCoy, Christopher David

Publication Date

2013

Peer reviewed|Thesis/dissertation

Extending and Characterizing Fuel Flexibility in Small-Scale Power Systems

By

Christopher David McCoy

A dissertation submitted in partial satisfaction of the

requirements for the degree of

Doctor of Philosophy

in

Engineering – Mechanical Engineering

in the

Graduate Division

of the

University of California, Berkeley

Committee in Charge:

Professor Albert P. Pisano

Professor Hari Dharan

Professor Seth Sanders

Fall 2013

Abstract

Extending and Characterizing Fuel Flexibility in Small-Scale Power Systems

By

Christopher David McCoy

Doctor of Philosophy in Mechanical Engineering

University of California, Berkeley

Professor Albert P. Pisano, Chair

The ultimate goal and hope for engines of the near future is the development of wide range fuel-flexibility within internal combustion engines. This research dissertation presents three innovations that have pushed the boundary of science and technology to enable this vision on the mini scale. First, the design and construction of a new small-scale, fuel flexible, engine dynamometer that allowed for precise measurement and control of mini engines operating on non standard fuels. Second, the fuel-flexible characterization of the O.S. Graupner Wankel engine and the successful production of output mechanical power between 10-500 W from a range of petroleum-based and bio fuels: gasoline, diesel, biodiesel, bioethanol and military-grade JP8 (among others). Lastly, a low-cost, multi-fuel switching system was designed and tested that controllably delivered a range of fuels to the engine and allowed for the first continual fuel-flexible operation using an array of fuels. In addition to these scientific contributions, it will be shown how the small-scale engine dynamometer and its peripherals were designed, constructed and tested such that future researchers can make advancements toward the ultimate goal enabling wide-range fuel flexibility on the small scale.

This work determined a number of the key parameters for small-scale fuel flexible engine operation (4.97 cc). Previous work only showed that fuel flexibility was possible in larger scale rotary engines and turbines—where operating conditions differ greatly from their smaller-scale counterparts. The present work extended the understanding of what engine parameters are critical for enabling fuel-flexible engine operation on this small scale and helped discover the strengths, weaknesses and opportunities of mini fuel flexible rotary engines which prior work had not described.

The design and construction of a new small-scale engine dynamometer was essential as no commercially available dynamometers on this scale existed and the legacy systems failed to capture all necessary engine data; especially those needed to characterize fuel flexibility. This dynamometer consisted of an engine mount and loading system, the

required sensors for measurement, the actuators to dynamically and repeatedly control engine and the integration of all these elements into a usable data acquisition system. The characterization consisted mainly of the maximum power outputs of the engine while running on specific fuels, the engine operating conditions during max power output, the stoichiometry ranges of each fuel in the context of the O.S. Graupner Wankel engine and output efficiencies. Other preliminary characterizations on emissions, combustion pressure and other typical engine tests were developed but not fully characterized but will be introduced.

The design and construction of a multi-fuel switching system was also integral to extending and characterizing fuel flexibility on this small scale. Early experiments only tested fuels independently and switched between them by hand. However, future systems would need to be able to change fuels on-demand and sequentially in real time. Therefore, a system that could accommodate the storage of multiple fuels and then deliver them reliably to the engine at the click of an on-screen fuel selector button was built, better syncing the fuel data with the engine performance data.

The resulting fuel-flexible engine characterization system was then tested amongst a variety of liquid hydrocarbon based fuels in order to create a fuel-flexible engine mapping for a Wankel engine of 4.97 cc displacement. During multi-fuel combustion, the following parameters were measured in an effort to fully characterize this engine: engine torque, mass flow rate of ambient air intake, stoichiometry, ambient temperature and humidity, ambient pressure, engine speed, mass fuel flow rate, engine housing temperature, engine exhaust temperature and loading brake temperature and the fuel selection. This data collection was possible through the design and integration of the LabVIEW data acquisition system architecture in concert four input / output devices: the NI-USB-6221, NI-USB-9162 and two ArduinoUNO microcontrollers. The design and integration will be fully described along with the new system potential and shortcomings.

In addition to the data acquisition, the system was also designed to enable future real-time control using conventional low-cost model engine servos such that the system could be fully automated. In the current system, there are eight actuation devices that control the throttle position, the glow plug heat, the fuel to air ratio, the dynamometer brake and four electrovalves that control the delivery of each fuel. The mechanical design and construction of all these control mechanisms are also described along with their added potential to enhancing fuel flexibility and opportunities for future improvement.

The fuel flexible dynamometer system, multi fuel switching system, data acquisition and system control enabled fuel flexible operation of a Wankel engine of 4.97 cc displacement. The maximum mechanical power produced from Gasoline, Glowfuel (methanol+nitromethane mix), JP8, Diesel and Biodiesel were 334 W, 508 W, 313 W, 239 W and 322 W respectively. Methanol did not require active glowplug power while

the 87 octane, diesel and JP8 fuels did. Good throttle response for both Methanol and JP8 was observed however the 87 octane operation, there was little to no throttle response during combustion. This dissertation research clearly demonstrates that small-scale Wankel rotary engines are fuel flexible across at least 6 different fuels: methanol, gasoline, diesel, JP8, biodiesel and ethanol.

This dissertation is broken down into six separate chapters: Chapter 1 Introduction that describes the motivations and background of this research, Chapter 2: Theory which gets the reader up to speed with the relevant engineering concepts, Chapter 3: Experimental Setup Design which describes how the fuel flexible characterization system was built, Chapter 4: Experimental Results which succinctly presents all data key data collected during this research, Chapter 5: Discussion and Analysis which are the conclusions drawn from the captured data and Chapter 6: Conclusions which briefly reiterates the key developments presented in this dissertation.

It is the hopes of the author that this research serves as a stepping stone in future development efforts and allows science and technology to arrive at a point where wide range and robust fuel flexibility is possible.

Front Matter

“Everybody has a plan until they get punched in the face.” Mike Tyson

Front Matter	i
List of Figures	ii
Dedication	xii
Acknowledgements	xii
Chapter 1 – Introduction.....	1
Why is this research important?.....	1
Standing on the shoulders of giants - background research.....	20
Chapter 1 summary.....	31
Summary of remaining chapters	32
Chapter 1 References.....	32
Chapter 2 – Theory.....	38
Review of Combustion	41
Rotary engine theory and design considerations.....	59
Chapter 2 Summary	68
References.....	68
Chapter 3 – Experimental Setup Design	70
Introduction.....	70
A fuel flexible engine dynamometer (FFED)	73
Clean sheet dynamometer design process and relevant challenges	75
Required engine sensors and measurement	88
Engine control	94
Multi-fuel switching system (MFSS)	105
Chapter 3 Summary	109
References.....	109
Chapter 4 – Experimental Results.....	110
Fuel-flexible characterization history and process.....	110
Mechanical power output results for each fuel tested	118
Measured and simulated fuel-flexible engine operating characteristics.....	122
Chapter 4 Summary	144
References.....	145
Chapter 5 – Discussion and Analysis	146
Fuel flexible engine performance discussion.....	146
Dynamometer results and commentary	148
Multi-fuel switching system (MFSS) review and commentary	150
Sensor and actuator integration.....	150
Recommended Future Work.....	151
Chapter 5 Summary	156
References.....	157
Chapter 6 – Conclusions.....	158
Conclusions from this research	158
Dissertation Close.....	159
References.....	160

APPENDICES 161

 APPENDIX A: Nomenclature and other useful definitions 161

 APPENDIX B: Useful theory and plots 163

 APPENDIX C: Sensor Calibration and Test Setup..... 166

 APPENDIX D: Previous fuel flexibility characterization research results 186

 APPENDIX E: Relevant Fuel Properties 191

 APPENDIX F: Mechanical Design Considerations 192

 APPENDIX G: O.S. Graupner Rotary Engine Considerations 192

 References..... 199

List of Figures

Figure 1: Solid model of the small-scale fuel-flexible engine dynamometer4

Figure 2: Electronically-controlled, multi-fuel switching system (MFSS).4

Figure 3: Fuel-flexible rotary engine sensor and actuator system to enhance fuel flexibility.....4

Figure 4: Dynamometer dashboard and control panel for the fuel-flexible engine system.4

Figure 5: January, 2010 – Haiti Earthquake Aftermath [11].5

Figure 6: The NetHope relief kit [12].5

Figure 7: The woman in this figure is the founder of wecaresolar.com who gives solar panels to hospitals, maternity wards and other power dependent places so that they can maintain light and other equipment on during critical health procedures [14].7

Figure 8: Fatigued soldier on battlefield [19]. These soldiers cannot perform optimally and presents safety risks for soldiers8

Figure 9: Another fatigued soldier resting on top of his equipment.8

Figure 10: The BigDog from Boston Dynamics has an impressive ability to carry payload and handle complex terrain. Its current powertrain is a very noisy, 2-stroke, 15hp engine [18].9

Figure 11: Google's self driving Toyota hybrid Prius. It is quite possible that someday cars like this will have a fuel-flexible engine as its battery counterpart [20].10

Figure 12: Doc. Emmitt Brown from the Back to the Future movie part two, fueling his time machine with fusion technology of the future [55]. 11

Figure 13: The graphic portrayal of the goal of fuel-flexible engine operation and its target applications. 12

Figure 14: The current portable power solutions have a separate energy converter for each type of fuel desired for energy extraction. Typically, portable generators use gasoline. 12

Figure 15: The goal of this research is to design a system around a small-scale rotary engine that can extract usable energy from an array of liquid hydrocarbon-based fuels. . 12

Figure 16: Aggregated fuel properties. Values pulled from the tables listed in “source” from [62,63] and the ME140 Reader produced by Prof. Carlos Fernandez-Pello at U.C. Berkeley, 2005. 13

Figure 17: An output power versus time plot as the engine switches from one fuel to another and adjusts engine parameters to maintain power output. Ideally, the curve would be a flat line with no interruptions in power production..... 15

Figure 18: Small-scale rotary engine technology along with other competing technologies. Rotary Engines: [1,46,47], Stirling Engines: [50], Piston Engines: [1,49], Batteries: [53], Solar [44,45] and Turbines: [52]...... 17

Figure 19: A Ragone diagram as presented by Tester from MIT in 2005..... 18

Figure 20: Taken from many sources of data, this Ragone diagram illustrates where the 4.97 cc O.S. Wankel engine exists but and the ideal target power range. See [9]. 19

Figure 21: Fu, et al. designed and fabricated three meso-scale rotary engines to test the limits of microcombustion [21]...... 22

Figure 22: A MEMS version of the Wankel Engine developed at UC Berkeley in the early 2000s made from Silicon Carbide [23]...... 22

Figure 23: A MEMS-based temperature sensor designed and fabricated by S. Wodin-Schwartz is embedded into a 4.97 cc Wankel Engine by C. McCoy to test survivability of MEMS devices in real combusting small-scale engines [40]. The circle identifies the location 5 x 5 mm² pocket for the MEMS temperature sensor..... 23

Figure 24: The integrated rotor apex seal and spring. Note the angled sidewalls known as the ARDE (Aspect-Ratio Dependent Etching) effect [25]. 24

Figure 25: Through the optimized process, Martinez et al. is able to maintain long vertical sidewalls with non-zero width bases, however striations are noted [25]. 24

Figure 26: After using the Taguchi Method to optimize the process over several key process variables (Time, Gas, Flow, Coil, Platen and Pressure), the etch performance is dramatically improved [25]. 25

Figure 27: Knobloch, et al. demonstrates the various etch profiles and process artifacts such as Silicon "grass" which could potentially affect smooth engine operation via a non-uniform sliding surface [24]. 25

Figure 28: Early development of mini-scale rotary engines. Designed as part of the MEMS REPS program at UC Berkeley [22]. 25

Figure 29: Albert P. Pisano reviews the contributions of the Berkeley Micromechanical Analysis and Design (BMAD) Lab [30]...... 25

Figure 30: Principal Investigator from the Combustion Processes Laboratory at U.C. Berkeley..... 25

Figure 31: The overview of the MEMS REPS project [30]. 25

Figure 32: Understanding the effect of chamber width on small-scale combustion [34]. 26

Figure 33: This work by B. Sprague focused on combustion dynamics and flame speed in small combustion chambers [35]. 26

Figure 34: Original dynamometer test stand designed specifically for small scale rotary engine testing [36]...... 26

Figure 35: Sealing on the micro and macro scales has always been a challenge. Heppner et. al. sought to understand why [37]. 26

Figure 36: Park, et al. utilized MEMS-based microvalves to do fuel delivery [48]. 26

Figure 37: A “down-axis” view of the 4.97 cc O.S. Graupner Wankel Rotary engine [1]. 26

Figure 38: The electrical braking system for the small-scale engine dynamometer [9]. ...26

Figure 39: McCoy et al. and the development of a small-scale engine dynamometer for fuel flexibility characterization [46]...... 26

Figure 40: The Rotary Engine Power Systems project thrust and the researchers who contributed. 26

Figure 41: Sprague et. al demonstrating 33W of un assisted power being produced by the 1500 mm³ engine [38].27

Figure 42: Magnetostatic actuator for fuel injection designed by S-W. Park, et al. [48]..28

Figure 43: Wodin-Schwartz, et al. investigated the effects of combustion on Si and SiC chips. Bonding and surface deposition were two main main challenges discussed [40]. 30

Figure 44: Rheume, et al., "Solid-state electrochemical sensor for monitoring lean direct injection engines." [42].....30

Figure 45: Experimental setup with a throttle control, belt driven dynamometer and manual engine start [1].30

Figure 46: Output mechanical power measured from a single unmodified rotary engine combusting a variety of fuels [1].30

Figure 47: Pressure traces of the combustion event. Poor data collection methods only yielded a snapshot of an oscilloscope screen [1].31

Figure 48: Various engine temperatures distributed around the periphery of the engine [1].31

Figure 49: Hypothesized technology development comparison between the piston engine and the rotary engine. The piston engine has been an evolutionary engine and the rotary engine will become a revolutionary engine.39

Figure 50: Since 2009, Makerbot Industries has began to produce hobby-grade 3D printers and have started a DIY revolution with many free designs and parts available for download on their website: www.thingiverse.com40

Figure 51: This is the structure developed by N. Dhillon and C. Hogue to create a thermal plane that maintains a constant temperature [66]......40

Figure 52: Cobalt Biofuels is a startup company that intends to bring biobutanol to the commercial marketplace and help the world achieve energy independence from renewable energy.....40

Figure 53: Various opportunities based on technology and economic trends.40

Figure 54: Ideal Diesel Cycle with heat entering at constant pressure and the work done between points 3 and 4 [77].42

Figure 55: Ideal Otto Cycle [77].42

Figure 56: a dual or mixed cycle with limited pressure and constant volume.44

Figure 57: O.S. Graupner Engine 4.97 cc performance specifications.46

Figure 58: The O.S. Graupner Wankel studied in this dissertation research [82].47

Figure 59: A comparison between the catalytic "hot spots" found in both piston and rotary engines.49

Figure 60: The approximate autoignition temperatures in K for various fuels. Extracted from various sources [84].51

Figure 61: Plots that illustrate the boundary between "no ignition" and "autoignition" ...54

Figure 62: The characteristic dimension a as found in a rotary engine. This dimension could be better observed with a cross-section view as there is a combustion pocket in the triangular rotor surface.55

Figure 63: Breaking down the combustion reaction rate based on units and variables. ...56

Figure 64: This form of the combustion reaction rate highlights the parameters which can be controlled and which are dependent on fuel type. The term “knob” refers to how the engine might be “dialed in” so as to permit wide-ranging and robust fuel flexibility.56

Figure 65: this emissions figure was borrowed from Borman and Ragland [76].58

Figure 66: Dr. Felix Wankel with an early version of his rotary engine [70]. 59

Figure 67: Key rotary engine components and distinct features. Face seals—which are typically inlaid in the flat faces of the rotor and follow the triangular contour of the rotor. These are not shown as smaller-scale rotary engines typically do not include them as they present a larger mechanical loss compared to the compression gain. 60

Figure 68: The rotary engine 4-stroke cycle as compared to that of a piston engine. Note that this rotary engine (top) has a side ported intake and a peripheral ported exhaust [83]. 61

Figure 69: This is an early generation, U.C. Berkeley designed, Wankel rotary engine along with its seals and requisite springs [86]. Due to the significant challenges at obtaining a functioning rotary engine at such small scales, engines were slowly made bigger until a working engine was obtained. 62

Figure 70: Trochoid housing, rotor, and crankshaft with eccentric lobe. This was the 1500 mm² rotary developed at UC Berkeley which eventually produced about 30 W of unassisted power [86]. 62

Figure 71: The small-scale O.S. Graupner Wankel engine with an engine displacement of 4.97 ccs. Hand model credit goes to Dr. Debbie Senesky. 62

Figure 72: Ven diagram of unique and shared engine components between the Wankel Rotary and the Piston Engines. 63

Figure 73: Cited from Fu, et. al in his design and characterization of microfabricated rotary engines. 65

Figure 74: Cited from Yamamoto, the image compares the number of parts required for a rotary engine (left) and a piston engine of equivalent power output (right) [80]. 66

Figure 75: The overall schematic of the fuel-flexible engine dynamometer and characterization system. The system includes fuel-flexible fuel delivery, measurement and control of all key engine parameters and data collection. 70

Figure 76: Early stages of the fuel flexible testing and control system. 71

Figure 77: overall test bench located in 44 Hesse Hall, UC Berkeley, California. 71

Figure 78: The fuel-flexible rotary engine testing setup at the Escuela Técnica Superior de los Ingenieros Aeronáuticos (E.T.S.I.A.), an aeronautical engineering school that is part of the larger polytechnic university (la U.P.M.) in Madrid, Spain. With a larger engine lab and more equipment available for the characterization of engines, the dynamometer characterization system was set up and modified to continue testing in this university. The primary modifications and tools used were the mechanical loading system, fuel switching system and the emissions measurement equipment. 72

Figure 79: First revision of the UC Berkeley small engine dynamometer. 73

Figure 80: An example of mechanical power output curves of a small scale rotary engine. 73

Figure 81: The general structure would have two elements: a engine mount and a dynamometer brake. 79

Figure 82: The shaft location needed to be precision located so as to reduce mechanical shaft losses due to misalignment. 79

Figure 83: The engine mount would also need to have basic thermal insulation, account for exhaust position and provide enough working space to mount / dismount. 79

Figure 84: The original sketches of a resistor bank filled with low-resistance and high wattage resistors attached to a large heat sink with cooling fans, supported by a low-cost, non-conductive and stable structure [89]...... 80

Figure 85: The final assembly of the resistor bank. The high power resistors are mounted directly to the heat sink with cooling fans (not visible from this photo)..... 80

Figure 86: A solid model of the mechanical braking element of the dynamometer. 82

Figure 87: Mechanical brake and servo mechanism for engine loading. 82

Figure 88: Main testing dashboard of the Fuel Flexible engine dynamometer. The upper left hand corner shows the temperature produced on the engine surface, the exhaust and the dynamometer loading brake. Just below shows the torque measurements. To the right are the air intake sensor measurements, the output mechanical power and when installed the combustion pressure measurements. The bottom half of the screen shows the digital controls, which allow the operator to dynamically change the throttle position, glow plug temperature, loading force, fuel delivered and rate of change of carburetor fuel needle valve (stoichiometry). 85

Figure 89: Dynamometer initial conditions and system setup dashboard. Each time the program is run, various settings need to be input to activate all the separate sensors, actuators, microcontrollers and other systems interfacing with the LabVIEW data acquisition system. 86

Figure 90: The Lujan emissions measurement system. This system was designed for auto emissions and was expected to potentially yield strange results as other similar systems (like Horiba) were specifically designed for automobile-scale emission volumes. 87

Figure 91: an example of the type of data collected during emissions testing. 88

Figure 92: Initial sketches for the torque measurement. 89

Figure 93: Design sketches load cell sensor mount with focus on adjustability. 90

Figure 94: Engine port drilling options for pressure measurement. The O.S. Graupner Wankel rotary engine did not leave much space..... 91

Figure 95: This image illustrates that no new chamber pockets / ports were drilled unnecessarily creating more unwanted dead volume (as in Cardes et al [90]. This was achieved with the help of the technical staff at the Universidad Politécnica de Madrid. . 92

Figure 96: This image attempts to show the landing surface for the pressure sensor. The dull brown ring is the crush washer for the glow plug, and the horseshoe shape is the flat surface landing for the sensor. However, the mouth of the horseshoe illustrates a leakage point for combustion gases and needs to be sealed. 92

Figure 97: A magnified view of the rotary engine with the Optrand Auto-PSI high temperature pressure sensor installed. 93

Figure 98: The ArduinoUNO microcontroller with the ambient temperature, humidity and pressure sensors..... 94

Figure 99: the electrical diagram of the motor starter plus dynamometer load switching system. 95

Figure 100: The mechanical loading system was designed with starting and effective loading in mind. 96

Figure 101: Schematic that utilizes a timer circuit to drive a servo. With a 5V power supply and a potentiometer, you can control the position of a servo. These were some of the original controls methods..... 97

Figure 102: The bulky box that contains a potentiometer to drive the PWM signal to any standard hobby signal. This solution was replaced by ArduinoUNO micro controllers upon their discovery. 97

Figure 103: Linear to rotary motion of throttle servo mechanism (top view). 97

Figure 104: Here is the 3D CAD model that illustrates the motion of the throttle linkage (this is a side view). 97

Figure 105: Small-scale carburetor schematic. The needle valve is typically to set the idle mixture. However in this research, this valve is constantly opened and closed in order to adjust stoichiometry. 98

Figure 106: O.S. Graupner Wankel carburetor with angular encoder mount. 98

Figure 107: Sketch of the encoder measurement of fuel air ratio. 99

Figure 108: Actual fuel to air ratio measurement system. 99

Figure 109: Sketch showing some of the key dimensions to determining carburetor fuel needle valve position. 99

Figure 110: The key dimensions in this figure are r , which is the radius of the flexible torque shaft, R , which is the radius of the belt hub and L_c , the center to center distance between the two belt hubs. 100

Figure 111: Calibration of the carburetor needle valve z-height. This height is proportional to the fuel delivery of the carburetor and is related to the stoichiometry. Data is presented in the bit value so as to be easily changed during testing but will be useful to assess fuel flow in the carburetor for stoichiometry calculations. 101

Figure 112: The Hobbico Deluxe Power Panel which helps manage power delivered to the glowplug and starter motor. 102

Figure 113: Servo mechanism to adjust the glow plug heat. Consists of flex torque shaft and several custom 3D printed clamping mechanisms. 102

Figure 114: The actual implementation of the glow plug adjustment mechanism. 102

Figure 115: Shaft couplers always presented problems until the drill chuck solution was implemented. 103

Figure 116: The drill chuck coupler system implemented to have a dyno fit for any size output shaft. 103

Figure 117: A dynamometer support failure due to high vibration and poor shaft coupling. 104

Figure 118: Sketch of how the structural loop—without a spline could cause unwanted bowing and flexing of the system. 104

Figure 119: Sketch drawing of fuel switching system. A.K.A. the "BarBuddy" creates the main structural support of all the fuel bottles (in this case, recycled wine bottles). The bottles are sealed with standard cork but have two tubes that pass through them. A pressure release and a fuel outlet. The fuel outlet tubes connect to one of four electrovalves that are built with viton internals that do not corrode in the presence of fuel. Then the fuels enter unions that converge four separate tubes into one that enters the engine. The electrical system is again controlled by an ArduinoUNO microcontroller and a set of relays to control the electrovalve actuator currents. 106

Figure 120: Original design compared to the actual machine. 107

Figure 121: Breadboarded prototype of the fuel switching electronic control system. The breadboard on the left contains the prototype with the relays and electrovalve ports. The breadboard on the right connects the logic circuit to the Arduino. 108

Figure 122: Printed circuit board and enclosure for fuel switching system. From prototype to printed circuit board. This is the controller box that is used to regulate fuel flow from the LabVIEW environment. A USB connection from the computer to the Arduino is what controls the signals to the relays..... 108

Figure 123: Maximum mechanical power output recorded for each fuel tested using the upgraded mechanical dynamometer. The fuels are listed in order of increasing specific gravity..... 112

Figure 124: Stoichiometry map that details the physical carburetor needle valve positions that represent the flammability range of the engine. Again, to understand the significance of these values, please see “LVP” or “Lab View Position” in the Nomenclature which is found in the APPENDIX. 113

Figure 125: Left: testing dynamometer for the O.S. Graupner Wankel Engine. Right: Close-up view of generator and test stand [90]..... 115

Figure 126: The 2009 version of the fuel flexible engine dynamometer with an electrical loading system..... 116

Figure 127: The 2009 dynamometer with all the required peripherals to operate and test the fuel flexible engine. 116

Figure 128: the updated fuel flexible engine dynamometer and its components. Not shown in this image: automated fuel switching system and the emissions exhaust collector. 116

Figure 129: the actual system that was re-assembled and enhanced at the Universidad Politécnica de Madrid. This image also includes a stainless steel emissions measurement exhaust collector that was designed by visiting research Nicholas Maiden. 116

Figure 130: The measured mechanical power output of the O.S. Graupner 4.97 cc Wankel. This is the native fuel for the engine. The glow plug is turned ON at start but is then disconnected upon reliable compression ignition. The curve “PmechC” represents a calculated version of the mechanical power because the calculation done in real-time by LabVIEW was delayed about 0.5s. 118

Figure 131: Mechanical power output of 87 octane fuel while running at 100% WOT. Current was constantly supplied to the glowplug during this test. 119

Figure 132: Mechanical power output of aviation grade JP8 jet fuel while running at 100% WOT. Current was constantly supplied to the glow plug during this test. 120

Figure 133: Mechanical power output of no. 2 diesel fuel while running at 100% WOT. Current was constantly supplied to the glow plug during this test. 121

Figure 134: Mechanical power output of BioDiesel fuel. Current was supplied to the glow plug during start but was later removed during this test..... 122

Figure 135: Determining the lower and upper flammability limits of glowfuel: methanol+nitromethane. The lower flammability limit is indicated by the lowest stoichiometric sensor value that maintained combustion. In this case, the LFL appears to be around -125. *Note: the negative value is arbitrary and based on how the stoichiometry angle encoder sensor is setup. The flatline at zero clearly suggests the engine is no longer running. 124

Figure 136: The rich flammability limit found while combusting Glowfuel. The LFL was recorded in the prior test to have a LVP of -125..... 125

Figure 137: Upon early testing, stable operating points were established but the rich flammability limit proved difficult to obtain. The dashed circle detailed in this figure is

interesting in that the engine spontaneously spiked in power without changing the throttle position nor the load brake position. However, as can be seen, the stoichiometry was being changed as a function of time with little to no affect on the output power. The temperatures can be observed to have changed, along with the mass fuel flow rate (from approx 0.25 g/s to about 0.5 g/s), therefore it appears that carburetor fuel flow valve regulator becomes wide open at about ~800 and does not stall the engine however does not explain the power spike. This likely suggests erratic engine operation or irregularities spawned by temperature changes within the system. 126

Figure 138: Lean and rich flammability limits of 87 Octane Gasoline. 127

Figure 139: The recorded lean flammability limit of JP8. 128

Figure 140: The recorded rich flammability limit of JP8. 129

Figure 141: Finding the lower flammability limit of the diesel fuel. 130

Figure 142: Lean flammability limit of BioDiesel. 132

Figure 143: Finding the rich flammability limit for BioDiesel. 133

Figure 144: The range of stoichiometries that support fuel-flexible engine operation. These data were collected with the glowplug continuously ignited. These tests typically concluded when carburetor or exhaust screws fell out. To understand this chart, please review LVP in the Nomenclature which can be found in the APPENDIX. 135

Figure 145: An attempt to combust several fuels consecutively without losing output mechanical power. By changing the stoichiometry via the carburetor needle valve, near optimal operating conditions can be quickly obtained and the engine can maintain combustion (the throttle and glow plug temperatures typically remained constant). 136

Figure 146: O.S. Graupner Wankel engine wearplate with embedded MEMS temperature sensor. 138

Figure 147: The OS Wankel in fact produced positive power with the MEMS sensor present inside the engine. However, upon breakdown of the engine, it was discovered that the MEMS sensor had been disintegrated and / or ejected out of the exhaust as it was no longer present. 139

Figure 148: Temperature profile with time when combusting standard GlowFuel (82% Methanol, 16% Nitromethane and 2% Oil) (120705-engine-test-methanol-04). The engine temperature is critical for preserving the engine during operation of non standard fuels. 140

Figure 149: Exhaust thermocouple position. 141

Figure 150: Engine housing thermocouple position. 141

Figure 151: Dynamometer break loading thermocouple. 141

Figure 152: One method observed to cool the engine was by running rich mixtures. It can be observed how the temperature of the engine decreases with richer mixtures and heats up on leaner mixtures. Time is plotted in seconds. 142

Figure 153: Engine emissions from methanol and the corresponding engine and exhaust temperatures. Top: Engine temperature is plotted with a light dashed line and the exhaust temperature is plotted with a dark solid line. Bottom left y-axis: %O₂: light dash-dot line with triangle markers, CO₂: light solid line with "+" markers: %CO: dark dashed line with "x" markers, and λ is signified by a light dashed line with square markers. 143

Figure 154: Engine emissions from gasoline (87 octane) and the corresponding engine and exhaust temperatures. 143

Figure 155: Emissions results for a BioEthanol fuel with corresponding exhaust and engine temperatures. Results are diluted due to exhaust extractor. 144

Figure 156: The engine speed is plotted along with emissions measurements. 144

Figure 157: Preliminary sketch for a fuel pre-heater system that would ideally utilize the waste heat from the exhaust to preheat heavier fuels introduced into the engine. 152

Figure 158: “McMillan Model 106 FLO-SENSORS are capable of measuring extremely low liquid flow rates from 15 mL/minute up to 10 L/minute with a full scale accuracy of $\pm 1.0\%$ or better [98]!..... 154

Figure 159: Location of problematic screws and hardware that become unfastened due to engine vibration..... 156

Figure 160: Taken from many sources of data, this Ragone diagram illustrates where the 4.97 cc O.S. Wankel engine exists but and the ideal target power range. See [9]. 164

Figure 161: This figure attempts to illustrate how the specific power output drops as fuel volume (with a constant specific energy) increases system weight. 165

Figure 162: Calculating the adiabatic flame temperature of methane as a function of equivalence ratio using Cantera. 166

Figure 163: Load cell is the cylindrical, quarter-sized, chunk of metal just beneath the weighted, blue Aluminum bar. It measures between 0 and 250 grams. 170

Figure 164: Here the load cell is being pulled in tension. The screw thread checker is being used as a plate to support the calibration weights. 170

Figure 165: Calibration weights used to calibrate the Sensotec load cell and compare Ohaus Explorer precision mass balance. 171

Figure 166: As can be seen in the above calibration plots, the sensor tends to drift. This could be caused by many things such as power supply voltage, setup biases, or other noise. However, the sensor maintains its linear response to mass. The offsets are typically from how the actual masses are loaded onto the load cell (i.e. the thread-checker plate above or any other platform or hook). 171

Figure 167: McMillan Co. intake air flow sensor. 172

Figure 168: The apparatus used to calibrate the air intake, mass air flow rate sensor. ... 173

Figure 169: Left most sensor is the Testo 425 air anemometer. Middle is a 75W 30V power supply, Above the power supply is the calibration unit. 173

Figure 170: The Testo 425 probe enters the air flow tube at the top of the photo. The tube continues on into the sensor being calibrated. 173

Figure 171: Calibration of the various airflow measurement devices..... 174

Figure 172: The ArduinoUNO microcontroller with the humidity, temperature and pressure sensors..... 175

Figure 173: Dynamometer with calibration motor and associated components..... 176

Figure 174: Electronic motor and speed controller. 176

Figure 175: A quick and easy voltage divider circuit, breadboarded with two resistors: 50 k Ω and 5 k Ω 177

Figure 176: Schematic of a voltage divider. This circuit was used to reduce the input voltage to the LabVIEW system as it is only capable of measuring between +10V and -10V..... 177

Figure 177: Shows the response of the electric motor power along with voltage and current generated by power supply. From the uppermost plot, the mechanical power

follows the electrical power being output from the power supply. Losses due to the ESC, motor efficiency and shaft misalignment should all be considered. 180

Figure 178: The engine speed in (RPM) and both electrical power and mechanical power are presented here to show how the magnitude change of the engine speed that corresponds to the amount of power and torque produced at that speed..... 180

Figure 179: A comparison of the input Electrical Power to the output, Mechanical Power. These should relate 1 to 1. 180

Figure 180: The Monarch Tachometer ACT 3A Display. The unit also comes with a laser emitter and collector to measure reflected, pulsing light [103]. 181

Figure 181: The Monarch Tachometer as used in the dynamometer test stand. The display is in the bottom, right hand corner and reads an engine speed of 0.0 RPM 181

Figure 182: The Optrand AutoPSI-TC pressure sensor has a 4mm tip with threads and can be installed directly in the combustion chamber. 182

Figure 183: Here the pressure sensor is installed in the 4.97 cc Wankel engine. Carfe 182

Figure 184: Standard O.S. Graupner medium glowplug. 184

Figure 185: The current that passes through the glowplug for a given glowplug LabVIEW Position (LVP). 184

Figure 186: the EBM-Papst 4 speed AC centrifugal fan used to refrigerate the O.S. Graupner Wankel engine. www.ebmpapst.com..... 185

Figure 187: Volumetric air flow produced by the AC fan for each of its various steps and air pressure differential. 185

Figure 188: Cardes et al. again presents the electrically-measured power output of the various fuel blends (in this case this is blending of GlowFuel with different amounts of nitromethane and lubricant oil) for constant load across the full range of throttle positions. The maximum power observed was produced by the GlowFuel and was approximately 210 W. * Designates continuous glow plug operation [90]. 186

Figure 189: Preliminary data on the fuel flexible capacity of the 4.97 cc O.S. Graupner Wankel engine in the early development stages of the mechanical dynamometer development. This was an attempt to replicate the 2005 data and confirm functionality of the newly developed dynamometer. This version lacked data logged mass fuel flow rates (due to errors in the communication between the scale and the data logger), electronic control of carburetor needle valve (regulating air-to-fuel mixture) and utilized a resistive-based loading system—which failed to test the full dynamic range of the motor and required a second operator to be present. 187

Figure 190: This plot compares the average power output across an engine speed achievable by the three fuels tested in this experiment (approx 9,000 RPM) and a rough estimate of the predicted power using measured efficiencies and energy density of the fuels. The Brake Mean Effective Pressure (BMEP) allows for the comparison of any motor regardless of its displacement. During this characterization, the dynamometer again lacked robust loading control, repeatable measurements for carburetor and poor measurement of fuel consumption (and therefore a lack of efficiency measurements). . 188

Figure 191: This is one of the first few power curves generated from the small-scale engine dynamometer. The strangeness of the curves comes from the method by which the engine was operated. Given the fragility of the engine, on top of the desire to preserve its functionality, the engine was not ran at full load. However, most dynamometers oscillate back and forth between fully opening the throttle and loading the

motor such that it does not over run or over rev the engine. In this case, the motor was operated at various engine speeds by varying the throttle, hence the atypical performance curves (120703-engine-test-methanol-02)..... 189

Figure 192: This figure was generated by the standard method of opening the throttle and increasing the load in order to manage the engine speed. Via this method, the maximum power and torque values should be measurable and easily attained. However the interesting fact remains that via this method, the maximum power of the motor was not realized nor did the engine speed reach the manufacturer’s specified maximum ratings (of nearly 1 horsepower) (120705-engine-test-methanol-04). 189

Figure 193: Mechanical power output of no. 2 diesel fuel while running at near 100% WOT (the motor failed to maintain reliable combustion at 100% wide open throttle). Current was constantly supplied to the glowplug during this test. This is No. 2 diesel fuel..... 190

Figure 194: Flammability limits, stoichiometry, autoignition temperatures and quenching distances of various fuels [105]. 191

Dedication

This dissertation is dedicated to my beloved mother and father for whom without their unconditional love and support, this dissertation would have never been possible.

Acknowledgements

The Ph.D. process is a long journey that could not be completed without lots of support. I would like to acknowledge the following people for their contributions to my journey:

Mom: Mom, you are the most encouraging, supportive, and loving person I know. I am so lucky to have you as a mother. You always gave me the courage to pursue my dreams even though many challenged your motherly instinct. Your giving has never known any bounds and you invested in me. Thank you for being you and providing your love without end.

Dad: Many thanks to you, Dad. You complement mom’s unwavering encouragement by helping me stay focused and keeping the eye on the prize. You also strengthened my persistence and determination to finish. And whenever there was something tough that needed to be said, you had the courage to say it. You always have been and will continue to be, a role model for me. Thank you for everything.

Prof. Albert Pisano: Thanks to one of the most charismatic, encouraging, and clever research advisers any graduate student could ever have. You not only taught me how to

do world-class research, but I also learned how to be an independent thinker and problem solver. Your willingness to allow your students to define their own journey through graduate school provided one of the most amazing experiences of my life: living abroad. While I left behind a lab of the best researchers and faculty in the world, I also gained a perspective that only few American researchers will ever have. I cannot thank you enough for giving me the opportunity to work with you and the BMAD team. I look forward to following your continued successes.

Brendan Shaughnessy: Thanks my homie for keeping me well-rounded; challenging my perspectives; and sharing some amazing and unforgettable moments with me. You have challenged me and my beliefs so that I could become a better person. Perhaps most importantly, you have helped me develop a rare combination of technical, emotional, professional, and social skills that will continue to bring me rare opportunities. Thank you for being you.

Somin Lee: Many kind thanks to my Joy Buddy: Dr. Somin Lee! You have been a great friend and role model throughout my entire Ph.D. process. Our late nights at People's Café and Philz were the backdrop of some amazing conversation and inspiring new ideas. I hope we get to write that book together soon before you are off in Michigan and publishing more cover-worthy research! I cherish our friendship dearly and I hope we can find ways to collaborate together in the future.

Mario Sanchez Sanz: I cannot say “thank you” enough to you, Mario. Without even knowing me, you were generous with your time, efforts, patience, office space, and friendship. I cannot thank you enough for all the continual encouragement and persistence in helping me finish my thesis. Your ability to excel in everything you do has been an inspiration and I hope we can continue to collaborate in the future! En el español de Yankee, espero que ya sepas que eres un buen tío que me has dado mucho para mejorar mis estudios, investigaciones, idiomas y mi vida. Por eso, tengo que agradecer mucho y tengo mucha confianza que triunfarás con tu carrera y tu vida nueva como un padre. Enhorabuena y llevo con honor la responsabilidad a ser “El Padrino Yankee” por vuestro hijo. Un abrazo muy fuerte Mario.

Eric Hobbs: Doc Hobbs!! Thank you for all your support and friendship throughout the years. You continue to be an inspiration and role model in my life, both personally and

professionally. If I could ever achieve even 1% of what Doc Hobbs has become, I would be a successful person. I look forward to working with you one day in the future and watching your continual success. Big thanks to Mandy and your family: Hayden, Nixon, and Cash!

Gabriele Vigevani: Dr. Vigevani: thank you. We have had some amazing times in the BMAD lab, surviving EE140 together, and trying to launch a web start-up. You will likely always be one of the smartest people I know and I hope someday soon we will be able to hang out and brainstorm the next big thing again. Many thanks again for keeping me focused when I was flying too high and for showing me what it means to be a great researcher and engineer.

John Reville: Dean John, thank you. Thank you for being a great friend, a great roommate, and for always looking out for me. You have been one of the few friends to give me the much needed "tough love" to get my act in gear and get my thesis completed. I have always admired and will continue to admire your attention to detail and the care you put into your work. I am also proud of you for taking action and becoming an entrepreneur! I have the utmost confidence that you can make that succeed and retire early!

Amine Berrada: You are a great friend and we have had some amazing times together over the years. I'm extremely excited for what the future beholds for us and I thank you for all the support you've given me while finishing my thesis. Let's make a real dent in this energy sector together!

Bernd Kamasi: Bernd! Thank you for all your help and support during my thesis. You came and rescued me in the summer of 2011 and we explored Europe together (which was a much needed vacation). You were always there to support my wild and crazy endeavors, using BuddyGrippers against better judgment, and then helping me sell them to others. You are a true friend and I look forward to hanging out and following all your successes!

Zubin Chagpar: Many thanks for all you have done for me, Zubin! We have only known each other for a short time, but it has been amazing learning from you and I am

excited about the impact that we are going to have on this earth. I hope we get to work together much more in the future and I look forward to watching you achieve great things!

Unai Liki: Qué pasa, tío!! Muchísimas gracias por todo me habías dado cuando trabajabamos juntos allí en la ETSIA. Me ha gustado mucho en conocerte y tu familia / vida en Vitoria. No voy a olvidar las experiencias que hemos compartido y espero en un día pronto que nos podamos quedar.

Miguel Hermanns: Many thanks, Miguel! You went out on a limb for me and we succeeded. You helped me bring one of the first market-testing classes into existence at the best engineering school in Spain. I am inspired by your courage to build a start-up in Spain, considering the ecosystem goes against you, and I regret that we had differing visions for the direction of the course. That being said, I still would not have ever been able to be successful with that class if it were not for you, and for that, I thank you kindly.

Matt Chan: Matty Matt Chan! Many thanks for being such a good friend and lab mate! You were among the key people that helped me stay sane during graduate school and I loved all the times we spent goofing off (shoving pillows in the ventilation and loading Gabriele's desk with water jugs). Best of luck in your future.

Fabian Goericke: Fabian--guten taag. It was great getting to know you during our time in BMAD and I thank you for all of our fun conversations. I appreciate dearly your strong viewpoints on life and engineering, and I look forward to watching you become a phenomenal engineer. I hope to come visit you someday soon in Germany.

Sarah Wodin-Schwartz: Many, many thanks Dr. Wodin-Schwartz! It was a ton of fun getting to know you during our time in BMAD and I am so very thankful for all of your support throughout the years. It takes a real friend to drop everything they are doing to help me piece together a tough night to help me locate my iPhone. I wish you the best of luck at Exponent and I look forward to following your successes.

Mick Fransen: Mick, many thanks for your unwavering patience and assistance in the UC Berkeley machine shop. I always enjoyed your energy and the many stories about all cool things mechanical you showed me. I hope someday you and I can participate in the Lemons race; it sounds like a real riot.

Lori Chen: Although you and I did not hang out much during my lengthy Ph.D. process, you were there at the end and gave me a chance to prove that I could bring value to your company. Many, many thanks for making me part of your team and I look forward to making our company the safest, most reliable, and most affordable gas utility in the nation.

Rob Raisch: Rob, you are like a brother to me and a consistent source of positivity and encouragement. Your continual struggle to achieve your dream is inspiring and I thank you for always being there to motivate me to continue on. I look forward to watching your success--literally watching your success on the big screen--and I hope we can someday collaborate together on a world-changing project.

Mike Raisch: Mike--like Rob, you are like a brother to me. Although we have always been busy, your high level of achievement has always been an inspiration to me and I always wished I could be as diligent and insightful as you have been during your academic career. You are one of the few people that I know who will have been in school longer than I, and I wish you the best in all of your future endeavors. The health of our society depends on you and you are the best man to tackle that challenge; I have no doubts.

Mike Neuffer: Mike: many, many thanks for the years of continual advice and assistance in the lab. I still have your leak-down test drawing affixed in my lab notebook and it was very useful in understanding the leakage of our engine. I am sad we never got to ride motorcycles together, but there is still time! What are you doing this weekend?

Gordon Long: Gordon, your patience in a high-stress environment will never cease to amaze me. You seem to speak all forms of machine language like G-Code and that of the painful whines of machines that are being improperly used by newbie engineers. Lastly, I am very glad to know that at least one more adopted child will grow up in a supportive and loving family. I admire you and your wife's courage to adopt. You will make the life of your child very fulfilling and rich; I have no doubts.

Javier Herrera: Javier: nuestro tiempo, aunque corto, ha sido genial. Me ha gustado mucho en conocerte durante mis últimas semanas en Madrid y tu energía para invertir en el motor y el banco. Espero que también te haya gustado en participar en mis investigaciones y que hayas tenido una experiencia parecida de ir a la escuela postgrado. Eres un tío muy bueno y tengo ganas de ver tu carrera y tu futuro como ingeniero. Un abrazo fuerte, amigo!

Scott McCormick: Many thanks to you, Scott! I always appreciated your friendly demeanor and willingness to help us solve problems in Hesse Hall. Such a wealth of knowledge, it was always a pleasure to work with you and your team!

Pete Graham: It was awesome working with you, Pete! I appreciated all of our hallway conversations about motorcycles and car racing!

Samuel Callejo Delgado: Muchísimas gracias, Samuel, por tu ayuda y amistad durante mis investigaciones en la ETSIA. Eres un ingeniero de verdad y te admiro por tus capacidades en el mundo de investigación.

Prof. Seth Sanders: Many kind thanks to Prof. Seth Sanders for serving on my Ph.D. Thesis committee and for actually reading the thesis in depth.

Prof. Hari Dharan: Many thanks to you, Prof. Dharan. I really enjoyed working with you throughout my graduate career. From taking courses to attempting to try to answer your quals questions, your technical knowledge and ability to do both high-level and detailed analysis on mechanical problems is inspiring. I hope we can collaborate in the future.

Prof. Carlos Fernandez Pello: Prof. Pello! Tengo que agradecerte mucho por cambiar mi vida con la experiencia de estudiar en tu alma mater, la Escuela Técnica Superior de los Ingenieros Aeronauticos. Ha sido una experiencia inolvidable y increíble para formar

mi vida académica, profesional y personal. Espero que podamos seguir en contacto y quedamos otra vez en Madrid un día pronto!

Prof. Juan Ramon Arias: Muchísimas gracias, Juanra. Ha sido una experiencia genial en conocerte, tus estudiantes post grados, y tu familia. Me habías ayudado mucho en mi experiencia allí en la ETSI Aeronáuticos y me sigues sirviendo como un modelo de ingeniero de motopropulsión que yo conozco.

Prof. Angel Velazquez: Muchas gracias por permitirme terminar mis investigaciones en tu laboratorio. Ha sido unas de mis experiencias inolvidable de mi vida.

Bailey Bliss: Many thanks to you, Ms. Bailey Bliss. It was a pleasure working with you on the many side projects I conducted while finishing my Ph.D. thesis. I always appreciated your innovative solutions to trying to keep my life in order and your ability to run projects independently. I wish you the best of luck.

Shaina Burnette: Many, many thanks, Shaina, for helping me edit my thesis. Your initial structural changes were very beneficial and your critical and philosophical nature really helped make my thesis flow. I could not have done such a nice job without you. I wish you and your new family the best!

Lisa Urwick: Many thanks, Cousin Lisa! I really appreciated all your copy editing improvements to my thesis and your patience with me as a "manager." With so many projects on my plate, you were brave to ever get involved and I am glad you cut the cord when we could no longer apply the 6F principle. Thanks again and I am really glad we got to work together!

Carlota Dorn: To the outlier of the group, who always seemed to do better than me in our ESPM class; most likely due to your diligence and responsibility. I'm glad we've stayed in touch over the years and while you came in at the tail end, many many thanks in helping me finish my Ph.D. thesis. I'm much more excited about where we are going to go from here as a team and what amazing things you'll achieve (even if it is for an outlier).

To my family in general, my deepest thanks to everyone in my family who has always been supportive of all my crazy endeavors and who have helped me along the way in completing this Ph.D. I could have never done it without your unwavering support and encouragement.

Aitor Rubio: Muchísimas gracias, Aitor, por todo lo que me has dado durante mi estancia en Madrid. El programa Fulbright sigue siendo una de las mejores experiencias que he tenido en mi vida. Teneis algo muy especial con tu proceso de elegir estudiantes y estoy orgulloso por tener la capacidad a decir que "soy uno de ellos". Espero que todo vaya muy bien contigo y tu familia y que quedemos algún día pronto.

Matt Hopcroft: Huge thanks to you, Matt, for helping out with this fuel flexibility project. You had to manage me and my wild ideas, which takes a level of patience that not many have. I regret to inform you that I never ended up burning that Everclear through the fuel flexible engine, but I am sure it did not go to waste in the BMAD lab. I wish you the best of luck in your future endeavors and I hope we cross paths in SF soon!

Jan Kuypers: Although our time working together was short, I really enjoyed working with you, Jan. I was always very impressed with your technical abilities and your dedication to research. I know you had a strong impact on many graduate students in Prof. Pisano's lab and I have no doubt these skills will take you far in your career. I hope you have not spent my \$20 yet in the picture frame and that we can put it toward a couple of pints in Boston someday soon!

Debbie Senesky: Dr. Senesky, many thanks to you. I appreciated all of your continual insistence that I finish my thesis and offering yourself and your husband (Dr. Matt Senesky) as resources as I went through my quals experience. I am sorry to see that your judgment has wavered slightly in choosing to become a professor at Stanford, but we all make mistakes :-). I wish you and your husband the best of luck in your careers and I hope we can collaborate again one day soon.

Jim Cheng: Jim, you're the man and you know this. Many thanks for all your help throughout the years. You will always be the Jim I know with all the answers and I look forward to following you and all your career successes. Many, many thanks for helping

me jump through this last hurdle of submitting the thesis and I hope we can brainstorm more start-up ideas someday soon!

Miguel Reyes Mata: Miguel, muchísimas gracias por tu ayuda en la ETSIA. Siempre estabas allí cuándo tenía una pregunta o necesitaba ayuda con recursos en el laboratorio. Estoy seguro que ya eres un Doctor y espero que tengas un buen futuro como ingeniero industrial. Que nos vemos pronto!

A mi familia Española, quién me han dado un parte de tu corazón, por eso los tengo que agradecer. Para llegar en un país Nuevo y conocer la gente y el ritmo de la vida mientras de trabajar con metas distintas (terminar una tesis), no es tan fácil. Aunque, cuando alguien tiene una familia como vosotros, si, es fácil y una es una experiencia magnífico. Nunca voy a olvidar mi experiencia en tu país y espero que ya sepais que siempre vas a tener un parte de mi corazón. Besos y abrazos fuertes.

Walter Foxworth: Walter foxy Foxworth--it was a pleasure getting to know you and hanging out at the ETSIA. Never would I have guessed a Stanford student could roll with the Chonis tan bueno que tu y que tendríamos muchas experiencias inolvidables allí en Madrid. Espero que podamos volver juntos y tomar unas copitas en la Siesta (que creo que no se existe nada más).

Christina Clancey: Ms. Christina Clancey, many thanks for being such a good friend during our amazing Madrid experience. It was awesome watching you do great things in engineering and becoming a Masters student--even amidst all our crazy adventures. Siempre me ayudabas con mi Español y siempre tenías confianza que podría hablar. Muchísimas gracias por tu paciencia y amistad y espero que podamos volver a España juntos algún día pronto.

Lauren Ostrowski: DJ OstroWOWski, we had an amazing time in Madrid together. It was great getting to know you and I am glad we stayed in touch. You seemed to always be around during the most memorable times in Spain, so por eso tengo que agradecerte. Gracias por la presion que me pusiste con mi tesis y me alegro que ahora ya estamos terminado con las tesis. ¡Por fin! If this can happen, then for sure it's possible that they change our national anthem to "Party in the USA".

Anders Vest Christensen: Anders, you are one amazing dude and I am really glad that we got to rock out in Madrid together. It was fun brainstorming our various entrepreneurial projects (no matter how risqué), and you showed me how to have an amazing time in Spain. Thanks for being one of the many who continually applied the pressure to get the thesis completed and para salir cuándo yo no pensaba que mi hígado podría sobrevivir.

Antonio Garcia Serrano: Antonio, ha sido un placer inmenso en conocerte durante mi estancia en España. Eres un buen tío y gracias por tu amistad. No voy a olvidar nuestras experiencias juntos y espero que algún día pronto que podamos quedar y salir por el HonkyTonk! Un abrazo fuerte, mi hermano.

Jose Manuel Linares: José, ha sido un placer en conocerte, tío. Muchas gracias por tu amistad y ayuda durante mi estancia en Madrid. No podría tener una vida tan buena que me habías ayudado formar. Espero que nos veamos un día pronto...por allí en Madrid o por aquí en San Francisco.

Juan ETSIA: A mi equipo de cocineros: Juan, gracias por siempre cuidarme en la ETSIA. No voy a olvidar nuestra experiencia con nuestro amigo Don Simon y espero que podamos repetir algún día pronto.

Jesus Alonzo: El jefe! ¿Qué puedo decir? Me cuidabas como si yo fuera uno de tus hijos. Me alimentabas cada día con unos platos sanos y sin gluten y por eso, mi madre podría dormir bien, sin preocuparse. Eso dice mucho sobre tí. Me ha gustado mucho en conocerte y tu familia y quiero que sepas que estáis invitados a mi casa aquí en California cuando quieres venir. Un abrazo muy fuerte.

Jose de Marimba: Jose! Tengo que agradecerte mucho por facilitar un ambiente muy bueno para escribir mi tesis y trabajar. Siempre Bar Marimba tiene la cantidad de vino y sonido para trabajar a un ritmo perfecto. Os echo de menos y voy a pasar de Lavapiés para verte cada vez que esté en Madrid. Un abrazo fuerte y nos vemos pronto!

Alberto Atreche: Alberto, muchísimas gracias por tu amistad y ser un tío de verdad. Es raro cuando conoces alguien y instantemente ya sabes que esta persona es buena gente. Eres uno de este tipo y me lamento mucho que no pasamos más tiempo juntos. Gracias por ayudarme crear "Calimochón" y espero que podamos tomar unos algún día pronto. Un abrazo fuerte.

Vaib Puri: Vaib! It was great getting to know you and watch you build a business in one of the toughest economic climates on earth. I appreciated all your positive encouragement and giving me motivation to keep pushing on the Ph.D. I wish you the best in all of your future endeavors and I hope we can both meet someday soon on our own private jets!

Erik Schlie: Many thanks Prof. Schlie for giving Zubin and I the chance to teach one of the best courses I have ever taught in my life at one of the top ranked MBA schools in the world. You took a big risk on us to deliver a top-quality class on a rather new subject, and it was extremely fulfilling to me to help our students get one step closer to creating the next "big thing." Many, many thanks and I hope we can continue to work together to make IE Business School the best MBA school on the planet. All the best!

To all of those whom I may have forgotten, thank you, thank you, thank you!

Chapter 1 – Introduction

“Not all who wander are lost.” J.R.R. Tolkien

Why is this research important?

Imagine you were the lead coordinator of a natural disaster relief effort being rapidly dispersed in Indonesia. You are responsible for flying to the disaster site, assessing the immediate rescue needs and dispatching rescue personnel to these critical areas. You have to pack your rescue equipment and fly to the disaster site in less than 1 hour. You grab a 300 W communication hub (A NetHope Relief Kit [15]) and the requisite power source so that you will have nonstop communication with your rescue team. This requisite power source is a fuel-flexible engine generator that can be checked-in or carry-on luggage. This generator can burn any liquid fuel present at the disaster zone. This generator provides between 10 – 1000 W of reliable and replenishable power from sources local to the disaster site using rescue vehicle fuel, local fuels, or even contaminated fuels. You save time in departure and have more fuel options for your power needs, thus you can immediately focus on your rescue effort and potentially save more lives. Just imagine.

Or imagine you volunteer to support the war effort in Afghanistan and become part of the Special Ops Task Force in the Army. You have been covertly dropped off behind enemy lines with an elite Special Ops team to perform a critical but highly dangerous mission. You and your team execute your mission but the enemy is now well aware of your existence. You need to communicate with home base to coordinate an evacuation effort. However, your team was unable to pack the heavyweight primary cell batteries required to maintain the night vision, GPS, surveillance tech and other power-hungry equipment that is critical to your mission. Instead, you grabbed the all-new fuel-flexible engine generator with a liter of JP8 military-grade fuel that would power your equipment in case of any emergency. You fired up the generator, made the call to your general and a BlackHawk Apache helicopter swoops in minutes later and you and your team fly away to safer grounds. Just imagine.

Lastly, imagine driving to a gas station of the near future and seeing an array of fuel options: gasoline 87-91 octane, diesel, ethanol, biodiesel, bioethanol, biobutanol and syngas. With the fuel prices at over \$5/gallon for octane and biodiesel at \$4/gallon, and because you have fuel-flexible engine technology in your new hybrid, you are able to choose biodiesel. You are not forced to make this decision based on what conventional engines used to require, rather you get to choose the fuel that met your price range and environmental goals [67]. With a fuel-flexible engine—capable of extracting energy from any liquid hydrocarbon—your transportation and refueling options would be

dramatically improved, permitting a change from petroleum-based liquid hydrocarbons to more environmentally neutral biofuels. Additionally, as a nation we would be able to potentially reduce our dependency on foreign oil and give budding renewable fuel start-ups a key component to a biofuels infrastructure that supports their new products and our national security. Have you been able imagine what this new world might look like?

This is the vision of fuel-flexible engine technology. Today, our transportation fleet only teases at the thought of robust fuel flexibility. Without a transitional engine solution, which permits these new and experimental fuels from being used, mankind will continue to consume the last remaining bits of this precious resource.

No longer would stored chemical energy in a fuel be left to the restrictions of one specific type of engine or generator. With fuel-flexible engine technology, we would enable people with power needs to access this power with greater fuel options and availability; especially during critical and emergency situations.

But why haven't we seen a completely fuel-flexible hybrid vehicle or a portable fuel-flexible engine generator yet? This is because conventional piston engines are not very tolerant of a diversity of liquid-based hydrocarbons, which have a wide range of fuel properties (such as volatility, specific gravity, viscosity, octane ratings, etc.). Several issues related to fuel flexible engine performance include, but are not limited to: combustion stability, corrosion, operability, durability fuel delivery, fuel storage and other challenges [13]. From an environmental perspective, transportation vehicles are the only engines currently being incrementally improved to increase efficiency and reduce emissions based on the evermore stringent CAFE standards pushed forward by congress and other legislation (AMFA, Energy Policy Act, California Clean Fuels Program, AB 2076, AB 1007, AB 32. Etc.) [6].

However, there is an engine that contains unique and underexplored properties, which may enable the fuel-flexible operation that is desired. This engine is based on rotation, rather than reciprocation; compact planar geometries rather than bulky cylindrical pistons and rods, and unlike a piston engine, boasts high power density—one power stroke per rotation. But most importantly, it is an engine that reduces, prevents and is tolerant to engine knocking and because of its unique geometry, supports the compression and consequent combustion of many fuels. Its unique properties have placed the rotary engine as the centerpiece of the fuel-flexible portable power solution. Through analysis and experimentation, this research attempts to further the understanding of fuel-flexibility with respect to small-scale rotary engines.

In this dissertation, the extension and characterization of fuel-flexibility will be explored and several of the key problems of wide range fuel-flexibility on the small-scale

will be studied and resolved. These problems are primarily based in engine characterization, fuel delivery and engine control.

The characterization challenges were rooted in the actual performance measurement in small-scale engines and their subsequent characterization. Small-scale dynamometers that could perform heavy duty and long-term power testing were unavailable or substantially out of feasible price ranges. Therefore, a small-scale engine dynamometer was designed, built and calibrated. Additionally, this dynamometer had additional features directly relevant to fuel-flexible engine testing such as the multi fuel switching system (MFSS). Having the right tools and systems in place to measure and characterize the engine was absolutely essential to understand the fuel flexible potential of this engine.

The electronic data acquisition and control of the engine was also critical to the advancement of fuel flexibility. Having many changing input engine parameters and conditions, real-time control of various properties—such as the throttle, air-to-fuel ratio and engine loading—was important. Using a combined hardware software solution that included National Instruments data acquisition systems, Arduino microcontrollers and other servos, several engine variables could be dynamically changed and measured.

The MFSS was a key component that was designed, built and tested in order to quickly and accurately deliver a variety of fuels to the rotary engine. Fuel miscibility and corrosive properties required the usage of specialized components and fuel hosing such that fuels could be reliably delivered to the engine. Additionally, testing the actual fuel flexibility of the engine and dynamic switching of fuels was improved using this system. The non-repetitive, early manual changes led to air gaps in fuel lines stalling the engine. This new system gives the operator electronic control of up to 8 fuels and allows for continuous operation; which is a key part of enabling reliable fuel flexibility.

Therefore, the design and development of a small-scale engine dynamometer, an electronically-controlled MFSS and the requisite sensor and actuator system to produce usable work from a range of petroleum-based fuel and biofuels were the major goals of this research. With these tools developed, the engine characterization could be completed.

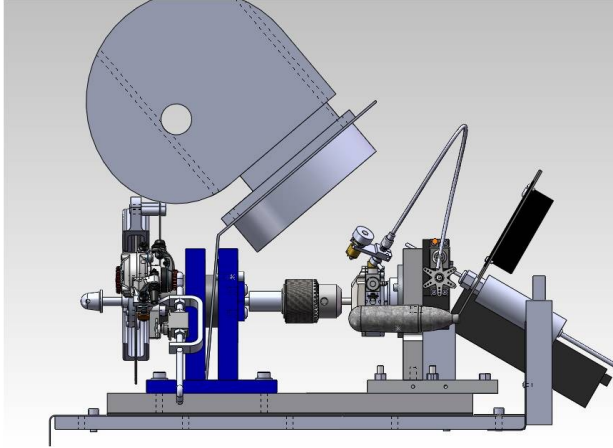


Figure 1: Solid model of the small-scale fuel-flexible engine dynamometer

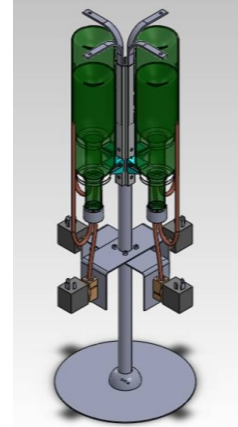


Figure 2: Electronically-controlled, multi-fuel switching system (MFSS).

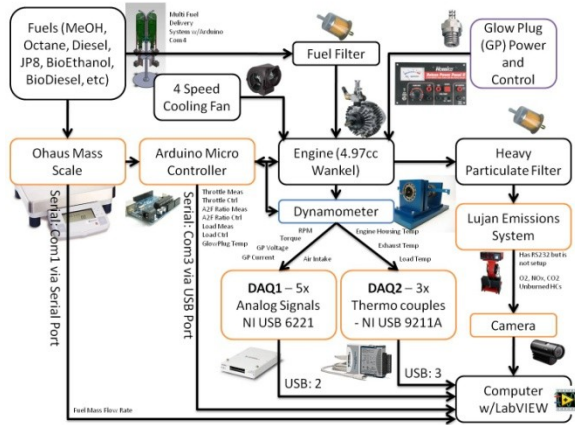


Figure 3: Fuel-flexible rotary engine sensor and actuator system to enhance fuel flexibility.

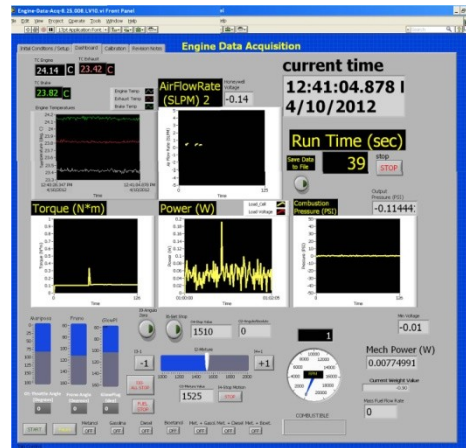


Figure 4: Dynamometer dashboard and control panel for the fuel-flexible engine system.

The proposed innovations and scientific contributions as presented above were derived from myriad sources including prior research done at U.C. Berkeley but additionally with insights from other researchers in the field. These innovations resolved several key issues to extending and characterizing fuel-flexibility in small-scale rotary engines and will be presented in detail throughout the remaining chapters.

Chapter 1 overview

Chapter 1 presents the reader with the vision and importance of fuel-flexibility, ideally motivating the research. Specific customer need cases are described and real life, hypothetical examples are presented. Later, chapter 1 defines fuel-flexibility in the context of this research. Lastly, a background research summary on work that was conducted both by international and U.C. Berkeley researchers is presented.

Direct applications of fuel flexibility

It is hard to neglect the constant concerns and fears of the declining supply of non-renewable energy resources that are consumed daily and are deeply integrated in every facet of human survival. Our nation continually looks for domestic energy security, lessened environmental impact and reduced effects from variable fuel costs [7]. Additionally, the growing demand for and dependency on portable systems and electronics are constantly increasing the need for small, portable power systems [33]. These two key features enable the utility of fuel-flexible engines in three primary applications: disaster relief, developing country emergency backup power and special ops military use.

Disaster relief and its need for fuel flexibility and portability

In late 2009, an executive from Cisco Systems brought to our attention the importance of communication systems during disaster situations for coordination of relief efforts in addition to the pains of supplying power to them. Their communication equipment, known as the Cisco Systems Nethope Relief Kit (Figure 6), greatly aids in these relief efforts [15]. Enabling communication via fuel-flexible sources of power could reduce casualties and improve the efficacy of rescue efforts.

However, access to the required 250 W of power is not always easily supplied by local sources such as solar panels or other power generation technology currently attempting to serve these markets [17].



Figure 5: January, 2010 – Haiti Earthquake Aftermath [14].



Figure 6: The NetHope relief kit [15].

In an emergency rescue situation where time is of the essence, portable power sources for communication equipment need to be quickly dispatched and ready for storage onboard a next-day economy class flight, fitting into overhead compartment bins and quickly passing through security. The Transportation Safety Administration (TSA) has specific rules and regulations for what types of chemicals and equipment that can be carried onboard [16]. Large supplies of batteries and other chemicals associated with fuel cells are typically not allowed in carry-on, nor checked luggage due to obvious safety concerns. Thus, the need to be able to quickly and confidently pack a portable power system that can produce power from local sources of stored energy (such as scavenged fuel, fuel from the rescue vehicles or other sources of liquid hydrocarbons) represents an opportunity to improve rescue efforts and save lives.

Developing countries & their need for on-demand, fuel flexible and portable power

Additional lives can be saved if reliable power technology can be accessed by developing countries during common medical procedures. In modern countries, constant and reliable access to power is taken for granted and if power is lost, back-up generators quickly start and allow doctors and surgeons the time to safely finish medical procedures. In developing countries, many factors can unexpectedly stop the power for uncertain amounts of time. Hospitals, suffering a power failure can cause doctors to lose sight of their hands and surgical tools, prevent essential medication from being administered and interrupt power to critical life-supporting equipment.



Figure 7: The woman in this figure is the founder of wecaresolar.com who gives solar panels to hospitals, maternity wards and other power dependent places so that they can maintain light and other equipment on during critical health procedures [17].

For the aforementioned reasons, a reliable, man-portable power source could greatly assist rescue personnel, doctors and other emergency personnel in their efforts to save lives.

Military demand for portable and fuel flexible power

Lastly, the United States military has an interest in highly portable power systems that are fuel flexible. Soldiers often times find themselves deep in warzone areas and in need of critical communication lines with headquarters. Imagine you are a soldier, carrying a 100-pound pack, 10 of which are batteries of unknown charge for your critical electronics and personal effects. What would happen if your mission changed and you had to survive for 3 more days without returning to base? How might you charge your batteries or power your communication equipment? If soldiers have access to fuel-flexible engine generators and could scavenge fuel from local sources, they might be able to charge one radio to send the last critical GPS coordinate. Currently wasteful practices, such as running Abrahams tank engines to keep onboard computers and GPS powered up, represent an unnecessarily large portion of wasted fuel, claimed to be one of the largest resources consumed by the U.S. Government and military abroad [18]. Not to mention the obvious danger it brings upon military personnel and resources. Additionally, new initiatives to reduce dependency on foreign oil and to power our military fleet with alternative fuel options are being investigated [19] (However as of 2012, the military is drifting away from its renewable energy focus [20]).

Soldiers also cannot simply carry a limitless number of batteries or gallons of fuel on their backs, thus they need lightweight, portable and flexible solutions. The average military backpack weighs about 100 lb and to carry anything more drastically fatigues soldiers (see Figure 8 and Figure 9). Additionally, these soldiers take fresh primary cell batteries at every opportunity as rechargeable ones never give confidence that they are fully charged. No soldier ever wants to leave for the battlefield without 100 percent fully charged batteries. Power options need to be clearly available and reliable.



Figure 8: Fatigued soldier on battlefield [22]. These soldiers cannot perform optimally and presents safety risks for soldiers



Figure 9: Another fatigued soldier resting on top of his equipment.

In fact, other military engineering companies have identified this problem and have been designing products more simply to carry soldier gear and other equipment, such as Boston Dynamics and Big Dog [21].



Figure 10: The BigDog from Boston Dynamics has an impressive ability to carry payload and handle complex terrain. Its current powertrain is a very noisy, 2-stroke, 15hp engine [21].

It is also quite possible that a fuel flexible engine power system could drive such machines like the Big Dog, not only by charging radios, but carrying payload as well (Figure 10). The military's continued need to maintain the security of our nation through energy independence also continues to expand the limits of technology; and the military too has placed their bets in fuel flexibility and portable power [7].

A grander vision for fuel flexibility – automotive applications

More than just supplying a fuel flexible power system to a few niche applications, a larger-scale application to fuel flexibility exists: fuel-flexible engine technology to automotive applications; specifically with hybrid engine technologies. By combining an internal combustion engine along with electrical powertrains, fuel can be conserved and emissions reduced. These energy regeneration technologies can be utilized to make short city trips without ever firing a cylinder (or rotating a rotor), reducing auto emissions. However, the moment the drive extends beyond the city or the car encounters a grade, the internal combustion engine kicks in and the highly energy-dense, petroleum-based fuel is consumed. This fuel is typically auto-grade gasoline (85-98 octane), but if the hybrid engine was a *fuel-flexible* engine, it is possible that drivers could choose a fuel that not only fit in with their environmental goals but also their price range [67].



Figure 11: Google's self driving Toyota hybrid Prius. It is quite possible that someday cars like this will have a fuel-flexible engine as its battery counterpart [23].

With miniscule infrastructures for bio and alternative fuels, a transitional solution is needed, which gives all transportation stakeholders an opportunity to take the next step towards renewable transportation technology. Renewable fuel producers face daunting challenges when competing with the pre-existing petroleum infrastructure and even with generous government subsidies (like corn-based ethanol [57]). They have trouble pricing their fuel competitively. If drivers do not have the option to choose a biofuel because their automobile is designed for only one single fuel, then renewable energy solutions and their infrastructural development will be further delayed [67].



Figure 12: Doc. Emmitt Brown from the Back to the Future movie part two, fueling his time machine with fusion technology of the future [58].

In the meantime, since wide-range, fuel-flexible engine systems do not yet exist, engineers are developing “add-on” systems that can permit some engines to run on several different fuels, including bio and renewable fuels [24]. But what exactly constitutes fuel flexibility? Can we strive to reach futuristic systems like that of Doc. Emmitt Brown from Back to the Future? Clarification and definitions are needed.

Fuel-flexibility and portable power defined

To better understand the scope and experimental goals of the research contained herein, some key components are defined.

Fuel-flexibility defined

“Fuel-Flexibility” as investigated in this research, is the ability of an internal combustion engine to produce usable power output from a wide range of liquid hydrocarbon based fuels. Wide range fuel-flexibility was until this research, only done in large-scale turbines (external combustion) [7] and to a limited extent, in other larger-scale rotary engines, like the Curtiss Wright military engines [26-28]. Not only did Jones *et al.* experiment with fuel-flexibility amongst fuels such as: Methanol Gasoline, Diesel and JP5, but they also explored supercharging as a way to improve performance. Until now, there has been little to no development of fuel-flexibility in smaller systems. The work that has been done to characterize fuel-flexibility in small-scale engines was conducted at U.C. Berkeley by several researchers [1], and the 4.9 cc O.S. Wankel rotary engine remains one of the smallest Wankel engines to have demonstrated a wide range, fuel-flexibility.

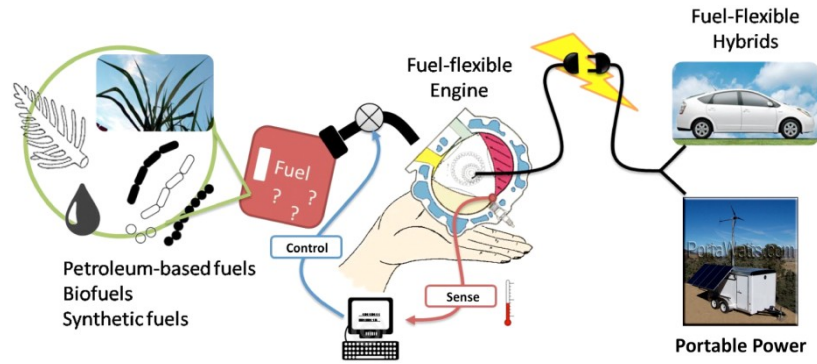


Figure 13: The graphic portrayal of the goal of fuel-flexible engine operation and its target applications.

Fuel-flexibility—in a general sense—is not limited to only liquid-based hydrocarbons. This range of fuels consumed could be expanded to include gaseous fuels and even potentially solid fuels (although likely through external combustion). This dissertation, however, focuses solely on liquid hydrocarbons. Researchers such as C. Fernandez-Pello, D.C. Walther and K. Fu [24], have shown that small rotary engines can also produce usable power combusting gaseous hydrogen and methane while C. McCoy and A. Cardes have demonstrated that fuel-flexibility is possible in 5 cc engines with liquid hydrocarbons [1].

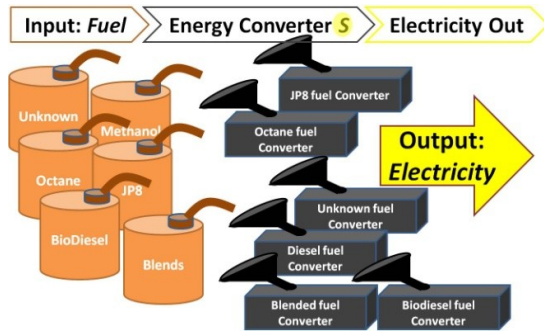


Figure 14: The current portable power solutions have a separate energy converter for each type of fuel desired for energy extraction. Typically, portable generators use gasoline.

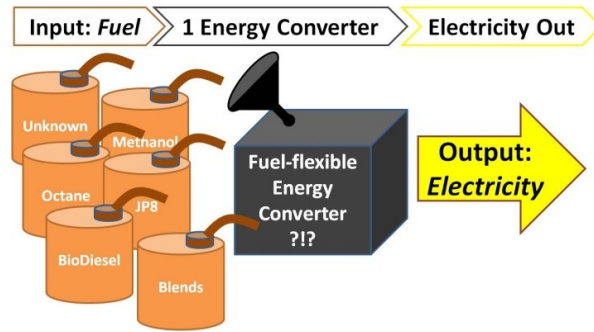


Figure 15: The goal of this research is to design a system around a small-scale rotary engine that can extract usable energy from an array of liquid hydrocarbon-based fuels.

Researchers have measured the fuel-flexibility of internal combustion engines [1,7,9,26,46] which typically involves measuring both the power output and the operating conditions of the engine. However, the real-time switching of fuels and the corresponding performance change—the output spike created when the engine switches fuels—has not been adequately explored. Thus to fully extend and characterize fuel-flexibility, the power should be measured across a range of fuels, the engine conditions

when using particular fuels and its ability to switch fuels in real time. The larger the range of fuel combusted and characterized, the more interesting the engine and the research. The table below highlights several important properties of fuels of interest to this research:

Fuel Name	Type	Chemical Formula	Specific Gravity	Molecular Weight [kg/kmol]	Latent Heat of Vap [kJ/kg]	HHV [kJ/kg]	AIT (K)	a/f	Source
n-Heptane	Liquid	C7-H16	0.684	100.2	318	48438.00	488	15.2	TA1
n-Octane	Liquid	C8-H18	0.703	114.23	301	48254.00	493	15.1	TA1
Gasoline	liquid	C8-H18	0.75	114.23	291	42500.00	553	15.1	TA7
Ethanol	Liquid	C2-H6-O (CH5-OH)	0.789	46.07	836	29668.00	638	9	TA1
BioEthanol	Liquid	C2-H6-O (CH5-OH)	0.789	46.07	836	29668.00	638	9	TA1
Methanol	Liquid	C-H4-O (CH3-OH)	0.791	32.04	1099	22663.00	658	6.5	TA1
JP8	Liquid	n/a	0.8	184.41	339	36112.00	513	15	TA1
Kerosene	Liquid	C13-H28	0.8	184.41	339	43100.00	483	15	TA4, TA7
BioButanol	Liquid	C4-H10-O	0.805	74.1	584	36112.00	616	11.1	TA1
Butanol	Liquid	C4-H10-O	0.805	74.1	584	36112.00	616	11.1	TA1
Diesel	Liquid	C12-H26	0.832	170.12	256	47838.00	273	15	TA1
BioDiesel	Liquid	C12-H26	0.832	170.12	256	47838.00	273	15	TA1
Light Diesel	Liquid	C8-H18	0.85	114.26	267	42500.00	483	15	TA7
Medium Diesel	Liquid	C14-H30	0.85	198.44	244	42500.00	483	15	TA7
Heavy Diesel	Liquid	C21-H44	0.85	296.65	232	42500.00	483	15	TA7

Figure 16: Aggregated fuel properties. Values pulled from the tables listed in “source” from [62,63] and the ME140 Reader produced by Prof. Carlos Fernandez-Pello at U.C. Berkeley, 2005.

To highlight the dependence of fuel-flexibility on various fuel properties, engine performance plots can be sorted by various fuel properties, such as specific gravity and volatility. It is still unclear which of the many fuel properties have the strongest effect on fuel flexibility. From early experimentation, the molecular weight appeared to be the parameter which affected the performance of the engine (likely due to its effect on viscosity, density, stoichiometry and volatility) [2].

The enablement of fuel-flexibility can be achieved in several ways. The engine itself can be redesigned and optimized to better accommodate a range of fuels. Systems can be built and added to the engine that can adapt to incoming fuels, loading conditions and the output properties of the engine. Lastly (or in addition), the range of fuels can be reduced to minimize fuel shock to engine system with respect to fuel changes, thereby requiring that the fuels be controllably blended or delivered to a “well-prepared” engine (well prepared suggesting that sensors inform control systems more-or-less what fuels will be introduced to the engine and how to change operating conditions).

Preliminary research results and intuition suggest that low-cost controls solution presents an effective solution in terms of actual development and implementation as designing, manufacturing and testing new engines and their components requires

significant investment. A controls solution can still lead to insight about the fuel flexible rotary engine being tested in this research and also be transferred and implemented into other similar engine systems (as opposed to specific engine modifications to this 4.97 cc rotary engine).

There are many strategies to better enable fuel-flexible systems of the future and this dissertation attempts to guide these efforts. R&D will ideally address the validity of the many potential solutions. Ideal fuel-flexibility should be able to take any liquid based hydrocarbon, in any order, and produce the maximum power and/or maximum efficiency it can from the given fuel. Ideally, the engine is sufficiently tolerant (i.e. it has been shown to operate and produce power from non-standard fuels) apart from the fuel for which it was originally designed to combust (as in the case of the O.S. Graupner, this is a Methanol-Nitromethane blend with typically five percent lubrication oil [1]). It's believed that this small-scale O.S. Wankel rotary engine can combust many fuels and fuel qualities, for example if the fuel is not pure or has contaminants. If the fuel has been diluted with some percentage of water, salt water, other airborne diluents or other chemicals, the goal remains to always be flexible and adjust the parameters of the engine to maintain continual and reliable power output. Thus, the goal is to use a system of sensors and actuators to extend the capability of a fuel-flexible engine and producing reliable power with any type, quality or amount of fuel introduced in the engine.

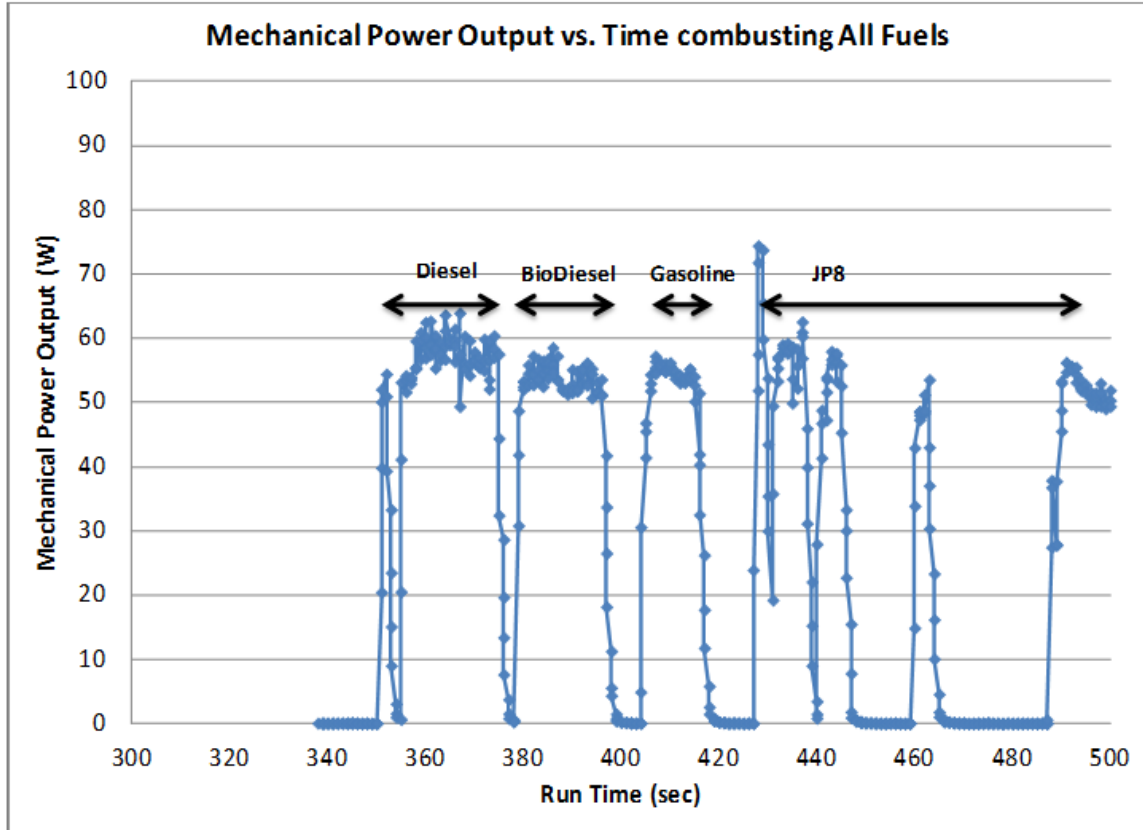


Figure 17: An output power versus time plot as the engine switches from one fuel to another and adjusts engine parameters to maintain power output. Ideally, the curve would be a flat line with no interruptions in power production.

The fuel-flexibility goal for this dissertation research is to minimize the power jump that is noted during fuel changes ΔP_{min} , while maintaining positive power output; dynamically adjusting the available small-scale engine parameters (such as percent wide open throttle, equivalence ratio, engine temperature, etc.). However, without the proper fuel flexible characterization of the engine, future research will be left without a sound basis of which variables should be actively controlled and to what degree they should be adjusted.

Portable power defined

In the research conducted in the MEMS REPS (Rotary Engine Power Systems) projects at U.C. Berkeley, terms such as “small-scale”, “mini-scale”, “micron-scale”, “portable”, and “ultraportable” were used to describe the power systems being investigated and developed. Typically, the length scale for the characteristic dimensions was a way to categorize one system or another. The micro-fabricated Wankels that K. Fu and A. Knobloch developed in the early 2000s were micron-scale devices while the larger motors that D.C. Walther and M. Swanger developed were on the mini-scale (as

dimensions could all be conveniently described in millimeters). This research falls within the mini-scale category, as most characteristic dimensions are in millimeters.

However, small does not necessarily mean portable. Devices, such as MEMS sensors and actuators, are very small but not always robust. These small devices (especially on the micron scale) are affected by different physical phenomena not typically considered in common engineering analysis. For example, when working with MEMS, inertial effects become less important but airflow and damping dominate dynamic behavior (which are typically ignored on larger scales) and, therefore, need to be carefully considered. In order to ensure portability, the device needs to not only be small, but also robust. This would suggest that any proposed solution should consider its capacity to resist shock, accommodate a range of temperatures, tolerate fuel impurities, adapt to various engine orientations, etc. In this research, the robustness sought was the fuel-flexible range achievable for this engine.

The portability desired for the power systems in this project is the ability to be “man portable,” such that a robust system could be easily transported by an individual wherever he or she may go. This portability is important and also generates some of the key motivations and challenges of the research conducted. Humans are already accustomed to several portable power systems, such as generators and batteries. Researchers and other early adopters of new technologies are likely also be familiar with fuel cells, super capacitors and mini turbines (which are all still their early development). However, in terms of dynamic response and wide-ranging fuel-flexibility, the rotary engine stands out above the rest. Fuel cells suffer from high cost and durability [4]. Stirling engines, while highly fuel flexible, suffer from low dynamic response times (in addition to solar and fuel cells), high cost and low power density [5,8]. Piston engines are highly refined but suffer from knocking during its limited fuel-flexible operation and tiny moving parts. Turbines, while demonstrated to be highly fuel flexible [7], require higher turbine speeds to achieve the requisite power output and make the system prone to failure as any imbalance at high speed could cause serious safety and system issues.

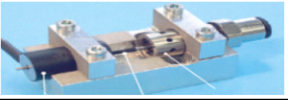





Current Portable-Power Technologies	Figure	Fuel-Flexibility (F)	Specific Power [kW/kg]	AHP Score
Turbines		Yes (Large-scale)	0.8	4.8
Stirling Engines		Yes (external combustion)	0.11	5.0
Solar		No	0.150-0.170	5.0
Batteries		Indirectly	0.250-4.5	5.7
Piston Engines		Narrow range	0.4-7.5	6.8
Proposed Solution: Mini Rotary Engine Technology				
<i>Small-scale Wankel Rotary Engine</i>		<i>Wide range</i>	<i>0.2-2.8</i>	<i>8.0</i>

Figure 18: Small-scale rotary engine technology along with other competing technologies. Rotary Engines: [1,46,47], Stirling Engines: [53], Piston Engines: [1,49], Batteries: [56], Solar [44,45] and Turbines: [55].

As seen in the above technologies (Figure 18) are not all created equal and often times have their particular strengths and weaknesses. One system may have high power delivery for a few minutes and another may be able to deliver low power for days on end. Thankfully, a pioneer in small-scale power systems, David V. Ragone, developed a plot which helps visualize these technologies based on their power and stored-energy capacities [3]. One such plot can be seen below where the Rotary Engine as tested fits into this plot:

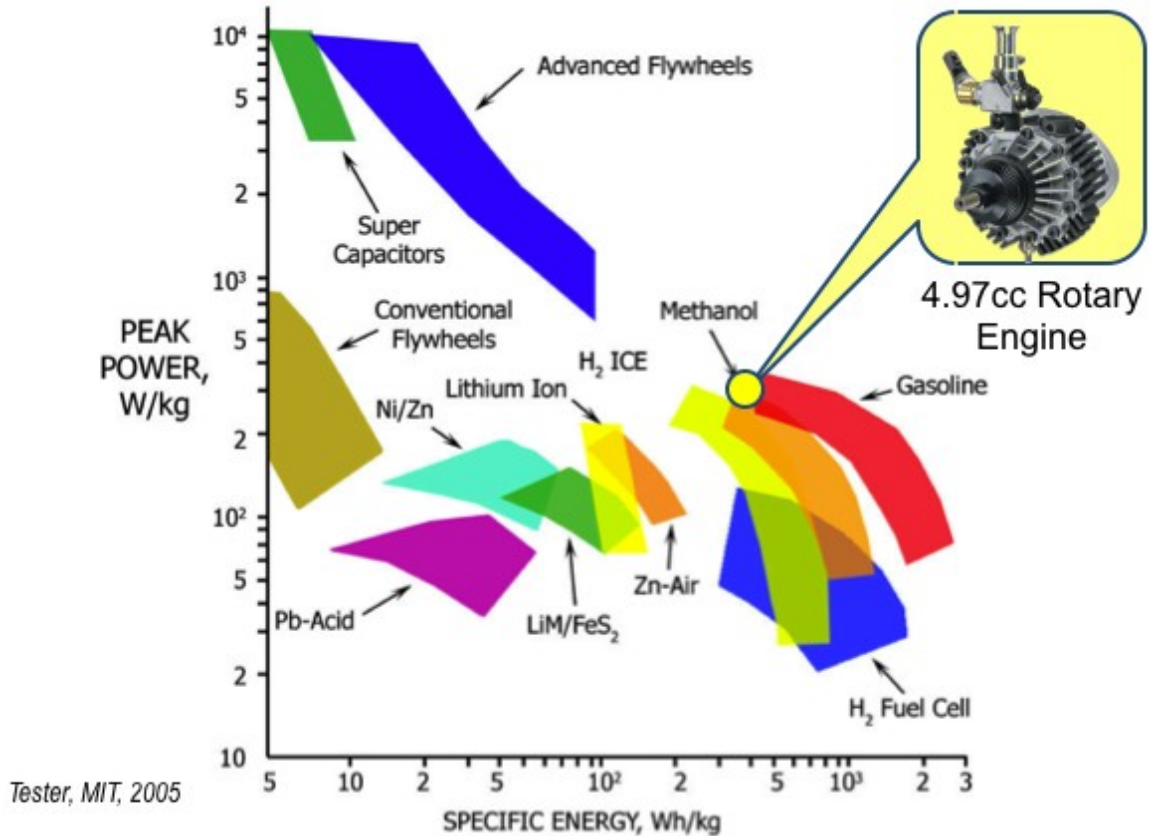


Figure 19: A Ragone diagram as presented by Tester from MIT in 2005.

It is noted that the scales are plotted in logarithmic form with energy density typically plotted on the y – axis and power density plotted on the x – axis. Thus, diagonal lines of unity divide technologies by their lifetimes or “characteristic times” at their maximum power delivery [3]. Capacitors, as can be noted in the plot, can only deliver high power for very short periods of time. Whereas in the opposing corner, technologies like “fuel cells,” are unable to deliver high power but can deliver low power for long periods of time.

Man-portable power systems based on internal combustion engines present an interesting data point in the sense that engines by themselves produce no power. They continually extract energy out of *fuel* and convert it into usable electrical or mechanical power. The static size of the engine, its power and energy, are largely based on the fuel storage capability of the system and thus depending on the size constraints of the application, or availability of fuel, tanks of various sizes can be selected.

Researcher, J. Revillé, went to great lengths to recreate and update the relevant small-scale power technologies on a Ragone Diagram, which can be seen below (Figure 20).

Ragone Diagram of Various Power Sources

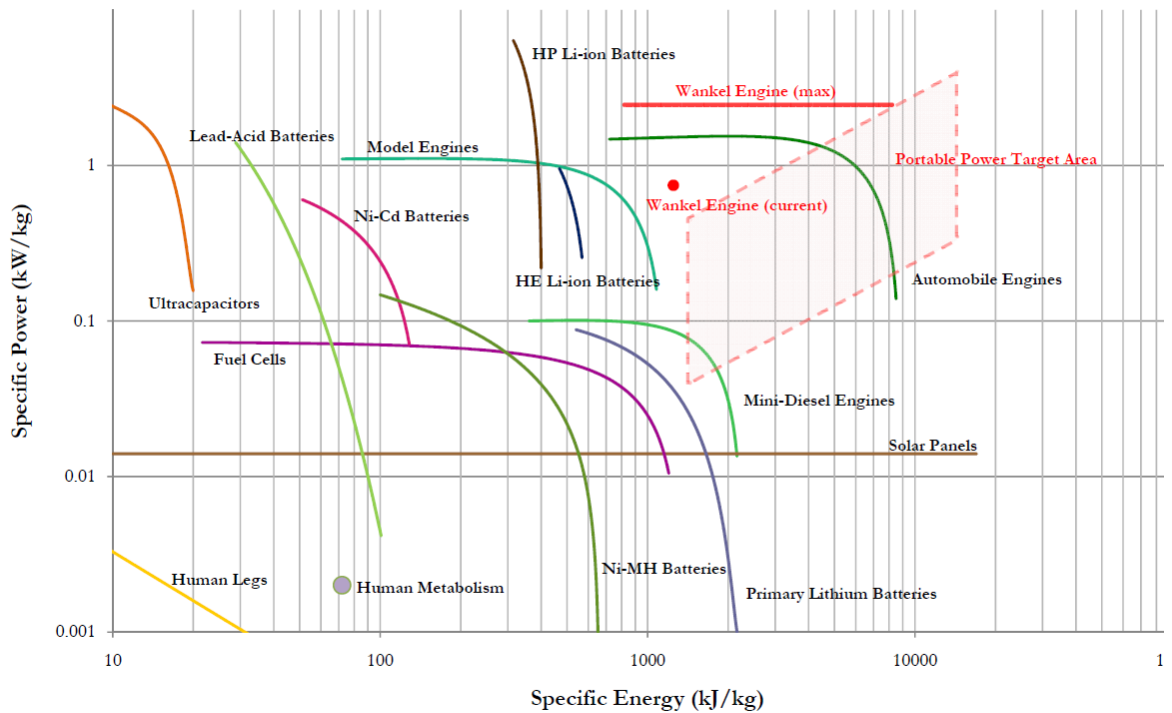


Figure 20: Taken from many sources of data, this Ragone diagram illustrates where the 4.97 cc O.S. Wankel engine exists but and the ideal target power range. See [9].

Power output can be a function of remaining stored energy potential, therefore, in many cases we observe a tapering off of specific power output as a function of specific energy (as mass increases with the addition of more fuel, thus driving down the specific power). Since the stored potential energy of fuel remains constant as power is being delivered (assuming an engine is operating at maximum potential), there is no taper as noted in the “Wankel Engine (max)” curve above (see Figure 20).

In an ideal world, the most useful technologies would have high specific power and high specific energy, placing these technologies in the upper right hand most corner of this plot. The rotary engine used during this research targets this ideal regime (10 – 1000 W, Figure 20).

However, to reach this point in the plot, there are several key challenges that need to be overcome. The maximum-power-output-to-weight ratio but even more importantly, enabling and increasing the fuel flexibility of the system while still remaining “man portable”. These Ragone plots only tell part of the story since high specific power and

energy are just two of the desired characteristics of this power system. Achieving fuel flexibility combined with portability would relieve the key pains observed in the primary motivators for this research. But like any thorough investigation, the hunt for the key issues and challenges starts with a look into the past and who has discovered what before now to solve this problem.

Standing on the shoulders of giants - background research

All scientific research builds upon the great works of the past, thus continually advancing science and technology. This case is no different. Many researchers have already contributed to making portable power and fuel flexibility feasible technologies for the future. Therefore, it is essential that the background of fuel flexible engine development, which has had tremendous influence on the direction of this research, be adequately understood.

In this research, fuel flexibility is again being limited to liquid petroleum-based hydrocarbons for fuel, flexibility meaning the range of fuels tolerated by a system and with regard to portable power. This constitutes “man-portable” devices (power supply technology that could be carried by the user).

Prior research advancements to fuel flexibility and portable power

Looking first at fuel flexibility, there are several important researchers outside of UC Berkeley who have made progress in this field. Several great reviews on micro and meso scale combustion exist; coming from K. Maruta [10], and Y. Ju [11]. The high density of fuels makes them ideal candidates for portable power technologies but their use in one single engine platform is limited by combustion fundamentals. Typically heat losses, flame-wall interactions and diffusion are among the standard combustion phenomena present that limit power capabilities on this scale.

Dunn-Rankin, Walther and others describe the opportunities and challenges present in “human-compatible” portable power [60]. Solutions presented are within the electrochemical, thermochemical and biochemical domains. Fuel cells show great promise as an energy source but cannot deliver high peak powers nor respond dynamically. Small engines—like the one presented in this research—can output high power but cannot do so at high efficiency. Biological systems like hummingbirds show great efficiency at producing metabolic power and are largely underexplored.

Engines are typically the common platforms converting chemical energy into mechanical energy and several researchers have made good progress in achieving wide-

ranging fuel flexibility. Johansson, Christensen, and Hultqvist are three such researchers who were able to put a variable compression ratio into an HCCI engine making it nearly capable of producing power any liquid fuel [12]. Other non-standard engines—like an external combustion, Stirling engine—shows promise for enabling wide-ranging fuel flexibility. D.G. Thombare *et al.* show that with proper design of the heat exchanger and drive mechanism, can produce power at low temperatures.

Combustors and turbines have also been looked at for fuel-flexible development. T. Lieuwen *et al.* discuss blowout, flashback, dynamic stability and autoignition issues within combustors due to natural gas composition variability and the potential use of other fuels like syngas [13].

Other researchers worldwide have attempted to solve similar problems in relevant fields. Some examples are the Siemens Fuel Flexible turbine systems, which use external combustion within a turbine to generate fuel-flexible power on a larger scale. Curtiss Wright and NASA also developed systems that used larger rotary engines to produce power and move vehicles on a variety of fuels [30]. The United States Military as well used rotary engines in their raptor unmanned aerial vehicles (UAVs) due to their high-power-to-weight ratio and their potential in combusting a range of fuels such as JP8 [1].

The Berkeley Micromechanical Analysis and Design (BMAD) Lab and the Combustion Processes Lab (CPL) at U.C. Berkeley, provide the foundation of this doctoral research. Below is a brief overview of their efforts which has helped identify the scope of the fuel-flexible power systems project and the intended advancements to science in which this research attempts to contribute.

Berkeley contributions to rotary engine power systems in the late 1990s and 2000s

“There is plenty of room at the bottom.” ~Dr. Richard Feynman

With power demands increasing, researchers explored technology options and identified the high energy density of fuels as one promising solution to portable power. This research intended to explore the feasibility and potential of micro combustion, on both the micro and mini-scales. The excitement of combining the world’s best micro fabrication and MEMS techniques to the development of portable power solutions in addition to the advanced combustion research taking place at the time, led to synergetic development of engines in both the micro and mini-scale platforms.

Specifically on the micro scale, topics such as micro-scale combustion, fuel delivery, advanced engine fabrication techniques, MEMS automotive sensors and other micro rotary engine applications (pumps and compressors) were researched and developed. The mini-scale topics included fuel flexibility, rotary engine design, dynamometer design and fuel processing.

Micro-scale Rotary Engine Power Systems (REPS) development

Beginning primarily with Fu, the technical feasibility of making rotary engines on the micro scale was assessed [9-11]. These researchers were attempting to make rotary engines with housing volumes under 1 mm^3 and rotor swept volumes of 0.08 mm^3 [24]. In collaboration with Case Western Reserve University, a first generation molded SiC meso-scale rotary engine was developed [26]. Fu concluded that there are no fundamental phenomena that will limit micro-scale combustion, however; he did note that heat loss and sealing issues would present formidable challenges. Additionally, fabrication challenges regarding alignment and assembly also would need to be addressed [21,23,24]. Thus, when considering the design of auxiliary systems for the 4.97 cc O.S. Graupner, heat transfer was carefully considered and addressed accordingly (such as isolating the engine from the aluminum support plate and using the fuel both as a lubricant and refrigerant).

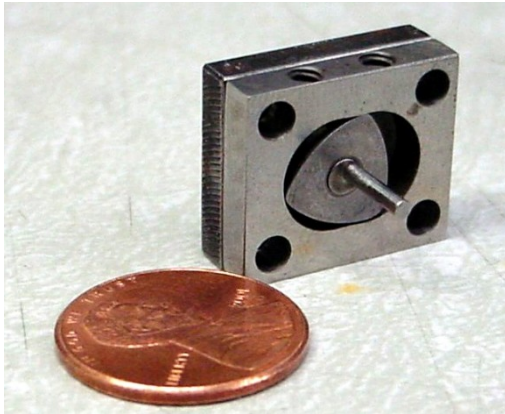


Figure 21: Fu, *et al.* designed and fabricated three meso-scale rotary engines to test the limits of microcombustion [24].

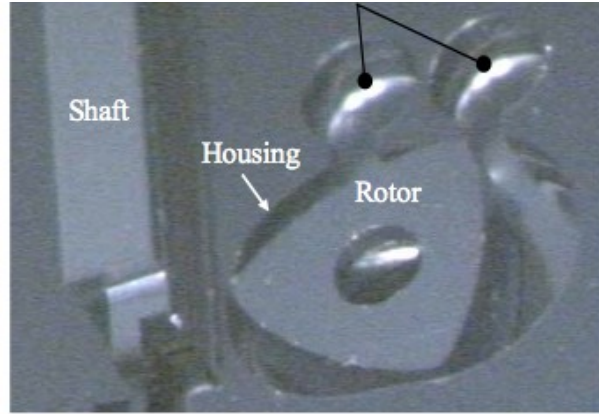


Figure 22: A MEMS version of the Wankel Engine developed at UC Berkeley in the early 2000s made from Silicon Carbide [26].

These engines (as seen in Figure 21) were operated using gaseous H_2 – *air* with both spark and glow plug ignition. They demonstrated 2.7 W of positive power at 9,300 RPM. The researchers concluded that heat loss and pre-ignition were problems that needed to be resolved. Due to the challenges with lubrication and H_2 management,

these types of gaseous fuels were not explored for this fuel flexibility research and are for future research efforts.



Figure 23: A MEMS-based temperature sensor designed and fabricated by S. Wodin-Schwartz is embedded into a 4.97 cc Wankel Engine by C. McCoy to test survivability of MEMS devices in real combusting small-scale engines [43]. The circle identifies the location $5 \times 5 \text{ mm}^2$ pocket for the MEMS temperature sensor.

Specifically regarding micro fabrication, Martinez *et al.* developed optimized DRIE processes for fabrication of the rotor and its micro springs [28]. This fabrication process was essential in order to form the dynamic combustion chambers of the rotary engines in the MEMS-scale applications [21,23-25]. Rotary engine geometry presents itself as a good candidate for MEMS-scale fabrication due to its planar nature, which is well suited for surface deposition or bulk-etching MEMS fabrication processes. Much of the scientific knowledge learned in this early phase of small-scale engine development led to the testing of MEMS sensors in larger combusting engines (Figure 23) [40,41].

Knobloch *et al.* also tackled the sidewall problems and achieved straight, $900 \mu\text{m}$ deep trenches using a three mask process (the number of masks is typically proportional to the complexity of a device and three is relatively low compared to other R&D processes). The researcher also notes silicon “grass” or black Silicon in the trench bases which can be mitigated by optimizing the pressure during the etch (Figure 27 below) [27].

In the SEM images below (Figure 25, Figure 26, Figure 27), it can be seen that Martinez *et al.* found ways to maintain nearly vertical sidewalls in high aspect ratio trenches [12]. Additionally, researchers such as Wijesundara developed coatings and

other post processing techniques in order to improve material robustness (with regard to temperature, wear, chemical corrosion, etc.) [26]. It is also not uncommon to see coatings on engine components, especially within the rotary engine. Researchers at Curtiss Wright and others have published several studies on coatings to improve rotary engine performance [29]. With various fuels being introduced to the engine, it may be necessary to choose special coated surfaces to catalyze combustion processes or protect the various components from material corrosion (as various fuels are known to corrode various metals and other common materials).

Considering the other potential opportunities using MEMS processing, the rotors can have ferromagnetic materials deposited within them as explored by Senesky, such as 40%-60% nickel-iron alloy (perm alloy); which is electroplated, in order to add a dual purpose to the rotor (to both generate electrical induction and to separate the combustion chambers). This material was selected specifically to match thermal expansion coefficients but also provide relatively high magnetic saturation [29,30].

Another significant challenge in MEMS devices that still exists today is the sealing of chambers after the last “release step”. As other researchers have published within BMAD (Chen, Y.M., and Frank, J.), the challenges to creating a sealed surface while also allowing a sufficient release step, is a problem for fully sealed combustion chambers and other types of MEMS fluidic valves [31-33]. With regard to the fuel flexible research, apex seal redesign was considered, however, since the sealing was not directly related to enabling fuel flexibility, it is left for future research endeavors.

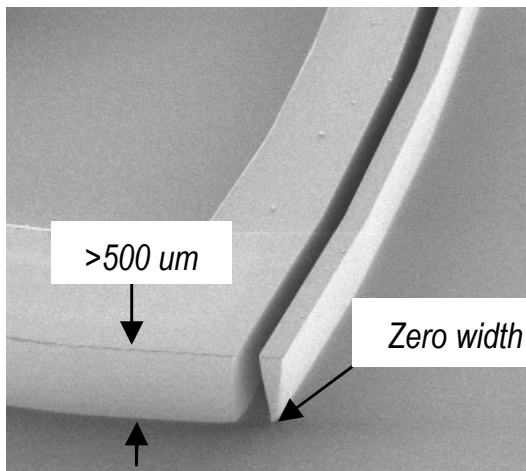


Figure 24: The integrated rotor apex seal and spring. Note the angled sidewalls known as the ARDE (Aspect-Ratio Dependent Etching) effect [28].

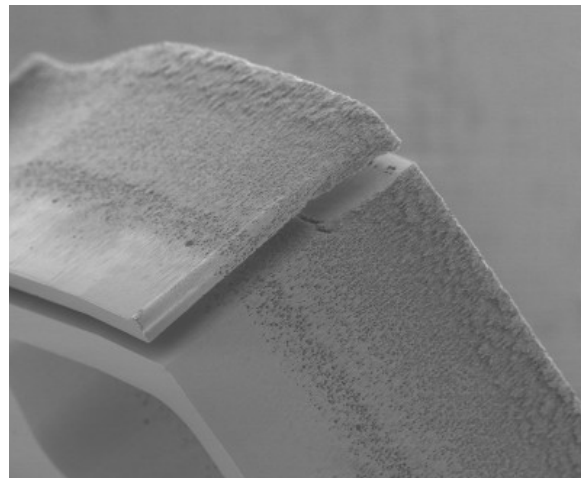


Figure 25: Through the optimized process, Martinez et al. is able to maintain long vertical sidewalls with non-zero width bases, however striations are noted [28].

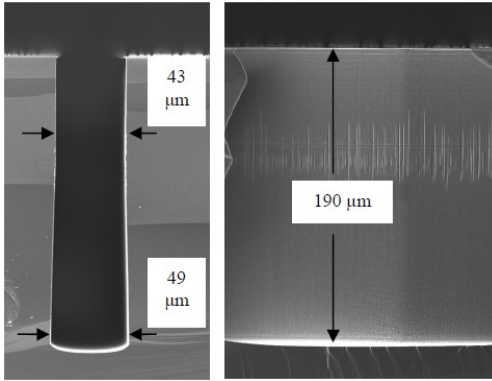


Figure 26: After using the Taguchi Method to optimize the process over several key process variables (Time, Gas, Flow, Coil, Platen and Pressure), the etch performance is dramatically improved [28].

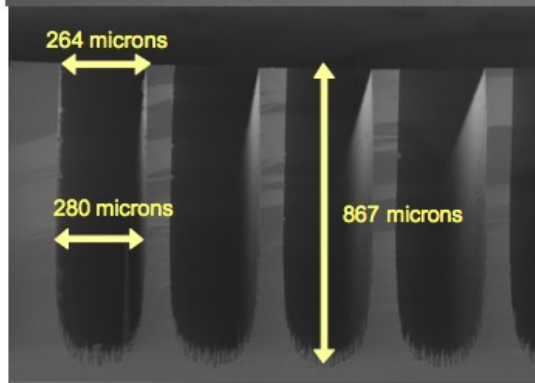


Figure 27: Knobloch, *et al.* demonstrates the various etch profiles and process artifacts such as Silicon "grass" which could potentially affect smooth engine operation via a non-uniform sliding surface [27].

The rotary engine in the mini-scale world

Researchers such as K. Fu, D.C. Walther conducted research in both the micro and meso worlds, but M. Swanger, B. Sprague, Y. Tsuji, S-W. Park, J. Heppner, A. Cardes, J. Revillé and C. McCoy were the members of teams who conducted the majority of their work on the mini-scale—or where the characteristic dimensions are typically in millimeters. These researchers specifically developed several aspects of the rotary engine power system: overall engine development, flame characteristics within small combustion pockets, mini and micro-scale fuel delivery, leakage flow analyses, preliminary fuel-flexibility characterization, dynamometer design and system development.

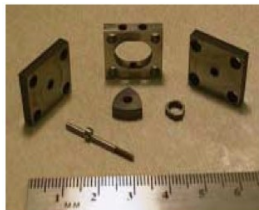


Figure 28: Early development of mini-scale rotary engines. Designed as part of the MEMS REPS program at UC Berkeley [25].



Figure 29: Albert P. Pisano reviews the contributions of the Berkeley Micromechanical Analysis and Design (BMAD) Lab [33].

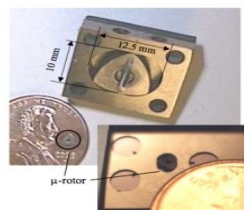


Figure 30: Principal Investigator from the Combustion Processes Laboratory at U.C. Berkeley

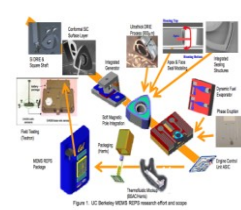


Figure 31: The overview of the MEMS REPS project [33].

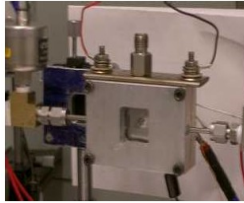


Figure 32: Understanding the effect of chamber width on small-scale combustion [37].

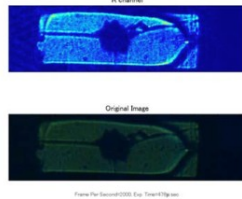


Figure 33: This work by B. Sprague focused on combustion dynamics and flame speed in small combustion chambers [38].

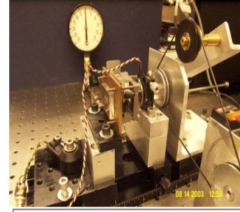


Figure 34: Original dynamometer test stand designed specifically for small scale rotary engine testing [39].

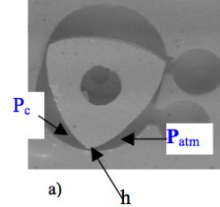


Figure 35: Sealing on the micro and macro scales has always been a challenge. Heppner *et. al.* sought to understand why [40].

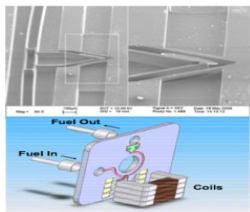


Figure 36: Park, *et al.* utilized MEMS-based microvalves to do fuel delivery [51].

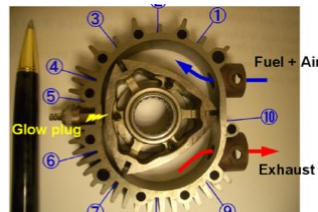


Figure 37: A “down-axis” view of the 4.97 cc O.S. Graupner Wankel Rotary engine [1].

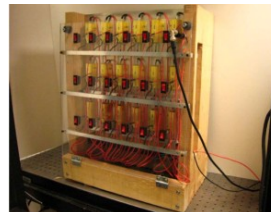


Figure 38: The electrical braking system for the small-scale engine dynamometer [9].

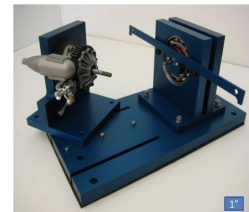


Figure 39: McCoy *et al.* and the development of a small-scale engine dynamometer for fuel flexibility characterization [49].

Figure 40: The Rotary Engine Power Systems project thrust and the researchers who contributed.

Swanger *et. al.* (Figure 34), primarily focused on the mini-scale development of the rotary engine, with emphasis on the 1500 mm³ and the 367 mm³ engines both designed and developed at U.C. Berkeley. Both engines were CNC machined from tool steel and many components were wire EDMed (Electro Discharge Machining, such as the apex seals). Each engine was tested and developed in similar manners using low-cost, custom-built dynamometers and can be proud that the 1500 mm³ engine is the newest rotary engine design since the publication of this dissertation. This engine has produced un-assisted power output and was fully designed by U.C. Berkeley researchers. Swanger and colleagues over the span of a few years were able to develop engines that produced 33W of unassisted power (Figure 41) [41]. The 367 mm³ never ran without assistance but was on the path to power production as well.

The challenge in this period was effectively collecting data and monitoring all engine input parameters and comparing them to their outputs. It was highly empirical research and could have benefitted from a more analytical approach. Additionally, the dynamometers used in these experiments were operated typically outside the operational limits of individual components; namely the loading and starting motors. Many of these

dual-purpose load / start Maxon motors froze up due to overheating and over-running. These research challenges will be presented and resolved within this dissertation (although was not without its own unique challenges).

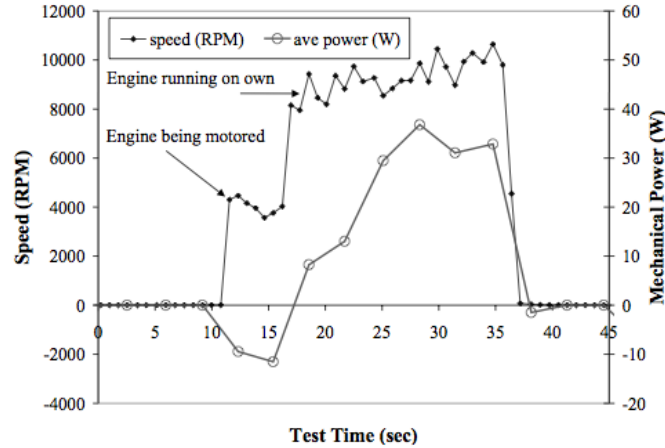


Figure 41: Sprague et. al demonstrating 33W of an assisted power being produced by the 1500 mm³ engine [41].

A big component to achieving the desired power output observed in Figure 41 is the fuel delivery systems researched and developed by S-W. Park [47,48]. As the droplet size for liquid fuels gets smaller, the more efficient combustion becomes. As less heat goes to evaporating fuel, more surface area exists to create reactions with oxygen and less fuel is wasted through non-combustion. However, as the size of the engine decreases, so must the maximum fuel droplet size because optimal combustion can only occur when all the fuel is evaporated. And because small engines suffer more from heat losses, therein lies another key challenge in developing fuel delivery systems on this scale. The following equation is derived from fuel evaporation equations, residence times of a rotary engine and droplet geometry.

$$(1) \quad d_o = \sqrt{\frac{C_o \lambda_b \theta_{crankshaft}}{\omega_{crankshaft}}}$$

Where d_o is the initial droplet diameter, C_o is a unit conversion constant, λ_b is the droplet evaporation constant, $\theta_{crankshaft}$ is the angular displacement of the crankshaft, and $\omega_{crankshaft}$ is the angular speed of the crankshaft. It is important to note that

residence times in rotary engines are independent of scale relying on the angular position of the rotor [42]. Residence times are on the order of 1-100ms.

Additionally in fuel injection, essential shaft power is consumed in order to maintain fuel pressure in fuel pumps and with the output power on the order of 100-1000 W, fuel pumps consume a significant percentage of the power output. This is known as parasitic power and significant efforts are made to reduce its magnitude.

Other challenges also exist on the small scale in terms of fluid management of liquid fuels and valving. Electronic circuitry needs to be protected from shorts caused by flowing liquids and also needs to be carefully regulated to maintain the desired stoichiometry. In this respect, S-W. Park optimized a linear, magneto-static actuator for fuel delivery so as to prevent shorts and include valving technology capable of atomizing fuel on this small scale [50].

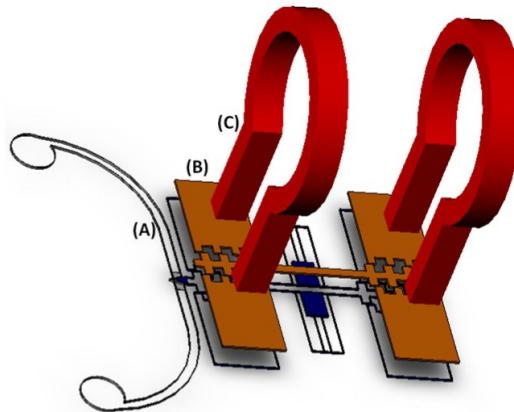


Figure 42: Magnetostatic actuator for fuel injection designed by S-W. Park, *et al.* [51]

Expanding on fluidic challenges, the leakage flow analysis conducted by J. Heppner highlighted that apex seals and springs are necessary to maintain sufficient compression ratios. His modeling showed that the leakage is approximately proportional to $Q \sim h^3$ where h is the gap between rotor apexes and the epitrochoidal housing (h is referenced in Figure 35 above). With this in mind, apex seal springs were always checked for wear and proper functionality so as to maintain compression [40]. Since this was not a specific problem addressed in this dissertation research, it is suggested for future work (in Chapter 5).

Integrated sensors and actuators for combustion applications

Additionally, the use and integration of MEMS features and devices within rotary engines are predicted to significantly improve their performance. Most modern vehicles to date use many sensors to monitor performance, however; they are typically input and output based, not *in-situ* measurements of combustion. Automobile engines today still rely on “fuel maps” in order to adjust to changing environmental and ambient conditions and are elected for geographic areas where fuels are sold in different compositions and to different standards. This presents significant limitations for the technical development of engines, being limited to only one selected fuel. Thus, within in the BMAD research lab, many students work on developing MEMS sensors that go *inside* the combustion chamber, providing real-time sensor data of *each* combustion chamber. Access to in-situ measurements of cylinders can improve engine power output, efficiency, fuel flexibility and other performance parameters. Thus the fuel flexibility research serves as a platform for MEMS harsh-environment sensor development as well.

S. Wodin-Schwartz *et al.* demonstrates that Silicon Carbide sensors can be placed inside harsh combustion environments (Figure 23) in order to measure and monitor performance [43]. In earlier work, oily residues atop these sensors were observed and in order to mitigate these effects, recommendations were made to add embedded heaters, maintaining elevated sensor temperatures [44].

Lastly, Rheume *et al.* designed and tested a new solid state electrochemical sensor for monitoring lean direct injection engines. This sensor not only detects oxygen presence but also responds to changes in pressure, potentially offering independent monitoring of each cylinder during operation. This sensor also provides improved performance compared to pre-existing sensors in that it has faster response times [45].

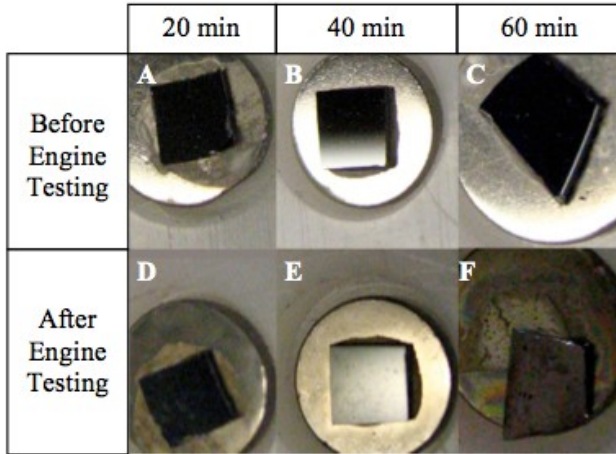


Figure 43: Wodin-Schwartz, *et al.* investigated the effects of combustion on Si and SiC chips. Bonding and surface deposition were two main challenges discussed [43].

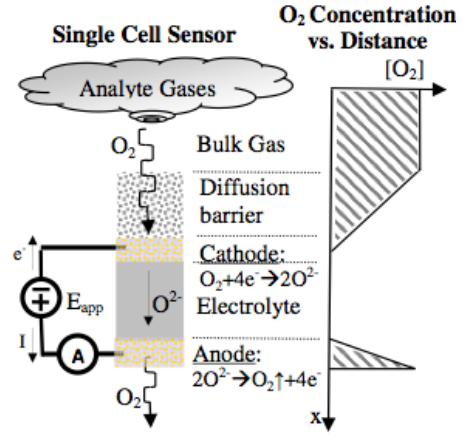


Figure 44: Rheume, *et al.*, "Solid-state electrochemical sensor for monitoring lean direct injection engines." [45]

Prior work in fuel flexibility for small-scale rotary engines

Amongst all of the world-class research conducted in this field, that of A. Cardes *et al.* provided the catalyst for this dissertation. His research was the first to operate a 5 cc Wankel engine on a variety of liquid fuels demonstrating the potential fuel flexibility of this engine. His research concluded that positive power could be produced from Methanol, Gasoline, Diesel and JP8 fuels—on the order of 100-300W. Additionally, other measurements by collaborating researchers were taken such as chamber pressure and temperature distribution across the planar faces of the engine (see Figure 47). Measurements concluded that the combustion event is non-consistent, even using conventional fuels and that there is in fact a large temperature gradient across the engine, defining a hot side and a cold side. Additionally, contributions by C. McCoy allowed for the direct measurement of the average engine pressure ratios for this engine yielding 6.4 ± 1 with $N = 10$ in dry, zero lubricant runs [1].



Figure 45: Experimental setup with a throttle control, belt driven dynamometer and manual

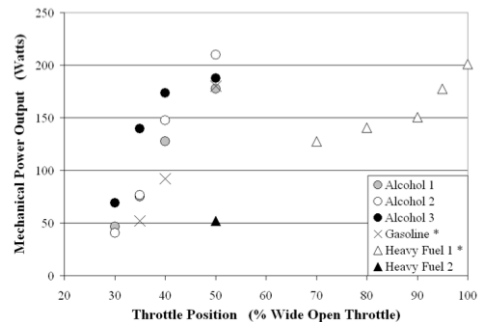


Figure 46: Output mechanical power measured from a single unmodified rotary engine combusting a variety of fuels [1].

engine start [1].

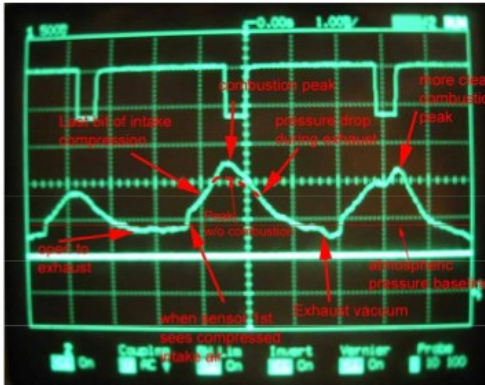


Figure 47: Pressure traces of the combustion event. Poor data collection methods only yielded a snapshot of an oscilloscope screen [1].

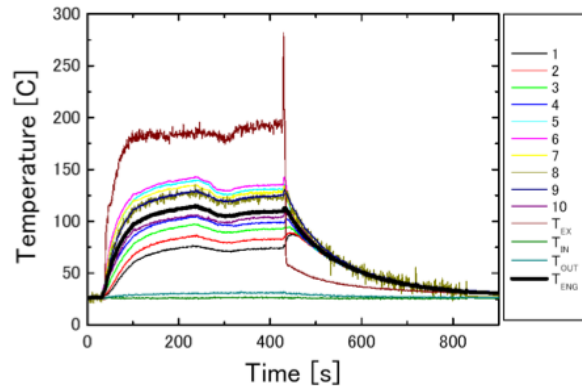


Figure 48: Various engine temperatures distributed around the periphery of the engine [1].

This research set the tone for the potential of fuel flexibility in small scales but lacked the key operating parameters: what variables are important for fuel flexibility, what range of fuels that can be combusted in a fuel flexible rotary engine, how fuels can automatically transition, and so forth. In the following chapters, the research presented provides answers to some of these questions and allows future researchers to build upon the shoulders of yet another giant so as to make further synergetic contributions to science and improve humankind’s understanding of the natural world.

Chapter 1 summary

Fuel flexible engine technology presents a scientific and engineering challenge in that engines today are designed to combust single fuels. However there is clear and present need for not only the ability to extract usable power from a diversity of fuels but also to make this power portable. Two applications on the small scale are for disaster relief and military emergency power. On the larger scale, fuel flexibility could provide a new transitional solution to enabling the consumption of renewable fuels in automobiles. These applications motivate the research teams efforts in extending and characterizing fuel flexibility in small-scale rotary engines.

This research built upon the vast works of others in areas of portable power and rotary engine characterization. The foundation of this background research has strong roots in U.C. Berkeley through their development of the MEMS Rotary Engine Power Systems project where micron-scale Wankel motors were designed, fabricated and tested. While no functioning motor was ever created on this scale, many key innovations were

developed that enabled new possibilities in MEMS fabrication and furthered the understanding of micro-combustion for portable power.

Additionally, the mini-scale research where technologies related to mini-scale rotary engines were reviewed and the technical and scientific challenges they presented to micro-combustion, fuel delivery, fuel flexibility, ignition, thermal management and rotary engine design and operation were reviewed.

Summary of remaining chapters

Chapter 2 intends to introduce some of the key theory of engines, heat cycles, rotary engine design, and other key equations that assisted the development of the fuel flexible engine dynamometer (FFED), the multi fuel switching system (MFSS) and the sensors and actuator systems that control the engine.

Chapter 3 describes in detail the actual design choices, fabrication and setup of these various systems.

Chapter 4 is the presentation of data and results from the various experiments that were conducted in order to characterize the fuel flexibility of the O.S. Graupner Wankel engine.

Chapter 5 discusses these data and draws conclusions. Additionally, several recommendations for future work are discussed.

Chapter 6 succinctly summarizes the work and conclusions of this dissertation research.

Lastly, the Appendices are presented as auxiliary material to help any other future researcher or interested reader on how they themselves might go about using the equipment described herein or developing a system on their own.

Chapter 1 References

- [1] Cardes, A.C., **McCoy, C.D.**, K. Inaoka, D.C. Walther, A.P. Pisano and C. Fernandes-Pello, “Characterization of fuel flexibility in 4.97 cc rotary engines,” MCS, Libson, October 6-10 2005.
- [2] Isaac, O.F., Okoro, K., Obodeh, O., “The need to know the right fuel for different engines in developing countries.” *Journal of Emerging Trends in Engineering and Applied Sciences*. (JETEAS) 2 (3): 495-498 (2011).
- [3] T. Christen, M. Carlen, “Theory of Ragone plots,” in *Journal of Power Sources*. Vol. 91, 2000. pp. 210-216.
- [4] Cacciola, G., Antonucci, V., Freni, S. “Technology up date and new strategies on fuel cells.” *Journal of Power Sources*, 100, 2001, pgs 67-69.

- [5] Thombare, D.G. and Verma, S.K. “Technological development in the Stirling cycle engines.” *Journal of Renewable and Sustainable Energy Reviews*. 12 (2008) 1-38 July 2006.
- [6] Turner, B., “E85, flex-fuel vehicles and AB 1493: integrating biofuels into California’s vehicular greenhouse gas regulations.” M.S. thesis, Energy Resources Group, UCB, Berkeley, CA, 2006.
- [7] Rahm, S., Goldmeier, J., Moliere, M., Eranki, A. “Addressing gas turbine fuel flexibility.” *Power-Gen Middle East*, Manama, Bahrain Feb. 17-19, 2009.
- [8] Mellde, R., Maasing, I., Johansson, T., “Advanced automobile engines for fuel economy, low emissions and multifuel capacity.” *Annu. Rev. Energy*. 1989 14: pgs. 425-444.
- [9] J. Revillé, “The Wankel engine and fuel-flexibility: an engine performance review,” M.S. thesis, ME Dept., UCB, Berkeley, CA, 2009.
- [10] K. Maruta, “Micro and mesoscale combustion.” *Proc. of the Comb. Institute*. 33 (2011) 6 Oct. 2010. Pp. 125-150.
- [11] Y. Ju, K. Maruta, “Microscale combustion: technology development and fundamental research.” *Progress in Energy and Combustion Science*. 2 Oct 2010. Pp. 1-47.
- [12] M. Christensen, A. Hultqvist, and B. Johansson, “Demonstrating the multi fuel capacity of a homogeneous charge compression ignition engine with variable compression ratio.” *SAE Technical Paper Series*. 1999-01-3679. Intl’ Fall Fuels and Lubricants, Toronto, Canada. Oct. 25-28, 1999.
- [13] Lieuwen, T., McDonell, V., Petersen, E., Santavicca, D. “Fuel flexibility influences on premixed combustor blowout, flashback, autoignition and stability.” *Journal of Engineering for Gas Turbines and Power*. Jan 2008, Vol 130.
- [14] Haiti Earthquake Image, <http://haitirescuecenter.files.wordpress.com/2010/01/jan-013-2010-e-103.jpg>. Accessed on 31 Mar 2010.
- [15] Net Hope Relief Kit. <http://www.make-digital.com/make/vol119/?folio=44#pg46> Accessed on: 4/1/2012.
- [16] Explosive & Flammable Materials, Disabling Chemicals & Other Dangerous Items. <http://www.tsa.gov/travelers/airtravel/prohibited/permitted-prohibited-items.shtm#9> Accessed on: 23 April 2012.
- [17] We Care Solar Photos. <http://www.wecaresolar.com/gallery> – Maternity Ward in Africa. Accessed on: 1 May 2010.
- [18] Johnson, K. “Pentagon’s First Energy Plan.” <http://online.wsj.com/article/SB10001424052702304665904576385843719478096.html?mod=djkeyword> Accessed: 15 June 2011.
- [19] Pfannenstiel, J. “We Sail the Ocean Blue, but We're Going Green, Too.” <http://online.wsj.com/article/SB10001424053111903454504576488170369227268.html?mod=djkeyword> Accessed on: 4 April 2012.

- [20] <http://www.wired.com/dangerroom/2012/05/senate-cuts-off-navy-biofuel/>
Accessed on: 29 May 2012.
- [21] M. Raibert, K. Blankespoor, G. Nelson, R. Playter et. al, “BigDog, the Rough-Terrain Quadruped Robot,” Proceedings of the 17th World Congress. The International Federation of Automatic Control Seoul, Korea, July 6-11, 2008.
- [22] Image. <http://standupforamerica.files.wordpress.com> Accessed on: 15 May 2010.
- [23] “TO DEMONSTRATE HOW EFFECTIVELY THE TOYOTA PRIUS HYBRID SELF DRIVING CAR WORKS, GOOGLE PUTS A BLIND MAN BEHIND THE WHEEL” <http://www.indiancarsbikes.in/cars/google-self-driving-driverless-toyota-prius-hybrid-blind-man-57678/> Accessed on: 1 April 2012.
- [24] Woosley, R.J., and Korin, A., “The Flexible Fuel Answer to OPEC: It costs an extra \$100 to enable a car to run on biofuels or natural gas. Washington should mandate the tweak.” <http://online.wsj.com/article/SB10001424052748703806304576243010385191274.html> Accessed on 23 April 2012.
- [25] Fu K, Knobloch A, Martinez F, Walther DC, Fernandez-Pello C, Pisano AP, et al. “Design and experimental results of small-scale rotary engines.” In: IMECE/MEMS-23924, Proc. ASME 2001 international mechanical engineering congress and exposition (IMECE), New York; November 11–16, 2001.
- [26] Wijesundara, M., Walther, D.C., Stold, C., Fu, K., Gao, D., Carraro, C., Pisano, A.P., and Maboudian, R., “Low temperature CVD SiC coated Si microcomponents for reduced scale engines.” ASME IMECE 2003, 15-21 November, Washington D.C.
- [27] Knobloch, A., Wasilik, M., Fernandez-Pello, C., Pisano, A.P. “Micro, internal-combustion engine fabrication with 900 μ m deep features via DRIE.” IMECE, 2003, Washington D.C. Nov 15-21, 2003.
- [28] Martinez, F.C., Chen, N., Wasilik, M., Pisano, A.P. “Optimized ultra-DRIE for the MEMS rotary engine power system.” EMNO4, 2021 October 2004, Paris, France.
- [29] Hege, J. B. (2001), Wankel Rotary Engine: A History, Jefferson, N.C.: McFarland & Co., c2001.
- [30] Jones, C. Ellis, D., Meng, P., “Multi-fuel rotary engine for general aviation aircraft.” AIAA-83-1340, 19th Joint Propulsion Conf., AIAA, SAE, and ASME. Seattle, WA, June 27-29, 1983.
- [31] Jones, C. “Advanced development of rotary stratified charge 750 and 1500HP military multi-fuel engine at Curtiss-Wright.” International Congress and Expo. Detroit, Michigan, Feb 27-Mar 2, 1984.
- [32] Senesky, M. “Electromagnetic generators for portable power applications,” in Mechanical Engineering. vol. Ph.D. dissertation: University of California, Berkeley 2005.

- [33] Walther, D.C., Pisano, A.P, “MEMS rotary engine power system: project overview and recent research results.” Berkeley Sensor Actuator Center, 2003.
- [34] J. A. Frank and A. P. Pisano, "Low-Leakage micro gate valves," in TRANSDUCERS, Solid-State Sensors, Actuators and Microsystems, 12th International Conference on, 2003, 2003, pp. 143-146 vol.1.
- [35] J. A. Frank, "Lateral Etching of Silicon: The Hole-in-the-Wall Fabrication Processes," in Mechanical Engineering. vol. Masters Berkeley: University of California, 2004.
- [36] J. A. Frank, "Planar Microfluidic Devices for Control of Pressure-Driven Flow," in Mechanical Engineering. vol. Ph.D Berkeley: University of California, 2004.
- [37] Y. Tsuji, B. Sprague, D.C. Walther, A.P. Pisano, A.C. Fernandez-Pello, “Effect of chamber width on flame characteristics in small combustion chambers.” 43rd AIAA Aerospace Sciences Meeting. 10-13 Jan. 2005. Reno, NV.
- [38] S.B. Sprague, Y. Tsuji, D.C. Walther, A.P. Pisano, A.C. Fernandez-Pello, “Observations of flame speed and shape in small combustion chambers.” Western States Section, Combustion Institute, Spring 2004. Davis, CA.
- [39] M. Swanger, D.C. Walther, A.C. Fernandez-Pello, A.P. Pisano, “Small-scale rotary engine power system development status.” Western States Section, Combustion Institute, Spring 2004. Reno, NV.
- [40] J.D. Heppner, D.C. Walther, A.P. Pisano, “Leakage flow analysis for a MEMS rotary engine.” Proceedings of IMECE. 16-21 Nov. 2003, Washington D.C.
- [41] S.B. Sprague, S.-W. Park, D.C. Walther, A.P. Pisano, A.C. Fernandez-Pello, Development and characterization of small-scale rotary engines, Int. J. Alt. Prop., in press.
- [42] S-W. Park, D.C. Walther, A.P. Pisano, A.C. Fernandez-Pello, “Development of liquid fuel injection systems for small scale rotary engines.” 44th AIAA Aerospace Sciences Meeting 9-12 Jan 2006.
- [43] Schwartz-S.W., “MEMS Sensing in an In-Cylinder Combustion Environment,” PowerMEMS, 2010.
- [44] Schwartz SW, Myers DR, Kramer RK, Choi S, Jordan A, Wijesundara MBJ, Hopcroft MA, Pisano AP (2008) Silicon and silicon carbide survivability in an in-cylinder combustion environment. In: PowerMEMS 2008, Sendai, Japan, Nov 9–12, 2008.
- [45] Rheume, J., Wolfgang, H., Dibble, R., Pisano, A.P. “Solid state electrochemical sensor for monitoring lean direct injection engines.” IMECE 2008 pp. 389-394.
- [46] Image. Haiti Earthquake.
<http://haitirescuecenter.files.wordpress.com/2010/01/jan-013-2010-e-103.jpg>.
Accessed on 31 Mar 2010.
- [47] Jones, P.A., White, S., Alan, J., “A high specific power solar array for low to mid-power space craft.” Spectrolab Inc., CA.

- [48] Wikipedia.org, <http://en.wikipedia.org/wiki/Photovoltaics> accessed on 1 Sept. 2009.
- [49] **McCoy, C.D.**, Revillé, J.P., Albert P. Pisano, “Fuel flexible engine design for optimal combustion.” MIT Energy Conference 2009, Boston, MA, March 2009.
- [50] Park, S.W., **McCoy, C.D.**, Mehr, A., Kuypers, J.H., Pisano, A.P., “Design optimization of a MEMS magnetostatic linear actuator.” IMAC 2008, Orlando, Florida, Jan 2008.
- [51] S-W. Park, D.C. Walther, E. Takahashi, A.P. Pisano, “On the Development of Micro-Scale Magneto-Static Actuator for a Planar Fuel Valve,” Proceedings of 7th PowerMEMS, pp. 141-144, 2007.
- [52] Dunn-Rankin, Pham, T., Karnani, S., Sirignano, W. "Liquid-fuel combustion in miniature power and propulsion systems." 6th Int'l Workshop on Micro and Nanotech. Dec. 2006, Berkeley, CA, USA.
- [53] Wood, J.G., Lane, N., “Advanced 35 W free-piston stirling engine for space power applications.” American Institute of Physics. CP654. (2003).
- [54] O.S. 49-PI Type II 30 Wankel Rotary. <http://www3.towerhobbies.com/cgi-bin/wti0001p?&I=LXPVE3&P=7> Accessed on 3 Sept 2009.
- [55] Peirs, J. Reynaerts, D., Verplaesten, F., "Development of an axial microturbine for a portable gas turbine generator." Journal of Micromechanics and Microengineering, 13 (2003) pp 190-195.
- [56] “Lithium-ion Battery.” http://en.wikipedia.org/wiki/Lithium-ion_battery accessed on 4 Sept 2009.
- [57] Pear, R. “After Three Decades, Tax Credit for Ethanol Expires.” <http://www.nytimes.com/2012/01/02/business/energy-environment/after-three-decades-federal-tax-credit-for-ethanol-expires.html> Accessed on 14 May 2012.
- [58] Dean, K. “On Sale in 2011: Air-Powered Car from Zero Pollution” <http://www.kerrydean.com/news/on-sale-in-2011-air-powered-car-from-zero-pollution-motors/> Accessed on 21 June 2012.
- [59] Power-to-weight ratio. http://en.wikipedia.org/wiki/Power_to_weight_ratio accessed on 5 Sept 2009.
- [60] Dunn-Rankin, D., Elisangela, M.L, Walther, D.C., “Personal power systems.” Prog. In Energy and Comb. Science. V31, (2005) 422-465.
- [61] Carlson, G., US Patent 7305939 - Addition of flexible fuel engine control system. Issued 11 Dec 2007.
- [62] Ceder, G., Byoungwoo, K., “Battery materials for ultra fast charging and discharging.” Nature 458, (12 March 2009) pp.190-193.
- [63] Mohr, P., Taylor, B., Newell, D. “CODATA recommended values of the fundamental physical constants: 2006” NIST, Gaithersburg, MD, 2007.
- [64] Quintiere, J. “Fundamentals of Fire Phenomena.” Maryland, Partial Reproduction, Ch.3-7, 2005.

- [65] Borman, Ragland, Combustion Engineering, McGraw Hill Publishing, San Francisco, CA 2001.
- [66] “Fluids – Latent Heat of Vaporization Chart”
http://www.engineeringtoolbox.com/fluids-evaporation-latent-heat-d_147.html
accessed on 6 Dec. 2012.
- [67] McCoy, G.A., et. al, “Alcohol-fueled Vehicles,” WSEO (1992).
- [68] Piemont, S. WIPO Patent: “device for identifying hydrocarbon fluids.”
<http://www.wipo.int/patentscope/search/en/WO1996015064> Accessed on: 10 May 2012.

Chapter 2 – Theory

“Don’t be more precise than the subject warrants.” ~Plato

The Wankel rotary engine—the first rotary engine to demonstrate working potential—was a wildly significant departure from the conventional piston engine as is commonly known today. Human nature has always feared radical change and the initial resistance to this new revolutionary engine (which boasted high power densities, reduced valving complexity, nearly perfected internal balancing and fully rotational motion) severely limited its development in the 20th century. By 2010, in contrast to the rotary engine, the piston engine had benefitted from over a century of intense engineering development, such that complex computer-controlled systems can go as far as to shut down pistons at high speed [66, 68], piston and battery hybrid systems help achieve a combined 42 mpg fuel economies [72], and experimental combustion methods such as Homogeneous Charge Compression Ignition (HCCI) engines meticulously control engine temperature, pressure and timing to continually improve engine efficiency [73].



Link to the History Channel's Modern Marvels: "Engines" episode, specifically their comments on the Rotary Engine (starts at 6:25 and has a 3 min. duration) [74].

The Wankel rotary engine—revolutionary at its inception and remains so today—lacks the years of consistent, incremental R&D advances from which the piston engine has evolved. While the piston engine will remain a key power plant for modern day automobiles and power machines—with heavy research investments, many incremental and evolutionary innovations surrounding CAFE fuel economy improvements and renewable fuel infrastructural research—the Wankel rotary is a revolutionary¹ innovation which fundamentally changes the geometry of four-stroke internal combustion engines and offers a new world of research opportunity. Like a child new to sports, there is a lot of opportunity for development and a “most improved” achievement is waiting for R&D efforts in Wankel Engines.

¹ Revolutionary in the context of an all-new and functioning, innovative internal combustion engine design.

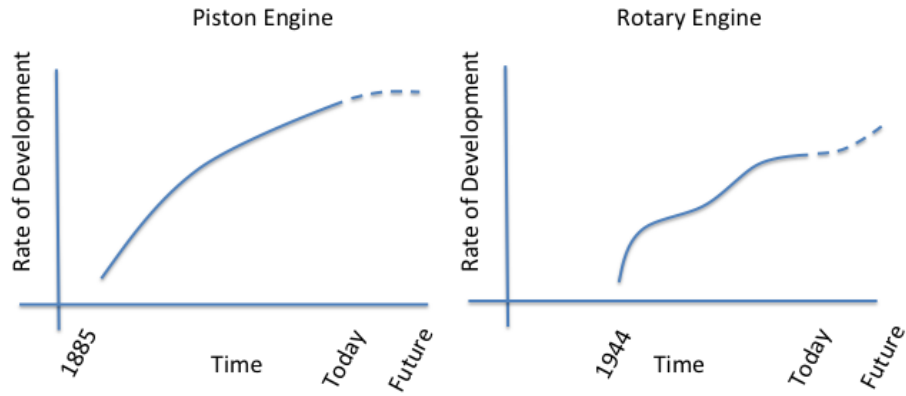


Figure 49: Hypothesized technology development comparison between the piston engine and the rotary engine. The piston engine has been an evolutionary engine and the rotary engine will become a revolutionary engine.

Even with the lacking supply of fuel-flexible portable power options, demand still exists. Notwithstanding the significant challenges that are present to enable fuel flexibility, these challenges create environments ripe for great opportunities. Therefore, a new, solution that can utilize the pre-existing combustion theories, infrastructures and knowledge, but additionally also provide radically new engine development opportunities, leverage newly developed manufacturing techniques, can bring hope that a similar century of advancement in engine technology is on the horizon. The Wankel Rotary Engine represents this opportunity and solution. The Rotary Engine—if given the same R&D attention received by the piston engine—could present new engineering advancements that technologists, entrepreneurs and thought leaders should not dismiss.

The Wankel rotary engine was advanced upon its release and challenged the state-of-the-art manufacturing and development technologies of the time. However today, many technologies exist and are mature enough to make rotary engine production much more cost effective and feasible; especially within R&D.


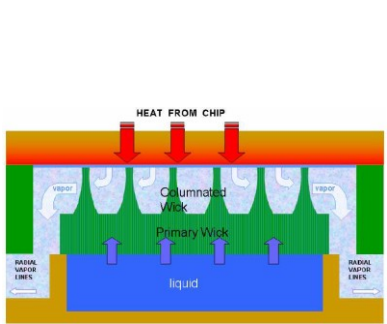

	<p>Advances in Materials and Manufacturing - New material development and manufacturing abilities have surfaced to enable and better facilitate micro-Wankel development, such as: Nanomanufacturing, Precision Engineering, CNC, 3D Printing and others [69].</p>
<p>Figure 50: Since 2009, Makerbot Industries has begun to produce hobby-grade 3D printers and have started a DIY revolution with many free designs and parts available for download on their website: www.thingiverse.com</p>	<p>Additionally, novel plating and microfabrication using high fracture toughness Silicon Carbide, presents opportunities to resolve long-standing concerns about the rotary engine such as wear, temperature management, corrosion and other material concerns [26].</p>
	<p>Advances in other relevant technology - Thermal management continually improves reducing the impact of early heat loss issues with technologies such as heat pipes, thermoelectrics and other cooling / heating strategies. With computer processors shrinking rapidly in size, technologies to sufficiently cool them have also shrunk and present potential options for cooling small engines.</p>
<p>Figure 51: This is the structure developed by N. Dhillon and C. Hogue to create a thermal plane that maintains a constant temperature [69].</p>	<p>The work of N. Dhillon and C. Hogue <i>et al.</i> at U.C. Berkeley, for example, generated a micro-loop heat pipe cooling system that was passive and microfabricated via silicon wafers in order to keep temperatures constant over a range of microprocessor power outputs. Technology like this provides more options to making the peripherals necessary to operate miniature rotary engines.</p>
	<p>Advances in Renewable Engine Technology: Fuel-flexibility and renewable fuels – Many companies are placing bets that biofuels will eventually replace the current fuel infrastructure but there is not yet any leader in biofuel production to date. Thus, having an engine that can accommodate a variety of fuels (both at consumer-level scale and also at the R&D test bench) presents an exciting opportunity to be part of the renewable energy solution [78].</p>
<p>Figure 52: Cobalt Biofuels is a startup company that intends to bring biobutanol to the commercial marketplace and help the world achieve energy independence from renewable energy.</p>	

Figure 53: Various opportunities based on technology and economic trends.

Therefore, with such an engine ripe for revolution and innovation, a vast opportunity awaits to review the requisite analyses to characterize and improve engine systems.

Review of Combustion

Combustion Cycles, Efficiency and Engine Performance Calculations

Even though the geometry of the rotary engine is radically different than its piston counterpart, it still operates on all the same fundamental combustion principles. The various heat cycles and combustion fundamentals (droplet evaporation, emissions, knocking etc.) are analyzed in similar manners but there are some differences. The key ones are pointed out and placed in context with the rotary engine tested in this research. The reader is encouraged to refer to standard combustion and internal combustion engine text books for an in-depth understanding (Borman & Ragland, Stone or Taylor, [76-78]).

The main equation that encapsulates much of the thermodynamic cycles is the First Law of Thermodynamics:

$$(2) \quad \Delta E = Q - W$$

Where Q is the heat generated and W is the work output. This difference is the total change in energy of a particular closed system. This fundamental law allows us to calculate and understand thermodynamic cycles, work output, heat released in chemical reactions and so forth. Thus, in the context of the small-scale rotary which suffers from heat losses, these heat losses represent a missed opportunity for extracting more work from a system for a given amount of stored energy that is injected into the system.

The Diesel Cycle

The O.S. Graupner Wankel Engine used primarily in this research, Rotary Engine 49-PI Type II (which will from now in this work, on be referenced as the O.S. Graupner Wankel), is a 4.97 cc rotary engine operating on a hybrid diesel cycle (Figure 54) in that it has compression ignition with the help of an activated catalyst glow plug at the onset. However during fuel-flexible operation, some fuels need this catalyst to remain hot to assist with fuel evaporation and maintain combustion, thus the Wankel Rotary in this research is acting in a somewhat hybrid cycle.

Diesel heat cycle efficiency

The benefit of a diesel cycle and diesel engines is that the efficiencies are typically higher than the Otto Cycle gasoline counterpart. This is because it operates on compression ignition, which requires higher compression ratios, driving temperatures higher (T_h) and therefore higher efficiencies. The Carnot efficiency, by comparison, is the ideal efficiency and according to current theory cannot be surpassed and serves as a

best case scenario. Modern automobile engines of today tend to operate around 25-30 percent thermal efficiency.

$$(3) \quad \eta_{Carnot} = 1 - \frac{T_c}{T_h}$$

However, for more accurate calculations, the thermal cycle efficiency incorporates the compression ratio of a particular engine.

$$(4) \quad \eta_{th} = 1 - \frac{1}{CR^{\gamma-1}}$$

Where $\gamma = k = c_p/c_v$, the ratio of specific heats and $CR = V_{max}/V_{min}$. The $\gamma_{air} = 1.4$ and is a function of gas / mixture temperature. Further refinement, taking into consideration of the cycle itself yields the modified diesel thermal efficiency

$$(5) \quad \eta_D = 1 - \frac{1}{CR^{k-1}} \left[\frac{r_c^k - 1}{k(r_c - 1)} \right]$$

Where $r_c = V_3/V_2$ as seen in (Figure 54), additionally, diesel engines are capable of achieving typically higher torques than that of the mechanical cycles.

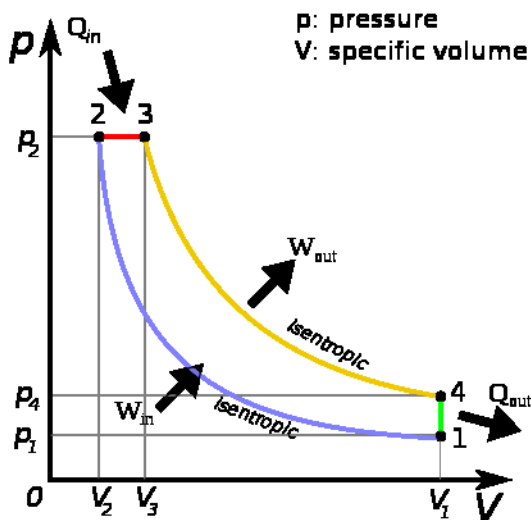


Figure 54: Ideal Diesel Cycle with heat entering at constant pressure and the work done between points 3 and 4 [80].

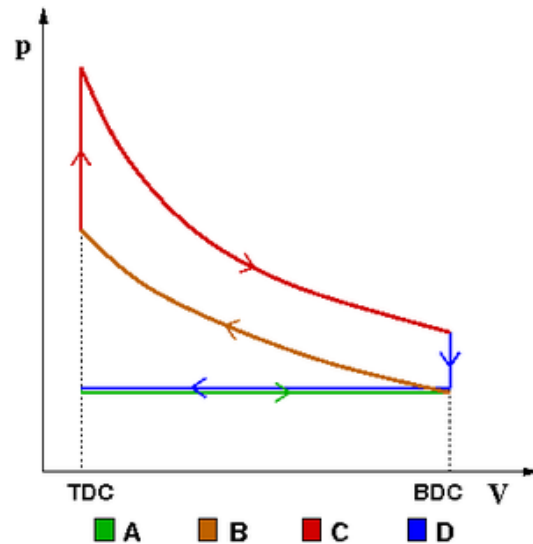


Figure 55: Ideal Otto Cycle [80].



Modern Marvels “The Engine” Rudolph Diesel, in 1892 patented the diesel engine and describes the differences [74]. (Video)

The Otto Cycle

Typical gasoline engines operate on the Otto Cycle (Figure 55). They are four-cycle processes and are typically spark-ignited thereby locally raising the temperature of a fuel-air mixture and subsequently causing heat release and pressure increases, driving the work output.

The Otto Cycle efficiency

The indicated and combustion efficiencies relevant to the Otto cycle efficiency are:

$$(6) \quad \eta_i = \frac{P_i}{\dot{m}_f LHV}$$

Where \dot{m}_f is the mass fuel flow rate multiplied by the *LHV* or lower heating value of the fuel, the term P_i is the measured power output of the engine.

The actual combustion efficiency, which breaks the combustion reaction into components in terms of mass flow rates of species and their heat of reaction, the following formula can be used:

$$(7) \quad \eta_c = \frac{(\dot{m}_f h_f) + (\dot{m}_a h_a) - (\dot{m}_e h_e)}{\dot{m}_f LHV}$$

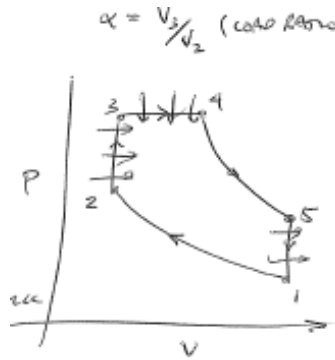


Figure 56: a dual or mixed cycle with limited pressure and constant volume.

The actual operating cycle of the engine is a hybrid between these two ideals. Especially as the fuel changes and has its specific octane rating (which is a chemical property which governs the spontaneous ignition point of a fuel), there is a hybrid of auto-ignition and spark / glow plug ignition. This does not operate on thermodynamic cycle efficiency as the heat addition is in two different stages: one part constant volume and the other, constant pressure. This hybrid cycle can be observed in Figure 56.

To approximate the predicted power output of the engine with a given fuel, the following formula is used:

$$(8) \quad P_{out} = \eta_{th} \dot{m}_f LHV$$

Where the \dot{m}_f is calculated by

$$(9) \quad \dot{m}_f = \omega \rho_{air} V_c \left(\frac{1}{AF} \right)$$

Where ω is the rotational speed of the engine in rad/s, ρ_{air} is the density of air, V_c is the chamber volume (which for the O.S. Graupner Wankel is 4.97 cc and the last term AF is the fuel to air ratio. These calculations provide order of magnitude values that help improve the design and diagnostics of the fuel-flexible dynamometer system.



Modern Marvels – “The Engine” In 1876, Nicholas Otto patented the first four-stroke system for the internal combustion engine [74]. (Video)

Brake Specific Fuel Consumption (BSFC)

The amount of fuel consumed for a specific power output is considered its specific fuel consumption. Mechanical efficiency is a function of the measured power output versus the calorific values of the fuel being burned. The amount of power being produced as shaft work is dependent on the design of the engine, its inherent losses, the completion of the combustion reaction, etc. Thus the measured power output versus the ideal power output (which would be to convert 100 percent of all stored chemical energy into usable shaft work) is known as η_o :

$$(10) \quad \eta_o = \frac{W}{CV} = \frac{W}{-\Delta H_o}$$

Where W is the measured power output and $-\Delta H_o$ are the calorific values of a specific fuel (the amount of energy contained within the bonds of the chemical structure). For example the reaction: $H_2 + \frac{1}{2}O_2 \rightarrow H_2O$ (*liquid*) has an energy of formation of: $-\Delta H_o \sim 142$ MJ/kg. Thus the brake specific fuel consumption (BSFC) is calculated by:

$$(11) \quad BSFC = \frac{r}{P}$$

Where r is the rate of fuel consumption and P is the output power. The BSFC has units of g/J or more intuitively, $\frac{g/s}{W}$ (which illustrates the rate of fuel consumption versus the power output of the engine). Any engine will have a different BSFC for different speeds and loading conditions. For example, a reciprocating engine has the highest efficiency when the intake is unthrottled and the engine is running at its peak torque. However, equations are not always operated at peak performance conditions to provide variable or throttled power output. From the BSFC, the efficiency can also be derived with the help of equation (8).

$$(12) \quad \eta_{th} = \frac{P_o}{\dot{m}_f LHV}$$

For example, using a $LHV_{methanol} = 19915$ kJ/kg, a $\dot{m}_f = 0.0045$ g/s and a power output of $P_o = 99.6$ W, the efficiency for this engine and this fuel is approximately: $\eta_{th} = 1.12$ %, These values were pulled from a dynamometer test of the O.S. Graupner Wankel engine studied in this research, hinting at the low efficiency of the tiny engine described in this research.

Brake Mean Effective Pressure (BMEP) – a means to compare engines

In the grand scheme of engine characterization, a performance comparison with other engines and other portable power technologies is typically made. Thus having a metric across engines to compare by is useful. The Brake Mean Effective Pressure (BMEP) does this exactly as it takes the volume capacity of the engine into account. This calculation includes the pumping losses and work consumed during the intake and exhaust strokes.

$$(13) \quad \begin{aligned} &BMEP \\ &= \frac{\text{Brake Work Output per Cylinder per Mechanical Cycle}}{\text{Swept Volume per Cylinder}} \end{aligned}$$

Since the engine being characterized in this dissertation research is a rotary engine, cylinders do not technically exist and the *BMEP* is therefore calculated by:

$$(14) \quad BMEP = nT \left(\frac{2\pi}{D} \right)$$

Where *n* is the number of revolutions per power stroke (in the case of the rotary engine, *n* = 1, in the case of a reciprocating engine, *n* = 1/2), *T* is the output torque, and *D* is the total displacement of the engine. In the case of the O.S. Graupner 49-PI Type Type II 30 Wankel motor, it has the following technical specifications from the user manual at TowerHobbies.com [82]:

Power Output ²	1.1 ps, 1.08 HP or 809 W at 17,000 RPM
Weight	450 g (15.88 oz)
Practical RPM	2,500 – 18,000 RPM
Displacement	4.97 cc
Engine Type	4 Stroke Wankel

Figure 57: O.S. Graupner Engine 4.97 cc performance specifications.

The frontal view of the O.S. Wankel can also be seen in Figure 58:

² Note: ps is the German term for horsepower meaning Pferdestärke.

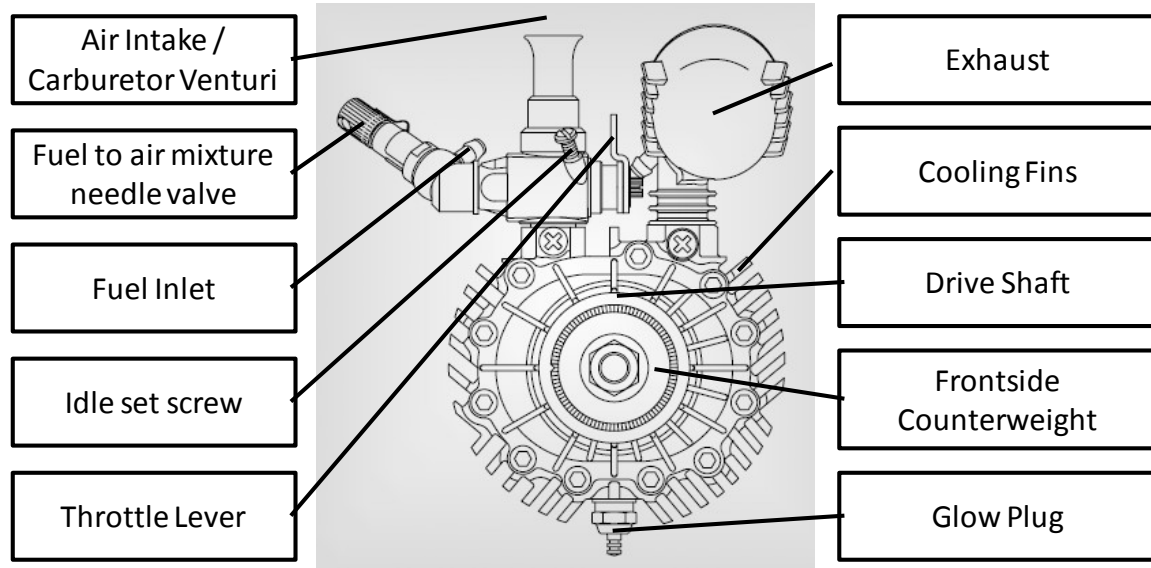


Figure 58: The O.S. Graupner Wankel studied in this dissertation research [85].

Review of Combustion and Fuels

Fuels are simply chemicals composed of basic elements (typically strings of hydrogen and carbon atoms) which have strong chemical bonds that when broken, release energy in the form of heat. Fuels often have variations such as oxygen atoms at various points in their hydrocarbon chains or they form chemical ring structures (like benzene) giving them noticeably different fuel properties. Again, this is where the ΔE enters in engine systems from equation (2).

Key aspects when thinking about fuels and their combustion are turbulence, stoichiometry (lean, stoichiometric or rich), evaporation, droplet sizes, disassociation, premixed or diffusion flame, chemical time, residence time, volatility, octane rating, and energy content. From crude oil, there are four types of fuels that are derived: paraffins, naphthenes, aromatics and asphaltics. The common fuels as ordered by their boiling range are: liquid petroleum gas, butane, petrol, jet fuel, kerosene, fuel oil and diesel fuel.

Specifically regarding petrol, two important features are its volatility and octane rating. Volatility is the natural tendency of a fuel to vaporize. The octane rating is the natural tendency of the fuel to resist knocking (which is auto-ignition during the compression stroke that produces negative work and can damage engines). The octane number of a fuel is derived experimentally and an octane of 0 corresponds to the knock-resistance of Heptane and 100 being set to that of iso-octane. Thus a fuel with 95 octane would be equivalent to a fuel blend between 5 percent Heptane and 95 percent Iso-octane. High-octane rating fuels are typically desired as they permit engines to be designed for higher efficiency as they can resist unwanted pre-ignition in high compression ratio engines. For example:

Compression Ratio	Octane Rating
7.5	85
10	100

Referring back to equations (4) and (5), the higher compression ratio increases the efficiency, which is typically always a desired feature in any engine (but often limited by added manufacturing costs). For some time, iso-octane fuels were “leaded” to improve the octane rating (as it changes the reactions which are typically responsible for knocking) however due to the unwanted health effects of airborne lead, fuels were restricted from future use of lead additives.



A John Madejski Academy quick video lecture on the combustion of fuels [74].

In contrast, Diesel fuel has one distinct property similar to the octane rating but is called its cetane number. The cetane number represents the tendency of a diesel fuel to self ignite. A high cetane number corresponds to a low octane rating.

Alcohols are hydrocarbons that have a double bond with an OH molecule attached somewhere along the HC chain. Alcohols are typically bad cold starters due to their lack of volatility but typically have high octane ratings. The power outputs of alcohol-based fuels tend to increase with rich mixtures, typically demonstrating high cycle efficiency and can also operate with lean mixtures. However, alcohol-based fuels normally have low volatility, low energy density, are miscible with water and have a tendency to pre-ignite. But alcohols also can be derived from renewable sources, which is an important attribute for this research. Because of their pre-ignition tendencies, “hotspots” exposed within an engine can cause unwanted knocking.

However, as will be seen later, rotary engines are naturally immune to these compression problems because of the natural hot-side/cold-side division, in which the compression phase is not located physically near the combustion phase and hot spots (like a in a piston engine as can be seen in Figure 59).

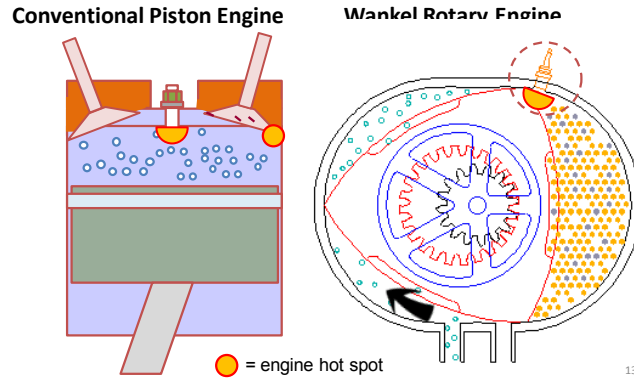
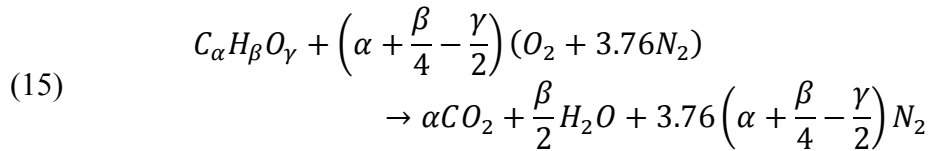


Figure 59: A comparison between the catalytic "hot spots" found in both piston and rotary engines.

Calculating stoichiometry of fuels

Combustion is simply a chemical reaction by which a hydro-carbon fuel reacts with air (in ideal conditions) and results in an energy release and a formation of products. This in general form looks like this:



Where $C_{\alpha}H_{\beta}O_{\gamma}$ represents the fuel and $\left(\alpha + \frac{\beta}{4} - \frac{\gamma}{2}\right)(O_2 + 3.76N_2)$ is the air (which are your reactants) that given a catalyst, react to create the products: CO_2 , H_2O and the non-reactive N_2 component. For ideal stoichiometric reactions, there are no other emissions species. But in reality, there are typically other harmful emissions such as NO_x , CO , and unburned hydrocarbons (UHC). The stoichiometric air-to-fuel ratio (AFR) for the fuels tested in this research have been presented below:

Table 1: Chemical formulas of tested fuels and their stoichiometric air to fuel ratios.

Fuel	Chemical Formula	AFR
Methanol	CH_3OH	6.5
Gasoline (iso-octane)	C_8H_{18}	15.0
Diesel	$C_{12}H_{26}$	14.9
Ethanol	CH_5OH	9.0
JP8	n/a	Approx that of kerosene
Kerosene	$C_{13}H_{28}$	14.9

Most automobile engines are run lean to conserve fuel and to ensure complete combustion (reducing *UHCs* in the emissions). However, this typically leads to higher engine temperatures thereby producing another unwanted exhaust emission, *NO_x*. The engine in this study was always intended to combust any incoming fuel at or near its stoichiometric value. However, given the limitations of the carburetor system, this was not always possible. In fact, this engine runs best on a rich mixture for its preferred methanol-nitromethane fuel as the fuel (which is used as a coolant and lubricant) evaporates, shooting energy and unburnt hydrocarbons out its exhaust, thereby reducing the fuel efficiency significantly.

The autoignition and flash point temperatures for various fuels

Autoignition is a function of pressure, temperature and the various characteristics of the fuel being combusted and its environment. Because the rotary lends itself to being fuel flexible based on its geometry, these curves are interesting because it shows at what pressure and temperature conditions a possible autoignition could occur. Because pressure can be related to the crank angle position and mixture temperature during compression is related to the residence time, it is important to take a deeper dive into this property of the fuel. Figure 60 illustrates these temperatures for a range of common liquid fuels.

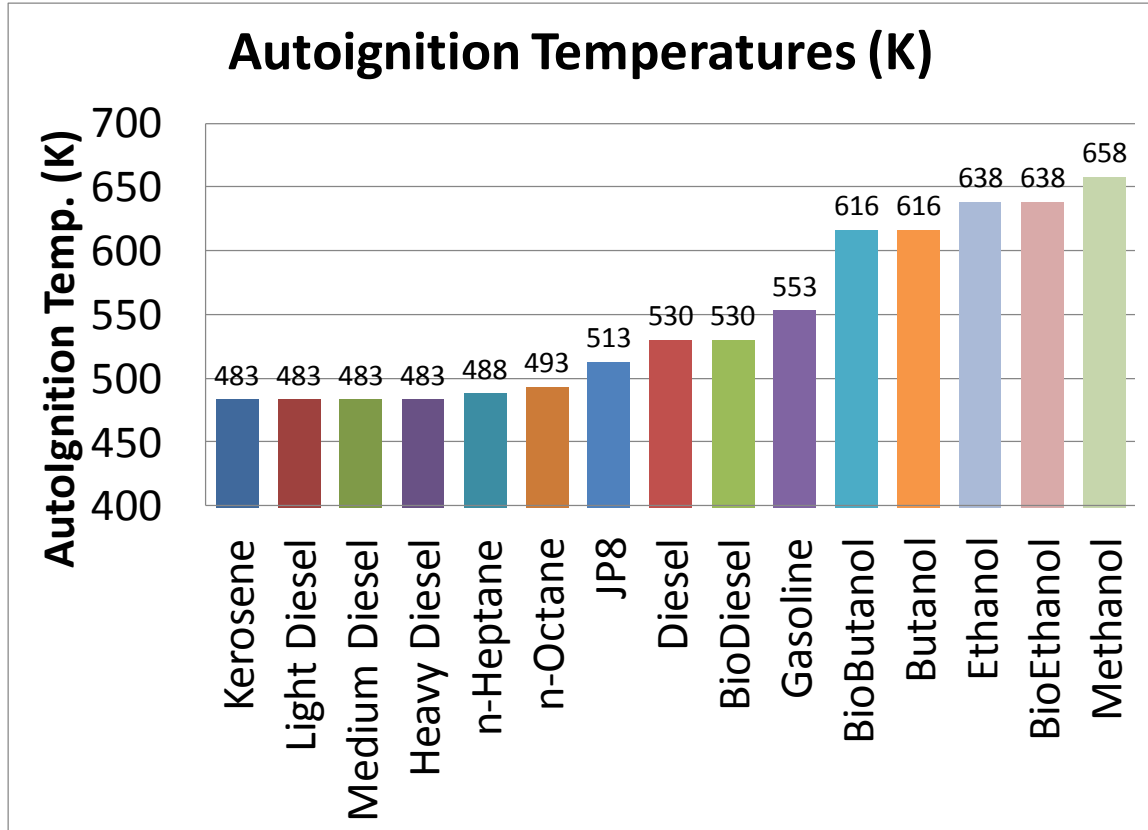


Figure 60: The approximate autoignition temperatures in K for various fuels. Extracted from various sources [87].

Another important property of the fuels used in this research is their flash point temperatures. The flash point temperature is when the fuel naturally begins to vaporize and can potentially combust; assuming the mixture stoichiometry is within the flammability ranges and a reaction catalyst presents itself (i.e. hot spot, spark, flamelet, etc.). Some fuels are highly volatile and vaporize well before STP (standard temperature and pressure). Others are not very volatile and thus, require heating and increased pressure and temperature to be combustible. These two extremes present “safety zones” in that gasoline, for example, with a flash point of $-40\text{ }^{\circ}\text{C}$, is so volatile that when it rests in a fuel container, it fills the tank with vapor making the mixture extremely rich—above the rich flammability limit (RFL). Conversely, diesel fuel has a flash point of $51.7\text{ }^{\circ}\text{C}$ and will not combust at room temperature, even with a lit flame above a pool of diesel fuel. The fuels that present dangerous combinations are the ones that begin to vaporize at temperatures at or near ambient conditions, mixing with air creating a stoichiometric mixture. Armed with this information, not only can the appropriate safety precautions be taken, but strategies on how the engine should react to various fuels become more apparent.

Table 2: The thermal properties of key fuels studied in this research.

Fuel	Chemical Formula	Flash Point (°C)	Autoignition Temperature (°C)
Gasoline (iso-octane)	C_8H_{18}	-12.2	280
Methanol	CH_3OH	11	385
Ethanol	CH_5OH	12.8	365
JP8	n/a	38	240
Kerosene	$C_{13}H_{28}$	38	210
Diesel	$C_{12}H_{26}$	51.7	210

Understanding the Semenov relationship

The Semenov relationship is a way to understand and predict autoignition based on comparing the heat losses of a combustion system to the heat generation due to combustion. This is particularly interesting to fuel-flexibility in rotary engines because the knock tolerance appears to be connected to the fact that the compression takes place on the “cold” side of the rotary engine. The compressed fuel-air mixture is only exposed to the “hot” side of the engine at near top dead center (TDC) and therefore does not combust until the engine is better prepared. In a piston engine, the hot exhaust and intake valves are constantly present during the compression phase and is much more prone to causing pre-mature autoignition or “knocking.” See Figure 59 for a visual.

The equations necessary for deriving the Semenov Relationship are put here for convenience. It is strongly suggested the reader review [87] for a more thorough description.

The rate at which heat is lost (\dot{q}_L) from the system is set equal to the rate at which the heat is generated (\dot{q}_R):

$$(16) \quad \dot{q}_R = \dot{q}_L$$

And as well, the when the rate of heat generation has increased to a point so as not to have the reaction suppressed due to a higher heat loss rate, the slopes of both curves are equal and this represents the T_c that causes autoignition:

$$(17) \quad \frac{\partial \dot{q}_R}{\partial T} = \frac{\partial \dot{q}_L}{\partial T}$$

The rate of heat generation and heat loss can be calculated and substituted into these two prior equations yielding:

$$(18) \quad \tilde{h} \frac{A_s}{V} (T_c - T_\infty) = A_o \left(\frac{P_c}{RT} \right)^{a+b} x_{fuel}^a x_{O_2}^b \exp \left(-\frac{E_a}{R_u T_c} \right) Q_c$$

For the left-hand side, \tilde{h} is the convective heat transfer coefficient of the system or vessel, A_s is its surface area, V is its volume, T_c is the critical temperature at the onset of autoignition, and T_∞ is the environment temperature. For the right hand side, A_o is the pre-exponential constant which is experimentally derived per fuel (similar to the activation energy E_a , reaction orders a and b). P_c is the pressure of the system, R_u is the ideal gas constant, x_f and x_{O_2} are the mole fractions of the fuel and oxidizer, respectively and Q_c is the heat of combustion (specific to the fuel).

This equality can be solved for P with a series of substitutions resulting in the following:

$$(19) \quad P_c = R_u T_c \exp \left(\frac{E_a}{(a+b) R_u T_c} \right) \left(\frac{\frac{h A_s R_u T_c^2}{V E_a}}{Q_c A_o x_f^a x_{O_2}^b} \right)^{1/(a+b)}$$

Using the basic geometric properties of the engine and the fuel properties of the fuels tested, the following critical pressure vs. critical temperature curves can be generated:

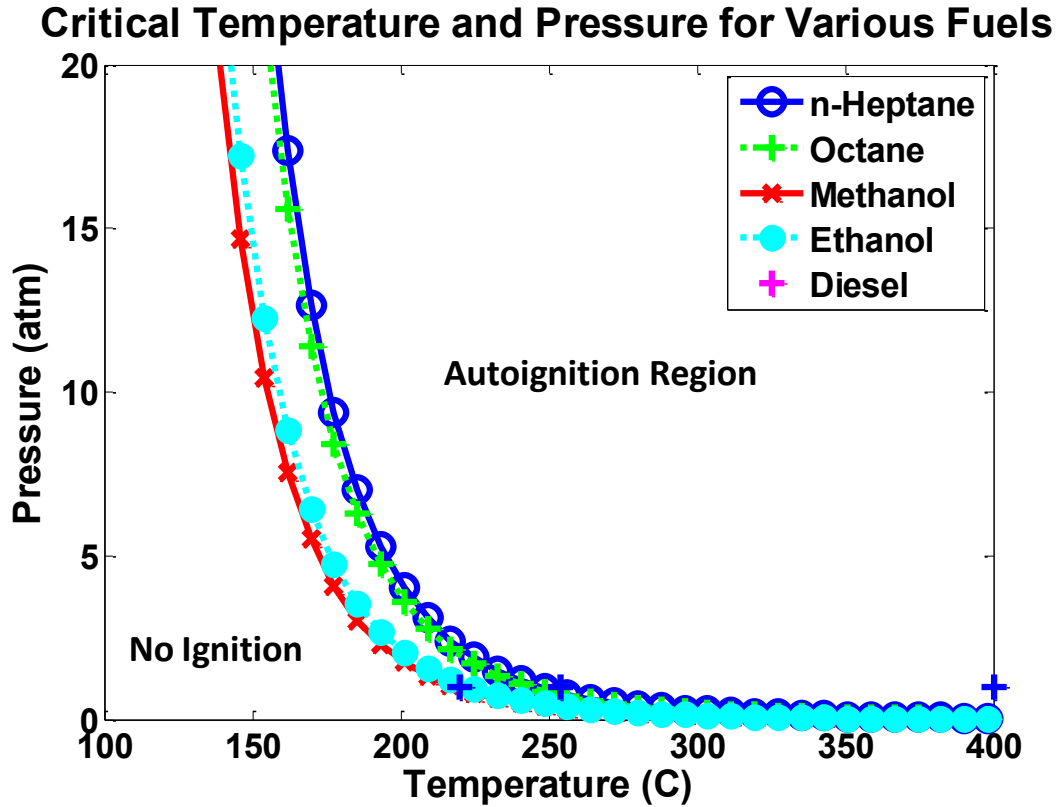


Figure 61: Plots that illustrate the boundary between "no ignition" and "autoignition"

Understanding fluidic flows relevant to combustion

The Reynold's Number is a key parameter upon which many fluidic and thermal relations are based. In the context of the engine, understanding the Reynolds number under various operating conditions helps in characterizing the turbulence (or lack thereof) in the combustion chamber, potential convective heating and cooling rates, etc.

$$(20) \quad Re = \frac{\rho Va}{\mu}$$

where ρ is the density of the gas, V is the tangential velocity of at the surface of the rotor, a is the characteristic dimension, which in this case is chosen to be radial gap height at top dead center and μ is the kinematic viscosity of the gas Figure 62.

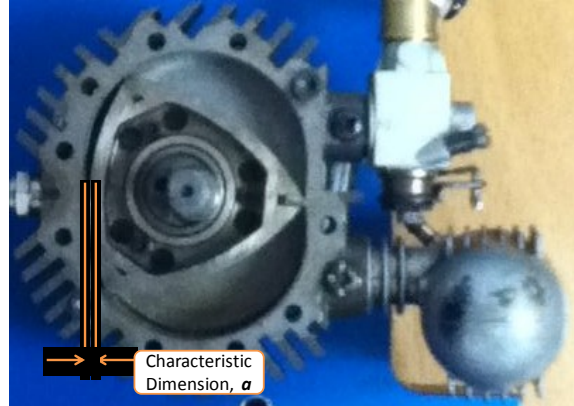


Figure 62: The characteristic dimension a as found in a rotary engine. This dimension could be better observed with a cross-section view as there is a combustion pocket in the triangular rotor surface.

Mixture rates, heat transfer and combustion are all improved by turbulent flow. A good fluids or heat transfer text such as Incropera and Dewitt will provide the correlations and how to use them correctly.

Calculating combustion reaction rate

Calculating the combustion reaction rate helps determine whether or not an engine can complete a combustion reaction given the engine speed and the consequent residence time. Additionally it illustrates how the various engine parameters affect the combustion efficiency and efficacy. The ignition delay is also based on these properties. The right-hand side of equation (19) is one version of this equation but it can also be represented by the concentration of the reactants as well:

$$(21) \quad \dot{q} = A_o [A]^a [B]^b \exp\left(-\frac{E_a}{R_u T}\right)$$

Where $[A]$, and $[B]$ is the concentrations of reactants A and B respectively. The remaining constants are similar to that of equation (19). Calculating \dot{q} yields a rate of fuel consumption and the units of A_o should be carefully assessed (Figure 63).

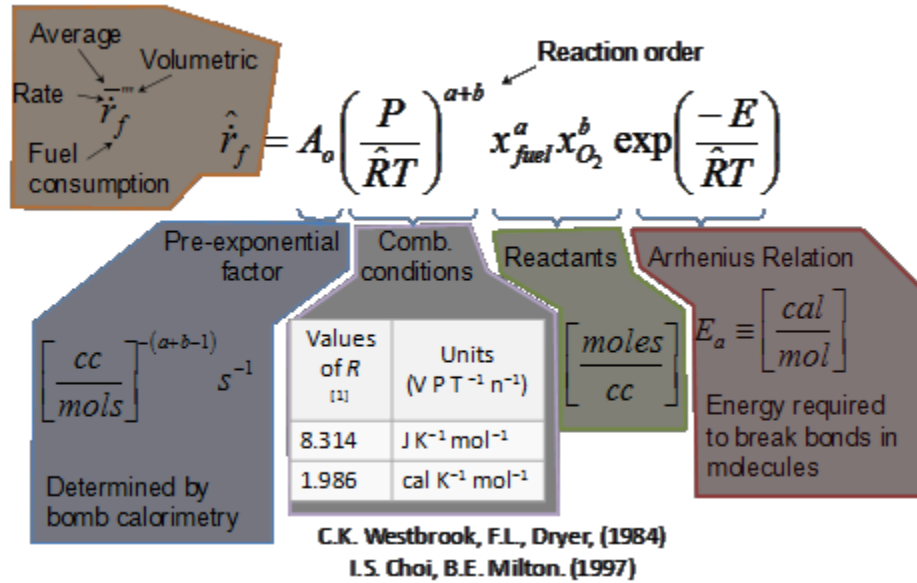


Figure 63: Breaking down the combustion reaction rate based on units and variables.

Continuing to investigate this equation, it can be noted that to better characterize and control fuel flexibility, the various terms which appear in this equation can be manipulated.

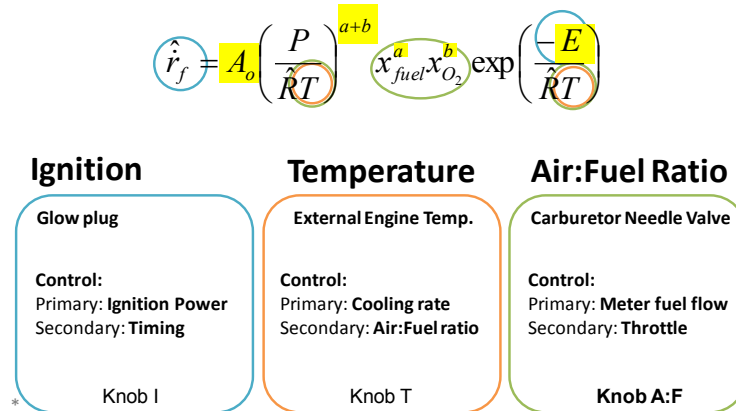


Figure 64: This form of the combustion reaction rate highlights the parameters which can be controlled and which are dependent on fuel type. The term “knob” refers to how the engine might be “dialed in” so as to permit wide-ranging and robust fuel flexibility.

Calculating mechanical power output

These equations are straight forward and basic but important to consider when running dynamometer tests. Output mechanical power in engines is calculated by:

$$(22) \quad P_m = \omega T$$

Where ω is the engine speed and T is the mechanical torque. Typically torque is calculated by the elementary equation:

$$(23) \quad T = Fr$$

Where F is the perpendicular force applied to a moment arm of length r . In the context of this research, a load cell is placed underneath a moment arm that transmits the torque generated by an engine or motor in a dynamometer.

Review of emissions

The basic performance specifications typically measured and monitored during engine characterization include power, efficiency, and fuel consumption, but the emitted species from the exhaust start another extremely important topic in combustion: emissions. Every combustion reaction has reactants and products. Ideally, the reactants and the products would not be harmful for human or environmental consumption. However, depending how a fuel is combusted, the type of fuel that is combusted and other engine operating parameters, the emissions can have a minimal or large impact on the surrounding environment. The plot below illustrates how certain combustion products are formed as a function of the engine stoichiometry. The engine characterized in this research was typically run very rich (in order to cool the engine).

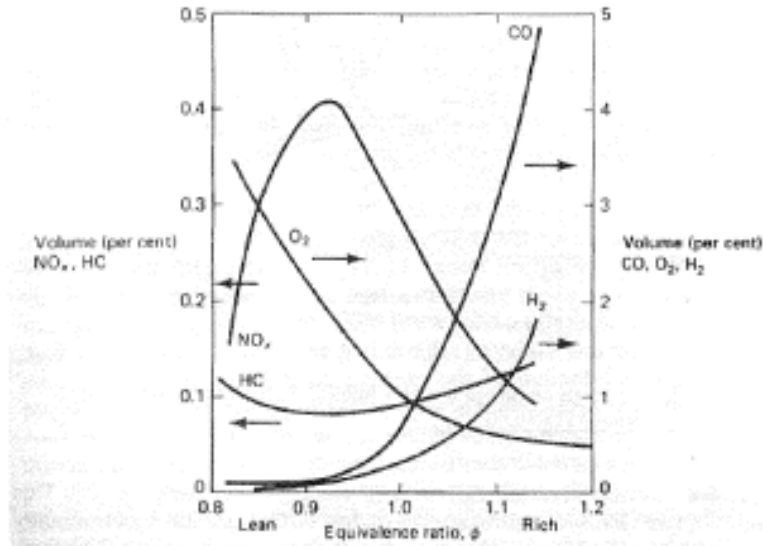


Figure 3.15 Spark ignition engine emissions for different fuel/air ratios (courtesy of Johnson Matthey)

Figure 65: this emissions figure was borrowed from Borman and Ragland [79].

In this dissertation research, emissions were in mind throughout the design phases. However, priority was placed on the fuel flexible range of the Wankel rotary and its output power/efficiency. Emissions are bad in large quantities, however during disaster situations lives are prioritized over minimal toxic exhaust particles. In contrast, for automotive applications one design decision can mean significant amounts of emitted CO_2 to the environment and likely prohibitive if the engine does not meet the strict CAFÉ standards.

With regard to small-scale engine emissions, we would keep an eye on the exhaust to better understand the engine operation. A dark bluish smoke signified that oil was likely being burned as part of the combustion process and white smoke is unburned hydrocarbons. The common species measured and observed in combustion reactions are: H_2O , CO_2 , Unburned HCs, CO , O_2 , NO_x plus others. Each has their own impact on the environment and, as can be seen by the figure, various engine conditions affect the output emissions.

It is also noted that the stock fuel—“glowfuel” which is a combination of methanol and nitromethane—tends to have better emissions properties than that of gasoline. Thus, even though the energy density of methanol is lower than that of gasoline, there is a potential to have improved emissions characteristics with a methanol or methanol-like fuel [90].

Rotary engine theory and design considerations

Basic principles and general considerations³

“Amongst competing hypotheses, the simplest answer tends to be best.”
~Occams Razor

History

Of the many “rotary-type” machines that had been conceptualized and worked on since the late 1500s, it was not until 1954 that Dr. Felix Wankel successfully developed a working rotary engine with the help of NSU in West Germany [83].



Figure 66: Dr. Felix Wankel with an early version of his rotary engine [73].

It was noted by Dr. Wankel that piston engines had several significant shortcomings. Reciprocating motion caused vibration, noise and power loss at high RPM. Additionally, the cranking mechanisms and engine geometry made the engine heavy in comparison to its available power output (low power density). Lastly, the valving mechanism required many parts and was complex. With these issues in mind, he developed a rotary engine.

Basic construction

“Simplicity is the ultimate sophistication.”
~Leonardo da Vinci

The beauty behind the rotary engine was that its construction reduced many of the complexities often found in a piston engine. These elements were merely an artifact of what manufacturing technology was proven at the time. Machining motions of boring, milling and turning—all basically rectilinear and round shapes and actions—drove the development of combustion chambers and pistons. The computer numerically controlled

³ Readers are strongly encouraged to read references [12][13] for in-depth history and technical details for Wankel and rotary engines in general.

(CNC) mills were not yet developed and the natural geometries identified by Dr. Wankel were not readily manufacturable during the early history of the piston development.

However, with fully automated lathes, mills, multiple axes and 3D printing machines, the prospect of cutting these trochoid and peritrochoid shapes has become elementary.

These basic geometries manifest themselves in several key components:

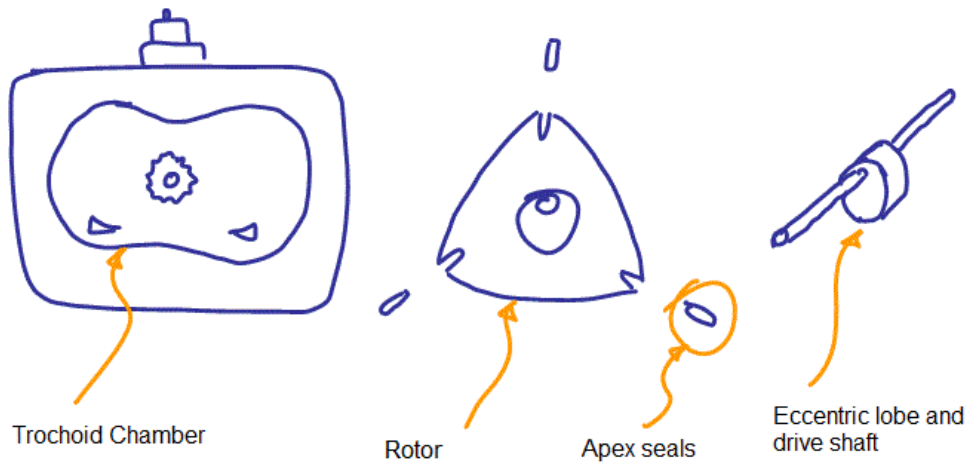


Figure 67: Key rotary engine components and distinct features. Face seals—which are typically inlaid in the flat faces of the rotor and follow the triangular contour of the rotor. These are not shown as smaller-scale rotary engines typically do not include them as they present a larger mechanical loss compared to the compression gain.

The rotor sits within the trochoid chamber and in concert with the involute gear and eccentric shaft, rotates in a planetary gear motion defining three ideally independent combustion chambers. These combustion chambers change geometry as the shaft spins, creating the four cycles of the Otto cycle. However, the key difference with the rotary engine and piston regarding the four-stroke cycle is the fact that for each shaft rotation there is one power stroke, whereas in a piston engine there is only one power stroke per two shaft rotations. Hence the power density advantage of the rotary in comparison with the piston engine.

This is a comparison between a 4-stroke cycle of a rotary engine to that of a piston engine:

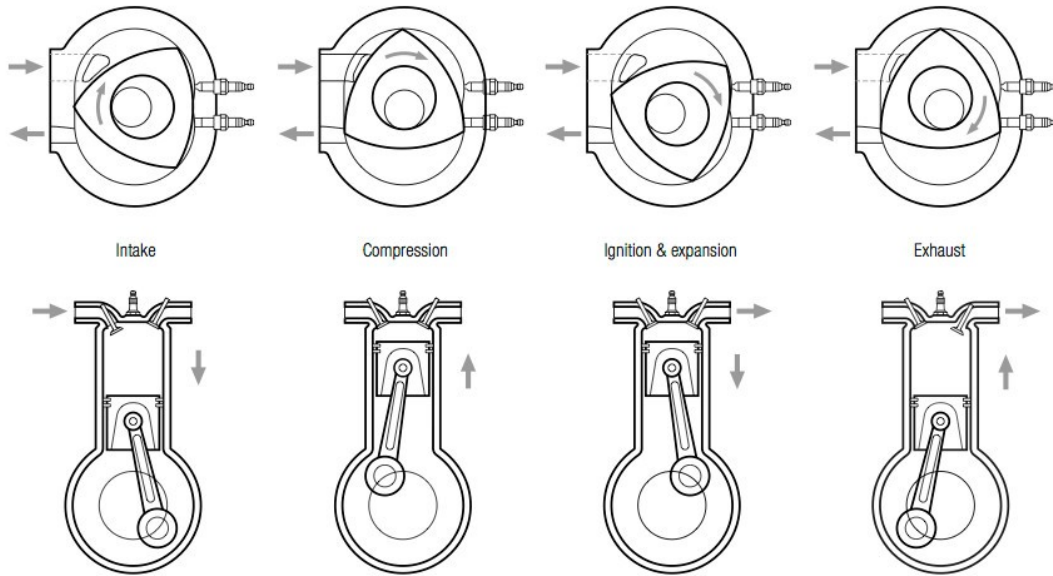


Figure 68: The rotary engine 4-stroke cycle as compared to that of a piston engine. Note that this rotary engine (top) has a side ported intake and a peripheral ported exhaust [86].

Aside from the significant geometry differences of the rotary engine as compared to the piston, the four cycles function the same. The pressure curves with respect to crank angle degree—as can be seen in Yamamoto’s work—show only minor differences as compared to the piston engine. However, the advantage is that there is one power stroke per shaft revolution making the engine very power dense. A piston has only 1 power stroke per two shaft revolutions.



The four-stroke combustion cycle is described in the context of the O.S. Graupner Wankel. (Video).

There were many versions of the rotary engine studied within the scope of the larger MEMS REPS project at UC Berkeley. As seen in Chapter 1, the work of Fu *et. al.* made micro-scale mini engines and Swanger, Sprague and Park *et. al.* all worked on new mini scale engines (Figure 69 and Figure 70).

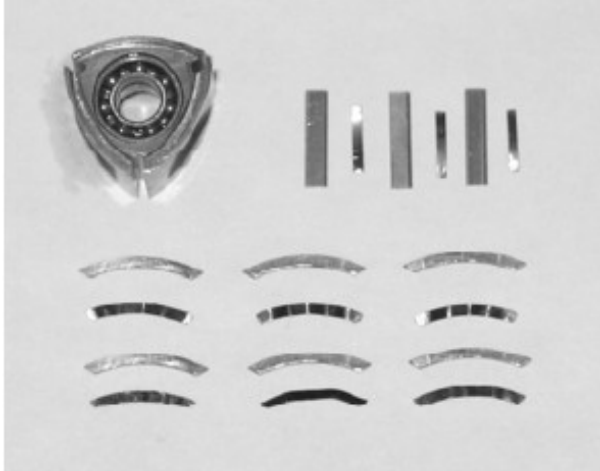


Figure 69: This is an early generation, U.C. Berkeley designed, Wankel rotary engine along with its seals and requisite springs [89]. Due to the significant challenges at obtaining a functioning rotary engine at such small scales, engines were slowly made bigger until a working engine was obtained.

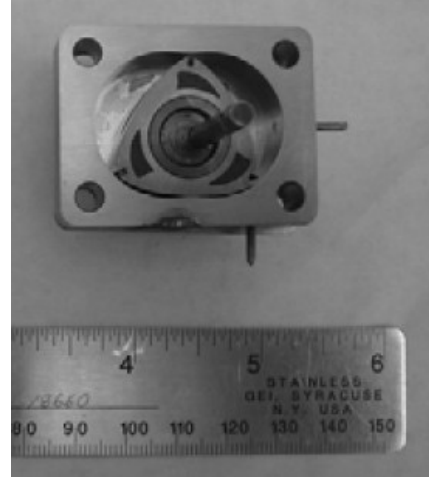


Figure 70: Trochoid housing, rotor, and crankshaft with eccentric lobe. This was the 1500 mm² rotary developed at UC Berkeley which eventually produced about 30 W of an assisted power [89].

The Wankel engine studied in this dissertation research (O.S. Graupner Engine PI 49) was only slightly larger at 4.97 ccs. The figure below shows some dimensions that were being measured during an engine inspection:



Figure 71: The small-scale O.S. Graupner Wankel engine with an engine displacement of 4.97 ccs. Hand model credit goes to Dr. Debbie Senesky.

The rotary engine, like a piston engine, functions on a four-stroke cycle. Therefore all the similar engine peripherals are still needed for rotary engines: throttle, fuel delivery, ignition, cooling, exhaust, emissions and other common components.

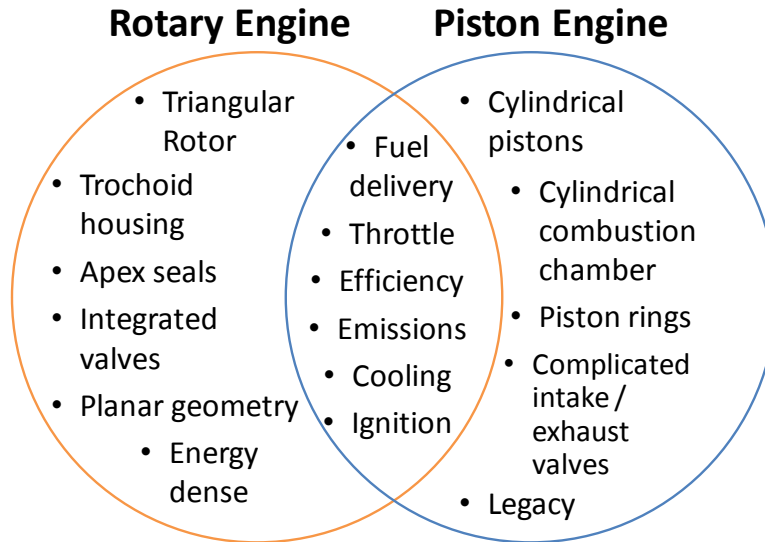


Figure 72: Ven diagram of unique and shared engine components between the Wankel Rotary and the Piston Engines.

From the basic to advanced development that has been introduced thus far, there are several key aspects to understanding the Wankel Rotary Engine and its opportunities and limitations from a technical standpoint. At the end this chapter lists additional media resources on the Rotary Engine as the simplicity of its operation is not well conveyed in words and pictures printed out in 2D.

Key advantages

“Any sufficiently advanced technology is indistinguishable from magic.”
 ~Arthur C. Clark

Let’s begin by starting with the macro-scale—consumer view—of the rotary engine. This revolutionary engine is often sought out by sports car enthusiasts for its high power to weight ratio, its smoothly balanced engine and the low center of gravity offered by a compact engine (Mazda’s RX series made the Wankel Engine commonly known to enthusiasts and engineers—although the mystery of its operation still keep many wrench monkeys at a safe distance). Additionally, Kenichi Yamamoto—the author of one of the rotary engine design “bibles”—offers the following key benefits to the Wankel Rotary Engine:

1. Power Density / Power to Weight ratios
2. Balanced Design. Rotary vs. reciprocating (smooth). Over rev capability. (pg. 8 Yamamoto)
3. Compactness / Planar design
4. Novel valving mechanism
5. Volumetric Efficiency at high speed

These are the benefits of the engine on a larger scale which have been “attractive enough” to gather the requisite attention and development of the modern automotive industry, but unfortunately not enough to make substantial developments on rotary engine technology.

However, as the target customer changes and the engine is scaled down, the features of the Wankel Rotary engine become more attractive to its piston counterpart and additional unique characteristics became even more interesting. For example, as machined parts reach sizes smaller than centimeters, costs start to rise. Therefore, the prospect of machining mini-scale valves, cam rods, and other complicated engine parts (as found in piston engines) make cost a prohibitive factor. However, the inherent features of rotary engines—such as integrated valving and planar structures—help alleviate manufacturing challenges on this scale.

As Haendler *et al.* at U.C. Berkeley stated in a 2004 article about the “technological arguments for micro-engines,” there are nine key components that make rotary engines attractive for mini- and micro- scale development. These nine key benefits can easily be remembered using the mnemonic: *MrLeafSir*.

1. **M**anufacturability
2. **R**educed complexity
3. **L**ow-cost materials
4. **E**nergy density
5. **A**ccessibility
6. **F**uel flexibility
7. **S**elf valving
8. **I**ntegration of MEMS devices
9. **R**echargeability

Manufacturability

The key attraction with regard to manufacturing rotary engines is its planar nature. Not only can new designs and shapes be quickly iterated, designed and then cut from planar sheets of material, assembly also becomes more one-dimensional and allows

for very slim form factors. Even more exciting was the thought to attempt and fabricate a MEMS rotary engine using the widely used batch microfabrication processes commonly used to make Intel Pentium chips and other integrated circuits.

Batch microfabrication is like a high-tech baking process where a plate of silicon material (known as a wafer) is modified by adding or subtracting materials in bulk using various depositing and etching processes. For ICs, this includes activities like adding insulating layers to prevent conductivity, doping to create semiconductor junctions, and metallization for electrical conduits. Layer by layer, electrical elements were defined in 2D and extracted or extruded to create the third physical dimension, thereby creating electrical devices. But could it be used to make other structures?

Thanks to the curiosity and creativity of researchers seeking to make this possible, both researchers and lab technicians tweaked the semiconductor process to create a new industry of devices known as MEMS (microelectromechanical systems). Primarily used in sensing devices, MEMS are commonly found in airbag sensors, mobile phone accelerometers, inkjet printer heads and low-cost pressure transducers. In the early 2000s, U.C. Berkeley researchers identified the manufacturing similarities between rotary engines and MEMS devices, and attempted to create a functioning MEMS rotary engine (this project was known as MEMS REPS: MEMS Rotary Engine Power Systems).

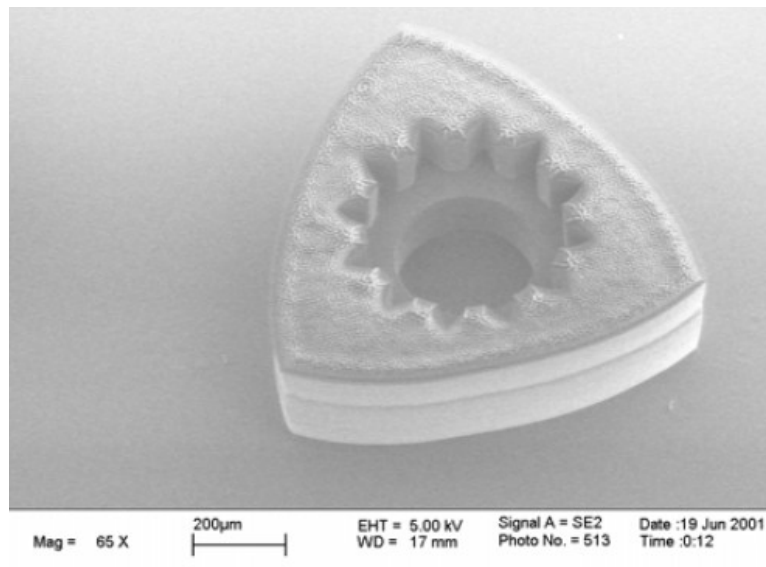


Figure 73: Cited from Fu, et. al in his design and characterization of microfabricated rotary engines.

Additionally, with the advancement of 3D printing systems, newer geometries and engine components—which were, until now, impossible to machine or manufacture in

standard methods—could be utilized in various aspects of the engine. For example, integrated springs into apex seals could be 3D printed out of titanium, which have high fatigue strength (strength to weight ratios and resistance to oxidation).

Reduced Complexity

Although many might argue the geometries of the rotary engine are complex, the simplicity and beauty of its operation and reduced components significantly reduce the complexity of the engine. Crankshafts, pistons, piston rings, valves, cams and more are the array of parts which are typically machined, molded, stamped, casted and which are assembled to form a piston engine. However, a rotary engine has many of these components are—due to geometry—built in to the engine yielding fewer key components.

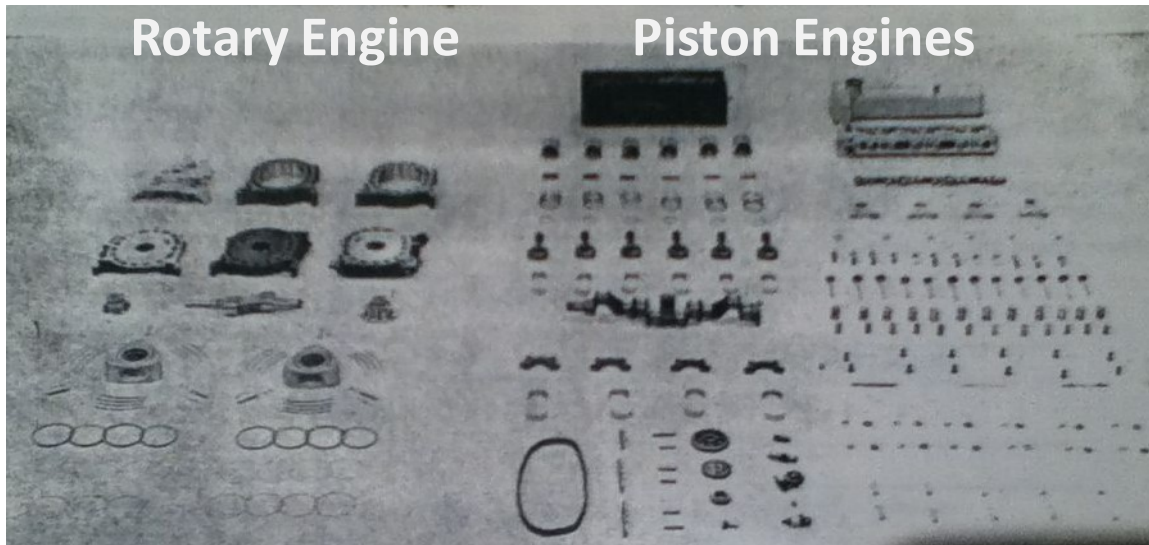


Figure 74: Cited from Yamamoto, the image compares the number of parts required for a rotary engine (left) and a piston engine of equivalent power output (right) [83].

Low-cost Materials

If the rotary engine can be fabricated both from metals such as steel and aluminum, it remains on par with piston engines. However, the ability to fabricate rotary engines into semiconductor materials such as silicon makes the cost of materials per engine low. As mentioned earlier, batch fabrication dramatically reduces cost as well if in fact rotary engines can be manufactured in this method.

Energy Density

The rotary engine maintains a high energy density by using liquid hydrocarbon fuels and a high power density with one power stroke per shaft revolution (compared to 1 power stroke per 2 shaft rotations in a piston engine). This is why many consumers in the 1970s thought they could buy a 1.8 L Mazda rotary vehicle and be buying an extremely “efficient” because they associated small displacement with low power. For the rotary, this displacement is sufficient to produce more than 200 horsepower.

Accessibility

The accessibility of rotary engines has again improved due to manufacturing technology, the desire to test new engine concepts and better understanding of engine design. Additionally, the fuel flexible nature of the rotary engine allows it to utilize more fuels and provide power in many more regions of the world.

Fuel Flexibility

The key feature being explored in this dissertation—fuel flexibility represents an opportunity to provide new access to energy that would otherwise, be inaccessible during disaster situations or in remote parts of the world. Fuel flexible engines—as a transitional solution—may also promote the production and consequent sale of biofuels as these engines can extract power from any number of liquid hydrocarbons.

Self Valving

The peanut-shaped trochoid housing coupled with the triangular geometry of the rotor, allows the engine to be self valving. As the rotor spins, it creates moving combustion chambers which pass by fuel-air intake and exhaust ports, creating the valving normally achieved in piston engines by the cam-rod-timing systems.

Integration of MEMS

As seen in Chapter 1, many researchers such as Fu and Knobloch attempted to make rotary engines work on the micron scale. While this work has transitioned to the mini-scale, MEMS sensor researchers continue to develop harsh-environment sensors to better measure the combustion processes found in engines. The Wankel engine studied in

this research served as a low-cost platform for harsh-environment MEMS sensing and testing.

Recharging

In 2012, people everywhere are familiar with the annoyance of charging mobile phones, computers and other portable electronics. Waiting for a full charge is not only annoying but requires a lot of time. Fuels simply need be placed in the tank and properly introduced to the engine and output power is maintained.

Chapter 2 Summary

Some of the basic theoretical tools related to combustion, engine performance and rotary engine construction were presented. Specifically, the science revolving around combustion in small chambers, with varying fuels and in rotary engines is presented and used to motivate the design decisions that are presented in the following chapter. It is advised to any reader who wants to better understand combustion physics, turn to one or more of the following texts: [76-78,84]. If the reader is specifically interested in taking a deep dive in to rotary engines, the following texts are essential: [80,81].

References

- [69] N. Dhillon, C. Hogue, “MLHP – a high heat flux localized cooling technology for electronic substrates.” Proc. of IMECE 2008. 2-6 Nov. Boston, MA.
- [70] “Engine-cylinder deactivation saves fuel.”
<http://www.jdpower.com/content/detail.htm?jdpaArticleId=925> Published 2/24/2012. Accessed on 3 May 2012.
- [71] Leone, T. and Pozar, M., "Fuel Economy Benefit of Cylinder Deactivation - Sensitivity to Vehicle Application and Operating Constraints," SAE Technical Paper 2001-01-3591, 2001, doi:10.4271/2001-01-3591.
- [72] The 2012 Toyota Prius. <http://www.fueleconomy.gov/feg/noframes/31836.shtml> Accessed on: 3 May 2012.
- [73] Yang, J., Culp, T., and Kenney, T., "Development of a Gasoline Engine System Using HCCI Technology - The Concept and the Test Results," SAE Technical Paper 2002-01-2832, 2002, doi:10.4271/2002-01-2832.
- [74] The QR Code Generator. <http://qrcode.kaywa.com/> accessed on 7 Dec 2012.
- [75] Aigner, F. Press Release. “3D-Printer with nano-precision,”
http://www.tuwien.ac.at/en/news/news_detail/article/7444/ accessed on 3 May 2012.
- [76] Bozicevic, Z., “Nanotechnology: Laser printers create grain of sand-size 3D cars, bridges in minutes.” <http://news.nationalpost.com/2012/03/30/nano-technology->

- laser-printers-create-grain-of-sand-size-3d-cars-bridges-in-minutes/ Accessed on 30 Mar 2012.
- [77] Wijesundara, M., Walther, D.C., Stold, C., Fu, K., Gao, D., Carraro, C., Pisano, A.P., and Maboudian, R., “Low temperature CVD SiC coated Si microcomponents for reduced scale engines.” ASME IMECE 2003, 15-21 November, Washington D.C.
- [78] Cardes, A.C., McCoy, C.D., K. Inaoka, D.C. Walther, A.P. Pisano and C. Fernandes-Pello, “Characterization of fuel flexibility in 4.97cc rotary engines,” MCS, Libson, October 6-10 2005.
- [79] Borman, G.L. and Ragland, K.W. (1998) Combustion Engineering, McGraw-Hill, Boston, MA.
- [80] Stone, R., Ball, J. (2004): Automotive engineering fundamentals. SAE International, 2004.
- [81] Taylor, C. (1985) The Internal Combustion Engine in Theory and Practice: Vol. 1 – 2nd ed, Revised: Thermodynamics, Fluid Flow, Performance. MIT press, Boston MA.
- [82] Tower Hobbies, “O.S. 49-PI Type II 30 Wankel Rotary” www3.towerhobbies.com/cgi-bin/wti0001p?&l=LXPVE3&P=7 accessed on 7 May 2012.
- [83] Yamamoto, K., “Rotary Engine”, Sankaido Co. Ltd., 1st Ed.
- [84] Ansdale, R.F. (1968) The Wankel RC Engine, Iliffe, London.
- [85] O.S. Engine, Rotary Engine 49-PI Type II, “Instruction Manual” (2006).
- [86] “Comparison of the 4 stroke cycle in a Wankel engine and a reciprocating engine” <http://www.autoevolution.com/news-image/how-wankels-rotary-engine-works-19241-3.html> Accessed on 9 Dec. 2012
- [87] S. McAllister, J-Y. Chen, A.C. Fernandez-Pello, Fundamentals of Combustion Processes. Mechanical Engineering Series. Springer, NY, 2011.
- [88] Image of Dr. Felix Wankel. Site Accessed on 17 Jan 2011: <http://www.chiangmai-mail.com/236/auto.shtml>
- [89] Sprague, S.B., Park, S-W., Walther, D.C., Pisano, A.P. and Fernandez-Pello A.C. (2007) ‘Development and characterisation of small-scale rotary engines’, Int. J. Alternative Propulsion, Vol. 1, No. 2/3, pp.275–293.
- [90] McCoy, G.A., J. Kerstetter, and J.K. Lyons, “Alcohol-fueled Vehicles,” WSEO (1992).
- [91] Piemont, S. WIPO Patent: “device for identifying hydrocarbon fluids.” <http://www.wipo.int/patentscope/search/en/WO1996015064> Accessed on: 10 May 2012

Chapter 3 – Experimental Setup Design

“There is no subject, however simple or complex, which—if studied with patience and intelligence—will not become more complex.” ~anonymous

Introduction

With a sound grasp on the theory and modeling of rotary engines and their fuel flexible potential, the next step is to empirically validate the results with real data. However the challenge in this research is that conventional tools to measure common engine parameters, such as: power output, engine speed, load, torque, temperatures and emissions to name a few, are not readily available. Therefore a dynamometer and its requisite peripherals were designed and built so the performance could be accurately measured and the engine could be characterized.

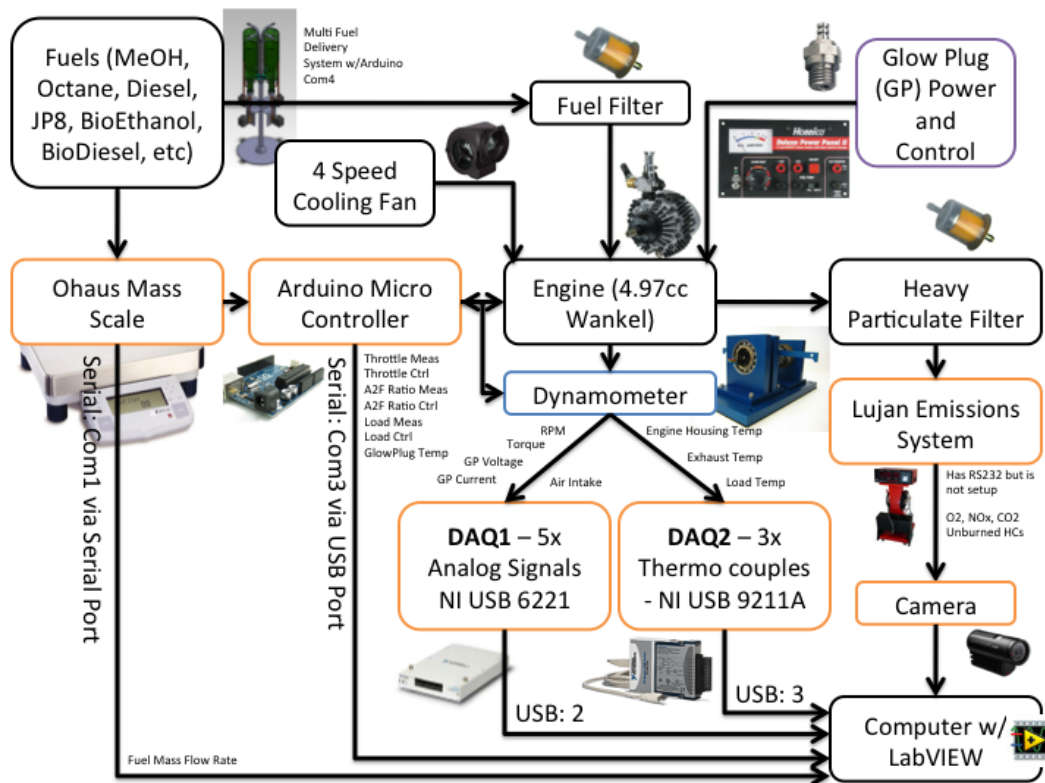


Figure 75: The overall schematic of the fuel-flexible engine dynamometer and characterization system. The system includes fuel-flexible fuel delivery, measurement and control of all key engine parameters and data collection.

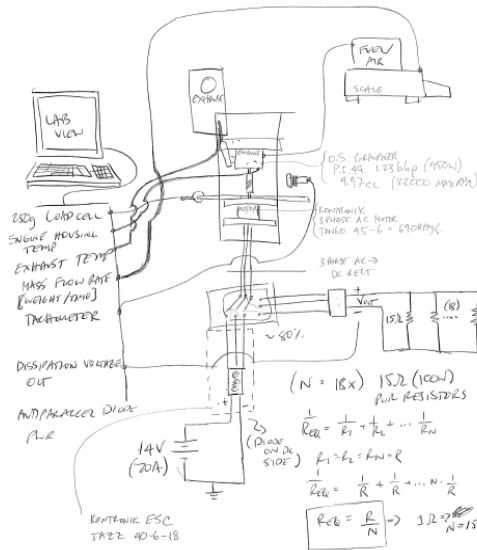


Figure 76: Early stages of the fuel flexible testing and control system.

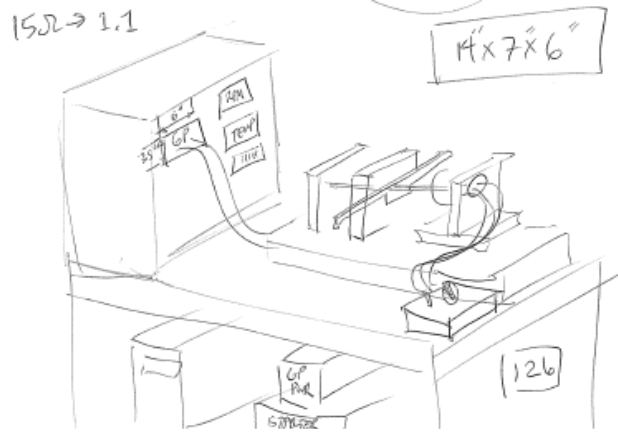


Figure 77: overall test bench located in 44 Hesse Hall, UC Berkeley, California.

In addition to the dynamometer design, other subsystems were needed to control the motor, the input fuel and the data acquisition. The design and construction of these systems were new and necessary for developing a characterized and functional fuel flexible engine. For example, a fuel switching system was necessary in order to achieve accurate control and delivery of combustible fuels.

Prior to beginning the research, it was unclear whether or not the engine would need a starter fuel or additives and in what order fuels would need to be combusted to maintain power output. Thus, having a quick-switching and reliable system to quickly change fuels would be essential. Therefore a computer controlled system, capable of selecting and blending up to 8 fuels, was constructed.

Therefore, in this chapter we describe the process of designing:

- A small-scale, fuel flexible engine dynamometer (FFED)
- The sensors required for extending fuel flexibility
- The software developed to read those sensors and
- The actuators implemented to control the engine conditions based on those measured signals
- A multi-fuel switching system (MFSS)

Resources for engine testing

During the course of this multi-disciplinary research, it was discovered that this engine research could be better conducted in a different university—specifically the Universidad Politécnica de Madrid—because of their engine testing resources and the

vast theoretical knowledge of combustion models. The following photo (Figure 78) shows the test bank in a laboratory in Madrid, Spain. The testing system was positioned in a full-scale engine testing lab next to two full-size automobile engines. Initial research started at U.C. Berkeley and in 2010, moved to Madrid, Spain with the help of a Fulbright Research grant.



Figure 78: The fuel-flexible rotary engine testing setup at the Escuela Técnica Superior de los Ingenieros Aeronáuticos (E.T.S.I.A.), an aeronautical engineering school that is part of the larger polytechnic university (la U.P.M.) in Madrid, Spain. With a larger engine lab and more equipment available for the characterization of engines, the dynamometer characterization system was set up and modified to continue testing in this university. The primary modifications and tools used were the mechanical loading system, fuel switching system and the emissions measurement equipment.

Additionally, several other systems were necessary to measure and enable fuel-flexibility: the fuel consumption rate, the fuel and air mass/air flow rates, glow plug temperature control and dashboards to display important engine information.

Integrating all these various devices and making them work together was a significant part of this research challenge. While these systems have been developed to some degree in larger scale engine systems, due to the millimeter-scale nature of this research, many of these measurement and control systems needed to be developed from

scratch or from legacy setups. Nothing was commercially available at the time and thus created one of the many challenges—and opportunities—of the research.

A fuel flexible engine dynamometer (FFED)

Dynamometer basics

The *dynamometer* is a common tool for measuring the performance of many types of vehicles and other “shaft-driven” power systems.

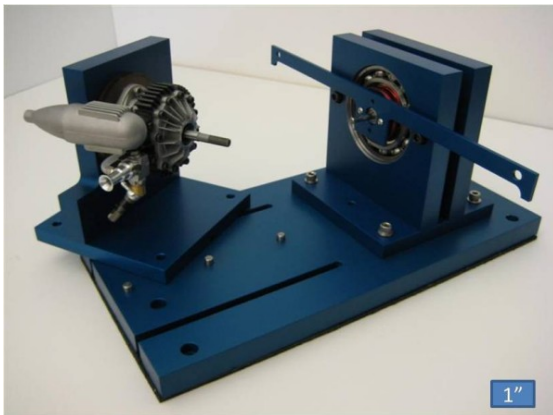


Figure 79: First revision of the UC Berkeley small engine dynamometer.

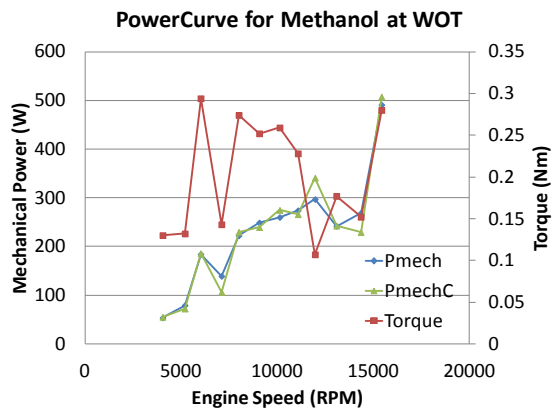


Figure 80: An example of mechanical power output curves of a small scale rotary engine.

There are various types of dynamometers used today that typically include the following basic components:

1. **Mechanical Coupling** - a connection to a driveshaft or the external output to power (i.e. wheels of a motorcycle, for example).
2. **Power Measurement** - A way to measure engine properties, primarily torque and RPM (to measure power), but other measurements are commonly taken (such as: air intake, exhaust output, engine temperature, ambient conditions, etc.).
3. **Engine Loading** - A way to load the engine (so as to simulate acceleration or a sustaining motion against drag).

With a mechanical coupling, power measurement and an engine loading element, a machine would have the key features of a dynamometer. However, the devil is in the details, especially when the details scale down in size.

One particularly common dynamometer is the “Water-brake” dynamometer and is used in many automotive applications. The car or motorcycle is mounted to a stage with the wheels being placed atop a big drum, which spins along with the wheels of the

vehicle. The exhaust is recorded using an emissions probe, the computers electronic control module (ECM) is accessed using a standard interface read by the dynamometer CPU (to record RPM, fuel injection properties, oxygen levels, etc.), fans are blown on the engine so as to simulate vehicle speed and then the engine is loaded. “Loading” refers to the resistance to rotational motion of the wheels and is of interest to performance enthusiasts because some vehicles’ performance properties vary with load (power, torque, emissions, etc.). A real world “load” would be a car traveling up a grade, an extremely fast acceleration or towing a heavy boat. This is why a semi-tractor trailer has a lot of power and is geared to have high torque but low top speed. And on the opposite end of the spectrum, a light-weight Honda Civic may have low power, but can achieve fast acceleration and higher top speed due to gearing. However it is highly unadvised to tow anything with this sort of vehicle.

To have appropriate loading, the dynamometer system needs to be able to dissipate the power produced by the vehicle in a safe and controllable manner. A designer needs to ensure that performance specs can be measured without having a vehicle become decoupled from the dynamometer, potentially threatening the lives of the operators. Thus, various loading systems were reviewed and the safest, lowest cost and simplest to design was selected. There are electronic loading elements (high-power resistors, rheostats and other resistive load solutions) and mechanical loading elements (water brake and mechanical brake).

For the electrical loading systems, the resistive braking, rheostat and conventional high power dissipation devices were considered. Ultimately, a three-phase, AC motor was selected that connected to a bank of high power, low resistance resistors for the first design iteration. This was perceived as the cleanest and most robust option at the time (leveraging know-how and experience from prior research endeavors).

For the mechanical systems, the water brake concept is most widely used. Water is added inside the drum upon which the test vehicle sits. As the drum spins and water is added, energy is absorbed by the water due to the rotational acceleration of the water. Water has a high density, is safe, can be added and drained controllably, and therefore presents an elegant solution. For the small-scale requirements of this research, a different method was needed to fit within design constraints.

A mechanical brake dynamometer is intuitively simple and has its pros and cons. The pros are that the mechanical forces of a brake and stopping mechanism used can be quickly assessed to know whether or not its braking forces can fully load the engine. (As will be seen, the electrical dynamometer theoretically had sufficient braking power, however failed to even partially load the engine.) The other pro is there are mechanical brakes easily available. The main con to a mechanical brake is the reduced precision in the applied load. Ideally you would like to have a precise way to characterize your

loading on the engine (especially as it changes over time), however the only measurement here is the servo position. See the following table for other pros and cons for various dynamometer types (Table 3).

Table 3: Essential user needs for dynamometers and relevant commentary.

User needs	Comments
<ul style="list-style-type: none"> ▪ A system that could measure mechanical power: where T is torque in and ω is engine speed in RPM. $P_m = T\omega$ ▪ A system that can measure the temperature properties of the engine. Specifically housing temperature, intake temperature and exhaust temperature. ▪ A system that can fully load an engine to stall or let it run freely. ▪ A system that can easily be dismantled and reassembled to test engines repeatedly and rapidly. ▪ A system that is adjustable and flexible for future experimental needs and unforeseen issues. 	<ul style="list-style-type: none"> ▪ Engine speed is relatively easy to measure using a shaft counter system (see APPENDIX C). ▪ Measuring mechanical torque is slightly more difficult because it requires the loading element to be “floating”— such that when the engine is loaded, the braking element can rotate, applying a force to a load cell to measure force applied. Therefore the applied force (F) multiplied by the moment arm (r) yields the torque, T. Long moment arms were observed to cause vibrational issues and noise in the measurements ▪ Loading can prove difficult and costly ▪ Design for manufacturing and assembly should both be considered.

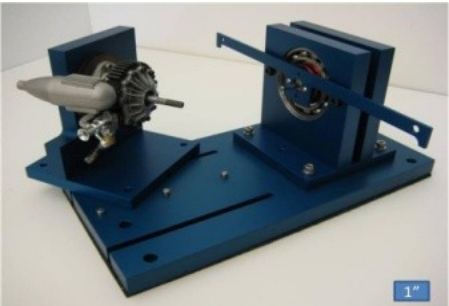
Clean sheet dynamometer design process and relevant challenges

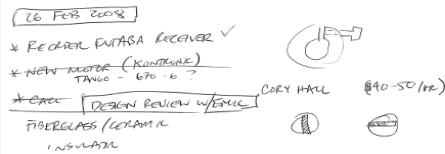
Leveraging prior work from other researchers, a combined system of an electric motor to both start and load the engine was first used. However, the same legacy system could not be used as it was designed to dissipate less than 10 percent of the power produced by the O.S. Graupner Wankel being tested. Additionally, the research by Cardes *et al.* utilized a larger motor however the resistive loading system utilized failed to fully load the engine and thus only a percentage of the total power was measured. Lastly, this design also suffered from excessive heat generation and the inability to change loading conditions on the fly. These were two problems the current research attempted to resolve.

“Leveraging the wisdom of a crowd” - design reviews

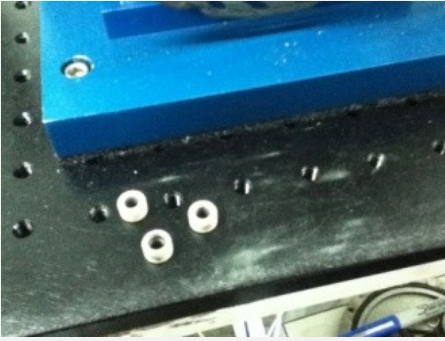
Design reviews helped tremendously formulate and optimize the design in addition to fostering the collaborative spirit of design. Considering the possibilities and limitations to this design, many people offered their feedback on an initial design. The comments were all primarily practical considerations that come from prior experience with similar systems or design in general.

Table 4: Design review sketches, commentary and reflections.

Sketches, commentary & photos	Post design review reflections
<p data-bbox="243 665 682 924">- NICKEL PLATING - MATERIAL / MACHINING RECOMMENDATIONS FROM PAST PISASD * ANTI SEIZE COMPOUND FOR BOLTS ALUMINUM * ADD HOLES TO TORQUE ARMS MOY COAT ~ SPACE PUL W/BE STEEL BOLT INTO ALUMINUM HEAD. TEFLON TAPE.</p> 	<p data-bbox="727 783 1372 1035">Nickel plating was suggested to improve durability, enhance corrosion protection of the dynamometer, but instead, a more common, low cost anodized solution was used which in addition to providing similar benefits, also reduced electrically conductive surfaces, maintained dimension precision and allowed for color change.</p> <p data-bbox="727 1077 1344 1182">Access holes were added to the torque arms and were conveniently utilized to balance out the loading mechanisms.</p>

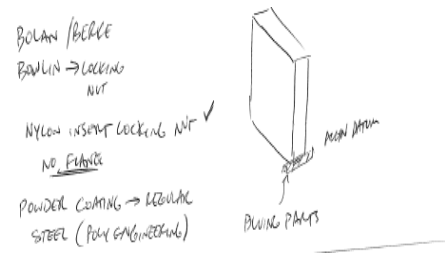


With regard to engine temperatures and isolating the engine (to enhance characterization), it was suggested to use ceramic insulators so that thermal conduction to the dynamometer was reduced.

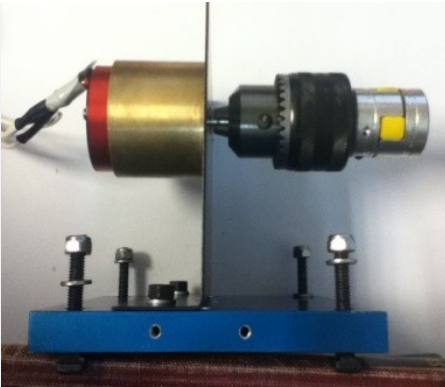


However, the ceramic standoffs used were brittle and did not withstand the repeated testing. The next solution was to use a slab of high-temperature and chemical resistant Delrin plastic as an insulator. However, extreme temperatures produced by the engine caused unacceptable melting and deformation.

Ultimately, a rubber pad with a high durometer rating and nuts as spacers was used instead.

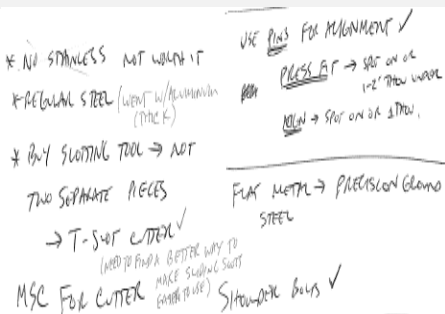


The following comments for locking nuts in the dynamometer proved important. The vibrations caused by the engine rattled many bolts loose regularly stopping experiments. Thus a combination of locking nuts (commonly found on skateboards and other vibration prone environments) and the use of thread locking cement were used. Locking wingnuts would also have been a good selection.



Powder coating was discussed to prolong the wear life, but again, in light of the advantages of anodization and maintaining the precision dimensions of the dynamometer, this process was not chosen.

No significant corrosion or damage to the dynamometer was ever observed during the over two years of extensive use. Some slight discoloration but that was the extent.



Pins, instead of shoulder bolts, were used to precision align the various components to the dynamometer. Pins were permanently press fit in the baseplate and the engine and electrical motor stands had snug fits such that they remained precision aligned.

16 APRIL 2008

GABRIELE'S TR FEEDBACK:

- * DON'T USE TORQUE ARM ON LOAD CELL, RATHER IMPLEMENT STRAIN SENSORS
- * JUST USE A FLEXIBLE ELEMENT.
- * NEXT TIME, MAKE LOAD CELL PART OF THE APPARATUS
- * MAKE ROUNDED TIPS ON TORQUE ARM



Although several of these recommendations were not implemented, in hindsight, the strain sensors may have been a much more cost effective and novel means of measuring torque. There may have been nonlinearity in this solution but considering the noise issues and load cell limitations encountered, a backup means of measuring torque would have been beneficial.

As well, the rounded point suggestion for the torque arm was implemented but in reverse. A sharp “point” was placed on the load cell itself such that an infinitesimally small point of contact was achieved (reducing noise and other measurement errors).

Design features of small-scale engine dynamometer

Design of the basic dynamometer structures

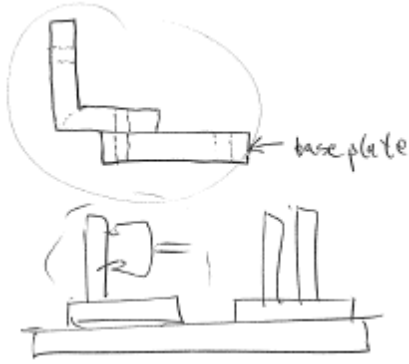


Figure 81: The general structure would have two elements: a engine mount and a dynamometer brake.

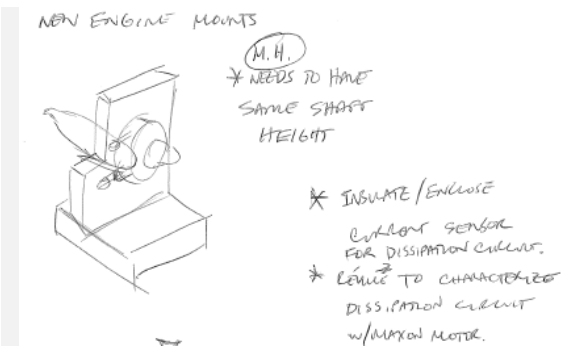
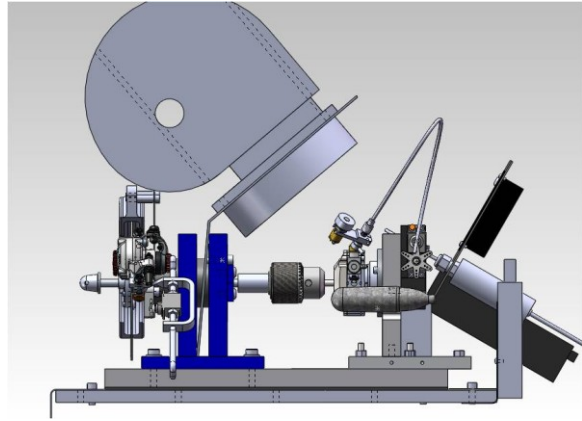


Figure 82: The shaft location needed to be precision located so as to reduce mechanical shaft losses due to misalignment.

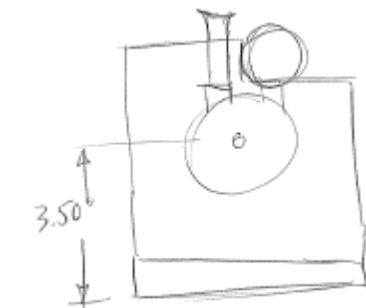
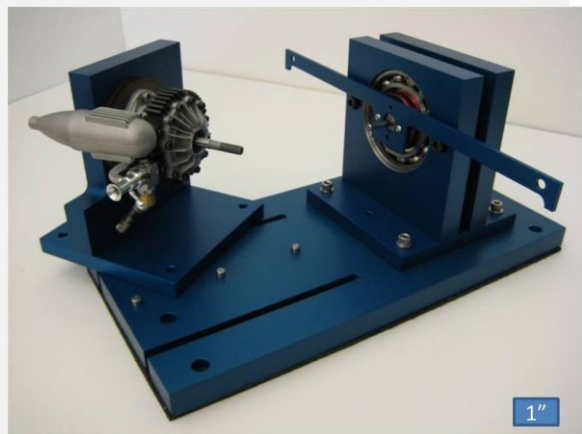
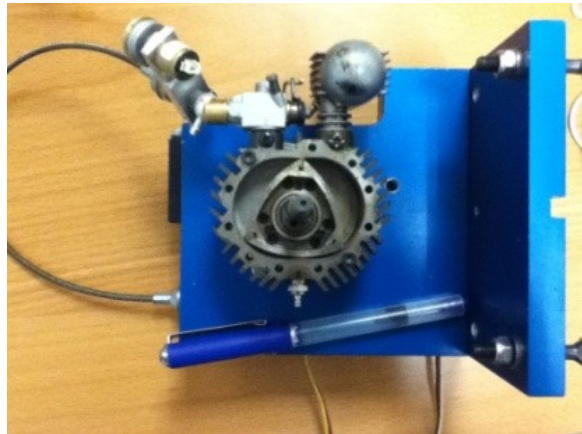


Figure 83: The engine mount would also need to have basic thermal insulation, account for exhaust position and provide enough working space to mount / dismount.



Engine loading elements

Electrical loading system

Electrically enabled solutions to measurement and control are always attractive because they move one step closer to digital environments (which often allow for

computer control and data acquisition). Simply measuring a voltage and a current to quantify a physical property was attractive and thus, the electronic loading system was designed, built and tested.

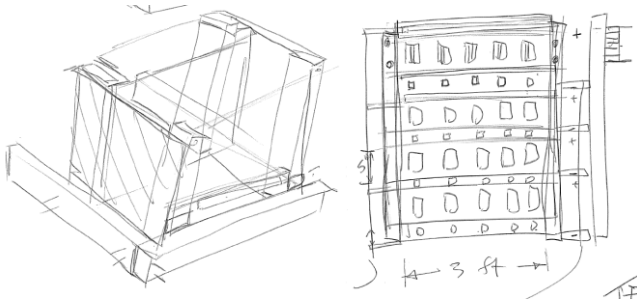


Figure 84: The original sketches of a resistor bank filled with low-resistance and high wattage resistors attached to a large heat sink with cooling fans, supported by a low-cost, non-conductive and stable structure [92].



Figure 85: The final assembly of the resistor bank. The high power resistors are mounted directly to the heat sink with cooling fans (not visible from this photo)

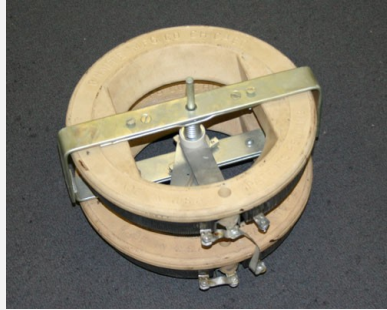
Several electrical loading elements were proposed but one by one they were eliminated from the final design. This included such as rheostats, several physically large, high-power, and low resistance resistors, toaster heating coils, and other low power dissipation elements, which can be seen in the table below.

Table 5: Various electrical loading elements researched.



High power, low resistance resistors

Good performance up to their power limit. Not easily adjustable nor is there a large range of adjustment.



High power rheostat

There is no good reason why a rheostat was not utilized in the design. All the technical specifications and device properties appear to have just what the original design requirements needed.



Medium power, low resistance, resistors

The smaller resistors in parallel allowed for a larger range in loading for the engine. These were ultimately chosen.

The chosen electrical system, utilizing a bank of medium power, low resistance resistors, attempted to key issues: easily adjustable loading conditions and the ability to dissipate the total output power of the Wankel Engine. Revillé *et al.* document the design of the resistive element, which includes independent, resistors all in parallel [92]. Each resistor was then electrically and thermally connected to an insulator frame and a large industrial heat sink.

Each resistor is in series with a switch that allows the variable loading of the engine. As each of the 18 resistors are switched on, they are added in parallel thereby increasing the physical torque load placed on the electric motor shaft which is then connected to the Wankel Engine under test. Power transfer theory demonstrates that the best power transfer characteristics occur when the load resistance matches that of the internal resistance of the electric dynamometer motor.

With low internal impedance for the dynamometer motor, the resistors needed to be placed in parallel and also have low ohmage values. A full description and analysis is provided in [92]. This loading mechanism allowed for more convenient data collection but was unfortunately unable to fully load the motor, however could not fully characterizing the potential of the engine. Additionally, it required the operation of a second researcher increasing the complexity of the performed tests. Lastly, when the electrical system was switched from the “starting” mode to the “measurement” mode, many electronic speed controllers were destroyed due to engine-generated current rushing into the precision electronics; overloading the circuit, releasing the characteristic burned

electronic scent and in the process burning about \$400 each time. Therefore, another solution was necessary.

Mechanical loading system

The concept of loading an engine and measuring its performance remained the same, however the loading mechanism changed—to something more intuitive to mechanical engineers—to a modern mountain bike disc brake. This development on first glance appears to be a step backwards in terms of measurement and accuracy—as the electrical system designed by Revillé *et al.* theoretically should have considerably better performance in this category, however the brake without doubt would allow the engine to be fully loaded to engine stall. Additionally, the other challenge with this system is achieving reliable, robust and repeatable starting of the engine.

While the electrical system proved sufficient to start the engine, it was not reliable in the long run. Instead, a brainstorming suggested that a mountain bike brake would also prove to be a low-cost solution. Additionally, using the standard hand-held hobby starters was more robust and required less dexterity. In this manner, one hand can be used starting the motor while the other hand is carefully adjusting the throttle position to start the engine.

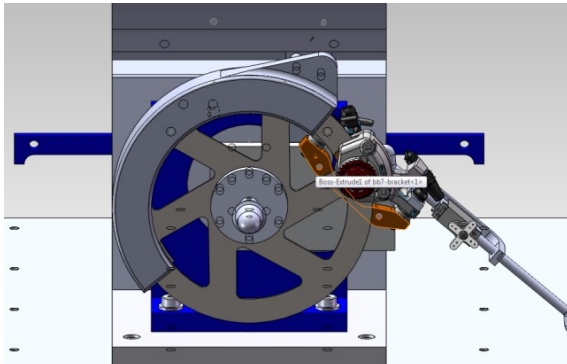


Figure 86: A solid model of the mechanical braking element of the dynamometer.

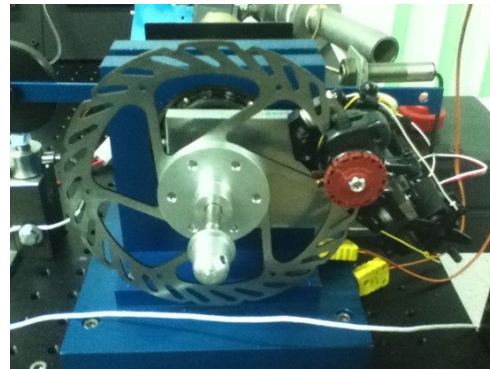


Figure 87: Mechanical brake and servo mechanism for engine loading.

Keeping funding constraints in mind, many parts of the mechanical loading system were scavenged, donated or bought with personal research funds, thereby permitting the development of a low-cost but functional loading mechanism.

In order to actively change / control the loading or braking force, a series of ideas were presented, again with similar constraints and it was decided that basic model airplane servos would be used. Typically, the actuator of the mechanical disk brake has

a tension applied to it by the rider during braking and there is an internal return spring when the rider no longer wants to decelerate.

However, the servos on this scale are not powerful enough to overcome the internal spring force and thus a solution to this problem was needed. A more expensive servo could have been purchased to overcome this spring force, but to maintain consistency with the servo actuation methodology, we sought to reduce the internal return force of the brake. The final solution, neglecting the many design details, resulted in removing the internal spring, creating a simplified servo mounting bracket and using two cables to both open and close the braking mechanism. Additional concerns were discussed about excessive heating since the brake would be traveling about 20 times more than normal operation (wheel RPM for a mountain bike is approximately 1000 and the engine can operate up to 20K) and therefore some approximations of final operating temperature were made. But with few theoretical models available to predict operations, a simple test was performed and provided real results. The test concluded that there are no short-term problems with this mechanism due to temperature. Mechanical intuition does suggest that long and extended periods of braking will elevate the temperature of the braking mechanism and this will have to be considered in future research.

Design considerations for fuel flexibility characterization

Designing a dynamometer system for one fuel is more straight forward than for designing for a range of fuels. Many researched fuels have corrosive properties and require rethinking in terms of fuel delivery, lubrication and engine operation. The general considerations when using multiple fuels in an engine system are strongly based on materials compatibility and corrosion.

Materials compatibility

First the fuel tanks and filling hardware should be compatible with corrosive fuels like methanol. General ABS plastics are soluble in petroleum based fuels and thus special materials need to be used. Typically materials such as Viton (which are often more expensive and more difficult to find) are used and resistant to a plethora of fuels. Fuel pumps, filters, pressure regulators and fuel delivery mechanisms (injectors or carburetors) should be methanol tolerant (as automobile engines which typically utilize gasoline, will not survive in a methanol environment) [94].

Data acquisition and control with LabVIEW

Typical control systems for general applications—where dynamic response is desired—have both some form of *sensing or input* and *controls or output response* that make optimal changes to the performance of a system. This section describes the efforts that went to sensing engine parameters and the computer aided controls that controlled the output response.

Data acquisition

Upon recommendations for data acquisition systems, LabVIEW regularly came up as the hardware and software of choice. A software system that allows you to create “virtual instruments,” LabVIEW tries to make the connection of software and hardware very simple for accurate, efficient and effective data acquisition.

The LabVIEW Front Panel

The front panel was designed in order to contain the key information about the engine in order to know whether all sensors and actuators were working properly.

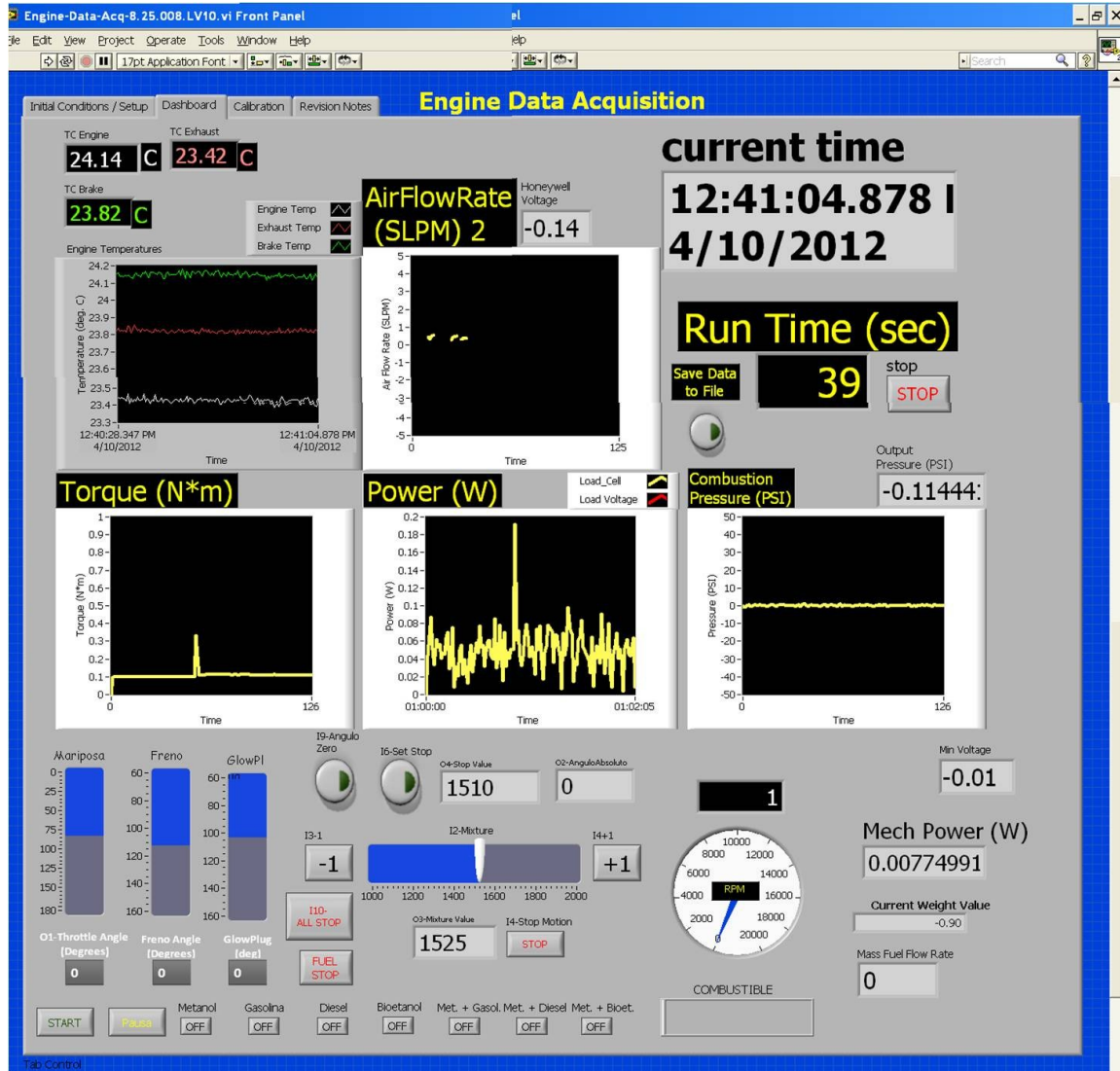


Figure 88: Main testing dashboard of the Fuel Flexible engine dynamometer. The upper left hand corner shows the temperature produced on the engine surface, the exhaust and the dynamometer loading brake. Just below shows the torque measurements. To the right are the air intake sensor measurements, the output mechanical power and when installed the combustion pressure measurements. The bottom half of the screen shows the digital controls, which allow the operator to dynamically change the throttle position, glow plug temperature, loading force, fuel delivered and rate of change of carburetor fuel needle valve (stoichiometry).

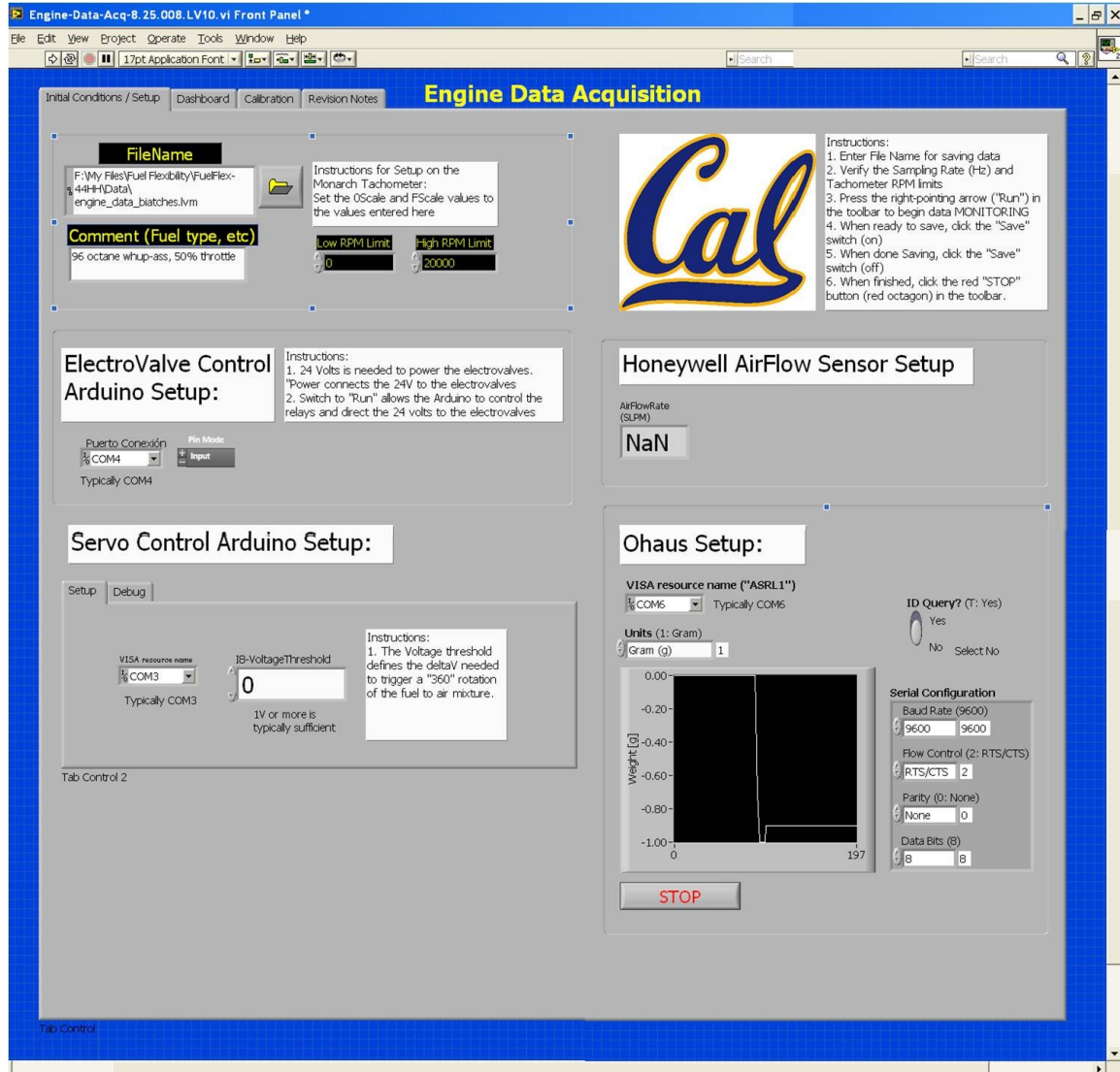


Figure 89: Dynamometer initial conditions and system setup dashboard. Each time the program is run, various settings need to be input to activate all the separate sensors, actuators, microcontrollers and other systems interfacing with the LabVIEW data acquisition system.

Small-scale rotary engine emissions characteristics

Today, output emissions from internal combustion engines is important, regardless the application. Thus, a preliminary characterization of the emissions output from this engine was conducted using the resources available at the Madrid, Spain laboratory. As this solution scales to larger sizes for other applications (primarily transport), emissions will be a point of concern. Therefore, it was an opportunity for this project to investigate the environmental impact of fuel flexibility on the small scale and provide insight and direction for future development in this project landscape.

Typically emissions are measured using predefined and heavily scrutinized testing procedures to equally compare emissions results of automobiles. On this scale, no real emissions procedures exist thus a larger-scale protocol was adapted by researchers Nicholas Maiden *et al.*



Figure 90: The Lujan emissions measurement system. This system was designed for auto emissions and was expected to potentially yield strange results as other similar systems (like Horiba) were specifically designed for automobile-scale emission volumes.

The first iteration of testing using the Lujan Gas Analyzer involved recording the measurements with a video camera, as a means to capture data. Recording the LabVIEW runtime (displayed large on the main dashboard) allowed for the emissions data to be synced up with the other measured engine output properties. However, this too was a tedious solution if many data points and test runs were desired and efforts to connect the emissions system via its RS-232 protocol continued in the background.

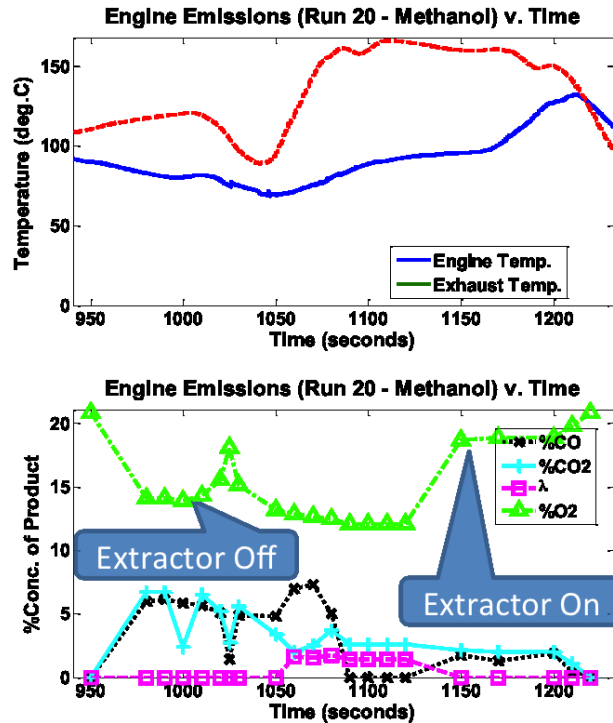


Figure 91: an example of the type of data collected during emissions testing.

In order to accurately measure output emissions from an engine however, a special reservoir needs to be designed such that oxides of the reservoir do not contaminate measurements, that probes are properly lined with Teflon so as not to contaminate or congregate species, etc. The remaining results should the reader be interested can be found in the appendix as they were not developed fully enough to draw any useful conclusions.

Required engine sensors and measurement

The sensing of the various engine parameters for this research is vital to the success of fuel flexibility. The O.S. Graupner Wankel engine as it stands, does not have sufficient capability to run fuel flexibly on its own without some human intervention. However, with the right set of sensors (combined with actuators and a control algorithm or fuel map), can better prepare an engine for the various fuels it may encounter.

Many sensors were purchased, calibrated used and integrated into this dissertation research. Some sensors went into direct characterization of the engine via the dynamometer and others would be required for safety or enabling fuel-flexibility. Specifics about each sensor can be found in APPENDIX C.

Dynamometer Sensors

Torque measurement

The torque measurement utilized pre-existing load cell as new sensor options were expensive and this equipment was available for use. However, the max force limits of the load cell were such that a torque arm needed to be designed that was long enough to measure a torque and yet still fall within the measurable range of the load-cell (500 g).

Table 6: Sensor hardware, measurement solutions and relevant commentary.

Using a pre-existing load cell from a former experimental setup, a torque measurement needed to be made where the perpendicular force applied and the moment arm are such that the midrange torque output of the engine is in the midrange output of the engine.

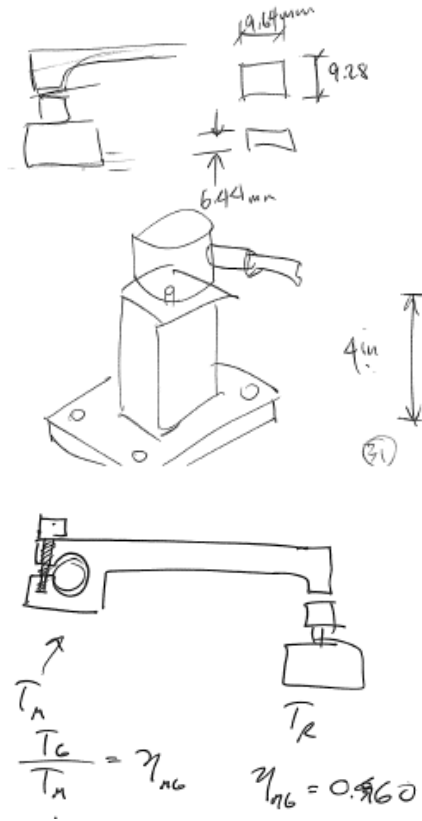


Figure 92: Initial sketches for the torque measurement.

Knowing the output torque range of the rotary engine and the limits of the load cell (APPENDIX C), the torque arm and sensor mount could be designed and fabricated.

However, as in many designs, design for assembly and flexibility were of key interest and ways to make each element adjustable was beneficial to the speedy setup and adjustment of the dynamometer.

Since the load-cell input platform is small and the torque arm should not be large, adjustment in and were desired. Thus a low-cost adjustment stand was designed and built in the student machine shop. Given reduced financial limitations, manually adjustable optical stands could have been purchased, however in this case, design was straight forward enough.



Figure 93: Design sketches load cell sensor mount with focus on adjustability.

This height stand attempted to utilize an angular surface to raise the height. This design was quickly eliminated for its coupling of the axis with one of the other axes and its complication to manufacture (at this time, rectilinear objects were the simplest to fabricate using standard lathes and mills).

While an interesting design, a standard stand with adjustments along standard axes was chosen.

Additionally, there are other important sensors and actuators that needed to be integrated in order to better characterize the engine and allow for the comparison between theoretical models and experimental results. These sensors specifically have been a combustion chamber dynamic pressure sensor, the fuel and air mass flow rates and the control of the fuel-to-air mixture. These sensors and actuators are specifically mentioned due to the challenges faced during the small-scale integration.

Combustion pressure sensing

The pressure sensor—an Optrand AutoPSI Plug—high temperature combustion pressure sensor needed both careful selection but also careful installation. The sensor tip functions from a piezoelectric transducer and has signal processing and filtering in an enclosure away from the engine setup. This cleansed signal is then passed into LabVIEW and directly compared and measured along with the other measurement points being inspected. This sensor as well is different from your standard analog output sensors in that it outputs a differential measurement; thus has a floating ground. The Optrand sensor was chosen for its stated high caliber pressure measurement capacities and low cost. Other sensors that compete in this market were 3-4x above our available price range. Especially when the sensor would be put in an experimental environment full of unknowns, fuels present, temperatures and various engine mounting points.

Mounting should be discussed, as it is non-trivial to create a minimally impactful measurement in such a small combustion chamber. The engine capacity cannot tolerate a significant increase in dead volume due to the presence of a new sensor. Additionally, this sensor can tolerate high pressures and temperatures at its sensor tip, however will burn up if hot combustion gases and fluids are able to pass over and along the side of the probe tip. Therefore, the manner in which the sensor is installed is critical for long-term usage and repeatable experiments. Additionally, its location with respect to top dead

center (TDC) is important for taking useful pressure measurements. Back during the initial characterization of the fuel-flexibility (by Cardes. *et al.* [93]), a similar sensor probe was installed however, one that had no threads and needed to be reworked to add scored surfaces—better adhering the probe into the pressure port. However, during testing, the sensor probe liquid cement failed (a JB Weld high-temperature liquid steel) due to high temperature and pressure and the sensor became a projectile and was damaged. Thankfully, enough data was collected to draw conclusions on the engine (i.e. inconsistent combustion, compression ratio, etc., see [93]), however this solution would no longer work. A more robust solution would be needed.

Given access to more funds to buy a second sensor in addition to precision drilling equipment, a second hole was drilled into the small-scale rotary engine, however the position for best output data and reliability needed to be considered.

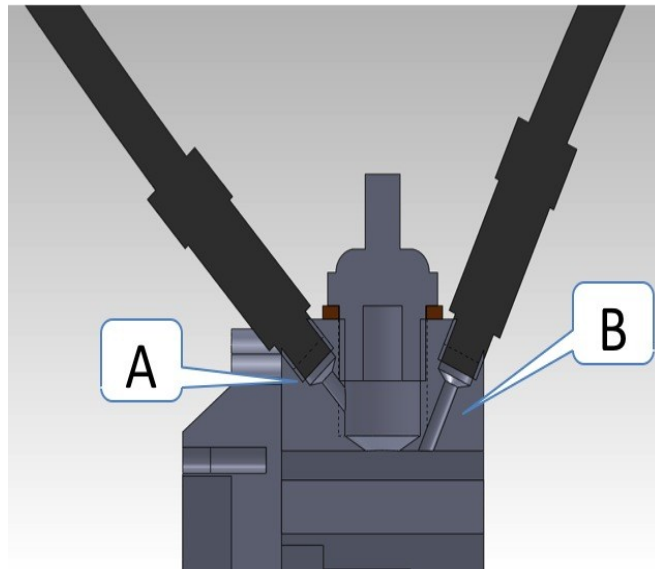


Figure 94: Engine port drilling options for pressure measurement. The O.S. Graupner Wankel rotary engine did not leave much space

In the figure above Figure 94, two locations, A and B were speculated for drilling into the O.S. Graupner Wankel engine. The design considerations consisted of what was feasible considering the hardened steel casing, what surfaces were best suited for drilling, how much dead volume would be created from the drilled port and what position would allow the most material for creating threads. Additionally, other spatial challenges surfaced coming from interference between the glow plug crush washer and the sensor base.

Position A was ultimately chosen for reduced dead volume and for having the “best” landing for the precision drill bit and machine. However, an unfortunate groove in the rotary engine prevented a sound seal and if hot gases could pass along the exterior of the sensor surface, there would be potential for unwanted overheating and sensor damage. Therefore a heightened landing pad was created via the high-temperature liquid steel, *JB Weld* such that a seal could be formed. This seal, more than simply preventing hot gas leakage, also is important for engine compression and functionality of the engine itself—thus was a much needed fix.



Figure 95: This image illustrates that no new chamber pockets / ports were drilled unnecessarily creating more unwanted dead volume (as in Cardes *et al* [93]). This was achieved with the help of the technical staff at the Universidad Politécnica de Madrid.



Figure 96: This image attempts to show the landing surface for the pressure sensor. The dull brown ring is the crush washer for the glow plug, and the horseshoe shape is the flat surface landing for the sensor. However, the mouth of the horseshoe illustrates a leakage point for combustion gases and needs to be sealed.

The other benefit to choice A (Figure 94) was the fact that pressure could be measured right at the glow plug and shared the same access to the fuel air mixture as the glowplug. Additionally, the pressure sensor will read at TDC and this is typically an ideal starting point for pressure measurement as it should give maximum or near maximum pressure values (at least for non combustion operation).



Figure 97: A magnified view of the rotary engine with the Optrand Auto-PSI high temperature pressure sensor installed.

Temperature Sensing

Temperature is a critical component in characterizing the motor during fuel flexible operation. Fuel evaporation rates and auto ignition—to name a few—are temperature dependent and thus, many points of temperature measurement were taken. The LabVIEW 9112, four-port thermocouple reader was purchased and used for accurate temperature measurement. Specifically the housing temperature, exhaust temperature and dynamometer brake temperature. Air temperature is measured by a combined temperature and humidity sensor apart of dynamometer system and measured only once per test run (see Figure 98).

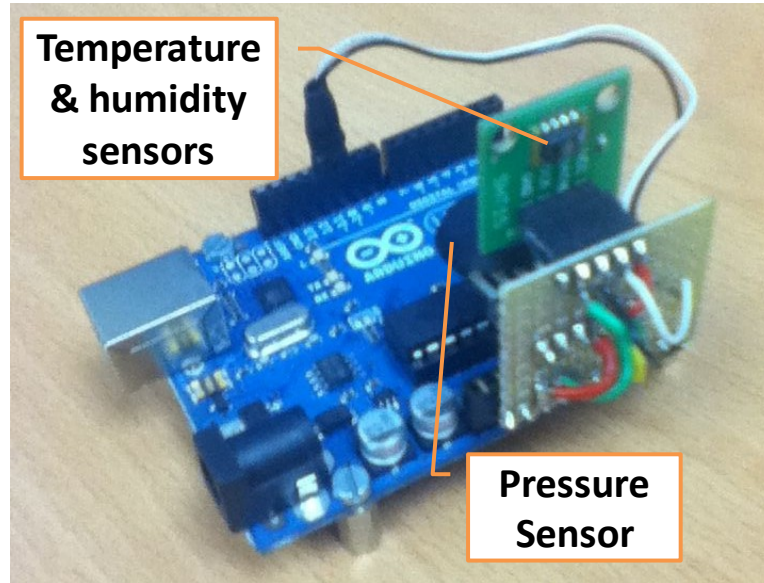


Figure 98: The ArduinoUNO microcontroller with the ambient temperature, humidity and pressure sensors.

This is for global adjustment of horsepower ratings based on location (altitude, weather, etc.). This was desired in case wild variations of the data would have been observed to radical changes in temperature, humidity or pressure.

Engine control

To fully enable fuel flexibility, active and repeatable control of the engine will be necessary as the required engine operating conditions are strongly dependent on the fuel introduced. Currently, the engine operator currently has to adjust and set the inputs to various engine parameters such as throttle position, air to fuel ratio, glow plug temperature and coolant speeds, etc. in order to maintain combustion and power output. Before this was all done manually and made characterization extremely difficult. But the long-term vision is one where these changes are made automatically using a sensor, actuator and microcontroller control system. The sensors have been reviewed and the actuators are the subject of this section.

Starting the engine

Ideally, the engine would have all the necessary controls available in standard engine testing banks; however as referenced earlier, few solutions on this scale existed prior and thus needed to be developed. One key element was the starting mechanism to the engine. Normally, hobbyists use a hand held starter motor, but in this application, the dynamometer loading element would be connected to the drive shaft of the motor, making it more difficult to apply this hand held starter motor. Thus, the electrical

loading system—which allowed for electric starting as well—was chosen as the first loading iteration.

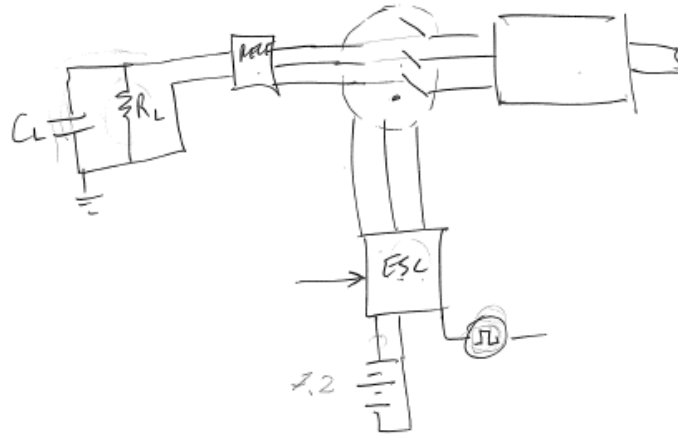


Figure 99: the electrical diagram of the motor starter plus dynamometer load switching system.

Ultimately, due to all the challenges with electronic speed controller, a mechanical solution was chosen and the engine was started with the standard hobby electrical starter motor.

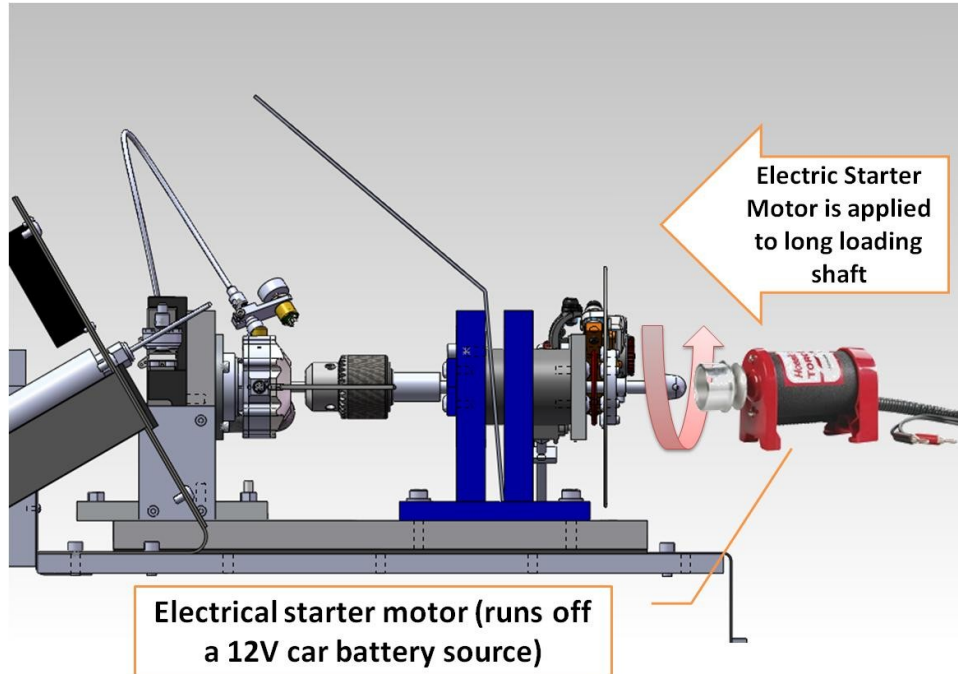


Figure 100: The mechanical loading system was designed with starting and effective loading in mind.

Throttle control

Typically, the only dynamically changing input to the engine is its throttle and the mechanical load applied to the engine. In this fuel flexibility research however, throttle, stoichiometry, cooling rates, selected fuels and other external parameters are dynamically changed and controlled to maintain combustion and reliable power output. Ideally, the operator of the fuel-flexible engine could elect to override the automatic control, but lacking any human input, a computer should dynamically control the throttle and maintain combustion. Thus, custom solutions were developed and the basic understanding of how servos work was investigated. Standard hobby servos require a 5 V pulse width modulation (PWM) signal with a highly specific duty cycle, which directly controls the position of the servo (if it is not a standard servo, like the stoichiometry servo that continually rotates, the duty cycle controls other parameters, such as angular velocity). The development of the throttle control is presented.

The first throttle control solution was a manual control that utilized a potentiometer, NE555 timer circuit and other standard circuit elements.

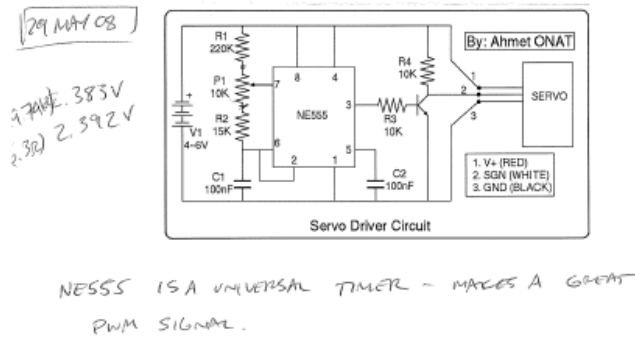


Figure 101: Schematic that utilizes a timer circuit to drive a servo. With a 5V power supply and a potentiometer, you can control the position of a servo. These were some of the original controls methods.



Figure 102: The bulky box that contains a potentiometer to drive the PWM signal to any standard hobby signal. This solution was replaced by ArduinoUNO micro controllers upon their discovery.

Additionally, with the need to measure accurate throttle positions, an attempt to model the exact position of the throttle based on the linear to rotary mechanism used can be found in Figure 18 of [92], and additionally, how this mechanism opens and closes the throttle valve in Figure 103 of this dissertation.



Figure 103: Linear to rotary motion of throttle servo mechanism (top view).

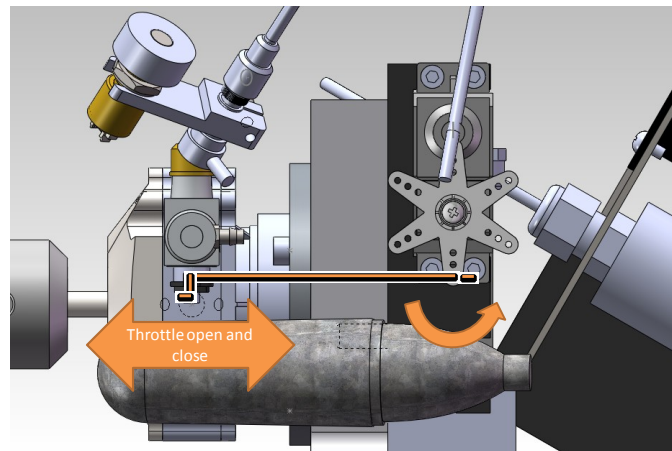


Figure 104: Here is the 3D CAD model that illustrates the motion of the throttle linkage (this is a side view).

Adjusting the stoichiometry

To dynamically adjust and measure the changing stoichiometry of the engine required some engineering. The challenge was to use some sort of electronic control to open and close a needle valve, which meters the flow of fuel to the carburetor. Because carburetors are known to be inferior to fuel injector technology with regard to efficiency and combustion control, fuel injector solutions were strongly considered, however

ultimately not used because of their parasitic power consumption (due to fuel pumps and required fuel pressure to atomize the fuel). A carburetor is typically passive in this sense and was designed already for this engine. Additionally, the added complexity of the fuel pump and injector systems on this small scale would add to the size reducing the portability. As the data will show, utilizing the carburetor for this preliminary characterization work was sufficient to demonstrate fuel flexibility. Future work could include fuel injection control and injection of many fuels.

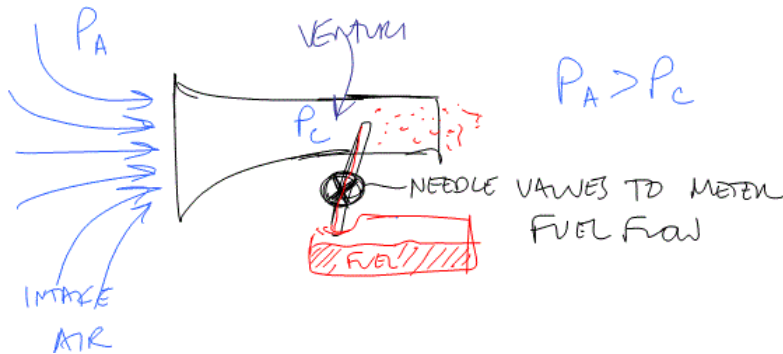


Figure 105: Small-scale carburetor schematic. The needle valve is typically to set the idle mixture. However in this research, this valve is constantly opened and closed in order to adjust stoichiometry.



Figure 106: O.S. Graupner Wankel carburetor with angular encoder mount.

Due to the design of the O.S. Graupner Wankel Engine, the carburetor stoichiometry adjustment needle valve is not on a conventional x , y , or z axis, and thus a solution with flexibility would be needed. What was needed was a mechanism that could transmit torque but attach at an unknown angle and then be easily adjusted and removed. Additionally, a means to reliably measure the position of the needle valve at any time was also needed such that the user (or a computer) could know the mixture stoichiometry and return to the optimal performance position for each combusted fuel.

The solution utilized was a flexible torsion shaft with a *HI-TEC* variable angular velocity robot servo. The angular position of the needle valve was measured by *USDigital* Analog angle encoder via a small rubber belt that tracked the torsion shaft as it rotated. In hindsight, a spring-loaded, linear micro potentiometer may have been a better solution as the needle valve has screw threads and a linear displacement is directly proportional to the fuel flow—rather than the current implementation which is a translation of rotary motion from one diameter to the next, somewhat like a bicycle chain and is prone to measurement and functionality issues/errors. Slippage from fuels and oils was prevalent and it was not a one-to-one gear ratio and the noted “degrees” were not equal to exactly that of the needle valve. It did however conserve at least as a more

consistent and actively recorded measurement (as compared to prior measurement by “feel”).

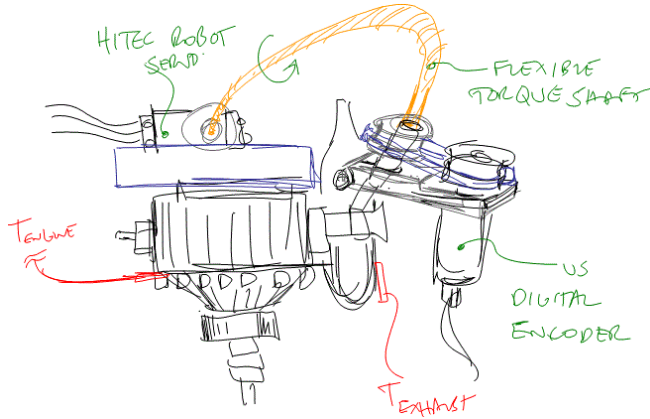


Figure 107: Sketch of the encoder measurement of fuel air ratio.



Figure 108: Actual fuel to air ratio measurement system.

Further, a relationship between the amounts of fuel flowing into the carburetor can be defined using basic gear and belt equations considering the diameters are known and the right-side element is a sensor and therefore measures rotation.

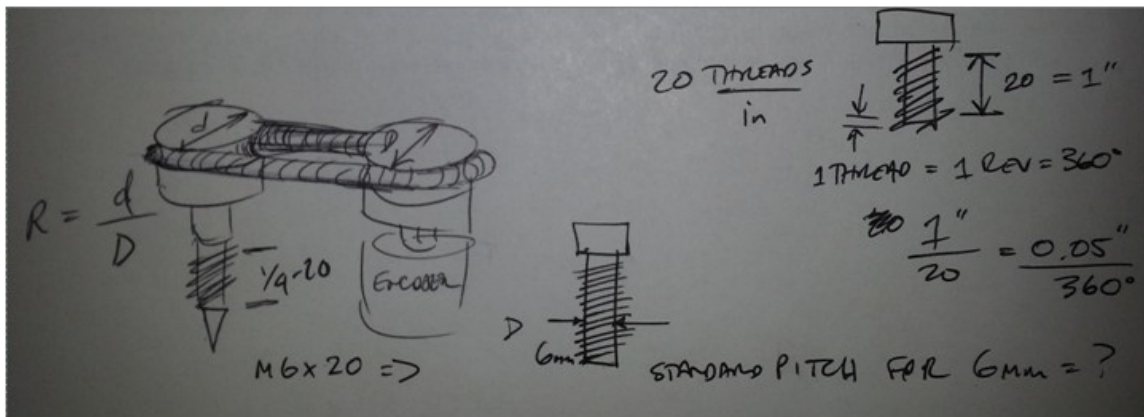


Figure 109: Sketch showing some of the key dimensions to determining carburetor fuel needle valve position.

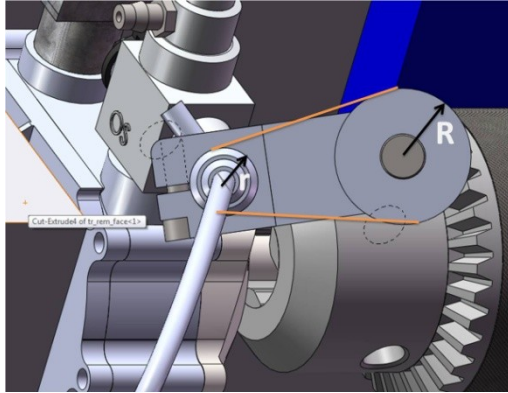


Figure 110: The key dimensions in this figure are r , which is the radius of the flexible torque shaft, R , which is the radius of the belt hub and L_c , the center to center distance between the two belt hubs.

$$\begin{aligned}L_c &= 1 \text{ in} \\r &= 0.375 \text{ in} \\R &= 0.75 \text{ in} \\ \sigma_{encoder} &= 163 \frac{\text{bits}}{\text{rev}}\end{aligned}$$

The encoder is measured in voltage and the Arduino converts that 5 V signal into 1024 bits. Therefore, it is 163 bits output into LabVIEW (LVM) per rotation of the encoder. However, the actual rotation of the needle valve is double that because of the belt gear ratio. Knowing that it is a $\frac{1}{4}$ -20 thread pattern, it can then be determined the needle valve opens 0.05 in per rotation. In this manner, the z height open of the needle valve can be calibrated.

In this manner a very basic calibration plot can be generated:

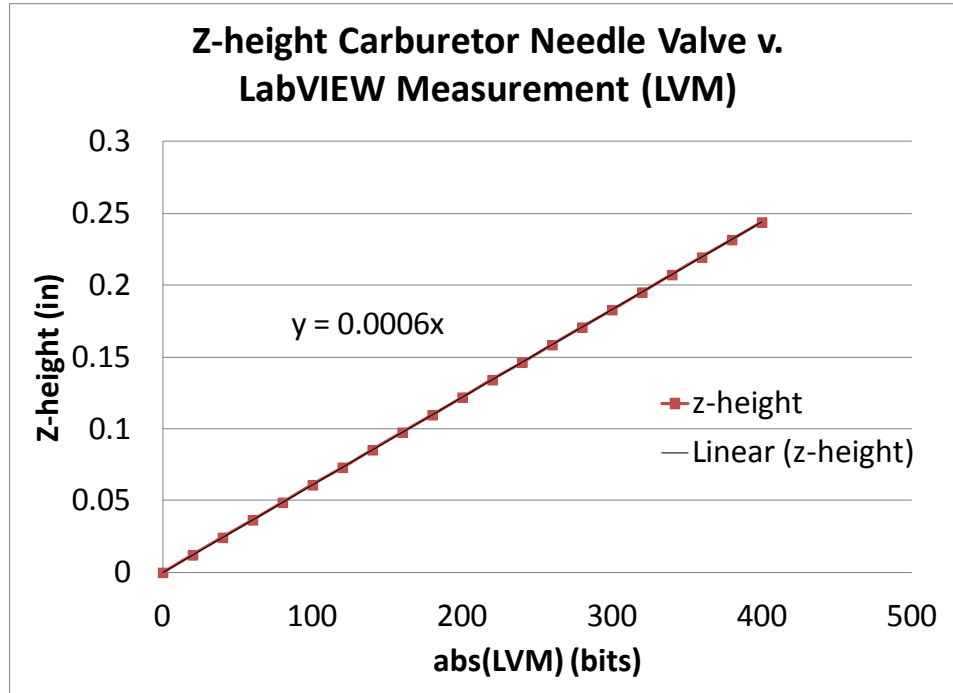


Figure 111: Calibration of the carburetor needle valve z-height. This height is proportional to the fuel delivery of the carburetor and is related to the stoichiometry. Data is presented in the bit value so as to be easily changed during testing but will be useful to assess fuel flow in the carburetor for stoichiometry calculations.

Dynamically controlling the glow plug temperature

The desire to dynamically control glow plug temperature has been strong ever since it was discovered that some fuels required the glow plug to be constantly “on” to maintain combustion while other more typical fuels, such as methanol, only needed it during start. Additionally, besides the digital option, “on” or “off”, researchers preferred to have better control and if at all possible, measure the amount of energy going into the glow plug (as this would not only help identify the ignition temperature, but would also factor into a overall power output of the engine).

Considering the options of controlling high current available, the first attempt was to reverse engineer the *Hobbico Deluxe Power Panel II* to understand the current delivery circuit and replace the potentiometer with either a digital signal or a digital potentiometer.



Figure 112: The Hobbico Deluxe Power Panel which helps manage power delivered to the glowplug and starter motor.

This proved to be more development than was desired and thus, a more intuitive, mechanical solution was implemented with the help of 3D CAD software and 3D printing.

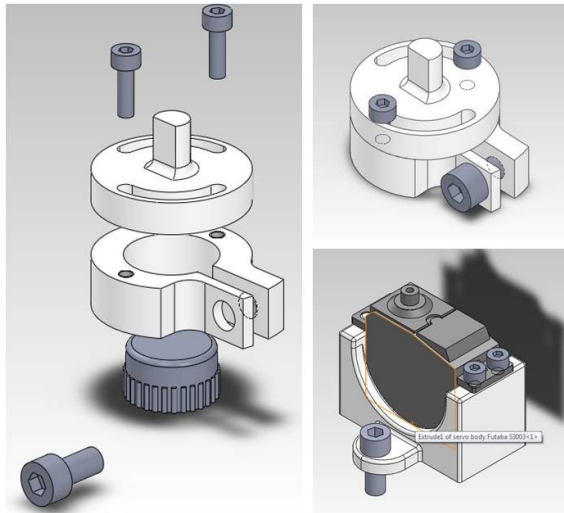


Figure 113: Servo mechanism to adjust the glow plug heat. Consists of flex torque shaft and several custom 3D printed clamping mechanisms.



Figure 114: The actual implementation of the glow plug adjustment mechanism.

With increased presence and access of 3D printing, this enabled the quick implementation of a solution to control the glow plug knob itself on the *Deluxe Power Panel II*. Using extra components that were purchased at the time of the stoichiometry actuator development, a similar torque shaft was used in this implementation.

Other critical system components

Shaft coupling between engine and dynamometer

Other elements to the dynamometer system that needed to be included were the coupling of the engine to the loading element.

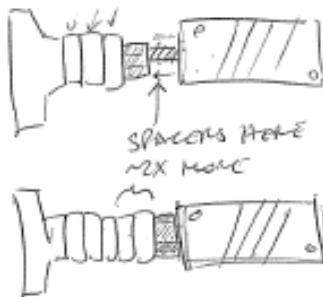


Figure 115: Shaft couplers always presented problems until the drill chuck solution was implemented.

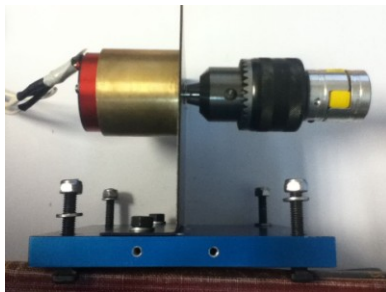


Figure 116: The drill chuck coupler system implemented to have a dyno fit for any size output shaft.

The output shaft of the rotary engine has $\frac{1}{4} - 28$ threads and is normally attached to propellers. Spacers and a robust shaft coupler was needed to properly affix each engine quickly and securely to the dynamometer system.

Every commercial shaft coupler tested typically failed with extended use. These couplers undergo torques, heat, and cyclic fatigue and jerk. This rough operation caused slippage and frequent engine breakdowns until a better solution was designed (see **Error! Reference source not found.**). Additionally, post-purchase modifications likely reduced the strength (to fit non standard diameter shafts).

Additionally, of the many allen-head screws required to breakdown and re assemble the engine dynamometer, any solution that made the removal of the engine more reliable and faster was a welcome change.

In Figure 116, (left) the brass sleeve concentric with a Kontronc model helicopter motor connected to (Right) a drill chuck head, flexible shaft coupling for easy and quick detachment of engines and motors under test. This heavier rotating mass also acted somewhat as a flywheel which helped keep the engine turning during rough fuel changes.

These couplers saw large torques and consequently high stresses as the motors that were being tested were claimed to produce up to 945 W of mechanical power. Additionally, with the engine spinning upwards of 20,000 RPM, a lot of potential energy is present in the shaft of this motor.

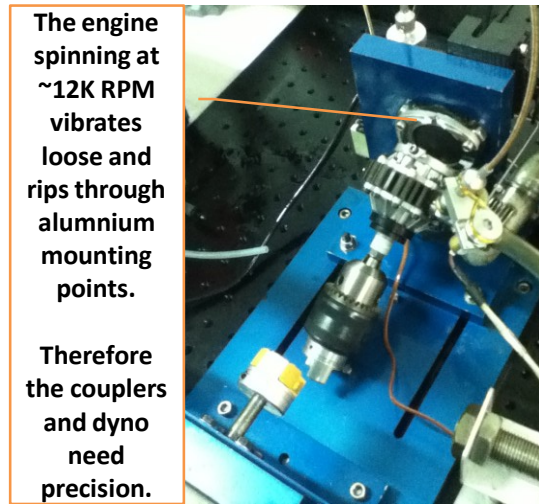


Figure 117: A dynamometer support failure due to high vibration and poor shaft coupling.

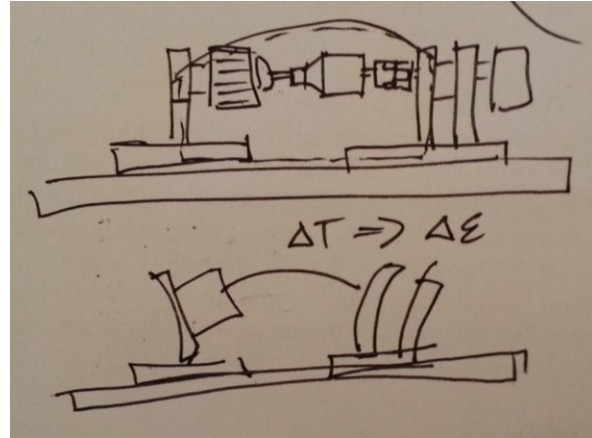


Figure 118: Sketch of how the structural loop—without a spline could cause unwanted bowing and flexing of the system.

Additionally, the engine producing combustion also transmitted much of that heat through its shaft and therefore was transferred into the coupler as well as the loading elements. This caused unwanted shaft expansion and would actually cause the closed loop system to bow (as evidenced by mechanical resistance during rotation at elevated system temperatures). This could have been resolved by a shaft spline which transmits rotation but allows for axial extensions and contractions.

The threaded shaft of the OS Wankel engine as well acted as a “screw” of sorts pulling the loading component towards the engine causing further binding of the system. Luckily, the system was designed with some flexibility and these issues were resolved. The coupling system was improved was by designing and using a universal drill chuck head as the receptor of the loading element (as to permit any type of small scale motor or engine to be tested).

To prevent further binding of the shaft thereby creating damage to the various dynamometer parts without adding a spline, the slide-in/out system for the engines to be mounted was left hand tight to allow for thermal expansion or contraction from the

threaded shaft and still keep the axis of rotation collinear (along with its unwanted consequences as in Figure 117).

For actual testing, there were engine protocols that attempted to maintain torque settings to ensure the most repeatable data. In this manner the characteristic dynamometer power and torque curves would be generated across various loads and engine speeds.

Multi-fuel switching system (MFSS)

From the onset of the research, having a multi-fuel switching system was a desired feature because switching fuels by hand was not only tedious and potentially dangerous, but it was a non-repeatable means for switching fuels. To judge the ability of the engine to switch fuels when the process is dependent on manual human intervention to quickly switch fuel sources is futile. Therefore a low-cost switching system was designed and built such that four fuels could be easily, reliably and consistently switched using one of four fuel tolerant electrovalves.

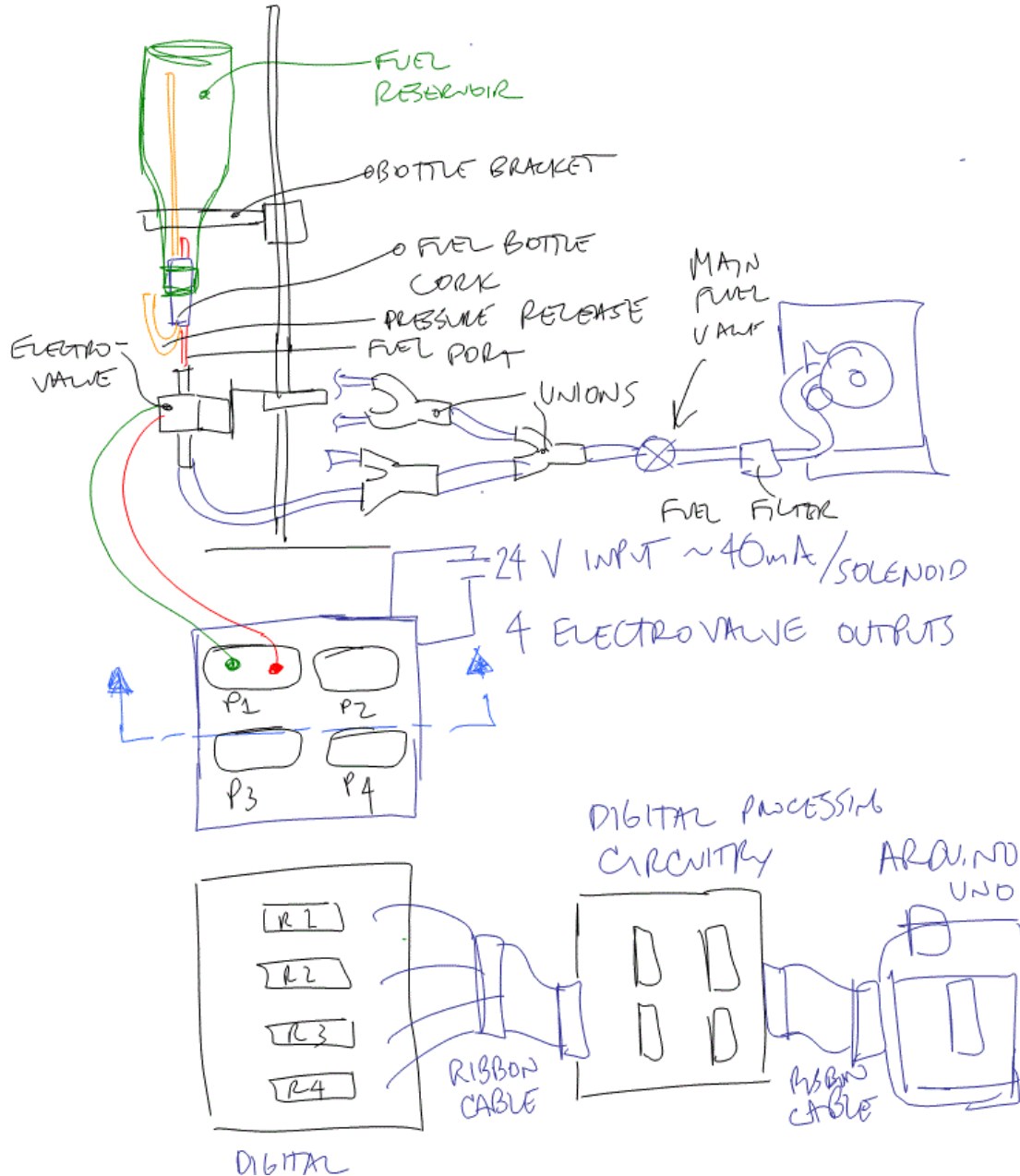


Figure 119: Sketch drawing of fuel switching system. A.K.A. the "BarBuddy" creates the main structural support of all the fuel bottles (in this case, recycled wine bottles). The bottles are sealed with standard cork but have two tubes that pass through them. A pressure release and a fuel outlet. The fuel outlet tubes connect to one of four electrovalves that are built with viton internals that do not corrode in the presence of fuel. Then the fuels enter unions that converge four separate tubes into one that enters the engine. The electrical system is again controlled by an ArduinoUNO microcontroller and a set of relays to control the electrovalve actuator currents.

Mechanical design

In addition to the electronic component, a pre-existing structure was utilized that gave four locations to place fuel bottles allowing for gravity feed fuel delivery (the

system known as the “BarBuddy” normally provides 25mL of a desired alcohol—aka a shot—into a consumption device—aka a shot glass—and was modified such that it could use empty wine or alcohol bottles for fuel bottles—which in Spain are in excess and free). This again combined both mechanical and electrical system design.

The mechanical design was more straightforward in that the BarBuddy system was already pre-built and simply needed a few modifications (for rapid and low-cost development). The shot measuring components were removed and replaced with a simple ringed support base whereby the neck of a fuel bottle could be placed upside-down and then cradled by the mount. Next, mounts for each of 4 electrovalves were needed and again was quickly designed for ease of assembly (adjustable height and rotation), low-cost (sheet metal and scavenged aluminum) and ease of manufacturing (symmetry, formable sheet metal). The unions utilized here were unfortunately made from plastic which did degrade in the presence of fuel. However, this is a slow process and data could still be collected.

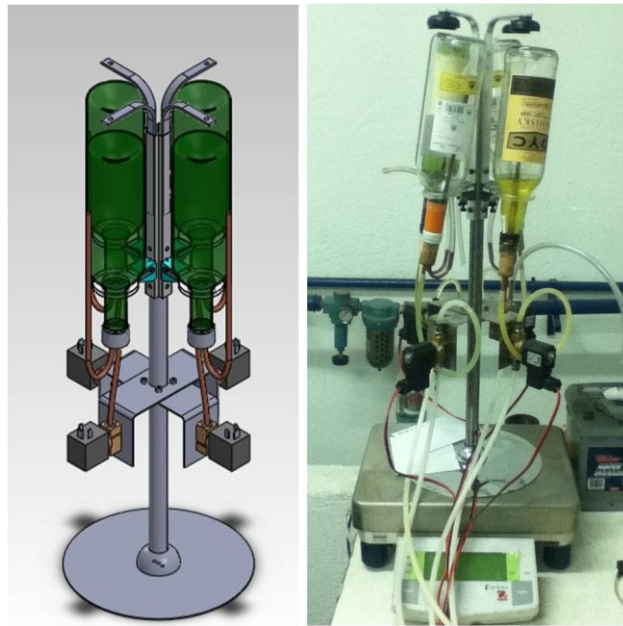


Figure 120: Original design compared to the actual machine.

This entire fuel switching system is then placed on top of a precision, *Ohaus Explorer* mass scale in order to measure the mass fuel flow rate entering the engine (Figure 120). The output from the scale can be read visually but as well, can be input into LabVIEW via serial communication and be compared against time, yielding a mass fuel flowrate accurate down to the nearest 0.01 g/s.

Electrical design

The electrical system (Figure 121 and Figure 122), is composed of a power supply, an ArduinoUNO microcontroller, a printed circuit board, and one relay + diode per electrovalve present in the system. Additionally, ADC1002 chips are used for the digital logic control. These circuit elements combined with a LabVIEW program enabled for Arduino control allow for the mechanical control of the fuels entering the engine.

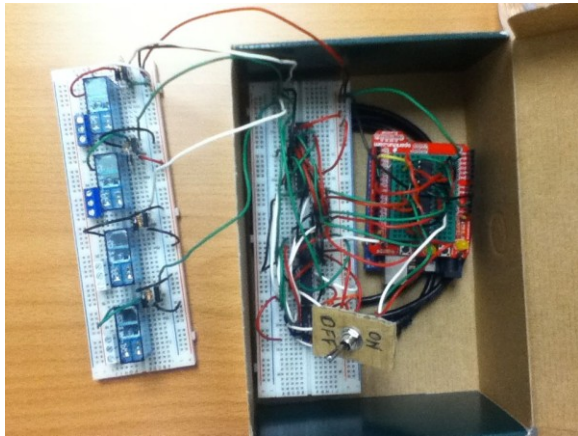


Figure 121: Breadboarded prototype of the fuel switching electronic control system. The breadboard on the left contains the prototype with the relays and electrovalve ports. The breadboard on the right connects the logic circuit to the Arduino.

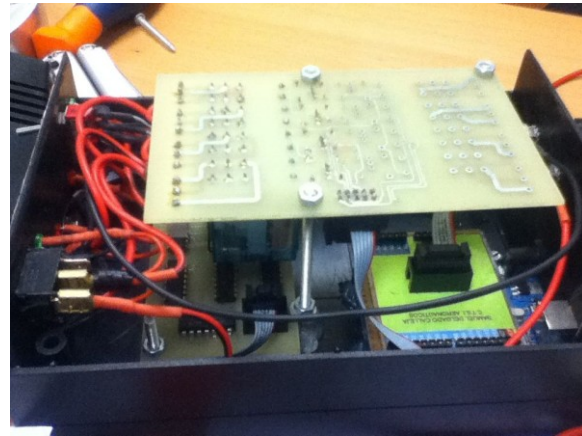


Figure 122: Printed circuit board and enclosure for fuel switching system. From prototype to printed circuit board. This is the controller box that is used to regulate fuel flow from the LabVIEW environment. A USB connection from the computer to the Arduino is what controls the signals to the relays.

Computer control

Control strategies for engines can be optimized for minimal emissions output, maximum power output, maximum efficiency and so forth. Many of the regulations regarding emissions are pushing for minimal emission outputs. To enable fuel flexibility, the system will need to measure its current condition based on the integrated sensor suite, utilize a specialized fuel-flexible control system and once the control strategy determines the optimal engine conditions, it sends signals to the actuators to change the engine conditions. There are many control systems that utilize various strategies to rapidly determine optimal conditions. With regard to small-scale engine technology, Fuzzy Logic control systems were utilized to reduce emissions in a small scale engine [96]. This system takes inputs from sensors, checks the input values against a basic set of rules which then define output signal responses for the various control actuators. The system is now prepared to have control strategies implemented.

These components are then controlled by digital outputs of the Arduino based on a 4-bit logic table of ones and zeros. These various digital bits correspond to each fuel or a blend of two (corresponding to two electrovalves “open”). With this basic setup, then further modification can be done in the LabVIEW “virtual instrument” environment. Typically this includes a more visually appealing interface and mouse and keyboard control of mechanical elements. Additionally, the system is scalable and can handle up to four more fuels or fuel blends.

This system provided a low-cost solution that enabled rapid refueling and switching of a host of fuels: methanol, gasoline, diesel, biodiesel and bioethanol.

Chapter 3 Summary

This chapter outlines the core development of the fuel-flexible, small-scale engine dynamometer, the multi-fuel switching system, the sensors required for extending fuel flexibility, the software developed to read those sensors and the actuators implemented to control the engine conditions based on those measured signals.

References

- [92] J. Revillé, “The Wankel engine and fuel-flexibility: an engine performance review,” M.S. thesis, ME Dept., UCB, Berkeley, CA, 2009.
- [93] Cardes, A.C., McCoy, C.D. , K. Inaoka, D.C. Walther, A.P. Pisano and C. Fernandes-Pello, “Characterization of fuel flexibility in 4.97 cc rotary engines,” MCS, Libson, October 6-10 2005.
- [94] McCoy, G.A., J. Kerstetter, and J.K. Lyons, “Alcohol-fueled Vehicles,” WSEO (1992).
- [95] Piemont, S. WIPO Patent: “device for identifying hydrocarbon fluids.” <http://www.wipo.int/patentscope/search/en/WO1996015064> Accessed on: 10 May 2012.
- [96] Lee, S.H., Howlet, R.J., Walters, S.D. “Small engine control by fuzzy logic.” *Journal of Intelligent and Fuzzy Systems* 15. (2004) pgs. 207-217.

Chapter 4 – Experimental Results

“If you can’t measure it, then you can’t improve it” ~Lord Kelvin

The goal of this research was to characterize and extend the fuel flexibility of a small-scale rotary engine. This characterization is achieved by measuring and drawing insights from the following key engine performance characteristics:

- Power output (W)
- Fuel-to-air mixture / Stoichiometry (Equivalence Ratio)
- Engine Temperature (deg. C)
- Exhaust Temperature (deg. C)
- Fuel mass flow rate (g/s)
- Air intake mass flow rate (g/s)
- Efficiency (percent)
- Engine Speed (RPM)
- Throttle position (percent WOT)

Knowing the performance conditions and operational parameters of the engine during fuel-flexible operation allows for its characterization and leads to ways for extending performance. The key figure for engine performance is the typical “power curve” where torque and output mechanical power are plotted against engine speed. These plots are produced for each fuel tested. Other simulations and experiments that further extend the viability of this fuel flexible engine—such as predicted fuel autoignition points, measured fuel-flexible emission outputs, MEMS sensor survivability in chamber, among others—were also conducted and are presented.

The data collected throughout this research is what allows future modifications and design enhancements to be made to fuel flexible engine technology. The changes and modifications that were made in order to improve the fuel-flexible dynamometer will be mentioned and referenced from Chapter 3.

Fuel-flexible characterization history and process

In addition to individual engine data for each fuel utilized, an overall picture of power output versus the various fuels provides insight into the true fuel flexible nature of the engine. Cardes *et al.* showed limited fuel flexibility in 2005 using an electrically-loaded dynamometer. The researchers collected data on four types of liquid hydrocarbons: GlowFuel (a mixture of methanol, nitromethane and castor oil), Gasoline (87 octane), Diesel and a military-grade JP8. While this research was pioneering and demonstrated the fuel flexibility of small-scale Wankel engines, it did not fully characterize the engine parameters nor present specific data for each fuel combustion (for

example mixture stoichiometry, engine temperatures, engine speed, etc.). Thus more complete characterization was desired; specifically with real-time collection of data, repeatability and automation.

Table 7: Temporal description of the fuel-flexible research testing.

Date	Results obtained	Researchers
2005	Initial fuel-flexibility results obtained manually using a electronically-loaded brake dynamometer.	Cardes, A., McCoy, C., <i>et al.</i>
2009	Fuel-flexibility results reconfirmed using a newly designed, fuel-flexible dynamometer with a resistive-brake taking real-time measurements via a high-performance datalogger.	McCoy, C., Reville, J., <i>et al.</i>
2012	Additional fuel-flexibility results with new fuels and measurements obtained using a refined fuel-flexible engine dynamometer that utilizes a multi-fuel switching system, a mechanical brake disc loading system and fuel-to-air mixture control	McCoy, C. <i>et al.</i>

The prior research results are presented in APPENDIX C and what is presented below are the most current results as of November 2012.

Bottom line up front: key data and results summary

Summary of mechanical power output

At this point, the 2009 dynamometer had been modified extensively with added sensing and control but most importantly, a wide-range loading mechanism. With these changes in place, the fuel-flexible characterization was improved.

For completeness and brevity, the details and compositions of the fuels combusted during these tests are presented in Table 8 along with the maximum mechanical power output recorded.

Table 8: Fuel characteristics and the maximum power observed during fuel-flexible combustion.

Fuel	Specific Gravity	Fuel Constituent 1	Fuel Constituent 2	Percent Volume	Max Power	RPM
Gasoline (87 Octane)	0.703	87 Octane	2T Synthetic Oil	0.96 / 0.03 / 0	333.7	9700
GlowFuel	0.791	Methanol	Nitromethane	0.82 / 0.18 / 0	507.5	15900
JP8	0.8	JP8	2T Synthetic Oil	0.92 / 0.07 / 0	312.8	9600

Diesel	0.85	Diesel	2T Synthetic Oil	0.98 / 0.02 / 0	239.2	12940
BioDiesel	0.85	BioDiesel	2T Synthetic Oil	0.96 / 0.03 / 0	322.2	9600

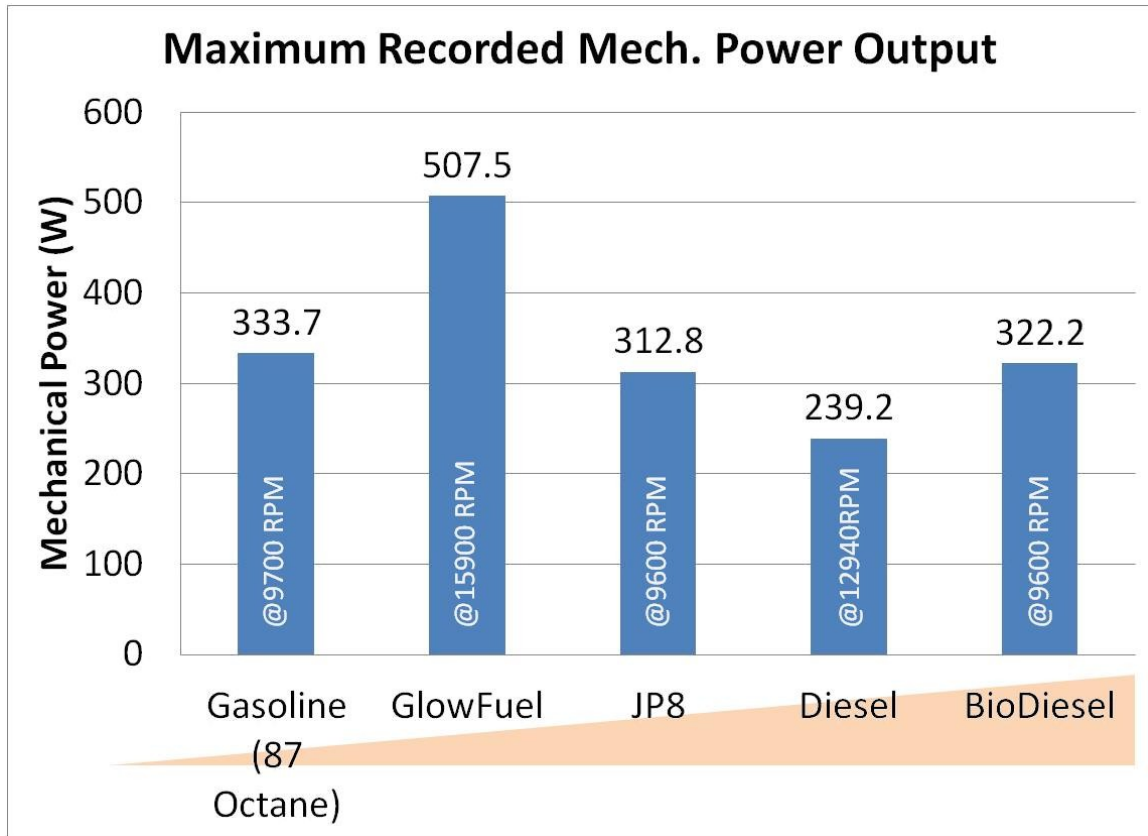


Figure 123: Maximum mechanical power output recorded for each fuel tested using the upgraded mechanical dynamometer. The fuels are listed in order of increasing specific gravity.

Stoichiometry map for the five fuels tested

The various fuels needed to be characterized with regard to their combustion stoichiometry such that the engine could run reliably when changing fuels. This map is the first attempt at understanding how to automate the engine to run fuel flexibly.

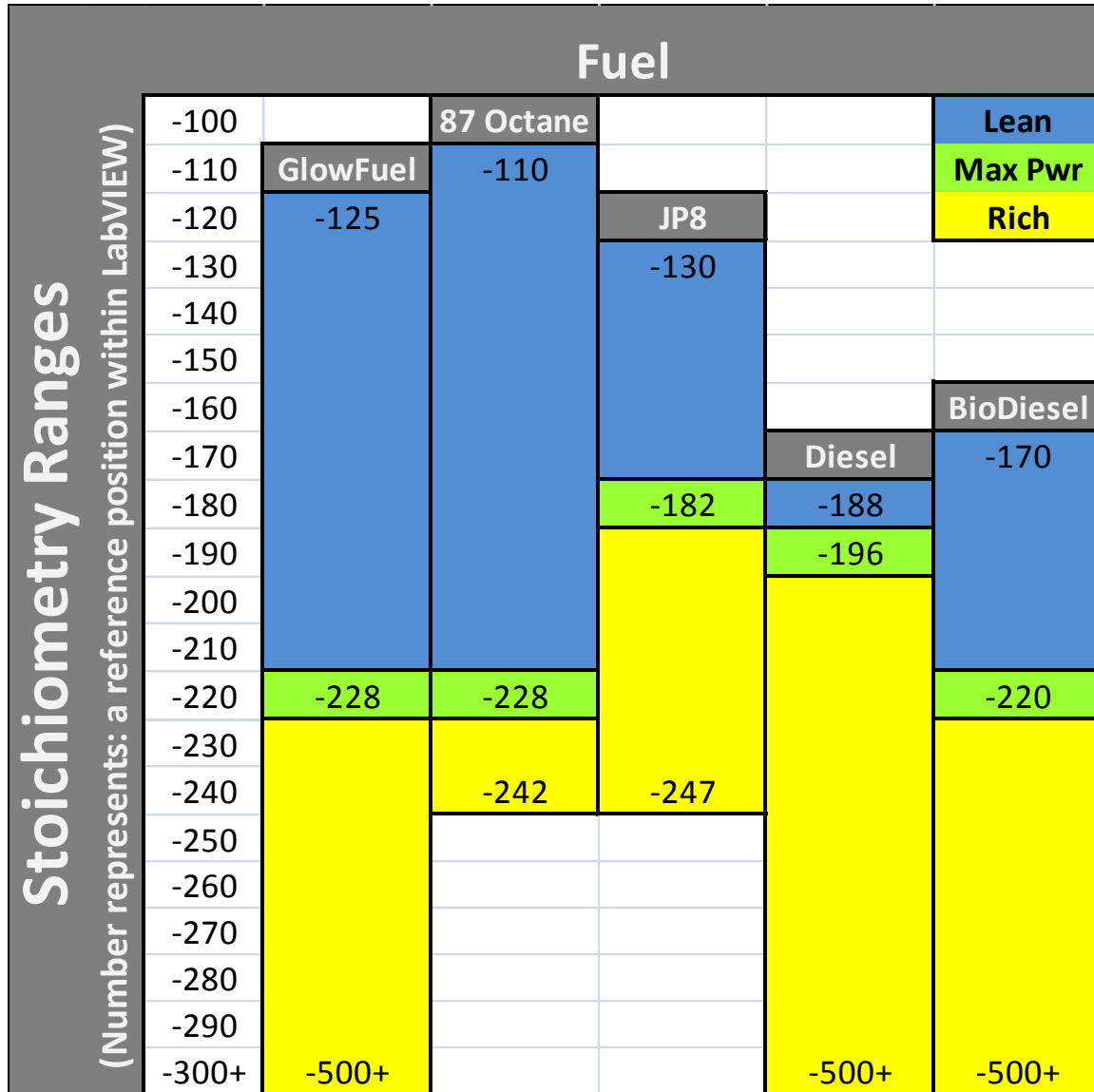


Figure 124: Stoichiometry map that details the physical carburetor needle valve positions that represent the flammability range of the engine. Again, to understand the significance of these values, please see “LVP” or “Lab View Position” in the Nomenclature which is found in the APPENDIX.

Characterization of fuel-flexible power output

Detailed data collection process

The data collection on these dynamometer systems was conducted per recommendations and tips presented at the Land & Sea website (a manufacturer of many styles and sizes of dynamometers) [190]. The basic data collection procedure however can be summarized in the following steps:

Fuel Flexible Dynamometer Test Procedure

- Connect the engine to the dynamometer.
- Connect all controlling servos and sensors.
- Start LabVIEW Fuel Flexible Dynamometer Software (enabling and prepping all sensors and connections to computer).
- Test for compression and ambient conditions (temperature, relative humidity and pressure).
- Connect fuel line (with filter).
- Start collecting data in the LabVIEW Fuel Flexible Dynamometer Software.
- Start engine using methanol fuel, standard glowplug and electric starter.
- Bring the engine to steady state temperature, varying such parameters as cooling fan speed, carburetor needle valve position, glow plug heat (or disable) etc.
- Slowly open up the throttle while increasing the engine loading.
- When throttle position is at Wide Open Throttle (WOT), ideally the engine has not stalled nor has damaged the dynamometer.
- Slowly begin relieving the engine load, thereby permitting the engine ramp up to full speed smoothly.
- When the full range has been measured, slowly ramp down the throttle and close the carburetor needle valve so that fuel does not leak back into the engine or out of the carburetor throat onto the test bench.
- If a non-standard fuel is tested (i.e. any non GlowFuel-based fuel), it is recommended that methanol is ran through the engine again in order to “clean out” the various fuel delivery components.
- Future tests can use the stoichiometry map in order to better tune the engine.

Calibration and assessment of carburetor needle valve position

In order to find a universal way to measure the position of the needle valve, some calibration is necessary. The position of the carburetor needle valve is computer controlled and adjusted by the operator. The needle valve position is measured by an analog angle encoder that is attached to the needle valve by a small rubber belt. This calibration was particularly important for the stoichiometry testing.

More testing and calibration resources

This entire testing procedure was a living document updated and edited by everyone who used the test setup. If quick access is needed, use the following media to connect with a smartphone:



This QR media tag will take the reader directly to the fuel flexible testing protocol

For the legacy systems (2005 and before), many of the adjustments and measurements were taken manually. The system that was built in 2009 added LabVIEW as an automated data collection system and by 2012, the same system had electronic control and measurement of the key engine parameters (throttle, carburetor needle valve position, mechanical loading, etc.) and new mechanical braking system that could load the engine until stall (the 2009 and earlier systems could not achieve this requirement). These data will be presented in section 0.

Legacy dynamometer (2005)

The legacy dynamometer built by Cardes, *et al.* lacked data logging software and the measurements had to be taken by hand, sequentially in the short periods of time where the engine ran stably. Throttle position was manually adjusted and the engine was loaded electrically and power output was measured across this load resistor (which is a neither non ideal loading mechanism nor power output measurement). The reader is referred to the Cardes *et al.* publication for more details [93]. Additionally, chapter 3 has commentary on the shortcomings of this particular dynamometer.



Figure 125: Left: testing dynamometer for the O.S. Graupner Wankel Engine. Right: Close-up view of generator and test stand [93].

The completely redesigned fuel flexible dynamometer (2009)

The 2009 system as it was described in detail in Chapter 3, had many upgrades from the Cardes system, but suffered from two key limitations: an electrical loading system and manual control of engine parameters (throttle, carburetor needle valve adjustment, electrical loading and glow plug temperature). However, this was a still a significant upgrade from the 2005 system in the sense that all sensor measurements were recorded by a data logging system with a 1 second sample rate.

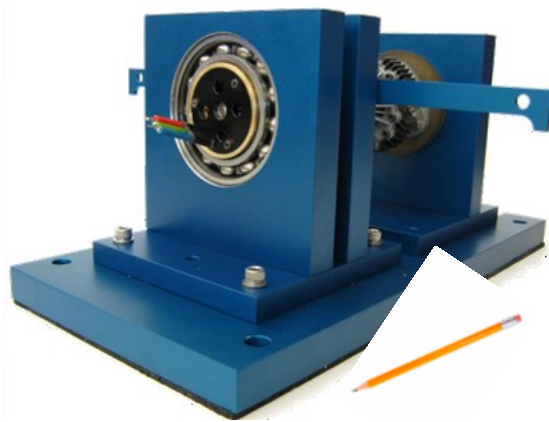


Figure 126: The 2009 version of the fuel flexible engine dynamometer with an electrical loading system.

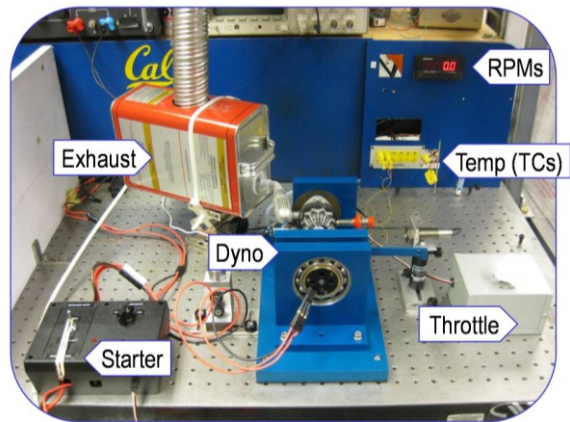


Figure 127: The 2009 dynamometer with all the required peripherals to operate and test the fuel flexible engine.

Improved and refined fuel flexible dynamometer (2012)

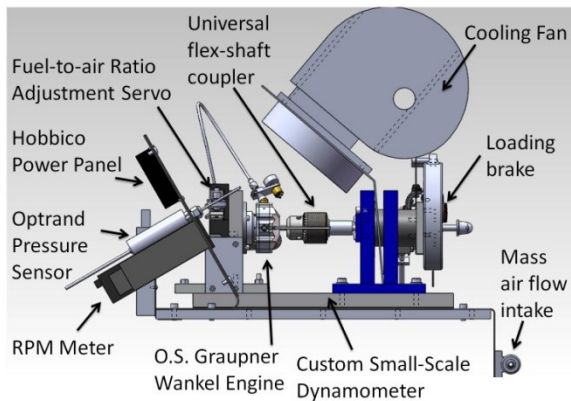


Figure 128: the updated fuel flexible engine dynamometer and its components. Not shown in this image: automated fuel switching system and the emissions exhaust collector.

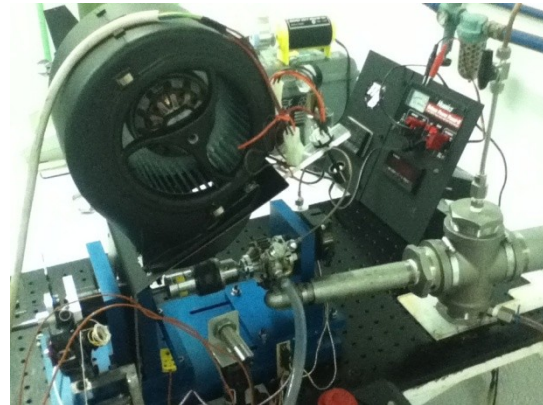


Figure 129: the actual system that was re-assembled and enhanced at the Universidad Politécnica de Madrid. This image also includes a stainless steel emissions measurement exhaust collector that was designed by visiting research Nicholas Maiden.

As the dynamometer continued to improve—namely with the inclusion of a mechanical braking system, electronic control of engine parameters and more sensors—the data became more reliable, better characterized and more repeatable.

This new dynamometer system could regularly set the glow plug temperatures (see glowplug calibration in APPENDIX C), throttle positions, carburetor needle valve and engine loading settings all at the push of a virtual button within the LabVIEW interface. This greatly improved the ability to run the engine reliably, collect data and maintain a vigilant watch on whether the system was in danger of overheating, breaking, causing damage or injuring researchers (thankfully the latter never happened, knock on wood).

Mechanical power output results for each fuel tested

Methanol

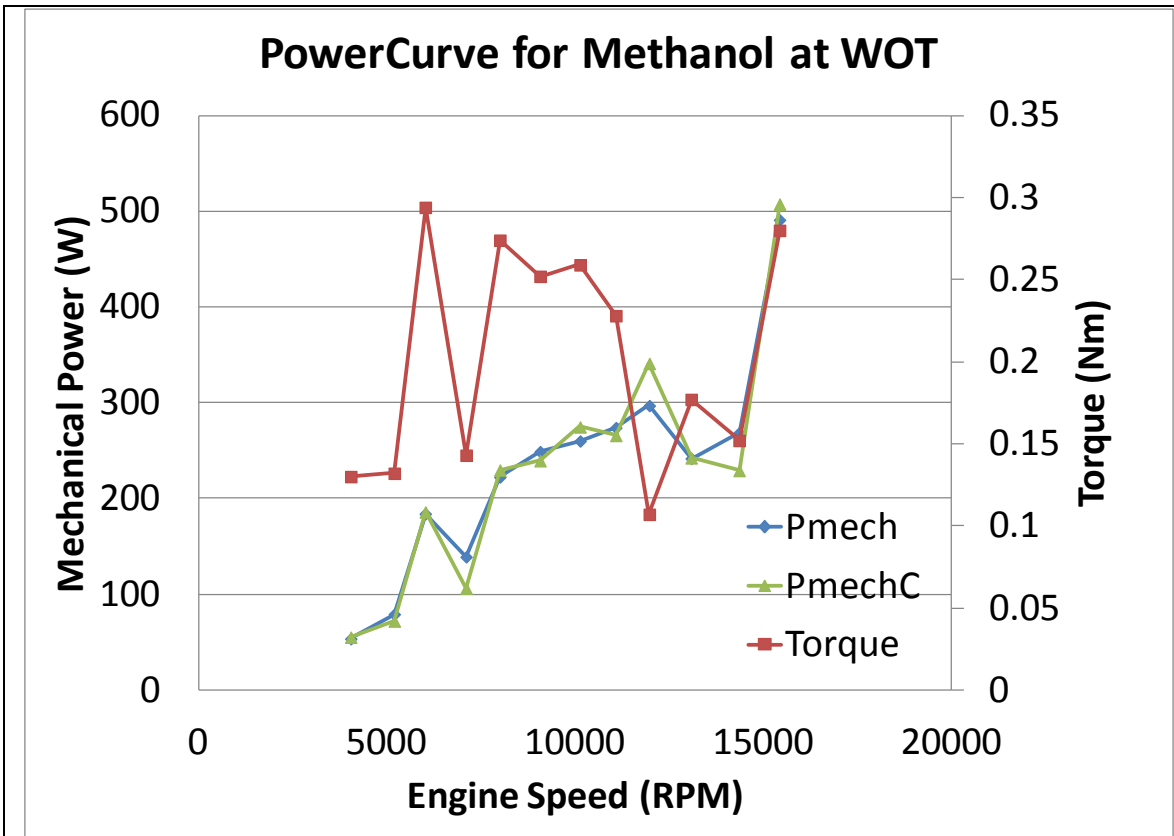


Figure 130: The measured mechanical power output of the O.S. Graupner 4.97 cc Wankel. This is the native fuel for the engine. The glow plug is turned ON at start but is then disconnected upon reliable compression ignition. The curve “PmechC” represents a calculated version of the mechanical power because the calculation done in real-time by LabVIEW was delayed about 0.5s.

Stoichiometry Value (LVP)	-228
Max Power	507.5 W @15900 RPM
Average External Engine Temp	52.3 °C
Average External Exhaust Temp	46.3 °C
Cooling fan speed (see Appendix C)	Level 3 - 850 m ³ /h
Mass Fuel Flow Rate	0.49 g/s
Maximum Efficiency Recorded	13.2%

Gasoline (87 Octane)

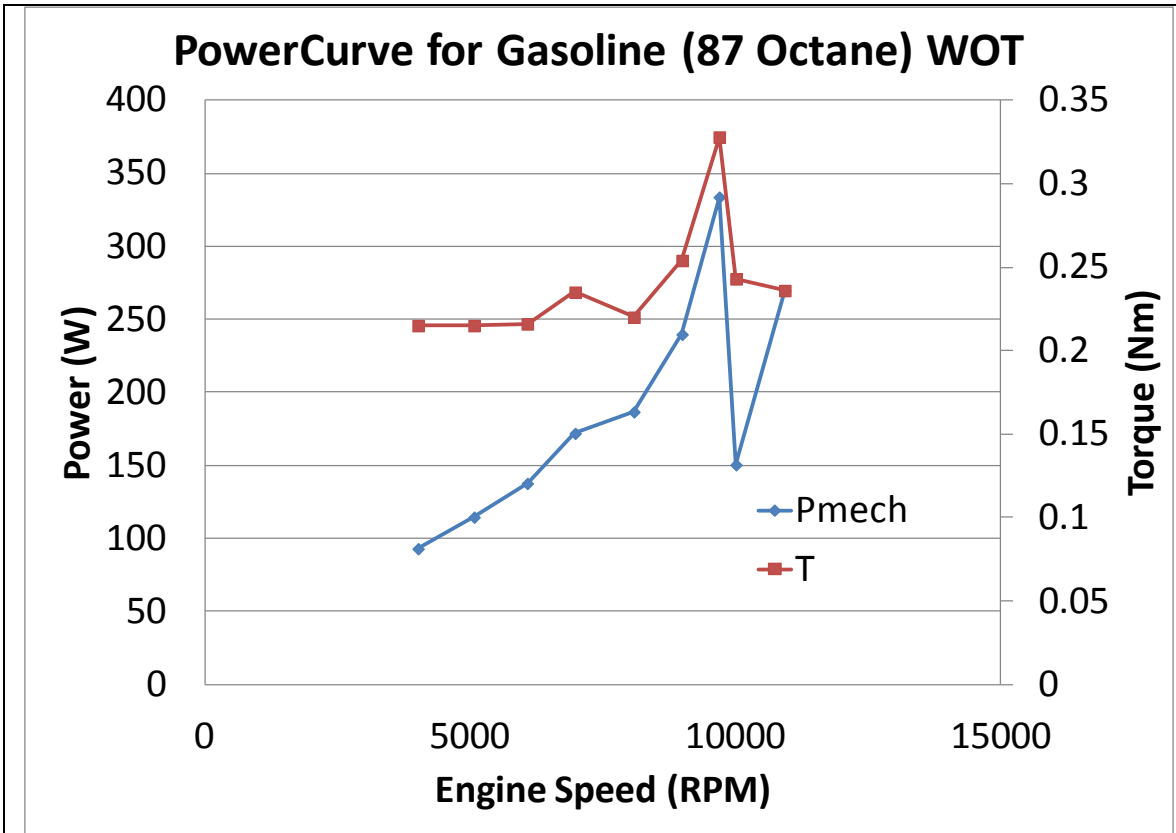


Figure 131: Mechanical power output of 87 octane fuel while running at 100% WOT. Current was constantly supplied to the glowplug during this test.

Stoichiometry Value (LVP)	-228
Max Power	333.7 W @9700 RPM
Average External Engine Temp	64.8 °C
Average External Exhaust Temp	77.5 °C
Cooling fan speed (see Appendix C)	Level 3 - 850 m ³ /h
Mass Fuel Flow Rate	0.09 g/s
Maximum Efficiency Recorded	15.9%

Jet Propulsion 8 (JP8)

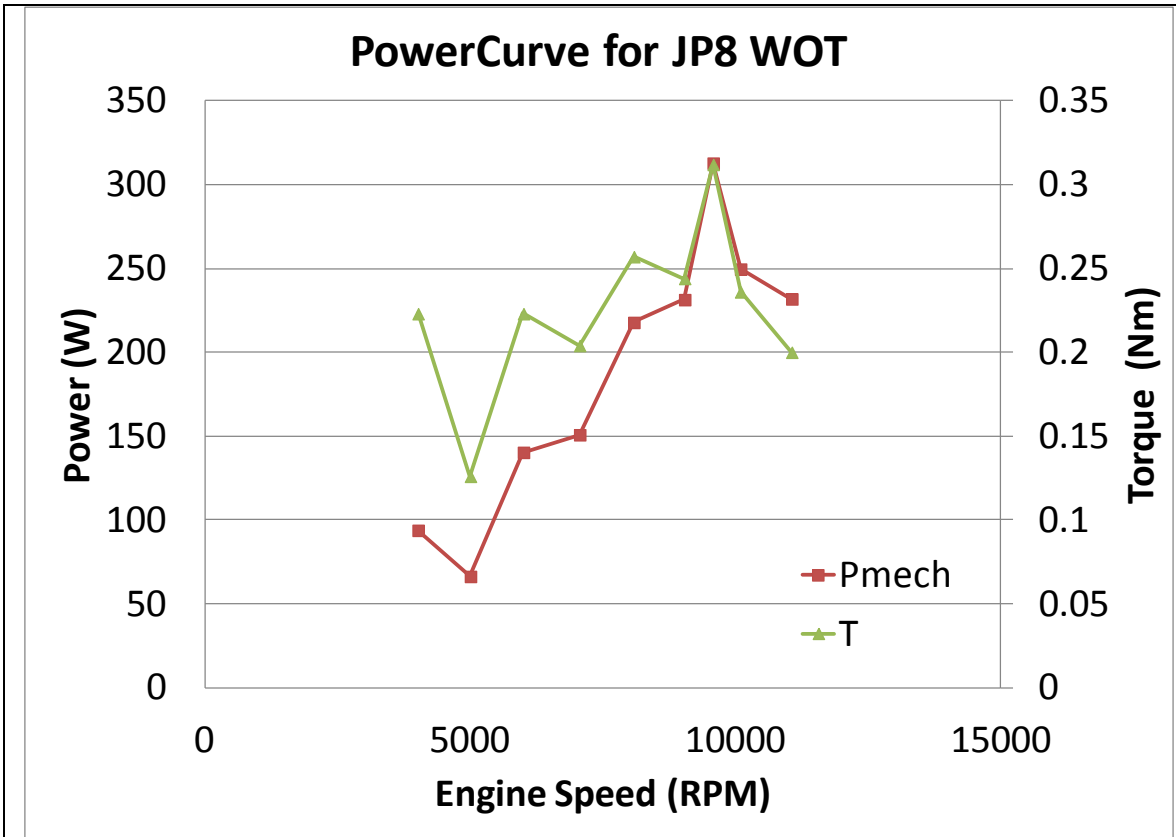


Figure 132: Mechanical power output of aviation grade JP8 jet fuel while running at 100% WOT. Current was constantly supplied to the glow plug during this test.

Stoichiometry Value (LVP)	-182
Max Power	312.8 W @9600 RPM
Average External Engine Temp	82.2 °C
Average External Exhaust Temp	66.4 °C
Cooling fan speed (see Appendix C)	Level 3 - 850 m ³ /h
Mass Fuel Flow Rate	0.22 g/s
Maximum Efficiency Recorded	3.0%

Diesel

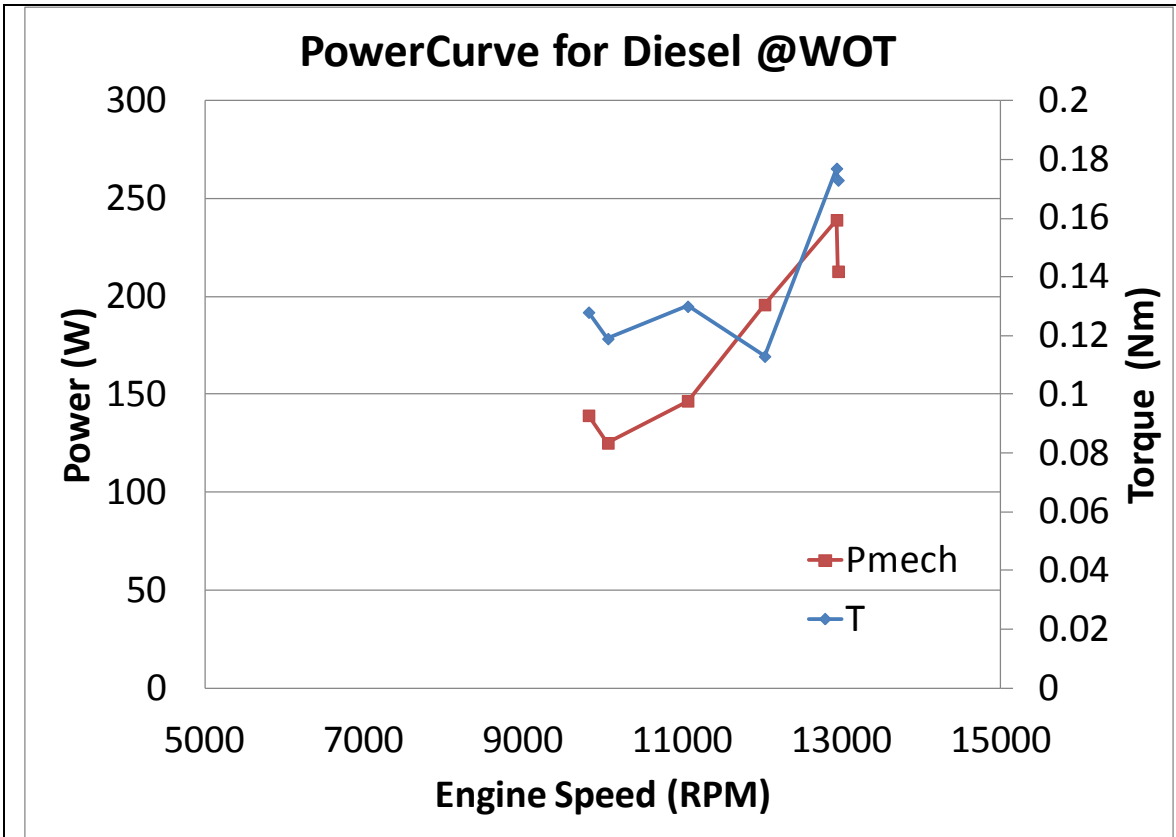


Figure 133: Mechanical power output of no. 2 diesel fuel while running at 100% WOT. Current was constantly supplied to the glow plug during this test.

Stoichiometry Value (LVP)	-196
Max Power	239.2 W @12940 RPM
Average External Engine Temp.	146.2°C
Average External Exhaust Temp	114.7 °C
Cooling fan speed (see Appendix C)	Level 3 - 850 m ³ /h
Mass Fuel Flow Rate	2.79 g/s
Maximum Efficiency Recorded	0.2%

BioDiesel

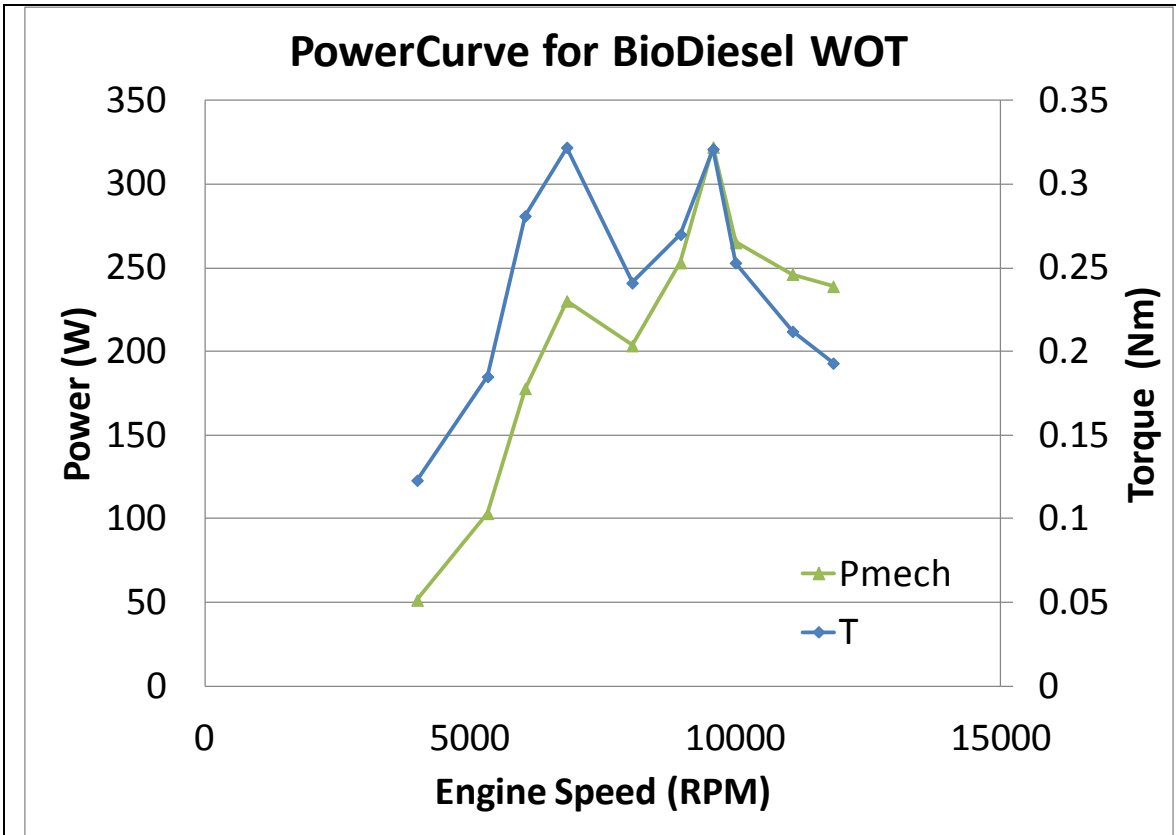


Figure 134: Mechanical power output of BioDiesel fuel. Current was supplied to the glow plug during start but was later removed during this test.

Stoichiometry Value (LVP)	-340
Max Power	322.2 W @9600 RPM
Average External Engine Temp	137.8°C
Average External Exhaust Temp	120.8 °C
Cooling fan speed (see Appendix C)	Level 3 - 850 m ³ /h
Mass Fuel Flow Rate	0.41 g/s
Maximum Efficiency Recorded	1.6%

Measured and simulated fuel-flexible engine operating characteristics

Stoichiometry values and flammability limits

Goal of stoichiometry experiments

The goal of the stoichiometry experiment was to determine the lean and rich flammability limits of each tested fuel (LFL and RFL, respectively) under fuel-flexible operation in a 4.97 cc OS Wankel engine. The carburetor on this engine has a fuel-flow metering needle valve and the fuel-flexible engine dynamometer has both an electronic

control and a measurement of the needle valve position within LabVIEW (any value controlled by LabVIEW will be known as the LabVIEW Position or LVP). The position values in the dynamometer system are calibrated to the flammability / stoichiometry characteristics of each fuel tested. Maruta *et al.* describe in more detail microscale flammability limits in the context of flame quenching and stability management [191]. To relate this LVM value to a z-height of the fuel valve needle, a plot is found in Chapter 3 of this dissertation.

This experiment is successfully conducted by running the engine on each fuel, achieving stable engine operation at a reliable stoichiometry, throttle and dyno brake loading positions and then, adjusting the carburetor mixture (lean or rich) until the engine stalls. The point of stall indicates either a rich flammability limit (RFL) or a lean flammability limit (LFL) and characterizes the limits of fuel-flexible combustion achievable by the OS Wankel engine.

Flammability limits of methanol+nitromethane “Glowfuel”.

The Methanol+Nitromethane “Glowfuel” is always tested first as it is the standard fuel used by the OS Wankel engine. After preparing the engine given the standard protocol listed in APPENDIX D, each stoichiometry test is conducted: richening the mixture until stall and leaning the mixture to stall. The steady-state operation of the engine using Glowfuel was achieved using the following measured engine parameters:

Table 9: Steady-state operating conditions for methanol+nitromethane "Glowfuel" mixture.

Throttle position	42% WOT
Engine loading position (LVP)	101
Cooling fan speed (see Appendix C)	Level 2 – 630 m ³ /h
Ambient Temperature	17 °C
Relative Humidity	50 %
Pressure	88.3 kPa
Glow Plug Current	LVP = 63 or 0.6A

Below in the following figure (Figure 135), this is a raw run where the mechanical power output is compared to the position of the carburetor needle valve. The value is arbitrarily negative and could technically change if the experimental setup is adjusted. The absolute value is the only value of importance and the values upon which the engine stalls. From plot however, the engine stalls are noted and the limits of the stoichiometry are observable.

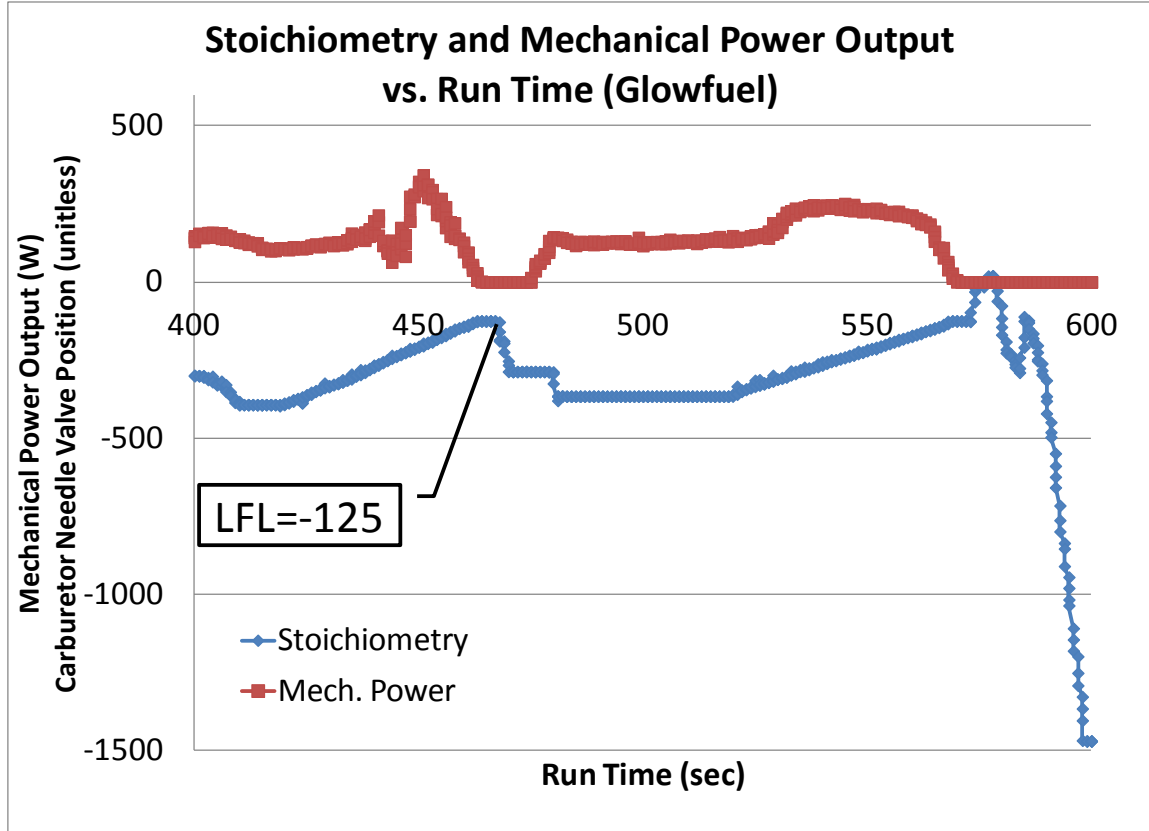


Figure 135: Determining the lower and upper flammability limits of glowfuel: methanol+nitromethane. The lower flammability limit is indicated by the lowest stoichiometric sensor value that maintained combustion. In this case, the LFL appears to be around -125. *Note: the negative value is arbitrary and based on how the stoichiometry angle encoder sensor is setup. The flatline at zero clearly suggests the engine is no longer running.

It is important to note however, the optimal value of operation is closer to -200 in terms of the sensor position. And the lower flammability limit occurs at -125 while the upper flammability limit appeared to be much much higher, around -1300. However, with repeated testing, values around -500+ (Figure 136) appeared to be capable of stalling the engine. The appears to be either wildly tolerant of rich mixtures of methanol+nitromethane “Glowfuel” or the carburetor needle valve cannot simply deliver any more fuel to the engine at the steady-state throttle position. The lower value is consistently around -125 and is concluded to be the LFL of the glowfuel.

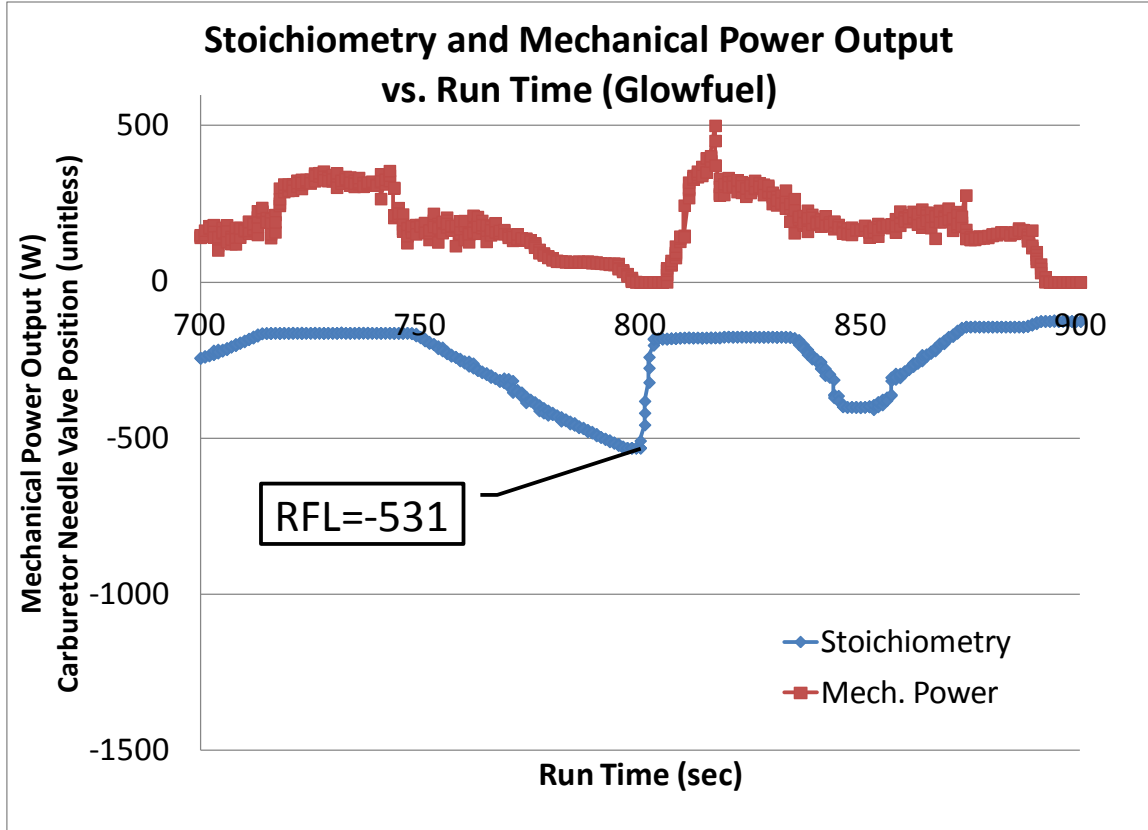


Figure 136: The rich flammability limit found while combusting Glowfuel. The LFL was recorded in the prior test to have a LVP of -125.

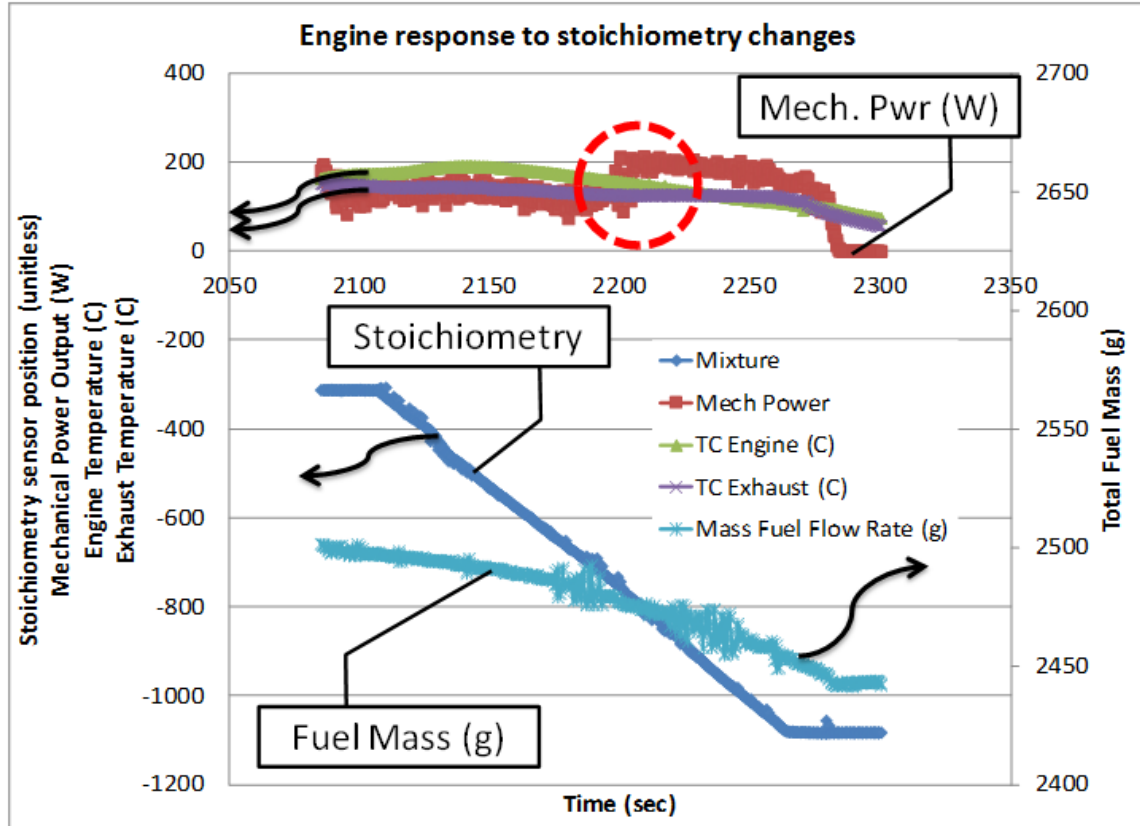


Figure 137: Upon early testing, stable operating points were established but the rich flammability limit proved difficult to obtain. The dashed circle detailed in this figure is interesting in that the engine spontaneously spiked in power without changing the throttle position nor the load brake position. However, as can be seen, the stoichiometry was being changed as a function of time with little to no affect on the output power. The temperatures can be observed to have changed, along with the mass fuel flow rate (from approx 0.25 g/s to about 0.5 g/s), therefore it appears that carburetor fuel flow valve regulator becomes wide open at about ~800 and does not stall the engine however does not explain the power spike. This likely suggests erratic engine operation or irregularities spawned by temperature changes within the system.

Flammability limits of 87 octane (gasoline)

Since earlier testing using the original version of the fuel flexible engine dynamometer, the control and performance of the OS Wankel engine while combusting 87 octane fuel has improved dramatically. Having more accurate control of the throttle in addition to dynamic adjustment of the carburetor stoichiometry regulation needle valve, the engine has even more response.

Table 10: Steady-state operating conditions for 87 octane (gasoline).

Throttle position	11% WOT
Engine loading position	145

(LVP)	
Cooling fan speed	Level 2 – 630 m ³ /h
Ambient Temperature	18 °C
Relative Humidity	43 %
Pressure	89 kPa
Glow Plug Current	LVP = 124 or 1.4A

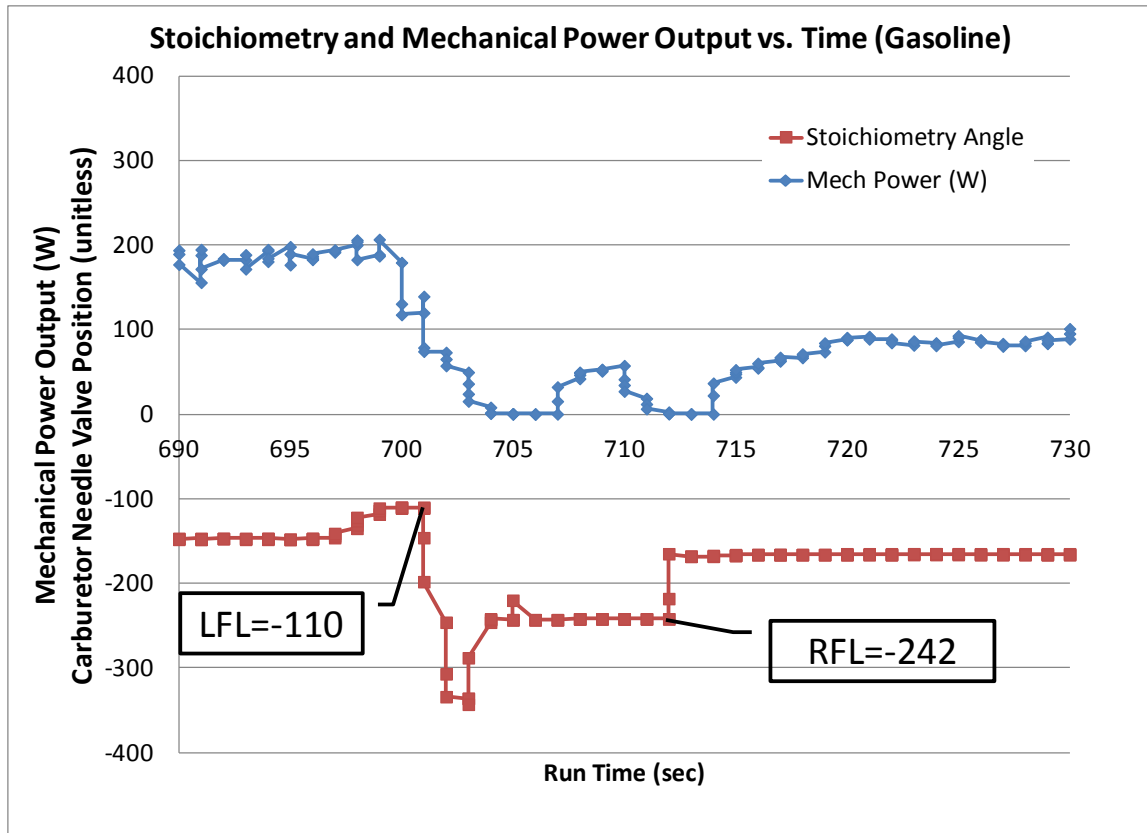


Figure 138: Lean and rich flammability limits of 87 Octane Gasoline.

Flammability limits of JP8 (military grade fuel)

The combustion of JP8 fuel is important specifically for military applications of fuel-flexible technology. The limits of flammability for JP8 were relatively simple to obtain using the dynamometer system. Other fuels (such as BioDiesel) proved more difficult.

Table 11: Steady-state operating conditions for JP8.

Throttle position	19% WOT
Engine loading position	149

Cooling fan speed	Level 2 – 630 m ³ /h
Ambient Temperature	18 °C
Relative Humidity	43 %
Pressure	89 kPa
Glow Plug Current	LVP = 118 or 1.4A

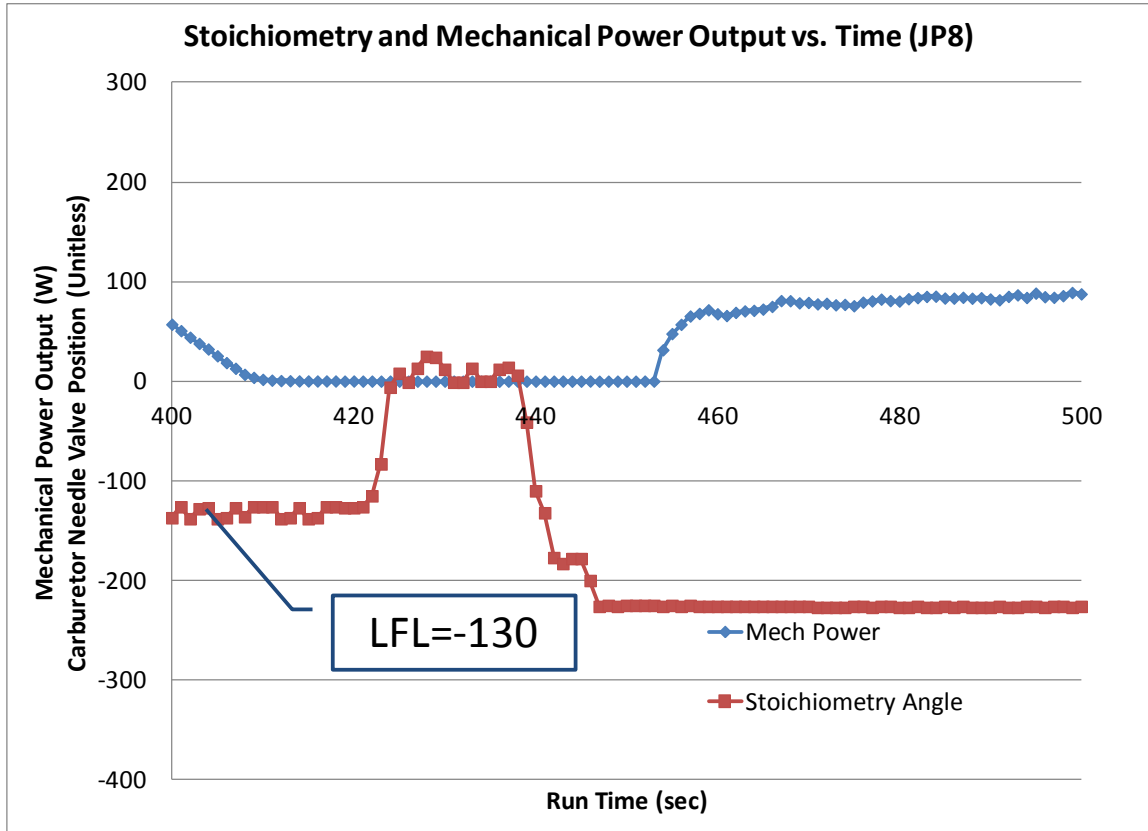


Figure 139: The recorded lean flammability limit of JP8.

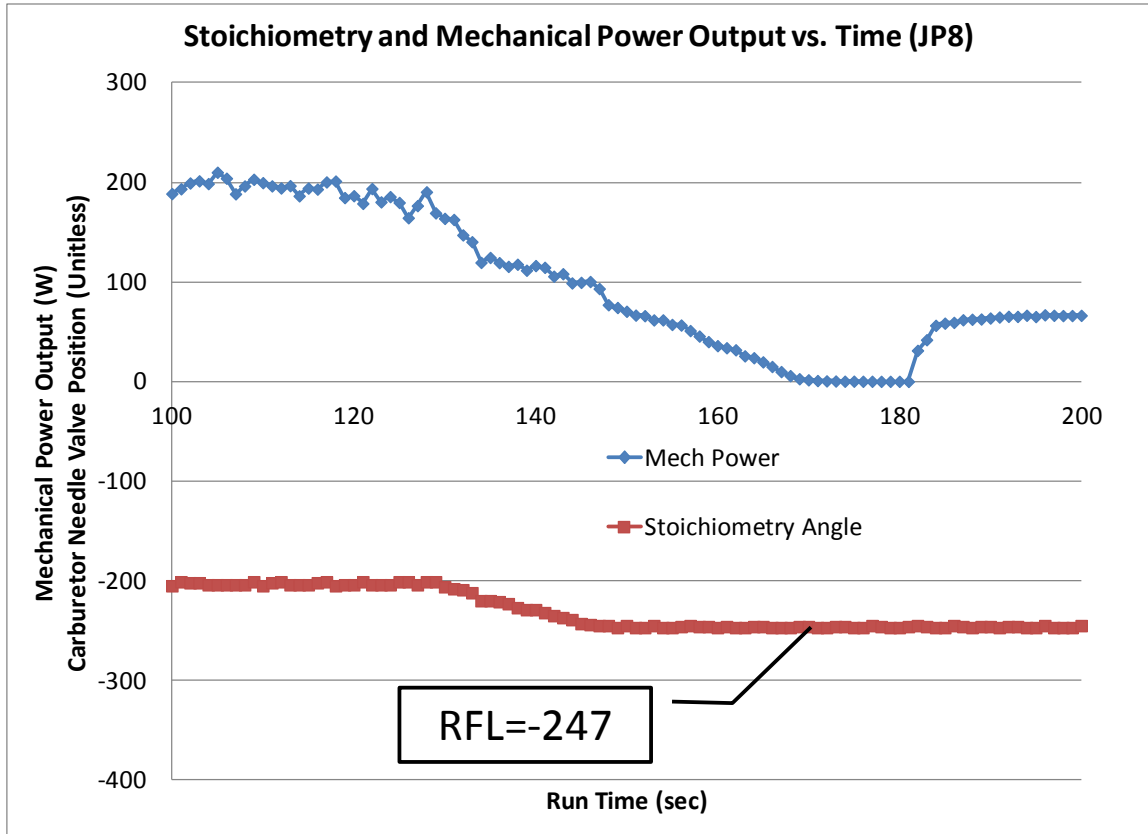


Figure 140: The recorded rich flammability limit of JP8.

Flammability limits of Diesel

The combustion of diesel fuel typically needs the glowplug ignited during combustion. The lower limit was found to be -188 and the upper limit went beyond the capabilities of the carburetor valve.

Table 12: Steady-state operating conditions for Diesel.

Throttle position	12% WOT
Engine loading position (LVP)	87
Cooling fan speed	Level 2 – 630 m ³ /h
Ambient Temperature	19 °C
Relative Humidity	36 %
Pressure	90 kPa
Glow Plug Current	LVP = 131 or 1.4A

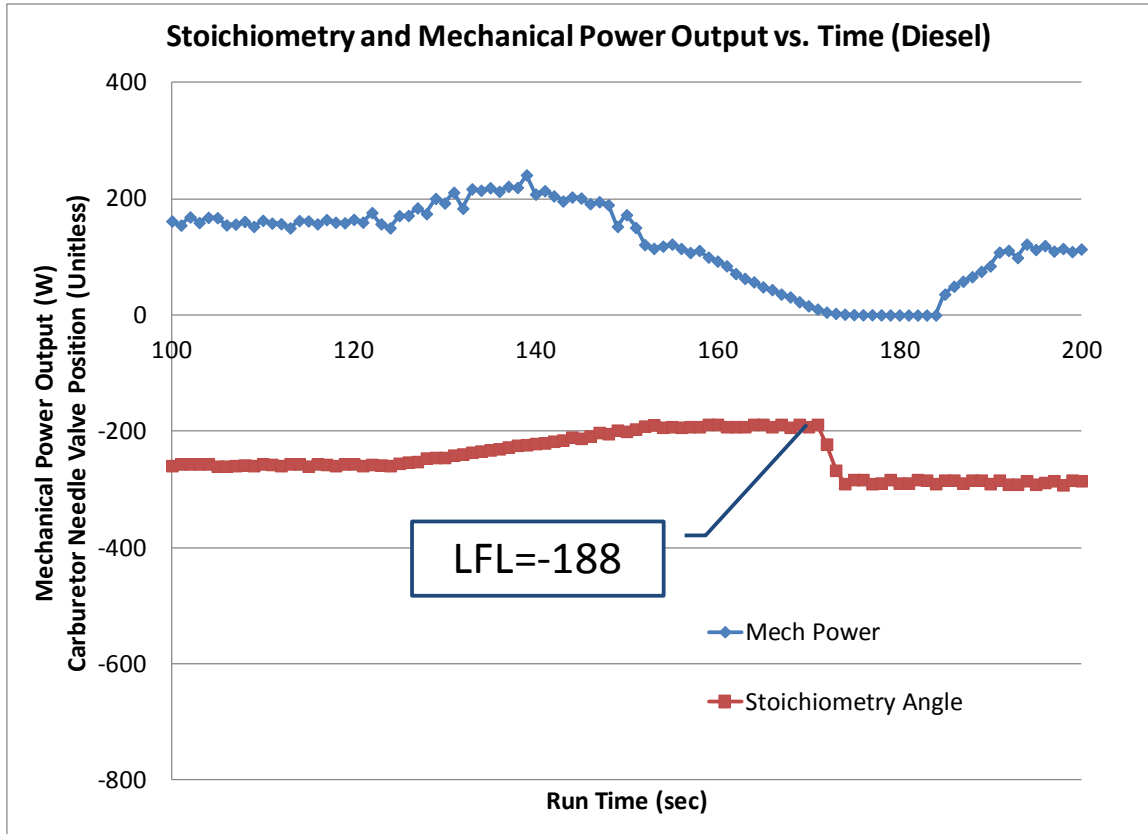
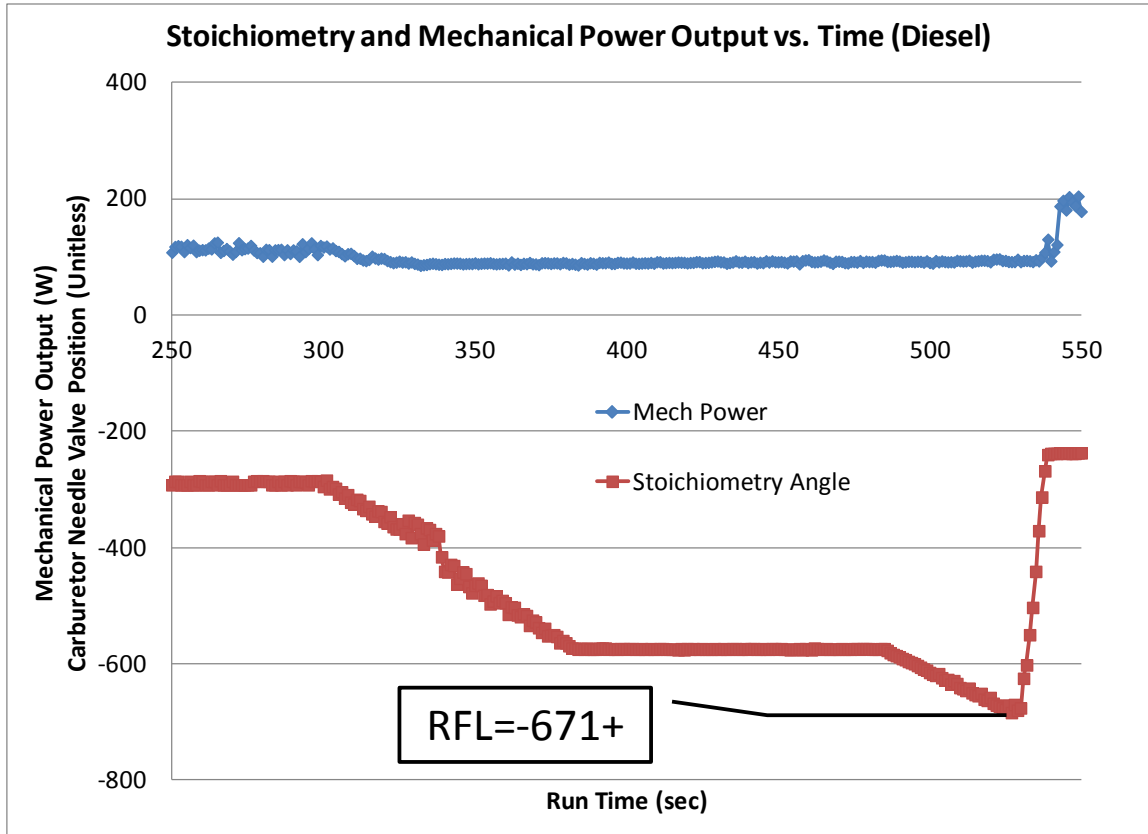


Figure 141: Finding the lower flammability limit of the diesel fuel.

As well, the rich flammability limit was unachievable due to the maximum flow fuel flow found in the carburetor.



Flammability limits of BioDiesel

The limits of BioDiesel were relatively clear and easy to determine given the prior experience from the measurement of the Glowfuel, 87 octane gasoline and the JP8.

Table 13: Steady-state operating conditions for BioDiesel.

Throttle position	12% WOT
Engine loading position (LVP)	87
Cooling fan speed	Level 2 – 630 m ³ /h
Ambient Temperature	19 °C
Relative Humidity	36 %
Pressure	90 kPa
Glow Plug Current	LVP = 131 or 1.4A

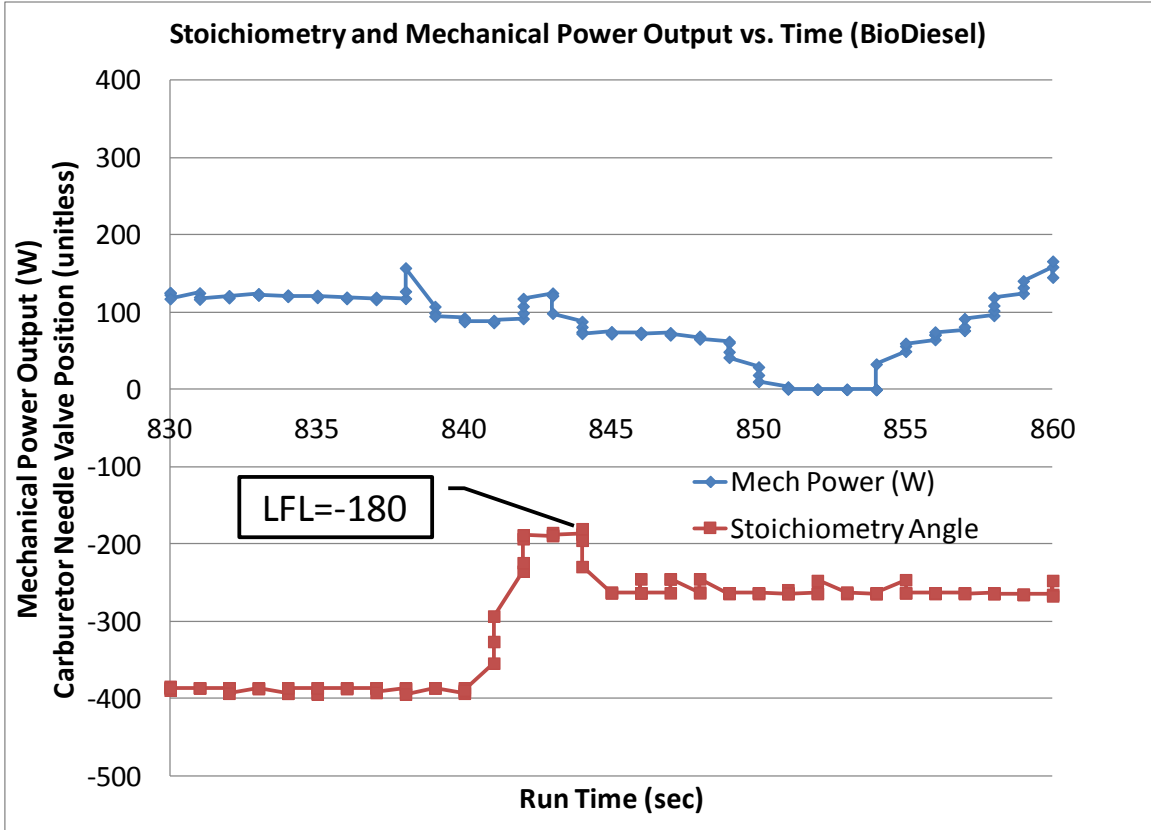


Figure 142: Lean flammability limit of BioDiesel.

For the rich flammability limit of BioDiesel:

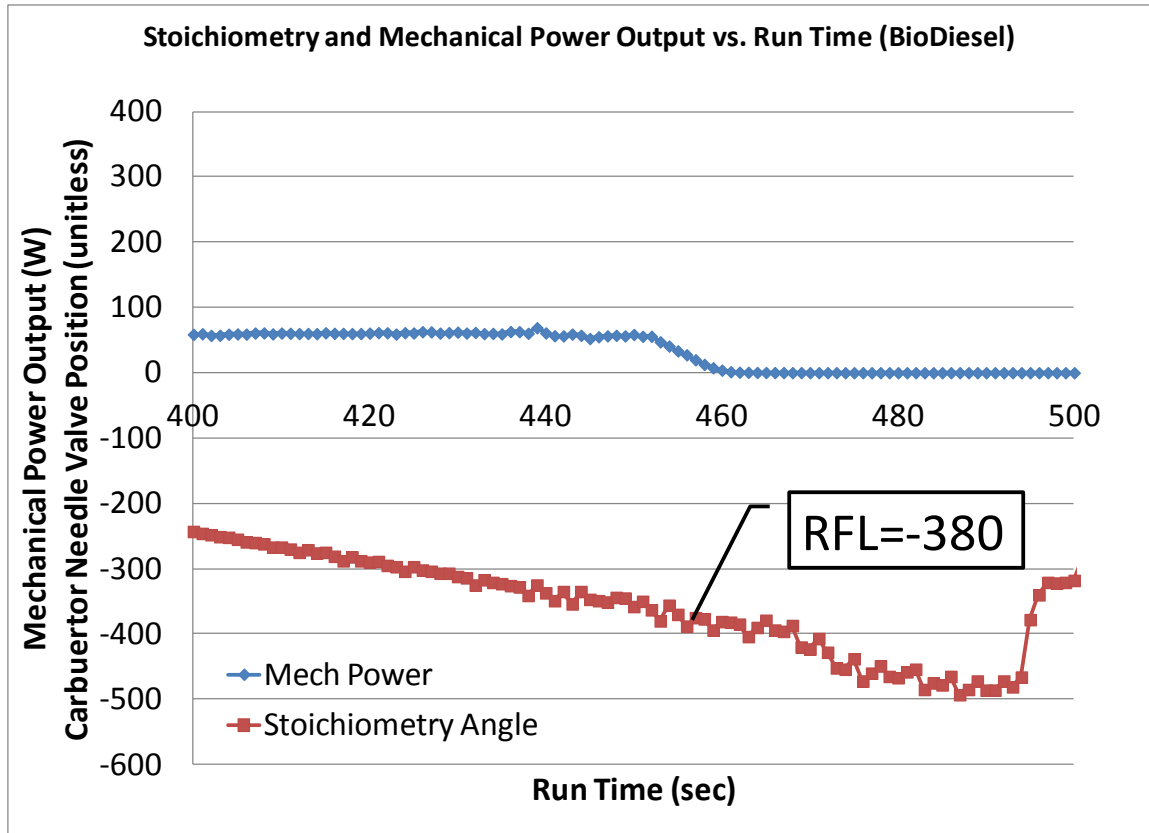


Figure 143: Finding the rich flammability limit for BioDiesel.

Stoichiometry experimental conclusions

After testing each fuel, it was determined that the lean and rich flammability limits could be obtained. The challenges that surfaced were finding some limits for the various fuels. For example, methanol proved difficult because the upper flammability limit could not be achieved by the maximum flow allowable inside the needle valve. Thus, the carburetor could not physically run and achieve the rich fuel limit for methanol.

For gasoline and other fuels, because their air-to-fuel ratios tend to be above 12:1, the rich flammability limit is easier to reach and the flexible range of stoichiometries using the stock carburetor is limited.

Table 14: The lean and rich flammability limits in the context of the fuel flexible dynamometer.

References: [192]	LFL (sensor LVP)	RFL (sensor LVP)	Measured Optimum Stoichiometry	LFL Limit in air (reference)	RFL Limit in air (reference)
87 Octane	-100	-242	-228	1.4%	7.6%

(Gasoline)					
GlowFuel	-125	-1300	-228	6.7-7.3%	36%
JP8 (Kerosene)	-145	-247	-130	0.7%	5%
BioDiesel	-170	-500+	-340	-	-
Diesel	-188	-500+	-196	-	-

Below is the range of LFL and RFL for each fuel in a visual presentation so as to better understand quickly the range of stoichiometries that should function for each fuel.

Stoichiometry Ranges (Number represents: a reference position within LabVIEW)		Fuel			
		87 Octane	JP8	Diesel	BioDiesel
-100					Lean
-110	GlowFuel	-110			Max Pwr
-120	-125		JP8		Rich
-130			-130		
-140					
-150					
-160	-228	-228			BioDiesel
-170	-228	-242		Diesel	-170
-180			-182	-188	
-190				-196	
-200					
-210					
-220	-228	-228			-220
-230					
-240		-242	-247		
-250					
-260					
-270					
-280					
-290					
-300+	-500+			-500+	-500+

Figure 144: The range of stoichiometries that support fuel-flexible engine operation. These data were collected with the glowplug continuously ignited. These tests typically concluded when carburetor or exhaust screws fell out. To understand this chart, please review LVP in the Nomenclature which can be found in the APPENDIX.

Maintaining combustion across all tested fuels

One of the main goals of this research is to allow this inherently fuel-flexible engine to run continuously on a variety of fuels. As has been presented, many fuels produce positive power in this engine, however initially each fuel was tested independently and output powers were not recorded consecutively. This stoichiometry characterization of the lean and rich flammability limits made continuous fuel-flexible operation much more achievable and below we present the results of a continuous run.

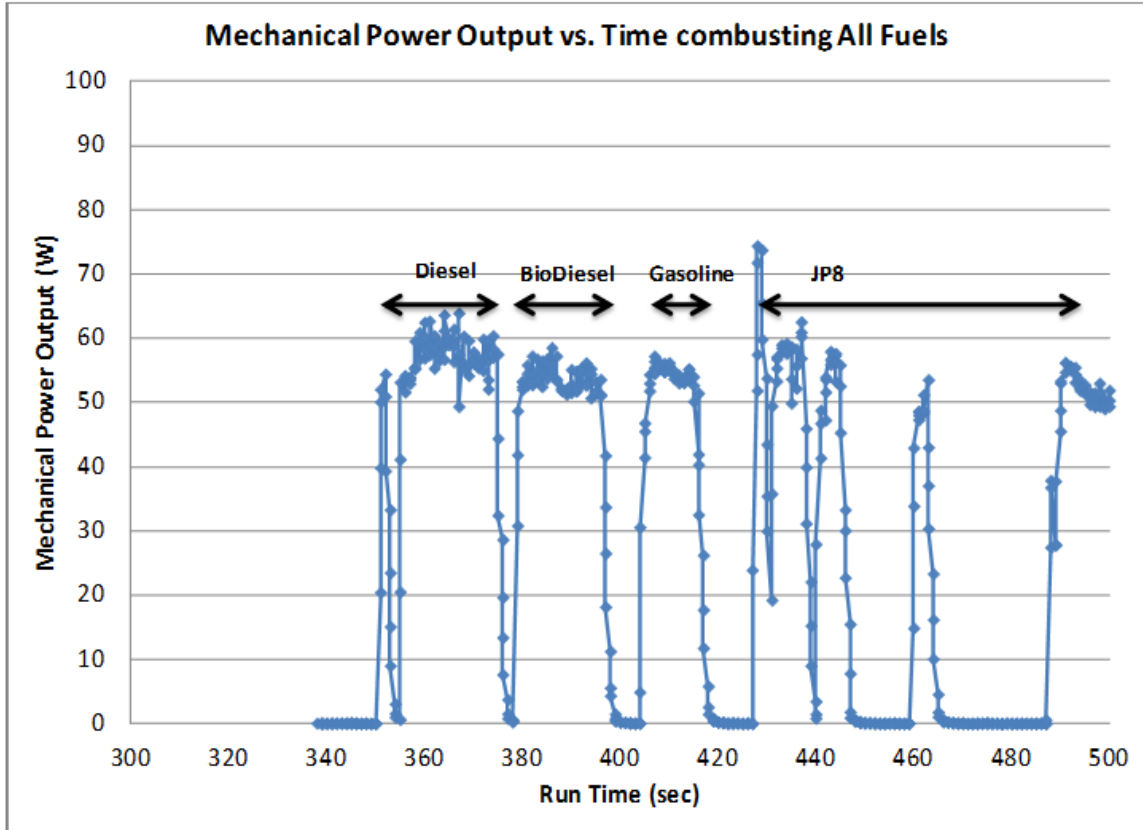


Figure 145: An attempt to combust several fuels consecutively without losing output mechanical power. By changing the stoichiometry via the carburetor needle valve, near optimal operating conditions can be quickly obtained and the engine can maintain combustion (the throttle and glow plug temperatures typically remained constant).

Measured efficiencies

The efficiency of the motor is calculated based on the total energy content of the fuel in comparison to the measured mechanical power output. This is calculated by utilizing the heat of combustion of each fuel and multiplying it by the dynamic fuel flow rate and comparing it to the mechanical power produced on the dynamometer. The fuel flow rate is measured using a precision mass balance and plotting it versus time. Due to the limitations of the scale, being precise only to ± 0.1 g, reading the fuel flow rate dynamically and accurately was challenging considering that the rotary engine consumed fuel on the order of 0.01 g/s. Additionally, light gusts of ambient room air coming from the fume hood and recirculating air caused the mass flow rate measurements to have some noise.

Considering these limitations, the efficiency calculations were approximated by determining an average fuel flowrate various engine speeds / throttle positions and calculating the efficiency for each power output recorded.

The maximum efficiency recorded of the motor across several different fuels can be seen in the table below. Normally the efficiency is calculated using the Lower Heating Value (LHV) but these values could not be found for each fuel therefore the more readily available Higher Heating Values (HHV) were used. In these calculations, the average mass fuel flow rate was used due to the inability of the Ohaus Explorer scale to measure precisely fuel flow rates on the order of 0.01 g/s.

$$(24) \quad \eta = \frac{P_{meas}}{\dot{m}_f HHV}$$

Fuel	η_{min}	η_{max}	η_{avg}
Glow Fuel (methanol + nitromethane) (RPM > 10K)	1.4%	13.2% @ 15433 RPM	6.9%
Gasoline (RPM > 6K)	3.9%	15.9% @ 11197 RPM	8.8%
Diesel	0.00%	0.18% @ 12940	0.12%
JP8 (RPM > 6K)	0.8%	3.0% @ 9586 RPM	1.5%
BioDiesel (RPM > 6K)	0.6%	1.6% @ 9583 RPM	1.0%

The best efficiency was demonstrated—surprisingly—with 87 octane fuel mixed with two-stroke engine oil. Regardless, the efficiencies in general are all very low. This is largely due to the inherent design of using the fuel to cool the engine. These rich mixtures use the enthalpy of the fuel to convect energy out of the system. Other fuels and their efficiency ranged from 0.12% to 8.8% percent on average.

Testing MEMS sensor survivability

Being that fuel-flexibility relies on a series of real-time engine monitoring and the ability to dynamically control and change engine parameters, new and smaller sensors are always needed. In-chamber combustion sensors which are being actively investigated, are expected to enable optimization of the combustion event and better improve fuel-flexible combustion.

In this experiment, the survivability of a silicon MEMS temperature sensor, bonded to the inside wearplate with a chemically resistant and high temperature ceramic adhesive.

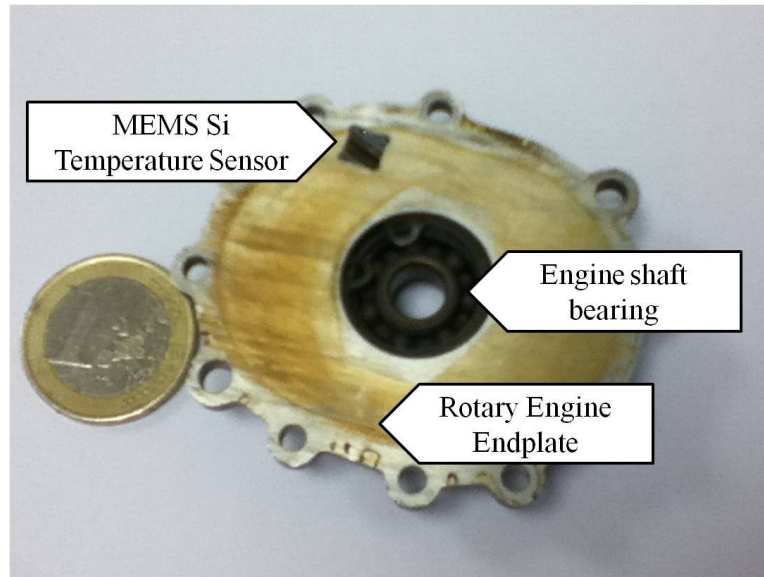


Figure 146: O.S. Graupner Wankel engine wearplate with embedded MEMS temperature sensor.

The procedure of this experiment was to run a baseline test with glowfuel and to ideally observe zero percent difference in the power output properties of the engine *with* the MEMS sensor and *without* the MEMS sensor.

Being that the automotive technology is destined to include sensors and actuators that are operating in the harsh environment of the combustion chamber, characterizing the survivability of such devices within this combustion environment is critical for sensor research and development. Especially because fuel flexible engine operation is largely dependent on engine parameters and the combustion characteristics of each fuel, embedding harsh-environment MEMS sensors into these engine environments have already begun. The goal of the plot below is to show that even in the presence of this silicon chip, the output performance of the engine remains unchanged.

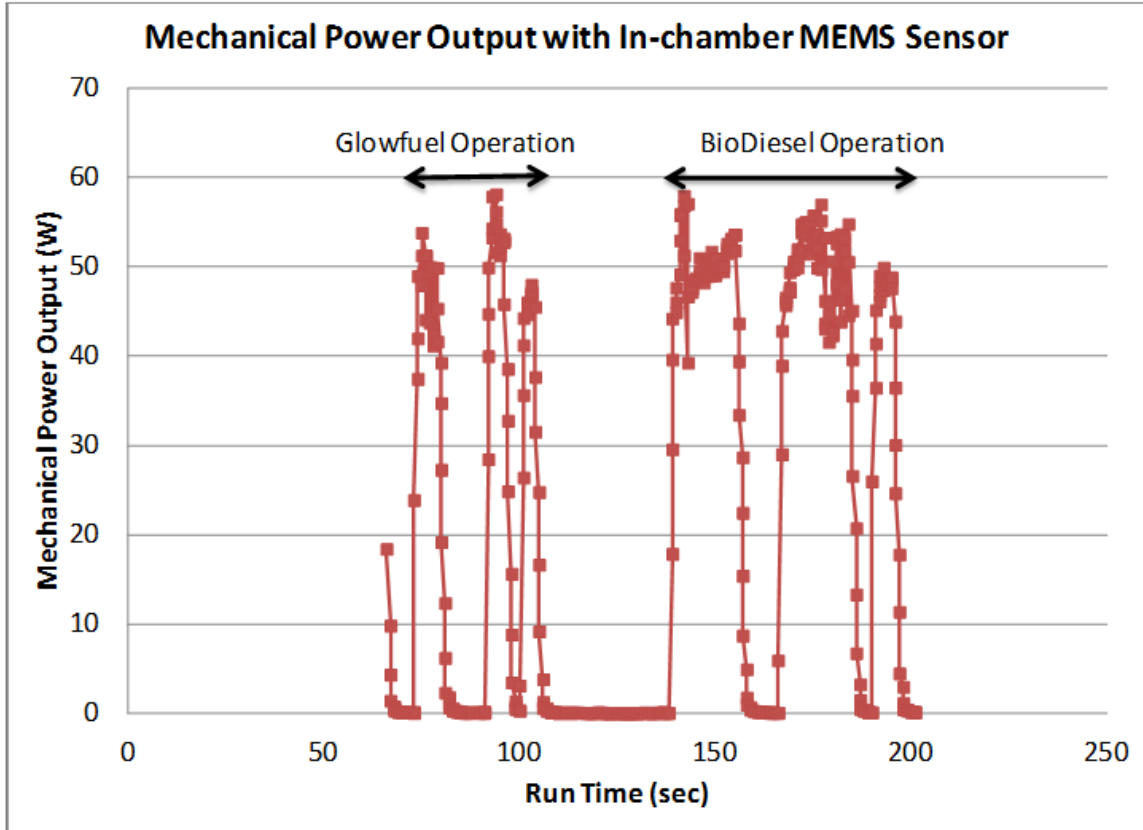


Figure 147: The OS Wankel in fact produced positive power with the MEMS sensor present inside the engine. However, upon breakdown of the engine, it was discovered that the MEMS sensor had been disintegrated and / or ejected out of the exhaust as it was no longer present.

Temperature characteristics

With the new ability to test the engine and compare a variety of engine parameters, various new insights about fuel flexibility and the OS Wankel engine operation could be extracted. Of particular importance for preserving the engine functionality and operation were the engine housing and exhaust temperatures. The loading brake temperature was also measured for fear of catastrophic meltdown as the braking mechanism is a mechanical disc brake for mountain bikes meant for rotational speeds of up to 1000 RPM. This brake has seen up to 15K RPM and continues to perform well.

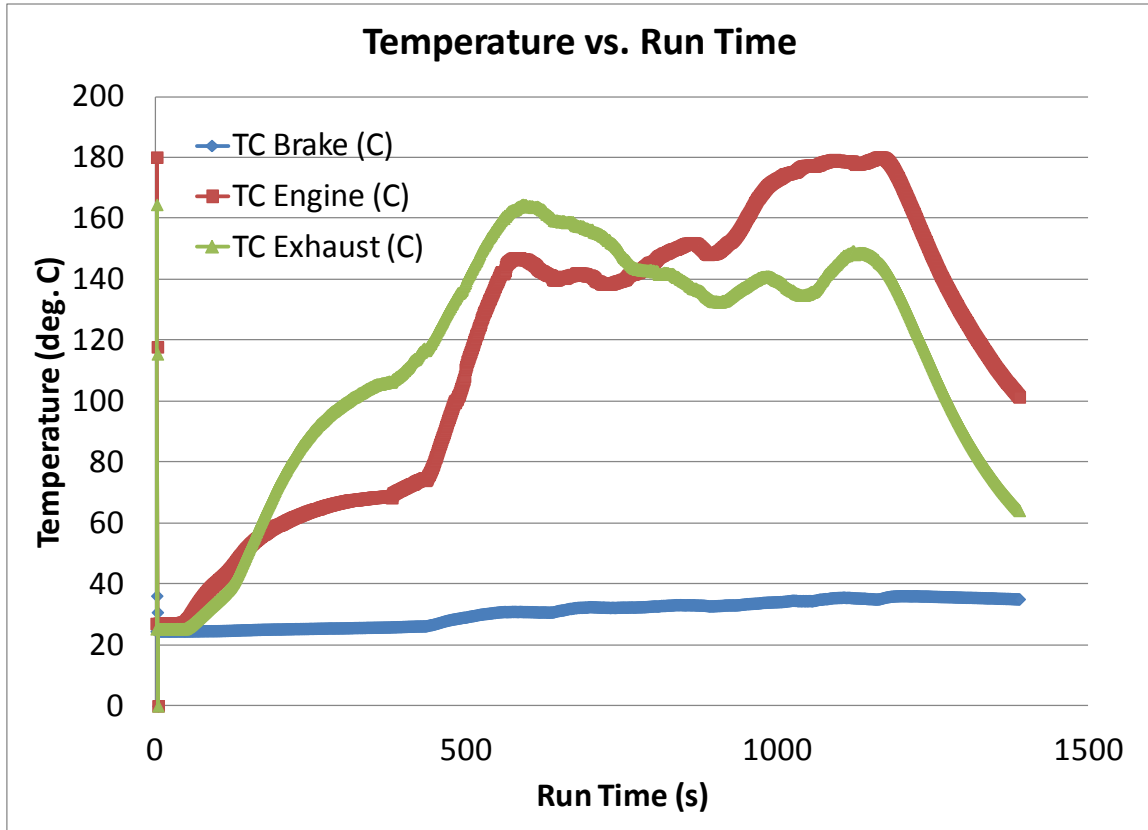


Figure 148: Temperature profile with time when combusting standard GlowFuel (82% Methanol, 16% Nitromethane and 2% Oil) (120705-engine-test-methanol-04). The engine temperature is critical for preserving the engine during operation of non standard fuels.

The exhaust temperature is unfortunately not measured in stream, but rather using an external screw that enters into the exhaust pipe and conducts the heat to the surface, contacting the thermocouple (Figure 149). The engine temperature is measured using a K-type thermocouple that is attached via the aluminum housing via an assembly screw (Figure 150). The brake temperature is measured for precautionary reasons to prevent damage to the mechanical loading system and reduce skepticism that the brake could handle the elevated speeds of the 4.97 cc O.S. Graupner Wankel engine (Figure 151). Follow the orange thermocouple cable until termination to find the measurement point.



Figure 149: Exhaust thermocouple position.



Figure 150: Engine housing thermocouple position.



Figure 151: Dynamometer break loading thermocouple.

Other useful thermal data is how the engine can be cooled by utilizing rich mixtures and thereby convecting the enthalpic heat content of the fuel. While extensive testing to find optimal stoichiometries for cooling were not conducted, the plot below shows that the temperature of the engine can be plotted against the engine stoichiometry and potentially be used to govern control algorithms.

$$(25) \quad T_{engine} = f(\text{Fan Speed}, \text{Stoichiometry})$$

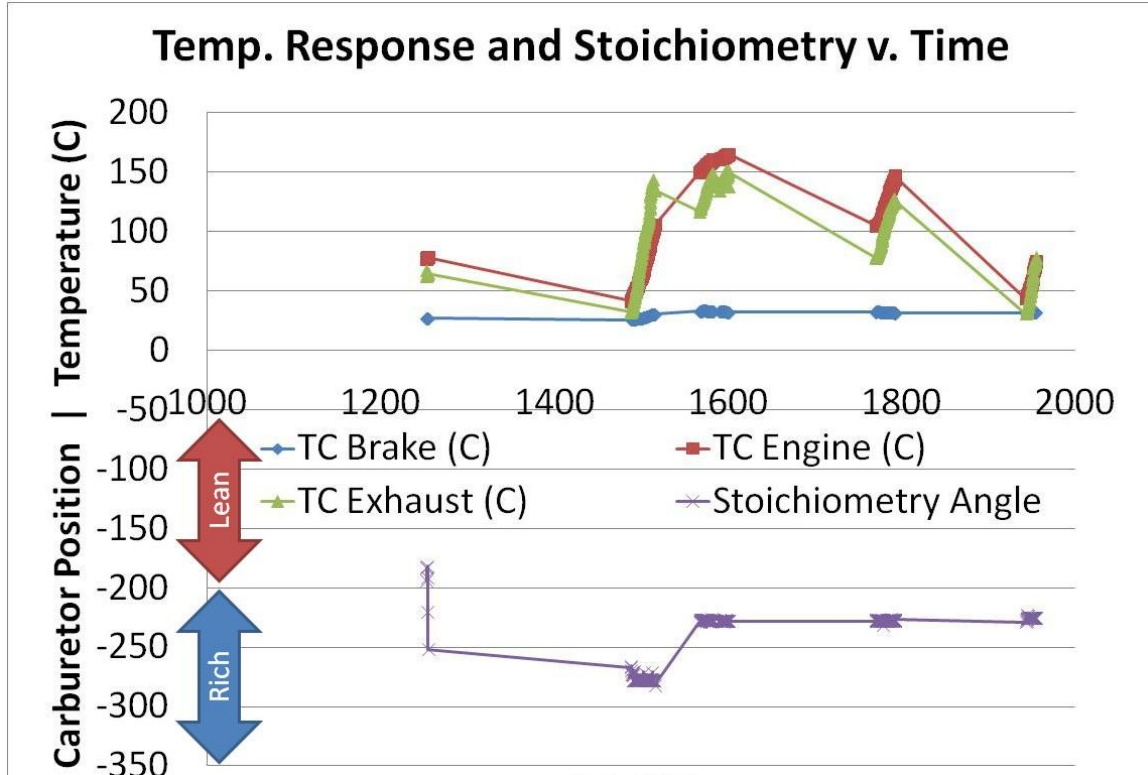


Figure 152: One method observed to cool the engine was by running rich mixtures. It can be observed how the temperature of the engine decreases with richer mixtures and heats up on leaner mixtures. Time is plotted in seconds.

Preliminary emissions results

The emissions are measured by a Lujan gas analyzer. The system measures the species percentage found in the exhaust port of the engine being tested. There are two probes: 1) which cools the exhaust gases to a temperature that satisfies the Lujan's measurement equipment and a 2) which is a direct probe to the exhaust (as the exhaust temperature did not always require external cooling). This calibrated system guarantees all measurements within 5% of their actual value and is typically used in automotive emissions testing.

The engine is a O.S. Graupner, 4.97 cc Wankel Rotary engine rated at 1.26HP at 17K RPM. It is a four stroke motor that operates in a hybrid regime between HCCI and pre-mixed flame combustion. The primary fuel for this engine is predominantly methanol with typically 5-20% nitromethane as an oxygenate and 2-5% castor oil for lubrication.

While not investigated in this research, methanol may serve as a valuable fuel for fuel-flexibility in the sense that it can be used to liberate hydrogen with fuel reformers helping to reduce emissions and improve performance [191].

Emissions present during methanol and gasoline combustion

The emissions characteristics for only three fuels have been collected. They are represented as percent concentrations of air in the exhaust stream.

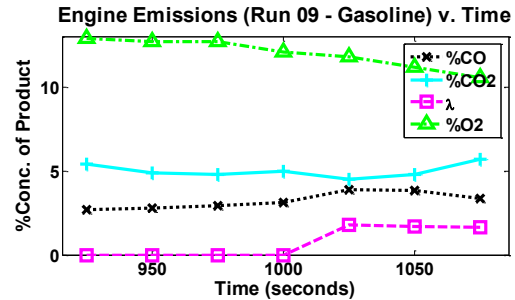
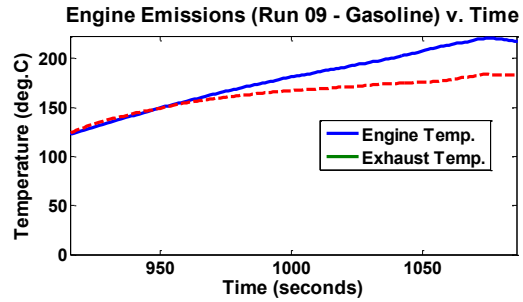
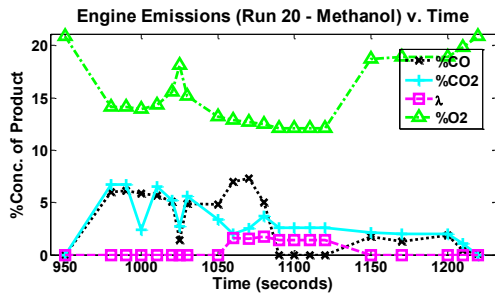
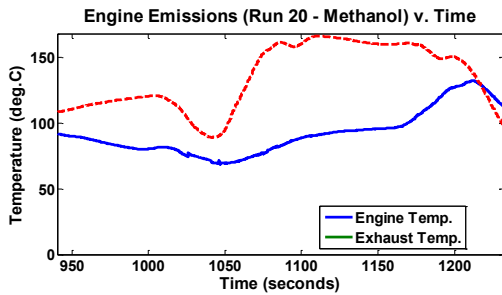


Figure 153: Engine emissions from methanol and the corresponding engine and exhaust temperatures. Top: Engine temperature is plotted with a light dashed line and the exhaust temperature is plotted with a dark solid line. Bottom left y-axis: %O₂: light dash-dot line with triangle markers, CO₂: light solid line with "+" markers: %CO: dark dashed line with "x" markers, and λ is signified by a light dashed line with square markers.

Figure 154: Engine emissions from gasoline (87 octane) and the corresponding engine and exhaust temperatures.

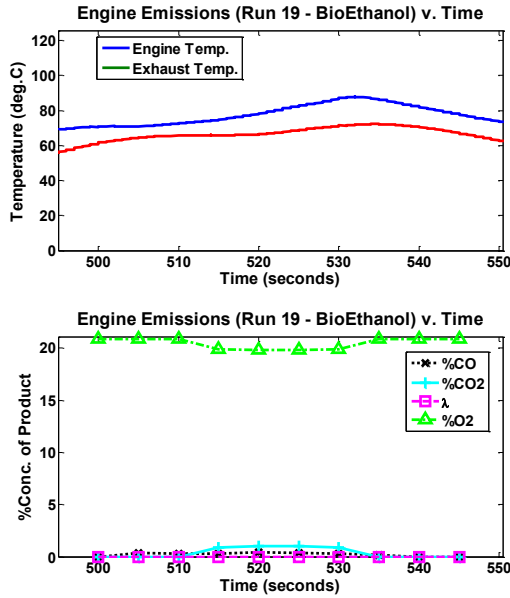


Figure 155: Emissions results for a BioEthanol fuel with corresponding exhaust and engine temperatures. Results are diluted due to exhaust extractor.

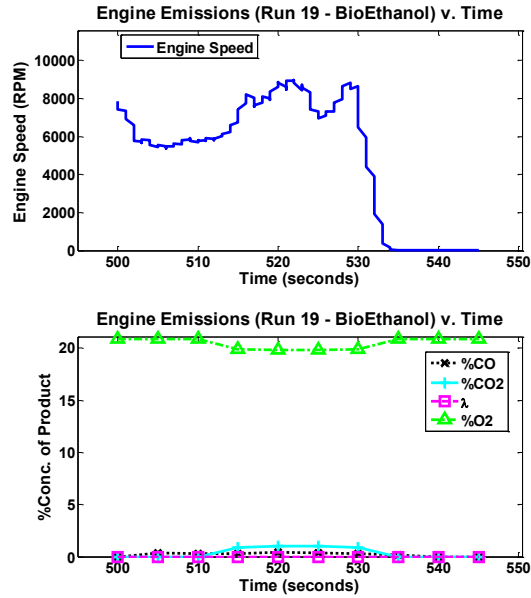


Figure 156: The engine speed is plotted along with emissions measurements.

Commentary on preliminary emissions experiments

Percent concentrations of emissions products from a small-scale fuel flexible engine have now been recorded. However, many improvements are needed before a full characterization of fuel-flexible emissions can be obtained. First, the method by which mechanical power is measured needs to be improved. The mechanical braking system—while an improvement from the former electrical braking method based on its ability to fully load the system—fails to mirror the input power of a known electrical motor, thereby not correctly measuring power. The losses due to mechanical friction within the engine, the transmission losses in the universal coupler, the frictional losses in the brake and the bearing upon which it sits, and any transduction errors due to the load cell that measures the force.

Second, the extractor system to evacuate combustion gases from the testing laboratory is very strong and needs to be properly adjusted and regulated so as not to corrupt the measurement. With the extractor on, the emissions results are severely diluted and the data reads as if the engine is not even having combustion.

Chapter 4 Summary

In this chapter, the key data demonstrating the functionality of the fuel-flexible engine dynamometer, the multi fuel switching system, sensor measurement, data acquisition, user control and engine actuation is presented. The data presented confirms

the fuel-flexible operation of a 4.97 cc Wankel rotary engine under five different fuels: methanol, gasoline, JP8, diesel and biodiesel. The power output ranges between 239 – 507 W.

A map of lean and rich flammability limits was produced such that other researchers and ideally control algorithms can utilize these data to better run the engine fuel flexibly. Methanol and the diesel fuels had the widest stoichiometry ranges.

The engine efficiencies were also determined based on the output power data and the energy density of the fuels. Surprisingly, gasoline produced the maximum efficiency observed of nearly 16 percent and that of diesel fuel was lower than 1 percent.

It was observed that the engine can run for a limited amount of time with a MEMS sensor embedded in the wear plate. Although the output power was reduced due to poor face sealing, the sensor appeared to survive at least in the presence of two fuels: methanol and diesel.

It was observed that temperature can also be varied as a function of engine stoichiometry leveraging the enthalpic properties of fuel via evaporative cooling to moderate the engine temperature.

Lastly, some preliminary results for output emissions are presented and can offer some general ideas and trends about output emissions under fuel flexible combustion.

References

- [188] Cardes, A.C., McCoy, C.D., K. Inaoka, D.C. Walther, A.P. Pisano and C. Fernandes-Pello, “Characterization of fuel flexibility in 4.97 cc rotary engines,” MCS, Libson, October 6-10 2005.
- [189] Dyno Tech Talk about Dynamometers and Testing. <http://www.land-and-sea.com/dyno-tech-talk/dyno-tech-talk.htm> Accessed on 16 August 2012.
- [190] Maruta, K. “Micro and mesoscale combustion.” Proc. of the Comb. Institute. 33 (2011) 6 Oct. 2010. Pp. 125-150.
- [191] Coward, H.F., Jones, G.W., “Limits of flammability of gases and vapors.” Bulletin 503, Bureau of Mines, U.S. Govt. Printing Office (1952).

Chapter 5 – Discussion and Analysis

“If you’re not making a mistake, it’s a mistake.” ~ Miles Davis

Fuel flexible engine performance discussion

The 4.97 cc Wankel Rotary engine is fuel flexible across several fuels

An engine that proves itself to be fuel flexible is exciting and represents a springboard for new fundamental research and development in power generation using pre-existing, new and alternative fuels. Additionally, this fuel flexible power generation was demonstrated on a small-scale, where typically combustion scaling challenges present fundamental technical barriers. Thus the fact that a 4.97 cc Wankel engine can produce useable mechanical power across (at least) five fuels (alcohols, octanes and biofuels) over a range of power outputs: 220 W - 507 W is an exciting advancement for alternative engines and small-scale power generation. In this research, it was demonstrated that:

- O.S. Graupner Wankel Engine is fuel flexible across several fuels: methanol+nitromethane (glowfuel), gasoline, diesel, JP8 and biodiesel
- The range of power output of the engine across all fuels was demonstrated to be between 220 W – 507 W
- Rotary engines can run continuously across four of five fuels with minimal stall events. Irregularities in combustion and the fuel sampled are .



Use your smartphone to watch all the relevant media: continuous engine operation under 4 fuels (both the short and extended versions and all other media presented in this dissertation).

The O.S. Graupner Wankel rotary only needs control of the carburetor needle valve to permit combustion across several fuels. Now while fuel injection would not only provide a better way to measure fuel input, control stoichiometry and likely improve the combustion event via improved turbulence and mixing, the carburetor sufficiency is very interesting from a systems standpoint. Fuel pumps, maintaining fuel pressures and activating injectors all represent parasitic power losses and when the output powers are on the same order of magnitude, it is promising that the carburetor can at least be used for the next phase of R&D should a dedicated fuel injection effort be absent in the project goals.

The control of engine parameters to maintain fuel-flexible combustion

One of the goals of this characterization was to understand what variables are the most important to enabling robust fuel flexibility. The dynamometer that was designed and built did allow the inspection of how each variable can affect the fuel flexible performance however each variable was not tested extensively.

Due to the varying properties of each fuel, the engine behaved differently during combustion of each fuel. Various adjustments of engine conditions were necessary to maintain combustion. The key engine parameters that were regularly adjusted to maintain fuel-flexible operation were: glow plug temperature, cooling fan speed, mixture stoichiometry, and throttle position.

Additionally the lean and rich flammability limits of combustion were experimentally determined and can now be used to better maintain engine operation within the expected range of stoichiometries.

The most obvious and important variable—the stoichiometry—was the main input characterized. The current engine dynamometer setup is ready to have controls algorithms implemented to change fuels on the fly. By using the fuel selector coming from the multi fuel switching system, a fuzzy logic controller could easily prepare the engine for known incoming fuels. Once a sensor that can predict or hint at the incoming fuel, then this decision matrix can be eliminated and the engine can simply detect the fuel and set the stoichiometry accordingly.

The other variables mentioned in bullet one, such as the glow plug temperature, clearly have an effect and in this set of experiments was more digital than analog. It was observed that every fuel except the glow fuel required that the glow plug remain on applying heat to the combustion event. It is highly likely that energy could be conserved using a spark ignition system however it was not tested in this research.

The long-term capacity of fuel flexible operation

The engine was typically run until it stalled. Unfortunately, this did not always represent a long amount of time (about 15 minutes). There are a couple of key issues that need to be observed when running for extended amounts of time so that the engine will not be damaged and will continue operation during future testing:

Proper and controlled cooling—the engine is at risk for serious damage when combusting a range of fuels because some fuels burn better at elevated temperatures which can threaten the life span of the engine. However, automated cooling could also be very interesting to verify the extent to which it can better optimize a combustion environment specific to an incoming fuel.

Sufficient lubrication—oil in proper mixtures is needed in order to prolong lifetime of the engine. This engine is not like most piston engines in that the oil is typically mixed with the fuel. This presents a point of improvement and future development although lubricating circuits in such small engines will introduce design challenges. The oil should be miscible with fuels that are introduced to the engine.

Fuel tolerant materials—a variety of fuels puts new material requirements on the engine peripherals. Specifically the fuel delivery system.

Engine vibrations—one problem that surfaced repeatedly and caused many problems. This may have to do with how the dynamometer was designed as it did not represent the model airplane to which these engines are typically attached. These vibrations caused nearly every screw in the system to become loose, causing the carburetor to leak at the intake, the exhaust to blow off and the most detrimental, shake itself off the dynamometer and rip itself out of its own mounting screws.

When these issues can be better addressed and resolved, more reliable combustion is likely to be observed.

Dynamometer results and commentary

After extensive use of this fuel flexible engine dynamometer, several design choices were verified as instrumental to the characterization. Others still need work however development is constantly dependent on available resources (graduate students, funding and time).

Engine loading design, selection and tradeoffs

The loading system represented one of the more challenging components to design seeming as each loading mechanism always seemed to offer a set of benefits with unfortunate tradeoffs. However, after this dissertation research, for this small scale engine dynamometer, the following comments can be made about each type of loading mechanism explored:

Best loading system chosen—electrical loading system was unable to fully characterize the power output of the O.S. Graupner Wankel engine. A mechanical loading system was able to fully load and stall the O.S. Graupner Wankel engine and would allow for full characterization across the entire operating range of the engine.

Although fears were present in using a low-cost mechanical brake for engine loading, a small hobby servo and mountain bike disc brake were sufficient to properly load and start the engine.

The fuel flexible dynamometer new capabilities and limitations

While the dynamometer designed, built, tested and utilized in this research provided the requisite characterization data, further development along the limitations could provide many more insights about enabling robust small-scale fuel flexibility.

Limitations

The main limitations observed in this fuel flexible dynamometer system were:

The mechanical torque measurement—the load cell measurement equipment was insufficient to measure the total torque output of the engine. Several design changes can be made extend range however it directly competes with the precision of the measurement. The torque arm geometry could be lengthened (which would introduce more measurement noise) or a new sensor with a larger dynamic range and precision could be installed (which would cost more).

The mass scale—the mass fuel flow rate measurement was limited by the precision of the Ohaus Explorer 20 kg, 0.1 g precision scale. A better system to measure the fuel mass flow rate—via weight, via volumetric flow, etc. should be identified and obtained. This limited the precision to which the efficiency could be measured. The fuel mass flow rate was not sufficient to measure in real-time due to the lack of precision of the mass balance. Fuel flow rate sensors were on the order of \$1000 which was out of the range of funding of this project.

Air intake sensor—the low-cost air intake sensor had a non linear output proportional to air flow rate and made real time calculations complicated. The data was so patchy and unreliable no real data could really be extracted from this sensor. At least, stoichiometry measurements using this sensor combined with the mass scale provided outrageously strange mixture stoichiometries.

Switching limited to only four fuels—currently the system can only switch between 4 fuels on the fly and blends of any of those four. The blending is not controlled (simply more than one electrovalve opens).

Vibrations—prematurely stop testing due to loosening of vital fasteners in the system: such as carburetor and exhaust mounting screws.

Capabilities

With the limitations known, the capabilities now offered for further fuel flexible characterization are as follows:

New characterization opportunities—the system is capable of measuring reliably and repeatedly the mechanical power output, the mechanical torque, engine speed, engine temperature, exhaust temperature, loading brake temperature, intake air flow rate, mass fuel flow rate and engine speed. With more dedicated testing, the affects of external housing temperature, glow plug heat and other controllable operating conditions on the fuel flexible potential.

Ready for automation—the dynamometer is ready for automation and controls implementation. A fuzzy logic controller would be the likely first choice however a mechanical engineering researcher who likes other control algorithms could use the LabVIEW + ArduinoUNO systems to control the engine.

Extending the range of fuels combusted—the key measurements of stoichiometry and power output have enabled the capacity to optimize and control fuel-flexibility across a range of at least 5 fuels. The only real limitation to testing other fuels would be the availability. Every fuel that was available when the dynamometer was working was tested. Many other fuels and blends are ready to be tested with this system.

Multi-fuel switching system (MFSS) review and commentary

The MFSS was an important step forward for finding low-cost components and materials that were compatible with fuels. However, this system is barely meeting the requirements for robust fuel flexibility. While the MFSS was designed and will allow for multiple fuel selection, it could be improved along these lines:

Head losses or addition of tank back pressure—however, head losses need to be reduced or some sort of back pressure is needed to drive the fuel flow into the carburetor. Gravity feed is not sufficient.

Additional exploration of materials compatible with multiple fuels—various fuels attack many polymers and plastics, thus the selection of proper materials is important for long term durability and usage. This was evidenced in the failed low-cost union joints when merging all fuel lines into one that enters the O.S. Graupner Wankel Engine.

Electrovalves and fuel delivery—a low-cost Arduino is capable of adequately controlling the electrovalves. A basic digital circuit that allows for fuel selection was sufficient for rapid fuel selection. This could be expanded and the next step might be creating a fuel tank ready to accept many fuels.

Sensor and actuator integration

One of the key differences between prior research and that which was conducted during this doctoral research was the addition of integrated sensors and actuators into one data acquisition and control center.

Sensor selection and utilization

The sensors used in the dynamic analysis of the engine ranged from \$30 to \$300, making a fuel flexible engine sensor system more than an affordable addition to potentially fuel flexible engines. These low-cost sensors are integral to making real-world customer solutions. The thermocouples and angle encoders were no more than US\$30.00.

Some sensors dedicated to characterization were more expensive—such as the dynamic combustion pressure sensor and the National Instruments data logging equipment—but overall, the sensors and hardware necessary to

control the engine and dynamometer system are affordable and basic. Other Arduino products such as the ArduinoMEGA could be utilized to potentially eliminate the LabVIEW system and the multiple ArduinoUNO microcontrollers currently present in the system.

Actuator selection and utilization

Actuators – real time control of the fuel-to-air ratio is necessary to permit dynamic fuel flexibility. Many fuels with varying chemical properties require significant adjustments during operation. Variations in engine temperature, glow plug temperature and engine speed all affect the performance output of the engine.

Control and management of sensors and actuators for improved fuel flexibility

The addition of Arduino microcontrollers in concert with the LabVIEW development environment added tremendous flexibility in quickly adding sensors, actuators and low-cost solutions to control.

Recommended Future Work

“Necessity is the mother of invention.” ~English Proverb

This is where the secret to the largest savings of time, money, effort and energy is located—the future work section. It is also where the author would have liked to explore if resources of time, money, energy and opportunity were plentiful. The innovations derived from typical research constraints (funding and time) furthered the research, characterization and understanding of small-scale, fuel flexible rotary engines.

Most problems encountered and opportunities envisioned in the research which were not directly related to the main research objectives are documented here and suggested for further investigation. This encapsulates all aspects of the characterization, dynamometer design, engine control, fuel flexibility and many other mechanical design and analysis. It is hoped that future researchers can use this section to maintain the scientific progress of fuel-flexible engine operation.

Pre combustion analysis

Considering that a fuel flexible engine should be able to produce reliable power on any liquid hydrocarbon fuel, a pre-combustion strategy was wanted in order to prepare the engine for incoming fuels. For heavyweight fuels like diesel, it was noted that the engine temperature would need to be elevated to maintain combustion (via reduced fan speed and constant glowplug ignition). The key conditions to maintaining combustion upon switching fuels is the throttle position, stoichiometry and engine temperature. The throttle position is important as it is proportional to the fuel flow into the engine and

therefore determines the time required to introduce a new fuel into the combustion chamber (on the order of 10-15 seconds using a fuel tube of 1 m). Additionally, the incoming fuel may be unknown and thus low-cost fuel detection sensor—if available—could better prepare the engine based on the optimal operating conditions as highlighted in Chapter 4.

Preheating the fuel for better evaporation

With the intention of improving the combustion of the variety of fuels exposed to the 4.97 cc O.S. Graupner Wankel engine, a waste heat fuel evaporator is suggested. The exhaust temperature for this engine was regularly measured to be around 100 °C and could have been used to preheat the fuel. Caution needs to be taken so as not to preheat the air (which lowers the air density, consequently reducing oxygen content and results in lower power output).

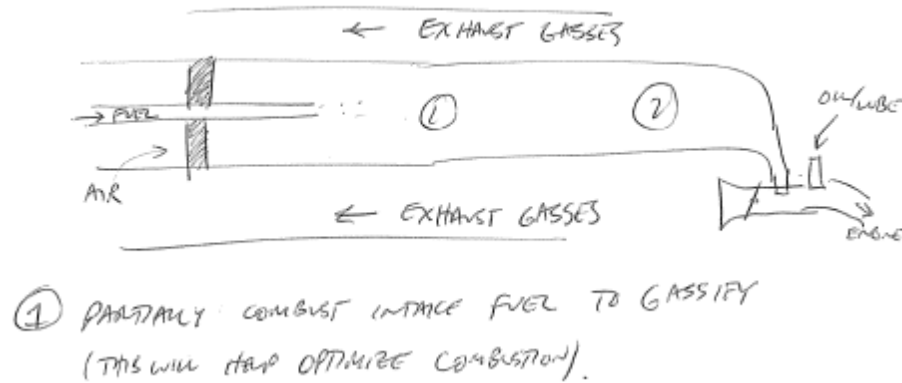


Figure 157: Preliminary sketch for a fuel pre-heater system that would ideally utilize the waste heat from the exhaust to preheat heavier fuels introduced into the engine.

A dedicated lubrication system

Initial goals of completely enabling fuel flexibility included the integration and use of a fuel sensor to help detect which fuel is entering the combustion chamber. A fuel flexible engine would likely have an array of distinct fuels available for combustion or would have any number of various fuel blends. The advent of refractive index and conductivity based or capacitive based fuel sensors provide various options such that engine conditions could be changed and calibrated to the incoming fuel.

In this research, lubricating oil was added in various proportions to each fuel (typically about 5 percent). The standard GlowFuel has oil mixed within from the factory and other non-standard fuels had either a mix of castor oil or two-stroke engine oil mixed in order to protect the engine. However, an optimal fuel-flexible engine solution would include some sort of self-sufficient lubricating system such that any fuel present in the engine had enough lubricating oil to keep the engine running reliably and safely (the

engine will burn up without lubricating oil). Thus some sort of intake spray lubricant that could be accurately controlled by a computer or microcontroller would be a great improvement to such an engine system.

Improving combustion via smoother engine and dynamometer operation

Many recommendations to add a fly wheel were offered mainly because of the variable combustion that was observed during testing. With the addition of the mechanical braking system and the universal shaft mount, this added to the rotational moment of inertia and improved the flywheel effect. However, no direct flywheel was designed for this system but it may have greatly improved the operation and reliable combustion. Considering that a light-weight system was desired, a specialized flywheel would be needed to maintain low weight but at the same time, add significant rotational inertia. From a design perspective, composite materials are ideal candidates for light-weight flywheels in the sense that their rotational strength can be tailored specifically for increased mass at the edges while at the same time, resisting radial strain. Thus, it may be useful for future experiments and characterization to add such flywheels.

Apex seal redesign

While not a direct issue to fuel flexibility, the apex seals are a point of concern for long-term reliability, improved compression ratio and efficiency. They are composed of a hardened steel rectangular piece with two leaf springs which apply the initial pressure to the “sidewalls.” The challenge is that these leaf springs lose their spring constant with time and present an inconvenient maintenance issue for long-term use of this fuel-flexible generator system.

Fuel flexible fuel injection

Fuel injection (FI) is a mature technology on the large scale and has many benefits. On the smaller scale and considering the scope of this research, the implementation of a fuel flexible fuel injection system was dismissed. Fuel injection boasts better mixing, enhanced vaporization of fuel and accurate control of delivered fuel resulting in better performance (efficiency, power output, etc.). Additionally, this is an electronic solution more ready for implementation in engine control systems.

However, when multiple fuels are required, a materials compatibility study with fuel valve internals and other hardware should be considered—for example, whether one fuel valve would be used for all fuels or if a better solution would be to have individual injectors for each fuel—should be investigated. The latter solution would require separate fuel tanks for each fuel, making the use of such a fuel flexible system more complicated for users. Additionally, several researchers have studied other ways to add pilot fuels and combine an injector along with the main fuel delivery system (either

another fuel injector or in this case a carburetor), in an additive manner rather than a completely substituted FI system [194].

This could possibly lead into the development of a self-separating fuel tank system where potentially the miscibility of fuels could be exploited to separate the contents of a fuel tank into its various contents.

Improved fuel flow rate measurement system

To dynamically measuring the fuel flow rate in realtime in a cost-friendly manner proved difficult. The systems available to us were at the precision limit of the fuel flow rate of the engine and therefore average fuel flow rates were used instead of real-time fuel flow rates (0.01 g/s). Liquid flow rate sensors are not typically designed for such high precision nor for such small flow rates. Therefore other systems for measuring fuel flow rate should be considered.

For example, McMillan Inc. makes sensors that can measure fuel flow rates of up to 15mL per minute and cost approximately \$1k and is still not as precise as the scale needed in this research. If a fuel injection system is utilized, this measurement can be done using the pulse rate, fuel pump pressure and knowledge of the nozzle characteristics.



Figure 158: “McMillan Model 106 FLO-SENSORS are capable of measuring extremely low liquid flow rates from 15 mL/minute up to 10 L/minute with a full scale accuracy of $\pm 1.0\%$ or better [192]!

PRODUCT
REQUESTED: 106-3-A-F4-C20-MT

Specifications:
15-100 mL/minute
12-15 VDC Power /
Pulse Output
1/4" PFA male flare fittings
20 foot (6.2 m) cable length
Mounting Plate
Installed (see options)

Characterizing blends of fuels and rapid switching of fuels

The multi-fuel switching system is nearly ready to permit the automated switching of fuels, pulsing of fuels and blending of fuels. Having electronic control of electronic fuel valves which lead into the carburetor of the motor, various fuel blends and switching conditions could be characterized.

Exhaust Gas Recirculation (EGR)

Exhaust gas recirculation could be an interesting addition to this fuel flexible system because of the tendency of this O.S. Graupner Wankel engine to run very rich (thereby maintaining and cooling the temperature of the engine). Thus, if unburnt hydrocarbons are readily output from the exhaust, EGR could not only raise and alter the intake temperature (thereby changing emissions and performance outputs), but it would also improve efficiency.

And considering this particular engine has poor emissions and many UHCs, this may also be a useful way to improve efficiency and reduce the environmental impact.

Implementation of Fuzzy Control System (FCS)

Considering the system is about 95 percent “fly by wire”, it is ready for a controls guru to implement a control strategy based on the characterization work detailed here. Considering the data collected per fuel (maximum measured power output, stoichiometry, etc.), a basic set of rules can be defined and responses based on these sensed inputs can be sent to a number of integrated controls. Researchers at the University of Brighton have already published preliminary work that describes a “Fuzzy Control System” for emission reduction by measuring intake manifold pressure and intake airspeed. From these measurements, their microcontroller then adjusts the injector pulse width—maintaining the stoichiometry of the combustion [96].

General mechanical problems and opportunities for improvement

The small-scale OS Wankel Engine has a lot of room for improvement. The following list can provide as the guide to problems future researchers will encounter until a solution is obtained:

Unwanted and vibration induced loosening of engine hardware—engine nuts, screws and bolts. No reasonable amount of Loctite™ will successfully maintain the torque settings for any length of time with this dynamometer. The carburetor and exhaust mount screws are the first to go and will cause problems (i.e. stop all data collection and require a dismount of the engine). Efficiency on average is less than 5 percent. Modern engines are typically between 25-30 percent. Therefore there is a lot of opportunity to improve this engine characteristic as well.

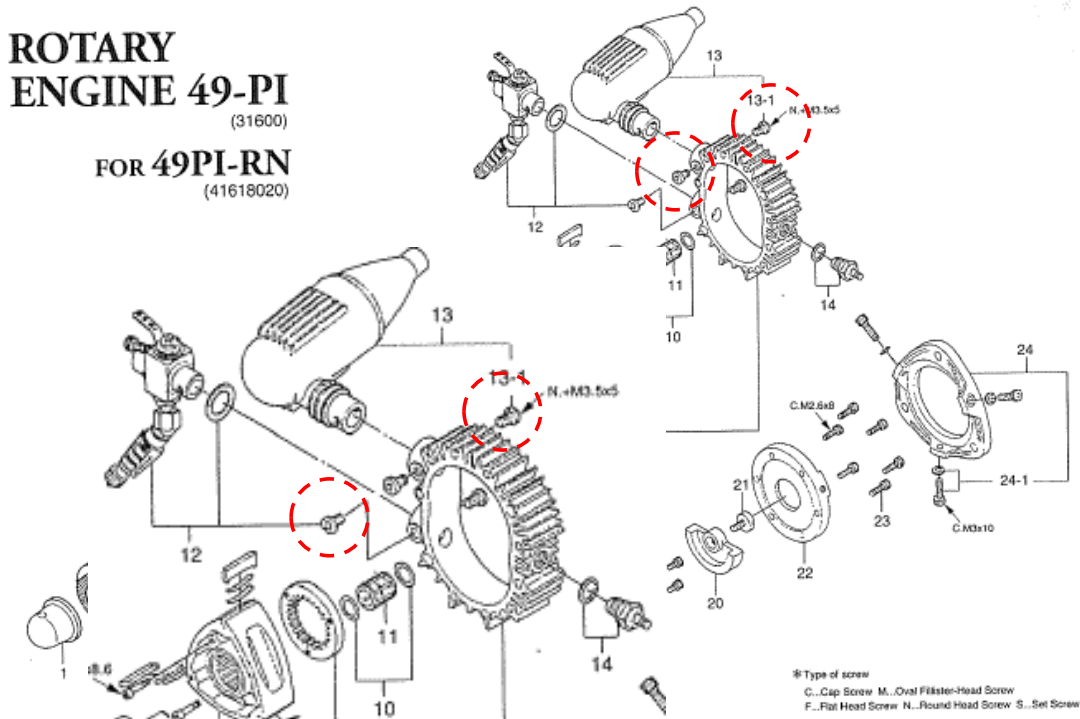


Figure 159: Location of problematic screws and hardware that became unfastened due to engine vibration.

The fuel delivery cables and connectors – these should be upgraded be of a material that can resist degradation in the presence of fuels.

Improved Design for Assembly / Disassembly – because the potential to damage the engine under these strange operating conditions is high, changes for improved disassembly and reassembly should be implemented. The dynamometer design began with the desire to have 100 percent metric hardware but unfortunately ended up with a mix of both English and metric hardware requiring two different sets of Allen wrenches. Additionally the reduction of screws or replacement of them for other quick-set connectors would be ideal. Thumbscrews were implemented where possible (for example in the optical breadboard where finger-tight adjustments were acceptable). This also includes reliable electrical connectors that typically capture data, control servos and power engine components. Losing key data to seemingly connected sensors is a depressing but regular occurrence.

Chapter 5 Summary

While much effort, energy, time and financial investment went into this limited characterization of a rotary engine, the system is now ripe for more characterization. Several tests can be conducted now without any further development to improve and extend the characterization of this fuel flexible engine.

Knowing the limitations and capabilities of the fuel flexible dynamometer system and the multi fuel switching system will allow any researcher to better understand fuel flexibility. These key limitations are the fuel flow rate and output mechanical power limitations caused by the sensors that measure them.

If however more time, money and energy via human resources are available to further develop the system, the future work section offers a host of ways to improve the characterization system.

References

- [192] Image: McMillan Flow Sensor.
<http://www.mcmflow.com/displayproduct.asp?PRODUCT=106> Accessed on 15 August 2012.
- [193] Lee, S.H., Howlet, R.J., Walters, S.D. “Small engine control by fuzzy logic.” *Journal of Intelligent and Fuzzy Systems* 15. (2004) pgs. 207-217.
- [194] Richards, G.A., McMillian, M.M., Gemmen, R.S., Rogers, W.A., Cully, S.R. “Issues for low-emission, fuel-flexible power systems.” *Journal of Progress in Energy and Combustion Science* 27, (2001) pgs. 141-169.

Chapter 6 – Conclusions

“The bigger the struggle, the greater the triumph” ~Butterfly Circus

Conclusions from this research

While complete and wide-range fuel-flexibility is the ultimate goal and hope for engines of the near future, this research adds to the existing body of knowledge with two humble, yet significant innovations.

First, the design and construction of a new small-scale fuel flexible engine dynamometer that allowed for precise measurement and control of small-scale engines operating on non-standard fuels. It was determined that fuel flexible engine dynamometers need have systems for damping significant engine vibration, need to have systems to adequately manage heating and cooling, require active control and measurement of a range of engine parameters: stoichiometry, throttle, engine and exhaust temperatures, emissions products and inlet fuel information.

Second, the small-scale engine dynamometer and the O.S. Graupner Wankel engine were utilized to successfully produce power from a range of fuels, non-standard to the engine: gasoline, diesel, bio-diesel and JP8. In order to achieve this, an experimental understanding of rotary engine operation using various fuels was necessary. Light weight fuels tended to demonstrate more stable combustion while heavier, diesel-like fuels required more elevated temperatures to promote combustion. Fuel maps for each of the fuels tested show their power output capability in the O.S. Wankel Engine platform and their upper and lower flammability limits; thereby providing a fuel-flexible engine operating map for this 4.97 cc engine.

Lastly, it has also been shown how the small-scale engine dynamometer was designed and constructed along with the many lessons learned through the experimentation in hopes that these results can be utilized by future researchers: enabling advancements towards wide-range fuel flexibility.

The novel design of a small-scale fuel flexible dynamometer

The design and construction of a new small-scale engine dynamometer was essential as no commercially available dynamometers on this scale existed. The legacy systems failed to capture all necessary data, perform endurance tests and control fuel-related parameters; especially the new needs for fuel flexibility. Building this dynamometer consisted of the design and construction of the overall geometry, the engine loading system, the required sensors and the integration of all these elements into a usable data acquisition system. This research highlighted the importance of stoichiometric control which could be achieved to some degree using the passive, stock

carburetors. Experiments also reinforced the need to be able to reliably control heat transfer processes to allow fuel vaporization of heavy fuels and reduce flame quenching.

The novel design of a fuel switching system

The design and construction of a multi-fuel switching system was also integral to extending and characterizing fuel flexibility on this small scale. Early experiments only tested fuels independently, but future systems needed to be able to change in real time. This research highlighted that a multi-fuel switching system could be built with low cost microcontrollers and fuel electro valves; allowing for continuous fuel-flexible operation. Future systems however will require low head loss connective tubing so that the carburetor is not choked and can properly deliver fuel to the engine.

The extension and characterization of fuel flexibility of a 4.97 cc Wankel Engine

The resulting fuel-flexible engine characterization system was then tested amongst a variety of liquid hydrocarbon-based fuels to create a fuel-flexible engine mapping for a 4.97 cc Wankel engine. Data was collected for the baseline fuel of methanol (plus nitromethane) and for non-standard fuels: gasoline, diesel, biodiesel and JP8. During combustion of these fuels, the following parameters were measured in an effort to fully characterize this engine: engine torque, mass flow rate of ambient air intake, stoichiometry, ambient temperature and humidity, ambient pressure, engine speed, mass fuel flow rate, engine housing temperature, engine exhaust temperature and loading brake temperature, and the fuel selection. This data collection was possible through the design and integration of the LabVIEW data acquisition system architecture in concert with four input/output devices: the NI-USB-6221, NI-USB-9162 and two Arduino UNO microcontrollers. The design and integration will be fully described along with the new system potential and shortcomings.

In addition to the data acquisition, the system was also designed to enable future real-time control using conventional low-cost model engine servos such that the system could be fully automated. In the current system, there are eight actuation devices that control the throttle position, the glow plug heat, the fuel to air ratio, the dynamometer brake and four electrovalves that control the delivery of each fuel. The mechanical design and construction of all these control and sensing mechanisms were also described along with their added potential to enhancing fuel flexibility and opportunities for future improvement.

Dissertation Close

The fuel flexible dynamometer system, multi-fuel switching system, data acquisition and system control enabled fuel flexible operation of a 4.97 cc O.S. Wankel rotary engine were all designed, built, tested and utilized to obtain the characterization

results achieved in this research. The maximum mechanical power produced from Gasoline, Glowfuel (methanol+nitromethane mix), JP8, Diesel and Biodiesel were 334 W, 508 W, 313 W, 239 W and 322 W respectively. A preliminary stoichiometry map was created in order to understand the total fuel flexible range currently achievable using the current system. With electronic data acquisition and control of the major engine components, the system is now ready for a plethora of future experiments.

With an operational small-scale engine dynamometer with fuel-flexible control, it is hoped that enthusiastic and talented future researchers can push the boundaries of science and engineering even further—leading the way to wide range fuel flexibility across all scales.

References

- [195] Lee, S.H., Howlet, R.J., Walters, S.D. “Small engine control by fuzzy logic.” *Journal of Intelligent and Fuzzy Systems* 15. (2004) pgs. 207-217.
- [196] Richards, G.A., McMillian, M.M., Gemmen, R.S., Rogers, W.A., Cully, S.R. “Issues for low-emission, fuel-flexible power systems.” *Journal of Progress in Energy and Combustion Science* 27, (2001) pgs. 141-169.

APPENDICES

“What seems so necessary today may not even be desirable tomorrow.”
 ~Anonymous

APPENDIX A: Nomenclature and other useful definitions

Books and scientific articles use special characters to reference physical properties or phenomenon but they are not always the same or consistent. Here is the list of symbols and definitions that refer to the physical properties and phenomenon researched in this work.

Term	Symbol	Description
3D Printing		The general manufacturing technique of additive manufacturing. Typically referring to fused deposition modeling but there are many forms. It is the process of forming 3D structures via the consecutive layering of materials.
BMAD		Berkeley Micromechanical Analysis and Design. An acronym that describes the research lab in which this research was at least partially conducted.
BMEP		Break Mean Effective Pressure. This is a quantity relating to the ability of an engine to do work independent of the engine size.
BSAC		Berkeley Sensor Actuator Center.
BSFC		Brake Specific Fuel Consumption. This is a measure of fuel efficiency for shaft reciprocating engines. It is the rate of fuel consumed divided by the power output.
Cetane		A unit of measurement used to characterize the resistance to knocking in diesel fuels.
CNC		Computer Numerical Control. Typically found in manufacturing equipment like a CNC mill or CNC lathe.
CO		Carbon Monoxide. Another unwanted exhaust emission commonly found in internal combustion engines.
CPL		Combustion Processes Lab.
DRIE		Deep reaction ion etching – a microfabrication technique that utilizes a combination of passivation and etch steps in order to create deep trenches in semiconductor materials.
Dynamic response		The ability of the fuel flexible engine generator to respond real-time to changing fuel inputs and engine conditions.
EDM		Electro-Discharge Machining. This technique was used by Dr. Joshua Heppner to create small apex seals with integrated springs out of silicon.
Equivalence Ratio	ϕ	The numerical comparison to the actual fuel-to-air ratio of the mixture to its calculated stoichiometric fuel-to-air ratio.

		Values less than 1 are considered “lean mixtures” and values greater than 1 are considered “rich” mixtures.
Flexfuel		A term and indicator utilized by General Motors automobiles that describes a vehicle that can accept E85 fuel in addition to regular octane fuel.
Fuel-flexibility		The ability of an engine to produce usable output power from 2 or more fuels.
g	<i>g</i>	Gram
HHV		Higher Heating Value
hp		Horsepower
In-situ		The process of performing a particular action (a test, measurement, procedure, etc.) while the system performs its primary task.
J	<i>J</i>	Joule
Lean Mixture		When the value of equivalence ratio is less than 1. Typically used to describe the setup or characteristics of the engine. Performance trade offs such as less power but improved emissions characteristics are associated with lean mixtures.
LFL		Lean Flammability Limit
LHV		Lower Heating Value
LVP		LabVIEW Position. Used to indicate the position of the carburetor needle valve under the combustion of various fuels. Since fuel flow rate on this scale was difficult to achieve, this indicator was arbitrarily created and utilized. Future research should find a better way to characterize this value.
Man-portable		Being of the capability to be carried by an average human. For the purposes of this research, between 10-50 lbs.
Maxon		Manufacturer of precision motors used in legacy mini-scale dynamometers.
MEMS		Microelectromechanical Systems. An acronym used to describe sensors and actuators that are made via standard semi-conductor processing techniques.
Meso-scale		Objects, features and all else with dimensions conveniently measured in millimeters, 10^{-3} m.
MFSS		Multi-fuel Switching System
Micro-scale		Objects, features and all else with dimensions conveniently measured in microns, 10^{-6} m.
Minimum Power Variation	ΔP_{min}	Symbolic of the power output jump when switching fuels
Mini-scale		Objects, features and all else with dimensions conveniently measured in meters.
NOx		Pronounced “nox,” NOx refers to several—typically unwanted—nitrous oxides found in exhaust emissions

		catalyzed by high temperature combustion.
Octane		A unit of measurement used to characterize the resistance to knocking in non-diesel liquid fuels.
Parasitic Power		Power which is parasitically consumed by engine peripherals necessary to enable small-scale engine operation; specifically fuel flexibility. An example would be fuel pumps, cooling fans, etc.
ps		A the German term for horsepower meaning Pferdestärke. 1 ps is equal to ~0.986 hp.
<i>r</i>	<i>r</i>	The rate of fuel consumption
RFL		Rich Flammability Limit
Rich Mixture		When the value of equivalence ratio is greater than 1. Typically used to describe the setup or characteristics of the engine. Performance trade offs such as more power but poorer emissions characteristics are associated with rich mixtures.
RPM		Revolutions per Minute. A unit of measurement of engine speed.
SEM		Scanning Electron Microscope
Si Grass		A phenomenon observed post deep reaction ion etching (DRIE); specifically during high-aspect ratio etched trenches.
Small-scale		Technologies measuring in the sub-meter range. See also micro-scale, mini-scale and meso-scale.
TDC		Top Dead Center.
Turbulence		The fluid flow phenomenon characterized predominantly by the Reynolds Number, Re. Turbulence improves engine performance in a variety of ways related to fuel air mixing and engine cooling.
UAV		Unmanned Aerial Vehicle.
UHC		Unburned Hydrocarbons. Harmful exhaust emissions catalyzed by incomplete combustion.
Ultra-portable		Being of the capability to be easily carried by an average human. For the purposes of this research, between 1-10 lbs.
WOT		Wide Open Throttle

APPENDIX B: Useful theory and plots

How to read a Ragone plot

Reading a Ragone plot or diagram can sometimes be confusing. A Ragone plot is typically plotted when one wants to show a range of portable power solutions.

Ragone Diagram of Various Power Sources

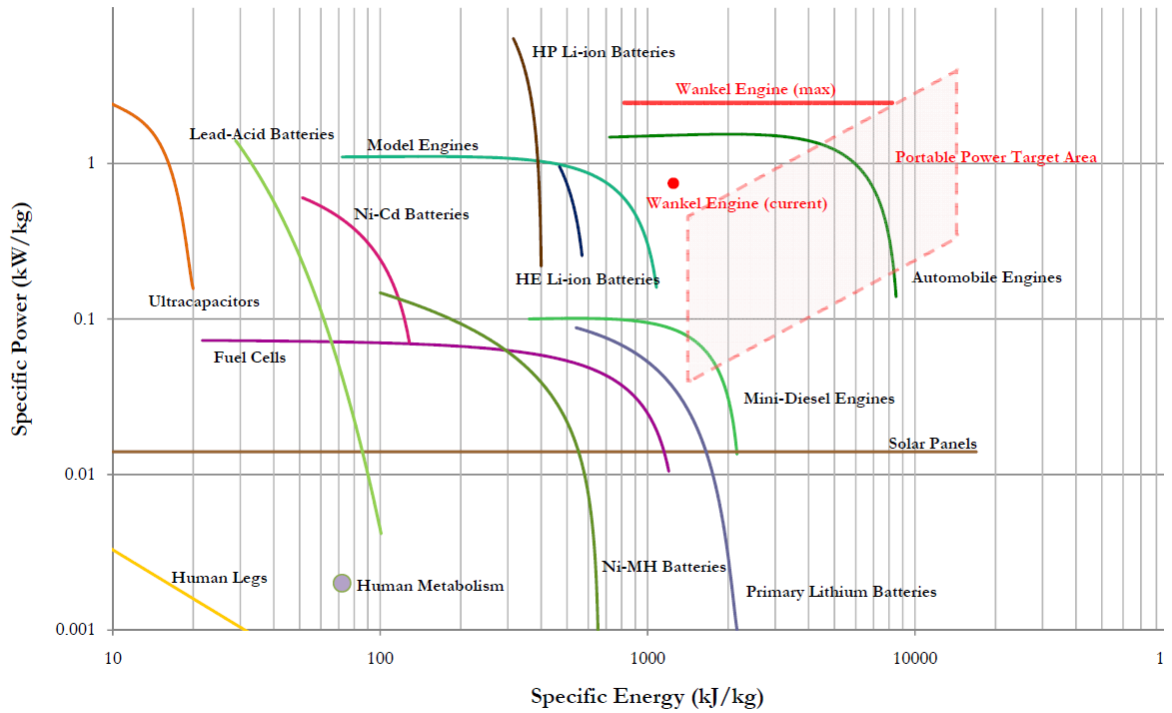


Figure 160: Taken from many sources of data, this Ragone diagram illustrates where the 4.97 cc O.S. Wankel engine exists but the ideal target power range. See [9].

The Ragone plot above borrowed from Reville *et. al.* Shows an u

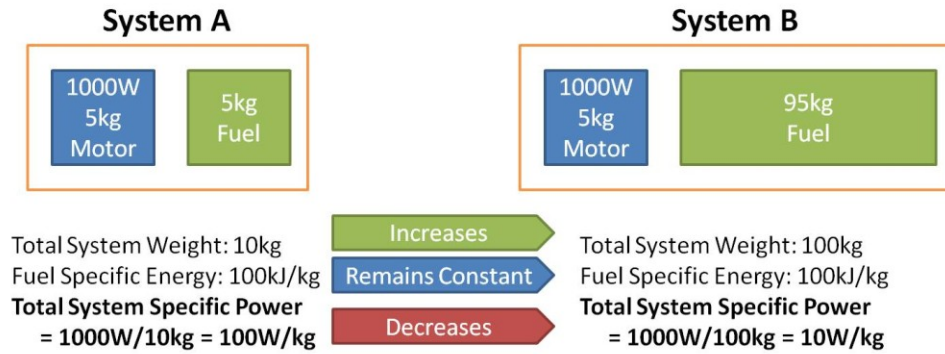


Figure 161: This figure attempts to illustrate how the specific power output drops as fuel volume (with a constant specific energy) increases system weight.

Calculating the adiabatic flame temperature

Another key parameter of fuels and their corresponding combustion is the adiabatic flame temperature — the maximum temperature a fuel and its mixture would reach if no heat left the reaction chamber. This can be conservatively assumed to be the maximum temperature a reactor or combustion chamber will see. Typically this temperature occurs at or near stoichiometric conditions. This temperature can be calculated under constant volume or constant pressure conditions using conservation of energy equations:

$$(26) \quad H_P(T_P) = H_R(T_R)$$

where

$$(27) \quad H_P(T_P) = \sum_i N_{i,p} \hat{h}_{i,p} = \sum_i N_{i,p} [\Delta \hat{h}_{i,p}^o + \hat{h}_{si,p}(T_P)]$$

And

$$(28) \quad H_R(T_R) = \sum_i N_{i,R} \hat{h}_{i,R} = \sum_i N_{i,R} [\Delta \hat{h}_{i,R}^o + \hat{h}_{si,R}(T_R)]$$

These adiabatic flame temperatures can be calculated using one of three methods: an average c_p value, an iterative enthalpy balance or using computer software (such as Cantera or Chemkin).

For example, the adiabatic flame temperature during combustion of methane, CH_4 as a function of the equivalence ratio is:

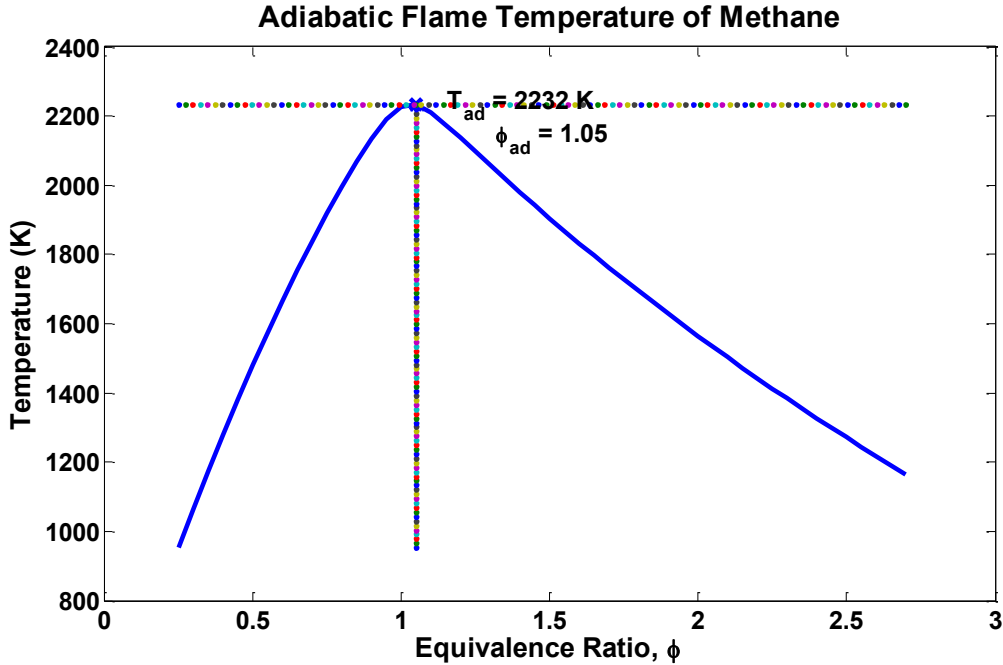


Figure 162: Calculating the adiabatic flame temperature of methane as a function of equivalence ratio using Cantera.

APPENDIX C: Sensor Calibration and Test Setup

For this research, the following sensors and actuators were utilized and calibrated to ensure the highest possible accuracy available.

#	Make	Model	Measurement	Units	Reference
1	Testo – Compact Thermal Anemometer	425	Air flow, air velocity	$m^3/h, m/s$	(PDF link)
2	Sensotec – 250g Load Cell	SN: 693479	Mass $\sigma = -37.45g/V$	grams	(Link to FuelFlex PBW)
3	Monarch - Tachometer	ACT – 3A	Engine Speed	RPM	(PDF Link)
4	Omega Thermocouples		Temp	Deg C	
5	CSA 1V Current Sensor	AN_117KI T	Current	1-40 Amps	(Web link)
6	Sensirion - Ambient Temperature and Humidity Sensor	SHT15	Temperature & humidity	0-100% RH	(SparkFun Link)
7	Motorola manifold absolute pressure sensor	MPX4115 A	Pressure	0-5V to kPa	(Link to PDF)

8	McMillan Mass air-flow rate sensor	Model 100	Mass air flow rate	L/min	(Link to datasheet)
9	Optrand Pressure Sensor	D222D6 AutoPSI	0-1000	PSI	(Link to website)
10	US Digital Analog Encoder	MA3-A10-250-D	±1	Degrees	(Link to website)
11	Honeywell Air flow (intake) sensor	AWM700	Intake Air flow	L/min?	(Link to datasheet)
12	EBM-Papst AC centrifugal fan	D2E146-HT67-02	Cooling Fan	m ³ /h	(Link to datasheet)

For a more complete list, use your SmartPhone to access this Google Drive Spreadsheet:



Use your smartphone to watch and access all the relevant media: Sensors and actuators used in the construction of the fuel flexible dynamometer.

General sensor calibration procedures and tips

Calibration is the process of determining sensitivities and capacities of any number of sensors for use in measurement. The general process is as follows:

1. Take any safety precautions necessary to take measurements carefully without causing any injury to yourself, others or property. If unsure, ask someone else nearby to check for any safety issues.
2. Search the internet for any pre-written calibration processes if the calibration procedure is unclear or no good guesses about how to perform a calibration can be made. Most calibrations take just a tiny bit of common sense and ingenuity.
3. Read any instructions or warnings, be sure to take any safety precaution seriously.
4. Setup the sensor to be calibrated so that it is ready to take measurements
5. Find a similar tool or sensor that
 - a. has a known calibration or can be rightfully assumed to be correct (a mass scale for example or beam balance)
 - b. and measures the same property of the sensor to be calibrated
6. Then take a series of measurements (typically at least 3 but better 5-6) across the range of the sensor.
7. Start at any point, measure to the maximum (if possible) then take measurements that decrease in value to the minimum.

8. For a quick calibration, points can be skipped and recorded in one or more directions. Don't hesitate to be creative, ever.
9. Once measurements have been recorded on both the "calibrated" tool and the "tool in calibration," use any method of choice to derive equation that defines the curve. Typically this will be linear (i.e. a load cell will have a voltage directly proportional to the weight or force placed on it).
10. Plot, determine slope. The slope is the sensitivity of the sensor.
11. Note any other abnormality or offset and generate an equation.
12. Save notes and repeat another day at another time to ensure repeatability.

There are probably engineering standard calibration methodologies and the author recommends reading these in comparison to the above guidelines. These are simply for quick reference should the reader have no freaking clue about calibration.

General testing and safety procedure

This testing protocol was pulled from the <http://fuelflex.pbworks.com> wiki where research collaborators updated and modified testing procedures as necessary.

Note, this procedure was produced for the electrical brake dynamometer.

Engine start-up and testing checklist

1. SAFETY FIRST! Safety Glasses and ear protection for everyone in the room. Stand behind an undergrad, if possible.
2. Ensure that all bolts / screws are tightened to their proper torque specifications (see this torque table for proper torque)
3. Start LabVIEW, ensure all sensors / actuators are powered up and ready to transmit data to computer (note dedicated powerstrip):
 - a. Turn on NI DAQ block (switch at back near power cord)
 - b. Plug in load cell
 - c. Plug in tachometer
 - d. Connect dissipation voltage cable. Verify presence of attenuator and / or the large voltage divider.
 - e. Set the max, min on the RPM meter* (See Jesse's Instruction Manual)
 - f. Set your sample rate to somewhere between 1-10 samples / second. We're taking 6+ measurements so we don't want to overdraw the system resources.
 - g. Clear all charts (right-click: Data Operations -> Clear Data)
 - h. Enter the fuel type, etc in the comments field.

4. Power up fuel scale.
5. Check the proper placement of thermocouples (the exhaust thermocouple can shift during operation / break-down)
6. Start cooling and exhaust fans
7. Start cooling fans (squirrel cage + overhead AirKing (aka Katrina) fans
8. Start cooling fans on dissipation heat sink (by turning on power strip)
9. Start exhaust suction pump / fan (at the wall over by the whiteboard)
10. Set voltage on Tenma power supply (12V) to adequately power glow plug (for start-up) and connect to Hobbico Power Panel. **see warning below for unnecessary burn up of glow plugs
11. Find the lab timer, and fill fuel tank. Be aware of what is on the scale when you start. It's only precise to 0.1 grams (and it has some error). Also, be aware that the fans put a downward force on the scale so average your measurements
12. Position both thermocouples: one in the exhaust, one on the engine housing near top dead center (unscrewing the housing bolt and pinching thermocouple may or may not damage measurement....beta test 1 will tell all)
13. Power up the high current power supply (20A, 14V) starter motor.
14. Securely fasten the flexible coupling from the electric motor to the engine

While engine is running

FLIP THE SWITCH ON THE STARTER CIRCUIT FROM START TO DISSIPATE. Otherwise we burn up \$200 speed controllers as fast as Bob Marley burned the weed.

Check to make sure the RPM IR light is positioned correctly as it may need realignment after each setup / break-down.

Generating Engine Power Plots

Methodology per Land & Sea's "Dynamometer Tech Talk"

1. Warm up engine
2. Open throttle to full load.
3. Regulate the RPM using the "absorber brake." This is our dissipation circuit
4. Slowly step through RPMs by relieving the absorber brake
5. Finish collecting data, back off throttle

Additional Details:

* (this is done via the Monarch box). Setting the max / min tells the computer what voltage corresponds to what RPMs. A Default would be: OSCAL = 0, FSCAL = 20000 => 0rpms = 0V and 20000rpms = 5V. Verify that these settings are correct on the LabView panel.

** Roughly 2 Volts, ~current of ~1.5Amps will be drawn. It is easy to burn out glow plugs on this power supply. Make sure your current coarse knob is set to 50% or straight up. This way your power supply will be in controlled-voltage mode. Then adjust to 2V watching the current & the glow plug light up. It'll get hot so be careful.

Sensotec 250g Load Cell

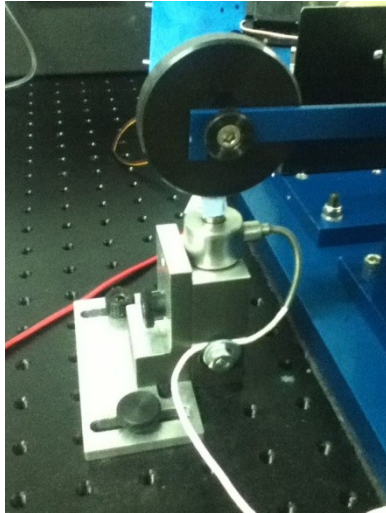


Figure 163: Load cell is the cylindrical, quarter-sized, chunk of metal just beneath the weighted, blue Aluminum bar. It measures between 0 and 250 grams.



Figure 164: Here the load cell is being pulled in tension. The screw thread checker is being used as a plate to support the calibration weights.

This 250g load cell was used to measure the torque generated by the engines under test in the dynamometer. For a given load, the sensor produces a proportional output voltage between -5 and +5V. Because these sensors are typically expensive, the dynamometer was designed around this sensor's capabilities.

Using the Ohaus Explorer mass balance to confirm the mass of the calibration weights, the load cell was calibrated.

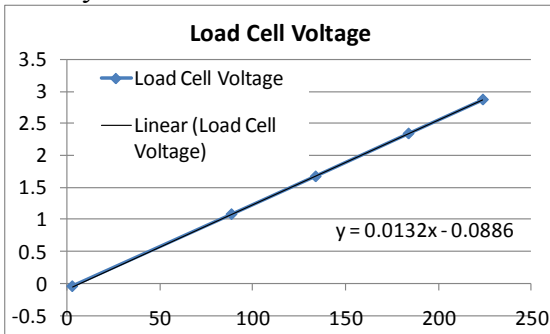
LabVIEW 8.1 was used to collect the voltage signal and confirm sensitivity values. The voltage outputs were collected in raw form and also using the LabVIEW 8.1 statistical averaging to steady output values.



Figure 165: Calibration weights used to calibrate the Sensotec load cell and compare Ohaus Explorer precision mass balance.

The plot below shows the calibration curve for the load cell for two different dates.

28 May 2010



2 June 2011

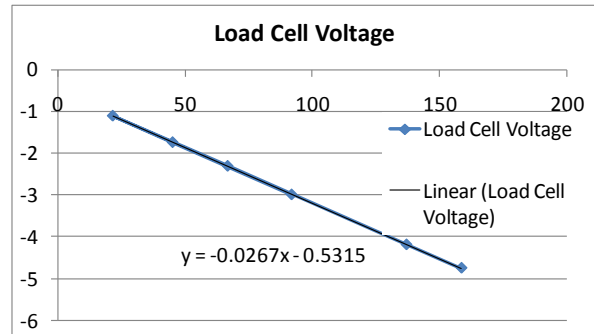


Figure 166: As can be seen in the above calibration plots, the sensor tends to drift. This could be caused by many things such as power supply voltage, setup biases, or other noise. However, the sensor maintains its linear response to mass. The offsets are typically from how the actual masses are loaded onto the load cell (i.e. the thread-checker plate above or any other platform or hook).

Calibration method and process modifications: Sensotec Load Cell

1. Obtain precision weights or any other weight that can be easily placed on both the scale and the load cell (Figure 165).
2. Check calibration weights with mass scale, note any differences
3. Then place, hang or affix mass on the sensing portion of the load cell, and record voltage

4. Repeat steps 2-3 until you have a sufficient number of points to confirm linearity. Typically 4-5 points although 3 are sufficient to define a proper slope or note errors in linearity.
5. Be sure to check for hysteresis by starting at a minimum and increasing the weight (or any measurement for that matter), reaching the maximum, then proceeding back to the original start point.

McMillan Mass Air-flow Rate Calibration

The mass air flow rate sensor provides mass flow rate data for the intake air entering the engine. Knowledge of this mass flow rate dramatically improves analysis of engine performance, providing estimates of oxygen intake, volumetric efficiency and other engine properties.



Figure 167: McMillan Co. intake air flow sensor.

Calibration and process modifications: McMillan Mass Air Flow Rate

The general calibration procedures apply but the following adjustments were made

This calibration required a special setup in order to contain a “known” airflow rate value. This airflow rate is needed to measure intake air of the engine. Again, there is likely a ASTM standard calibration process, however, due to time and financial constraints, a custom one was built.

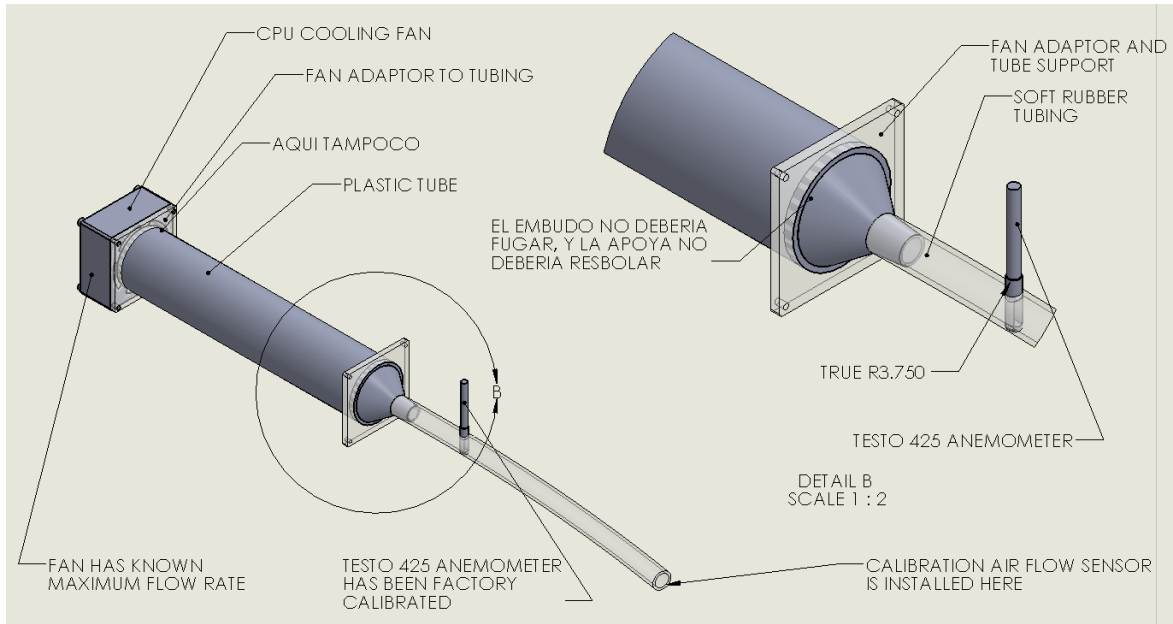


Figure 168: The apparatus used to calibrate the air intake, mass air flow rate sensor.

Here is the device as it was calibrated in the lab



Figure 169: Left most sensor is the Testo 425 air anemometer. Middle is a 75W 30V power supply, Above the power supply is the calibration unit.



Figure 170: The Testo 425 probe enters the air flow tube at the top of the photo. The tube continues on into the sensor being calibrated.

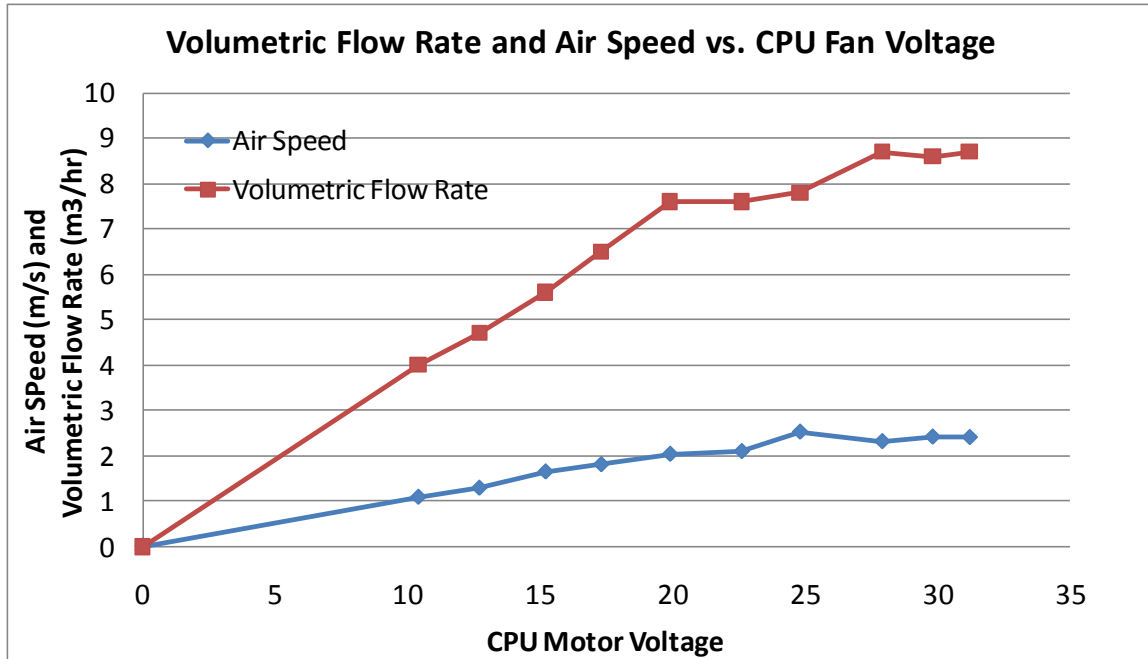


Figure 171: Calibration of the various airflow measurement devices.

Calibration method and process modifications for Air mass flow sensor

1. Install Testo 425 air anemometer into the soft tubing of the apparatus shown in Figure 168. Ensure that the sensing portion of the tip is inserted carefully and such that the arrow on the bottom of the probe points in the direction of the flow. Be extremely careful not to damage the tiny wires that sense the flow rate.
2. Ensure all devices are ready to be powered up and to take measurements
3. Power CPU fan to maximum voltage (see Ebmpapst 8214JN datasheet)
4. Assume you have the maximum value of air flow being provided by the fan
5. Record this value from the Testo 425 anemometer, record the value for the air flow sensor “in calibration.” Note the different units (one is *L/min* the other is *m³/h*).
6. Then decrease the velocity of the fan in increments such that you can at least take 5-6 different points.
7. When you get to the minimum velocity of the fan speed, take measurements back up to the maximum (they can be intermediary values) to check for any hysteresis or warm-up time issues.
8. Put the calibration data in to the spreadsheet or data manipulation software of choice and note the slope, i.e. the sensitivity.

Known issues and comments

The MacMillan air flow sensor operates on a nutating disk phenomenon. It also can be calibrated for various ranges of speed based on the position of the probing tubes

that enter the airstream. As of 7/1/2011, the nutating disk does NOT seem to spin and therefore does not output flow rate values (at least with the power of the CPU fan). Consult the manual to determine which “mode” the sensor is in. It is believed that the sensor was originally spec’ed to run in the range of 100 *l/min* which is appropriate for this engine and this calibrating fan, but it is speculated that because the CPU fan is a smooth function of fan voltage, there is a residual static friction which holds the nutating disk in place, thus the optical sensor cannot count the number of rotations per min or second. However, during engine testing, the sensor appeared to be working correctly and air intake values are in agreement with theoretical values at similar engine speeds.

Relative Humidity and Temperature Calibration

This IC purchased from sparkfun.com was used to measure the ambient temperature and humidity for dynamometer recalibration (as the performance of engines change modestly to these parameters, in addition to atmospheric pressure). This small IC comes calibrated from the factory but it behooves the scientist to double check reported values.

This sensor was used in concert with an Arduino micro controller. These inexpensive devices have been very useful in quick prototyping of controllers and to measure various parameters of the engine.

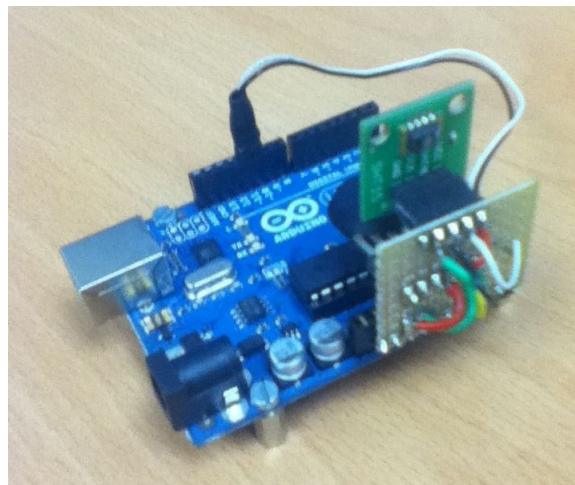


Figure 172: The ArduinoUNO microcontroller with the humidity, temperature and pressure sensors.

Calibration method and process modifications: “Sensor name here”

The general calibration procedures apply but the following adjustments were made

1. Process adjustment 1
2. PA2

Dynamometer Calibration

The dynamometer is one of the most important pieces of testing equipment that is needed for engine testing. Unfortunately, dynamometers measuring power output on this scale were not available during the start of the project. Thus it was decided to build a custom dynamometer to serve the research needs (as can be read in Chapter 3 of this work).

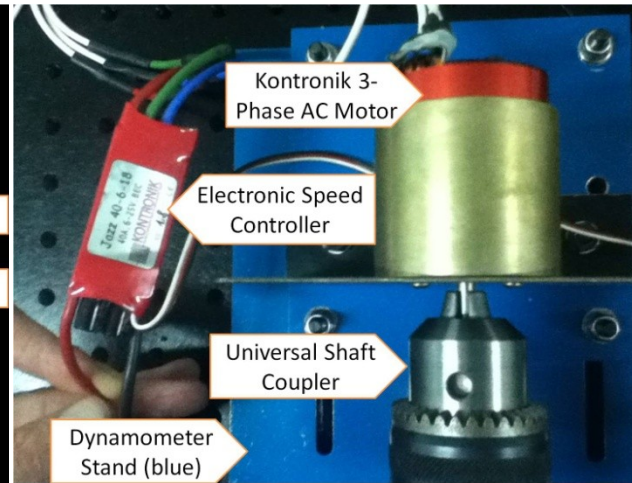
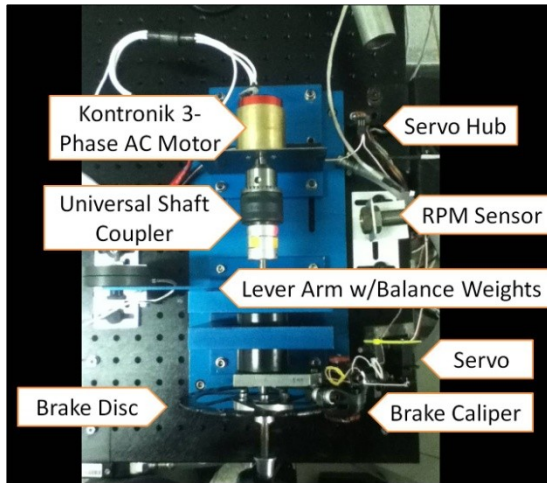


Figure 173: Dynamometer with calibration motor and associated components **Figure 174: Electronic motor and speed controller.**

But for calibration, the main part needing calibration is the dynamometer brake—which controls the amount of load on the engine. The calibration method is to use an electric motor of high efficiency, apply a load to it and then measure its output power using the torque, motor speed and braking method. The mechanical output power can be determined (P_m) using the following equation:

$$(29) \quad P_m = T\omega$$

Where T is the torque and is calculated by:

$$(30) \quad T = Fr$$

In which F is the force applied by the moment arm of length r (which is half the length of the moment arm as indicated in Figure 173, “lever arm with balance weights”). The force F is measured by a Sensotec 250g load cell as shown in Figure 163). The moment arm length is measured using calipers or simply known via the design drawing.

And the engine speed is measured using the Monarch ACT – 3A tachometer. This sensor outputs a voltage which is linearly proportional to the shaft speed. It measures the

number of “pulses per minute” which are directly related to “revolutions per minute” (RPM). This however needs to be converted to “radians per second” (*rad/s*) for the above power calculation.

$$(31) \quad \omega = \frac{1 \text{ Rev}}{1 \text{ min}} \left(\frac{1 \text{ min}}{60 \text{ sec}} \right) \left(\frac{2\pi \text{ rad}}{1 \text{ rev}} \right)$$

Which for quick estimates, can be approximated by:

$$(32) \quad \frac{2\pi}{60} \sim \frac{1}{10}$$

Which therefore suggests that for every 10 RPM there is roughly 1 Hz. Using the acquired measurements, and known physical values, the mechanical power can be calculated.

The power utilized by the electric motor is measured by the power being output by the power supply. Therefore, this electrical power output (P_e) can be calculated using measurements of voltage (V) and current (I):

$$(33) \quad P_e = VI$$

Where V is in volts and I is in amps.

Measuring Voltage in LabVIEW

Voltage is measured by the LabVIEW data acquisition system after reducing the voltage using a voltage divider (LabVIEW is limited to measuring voltages between -10 and $10V$). This voltage divider can be seen in the following images:

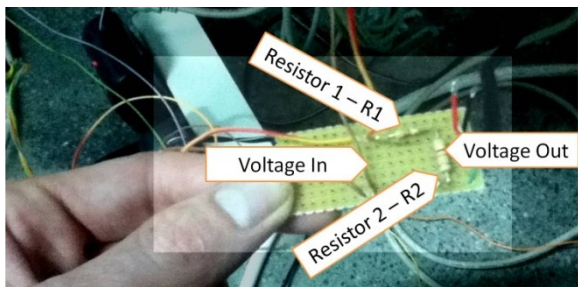


Figure 175: A quick and easy voltage divider circuit, breadboarded with two resistors: 50 kΩ and 5 kΩ.

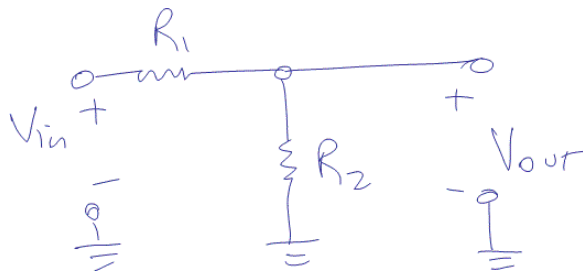


Figure 176: Schematic of a voltage divider. This circuit was used to reduce the input voltage to the LabVIEW system as it is only capable of measuring between $+10V$ and $-10V$.

There are probably much better, cleaner and more efficient circuits that can be made to reduce a voltage but since this was simply a calibration and the reduction circuit itself needed to be quickly calibrated to determine the linearity, this is what was designed and made.

The reduction in voltage can be calculated using Kirchoff's Laws.

$$(34) \quad \sum V_i = 0$$

$$(35) \quad \sum I_i = 0$$

Therefore, the output voltage, V_{out} can be determined algebraically through those equations.

$$(36) \quad -V_{in} + IR_1 + IR_2 = 0$$

This equation can be rewritten as

$$(37) \quad V_{in} = I(R_1 + R_2)$$

Now since the output voltage is simply the voltage across R_2 , this can also be determined.

$$(38) \quad V_{out} = IR_2$$

Which then can be used to solve for the current, I

$$(39) \quad I = \frac{V_{out}}{R_2}$$

Finally, this can be substituted into (37) and V_{out} can be determined as a function of V_{in} and resistor values R_1 and R_2 .

$$(40) \quad V_{out} = V_{in} \frac{R_2}{(R_1 + R_2)}$$

Reducing the input voltage by a factor of 10 would suggest that the expression in equation (40) should equal

$$(41) \quad V_{out} = \frac{1}{10} V_{in} = \alpha V_{in}$$

Where α in this context will represent the reduction factor. Which further suggests that

$$(42) \quad \frac{R_2}{(R_1 + R_2)} = \frac{1}{10} = \alpha$$

Therefore it can be determined that for a 10x reduction in voltage

$$(43) \quad R_1 = 9R_2$$

So picking more or less nominal resistor values, this ratio can be achieved. But so long as the input voltage is calibrated to the output voltage, any combination of resistor values around this ratio should work just fine. Therefore, a $51k\Omega$ and a $5.1k\Omega$ resistor was chosen. Voltage can now be measured using LabVIEW.

Note, voltages above 10 entering the LabVIEW data acquisition board will saturate and not yield accurate values. Further reduction may be needed and thus, α would change.

Measuring Current

The current measurement is made using a “current sensor” produced by GMW. The CSA-1V Test Circuit Kit for High Currents (AN_117KIT) is a low-cost sensor which allows the measurement of up to 40 Amps RMS and 100 Amps peak (for less than 1 second). This sensor is placed in series with the main drive voltage wires of the Kontronik Electronic Speed Control (ESC) as shown in Figure 174. Unfortunately, this sensor suffers from some noise issues as it operates using the generated magnetic field from the current movement. However, it is sufficient to calibrate the motor.

Calibration method and process modifications: fuel-flexible dynamometer

The general calibration procedures apply but the following adjustments were made

1. Setup an electric motor in the dynamometer stand.
2. Second, prepare the proper LabVIEW programs which are designed to record engine speed, force, torque, voltage from electric motor and current for electric motor.
3. Use arduino controller to control electric motor speed and braking force

Recording the data, the following plots can be generated:

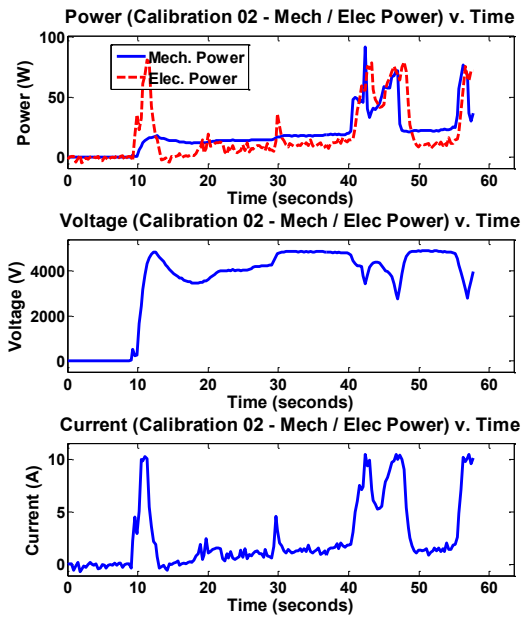


Figure 177: Shows the response of the electric motor power along with voltage and current generated by power supply. From the uppermost plot, the mechanical power follows the electrical power being output from the power supply. Losses due to the ESC, motor efficiency and shaft misalignment should all be considered.

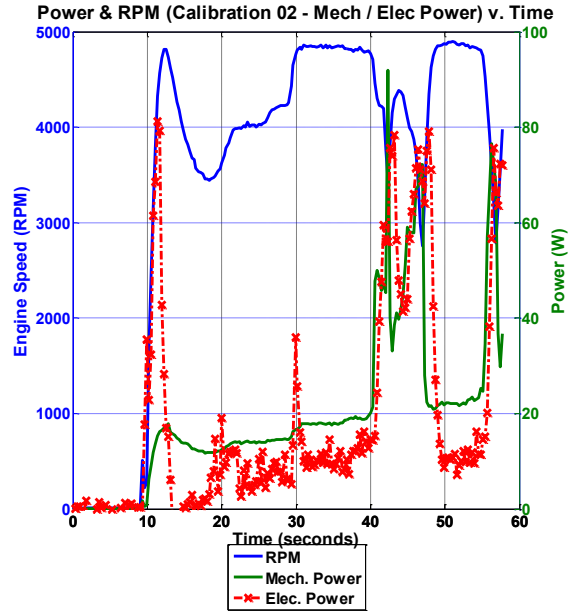


Figure 178: The engine speed in (RPM) and both electrical power and mechanical power are presented here to show how the magnitude change of the engine speed that corresponds to the amount of power and torque produced at that speed.

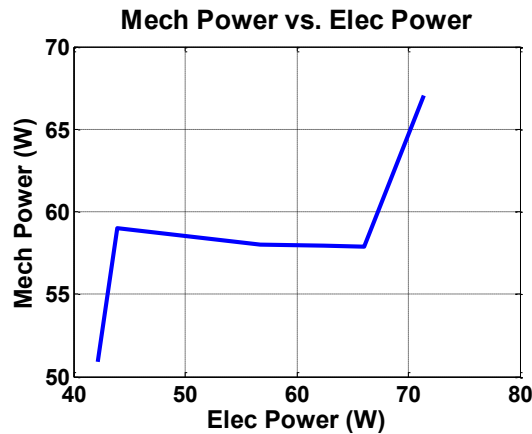


Figure 179: A comparison of the input Electrical Power to the output, Mechanical Power. These should relate 1 to 1.

Known issues and comments

The mechanical braking system leaves a lot to be desired in a 1 to 1 measurement of electrical power vs. mechanical power. However, as can be seen by a small window

range of measured power, the electrical power more or less equals the electrical power produced, therefore we can assume that the mechanical measurement is nearly as good as the electrical power output by the motor, and is a “real” mechanical torque generating “real” mechanical power. If a linear regression were to be imposed on the following graph in Figure 179, the fit would likely be poor but the magnitudes are in agreement. The researchers involved in this project are actively working to fix this issue.

Monarch Tachometer Calibration

The Monarch ACT 3A has proven to be a very reliable and robust tachometer for this research. It has a history with the rotary engine project, having measured the engine speed of the smallest mini Wankels that have been created to date.

The Monarch Tachometer functions by counting optical pulses that are generated by reflections from the motor shaft. These reflections are generated by a small piece of reflective tape that is placed on the shaft.



Figure 180: The Monarch Tachometer ACT 3A Display. The unit also comes with a laser emitter and collector to measure reflected, pulsing light [197].

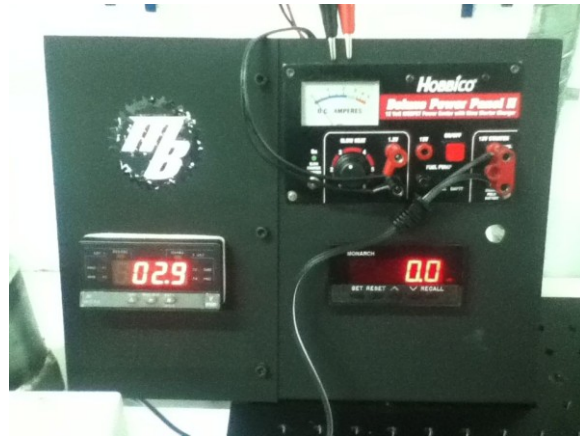


Figure 181: The Monarch Tachometer as used in the dynamometer test stand. The display is in the bottom, right hand corner and reads an engine speed of 0.0 RPM

Optical sensing element:

Reflective tape

Because this tool can measure up to 999,999 revolutions per minute and the rotary engines used in this research have maximum limits of approximately 20,000 RPM, this device can also be used to locate the position of the drive shaft. This is achieved by carefully placing reflective tape along the spinning element (in this setup, the reflective tape was placed along the circumference of the universal shaft coupler because there is more space, $D_c \sim 40mm$, on this spinning part compared to the drive shaft, $D_{ds} \sim 6mm$).

Calibration method and process modifications: “Sensor name here”

The general calibration procedures apply but the following adjustments were made

1. Find an electric motor with accurately controllable and known speeds
2. Or find an external RPM reader
3. Spin motor or engine to known speed, measure with calibrated device and compare with Monarch Tachometer.

Known issues and comments

Self-explanatory

Optrand Combustion Pressure Sensor (AutoPSI-S) Calibration

The internal combustion pressure sensor is an important measurement to determine how the combustion event performs in the rotary engine. Due to the extremely harsh conditions in a combustion environment, these sensors are typically pretty expensive and the search to find a high value, low cost sensor has been challenging. Ultimately, the Optrand AutoPSI-S combustion pressure sensor was selected based on past experience and other related researcher usage and recommendations.



Figure 182: The Optrand AutoPSI-TC pressure sensor has a 4mm tip with threads and can be installed directly in the combustion chamber.

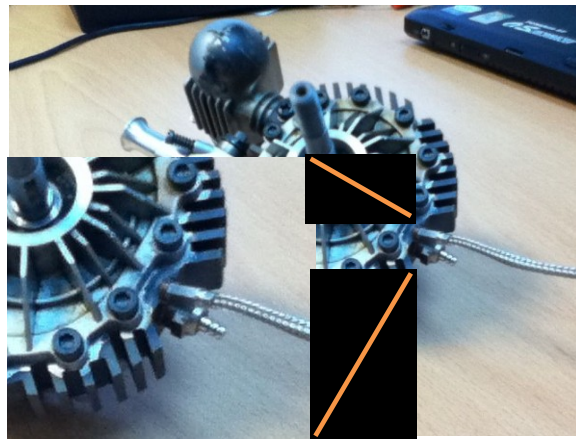


Figure 183: Here the pressure sensor is installed in the 4.97 cc Wankel engine. Carfe

Calibration method and process modifications: “Optrand AutoPSI-TC”

The general calibration procedures apply but the following adjustments were made

1. To calibrate the sensor in “static mode” there are one of two methods to enter static mode. Method 1 is to use a potentiometer and method 2 is to use an external voltage source. Both static calibration processes are described in the referenced service manual however method 1 needs elaboration and is described here.

2. The potentiometer needs to be placed “in short” between the diagnostic wire (green) and ground (black). The diagram, as sent separate via e-mail on 28 June 2011, was sent by Mr. Raph Wlodarczyk and is shown above.
 - a. As noted from Mr. Wlodarczyk “power up with pot at short, the sensor output should go to 7V and stay there, after a brief time it should either decay down to a value below that or remain at 7. If it stays at 7, increase resistance slowly until the output starts decaying and stop adjusting. It should settle at a voltage well above 0.5V. Once is has stabilized, adjust the pot so the output is slightly above 0.5V (0.55 is safe). If it is bottomed out at 0.5 to where the pot does not INCREASE the voltage immediately, it is too low and needs to be adjusted. The minimum it will sit at is 0.5V and any adjustments below that level will not have any effect on the output (it may reset).”
3. Once the 0.55V is achieved, the sensor is ready to measure statically and can be calibrated by any means available.
4. In this work, this sensor data was collected using an Arduino.

For reference, some pressure conversion factors:

1 PSI	6.89 kPa	0.7 kgf/cm ²	0.0680 atm
-------	----------	-------------------------	------------

Known issues and comments

The Oprtrand pressure sensor regularly poses challenges in small engines because of the small formfactor of the sensor tip and the potential to damage the sensor due to combustion heat and gases leaking by the sensor. Care and caution needs to be taken such that the pressure sensor is used correctly and that it is properly measured within the data logging system (in this research LabVIEW development platform was used).

Glowplug control and current calibration

The glowplug in most modern model engines is set to a constant temperature based on the materials, internal resistance and current applied to the glowplug (which is typically constant in a hobby environment. In this research, the glowplug temperature was changed dynamically based on the performance of the engine and



Figure 184: Standard O.S. Graupner medium glowplug.

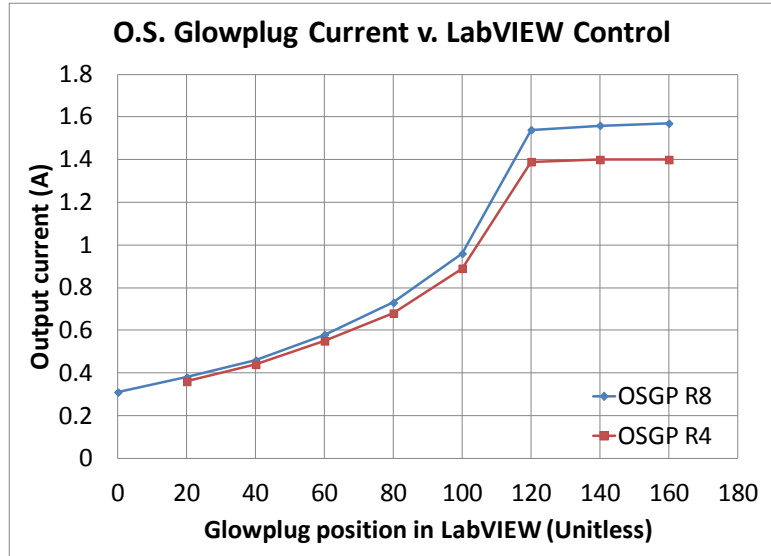


Figure 185: The current that passes through the glowplug for a given glowplug LabVIEW Position (LVP).

Calibration method and process modifications: “Standard Glowplugs”

The general calibration procedures apply but the following adjustments were made

1. Connect and utilize LabVIEW to control the glowplug servo position or the glowplug LVP.
2. Connect a multimeter in series with the glowplug cables
3. Measure current across the range of potential positions in LabVIEW.

Known issues and comments

It is not uncommon to see glowplugs burn up during extended use; especially at the higher currents. It is recommended to reduce glowplug usage during combustion if not necessary. Typically all fuels with the exception of the standard Glowfuel required constant glowplug current.

AC centrifugal fan

This cooling fan was utilized to refrigerate the engine during operation.



Figure 186: the EBM-Papst 4 speed AC centrifugal fan used to refrigerate the O.S. Graupner Wankel engine.
www.ebmpapst.com

Charts: Air flow

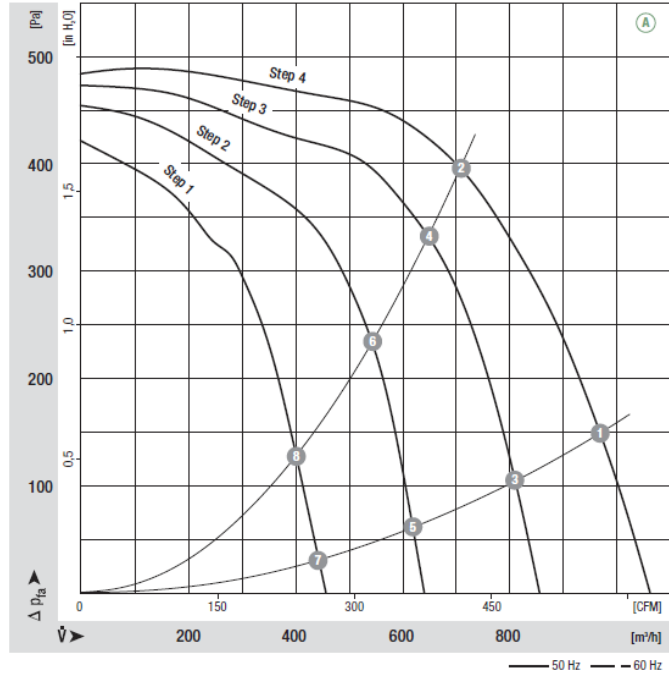


Figure 187: Volumetric air flow produced by the AC fan for each of its various steps and air pressure differential.

Calibration method and process modifications: “AC centrifugal fan”

The general calibration procedures apply but the following adjustments were made

1. Record ambient air temperature, pressure and humidity
2. Utilize the air flow measurement system to measure output flow
3. Test air flow several times across all speed positions, record and compare plot to measured value.

Known issues and comments

The fan is bulky and did not come with a stock speed switch. It is recommended if this part is purchased again, to find the stock speed switch.

APPENDIX D: Previous fuel flexibility characterization research results

Overall output power results from the 2005 research by Cardes et al.

Table 15: Cardes *et al.* tested a variety of fuels in 2005 in order to demonstrate fuel flexible operation of the 4.97 cc O.S. Graupner Wankel engine. This table shows the characteristics of each fuel tested along with bomb calorimetry measurements to determine the heat of combustion of each fuel [93].

Fuel Mixture	Fuel Constituents	% volume	Specific Gravity	Heat of Combustion
Alcohol 1	CH ₃ OH / CH ₃ NO ₂ / Oil	82 / 0 / 18	.81	18 kJ/g
Alcohol 2	CH ₃ OH / CH ₃ NO ₂ / Oil	72 / 10 / 18	.84	20 kJ/g
Alcohol 3	CH ₃ OH / CH ₃ NO ₂ / Oil	52 / 30 / 18	.90	17 kJ/g
Gasoline	87 Octane Gasoline / Oil	96 / 4	.74	43 kJ/g
Heavy Fuel 1	Diesel / Ether / Oil	89 / 9 / 2	.82	51 kJ/g
Heavy Fuel 2	JP8	100	Not Tested	Not Tested

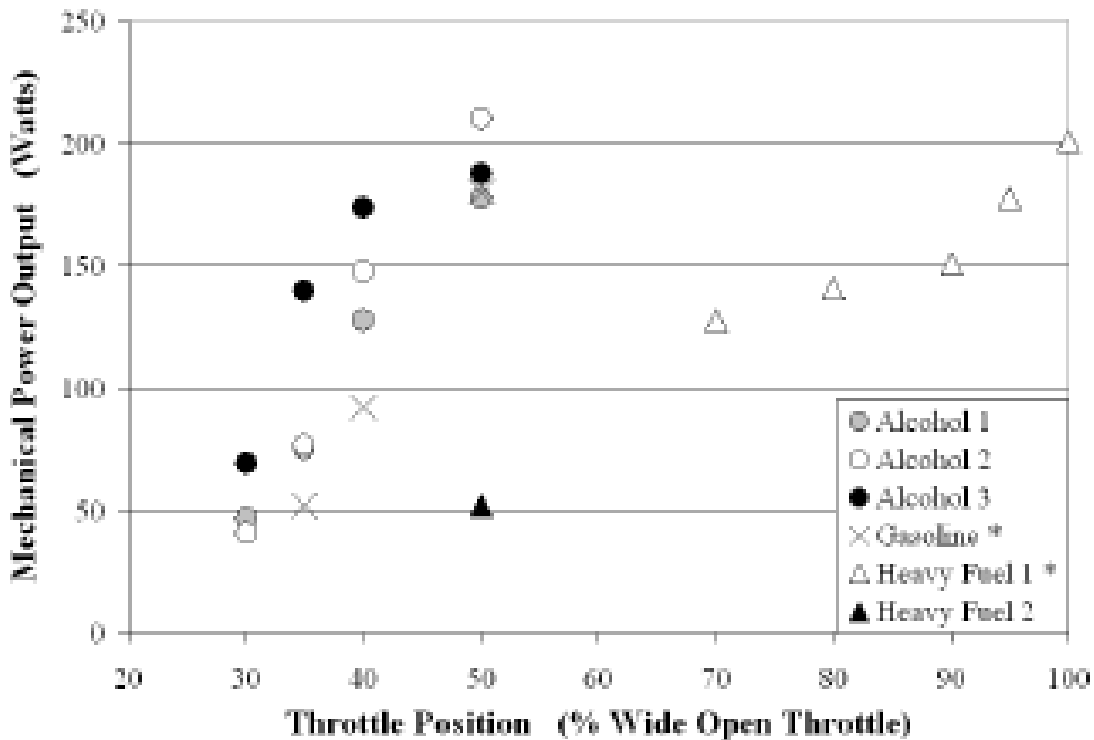


Figure 188: Cardes *et al.* again presents the electrically-measured power output of the various fuel blends (in this case this is blending of GlowFuel with different amounts of nitromethane and lubricant oil) for constant load across the full range of throttle positions. The maximum power observed was produced by the GlowFuel and was approximately 210 W. * Designates continuous glow plug operation [93].

These next two figures present more data reconfirming that the 4.97 cc O.S. Graupner Wankel engine is in fact fuel flexible using the new fuel flexible engine dynamometer developed during this doctoral research. This characterization was conducted using the newly designed—yet unrefined—mechanical-brake dynamometer. The deficiencies in the dynamometer used in 2005 and original testing procedures left significant room for improvement, hence why the new dynamometer as extensively described in Chapter 3 was built. The most critical components being, the loading mechanism, ability to measure air and fuel flow rates, measured and electronically controlled throttle, carburetor mixture and loading conditions which were all governed and controlled by a LabVIEW Virtual Instrument and data logging system.

Output Power results from 2009 using the new fuel flexible dynamometer

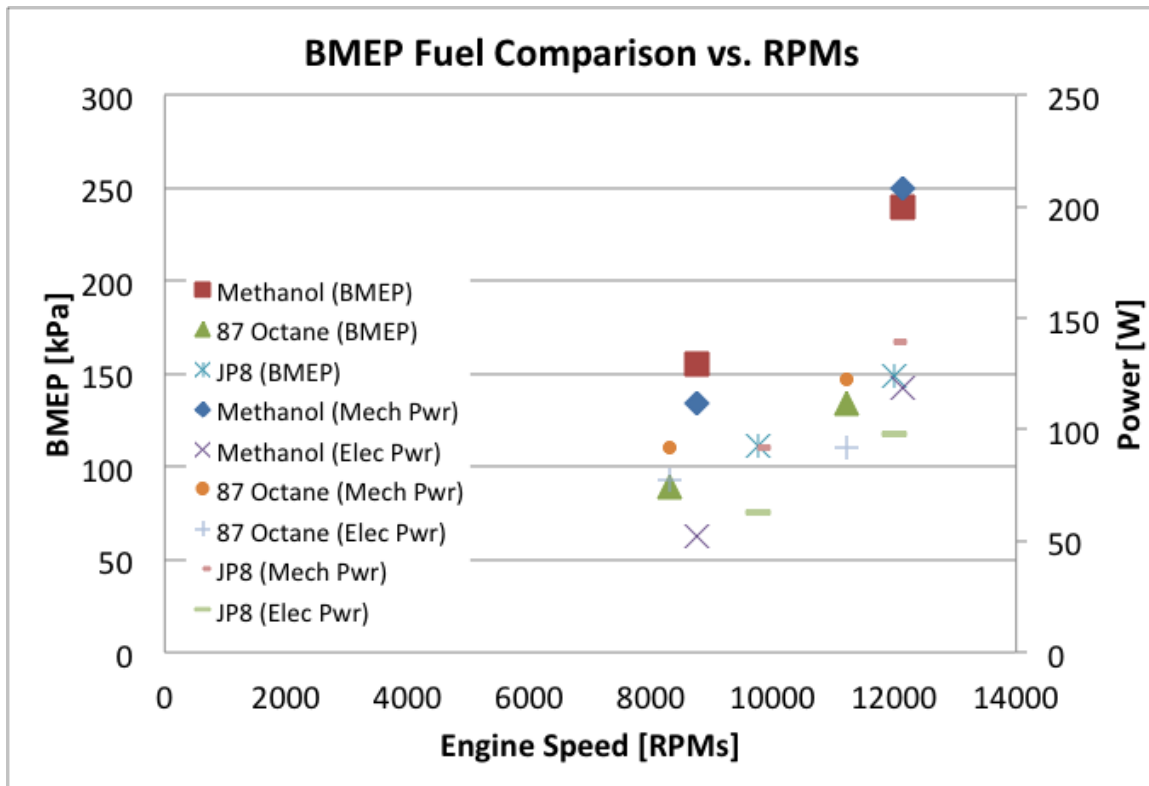


Figure 189: Preliminary data on the fuel flexible capacity of the 4.97 cc O.S. Graupner Wankel engine in the early development stages of the mechanical dynamometer development. This was an attempt to replicate the 2005 data and confirm functionality of the newly developed dynamometer. This version lacked data logged mass fuel flow rates (due to errors in the communication between the scale and the data logger), electronic control of carburetor needle valve (regulating air-to-fuel mixture) and utilized a resistive-based loading system—which failed to test the full dynamic range of the motor and required a second operator to be present.

Estimated and Measured Mechanical Power Output in a 4.97cc Wankel Rotary Engine

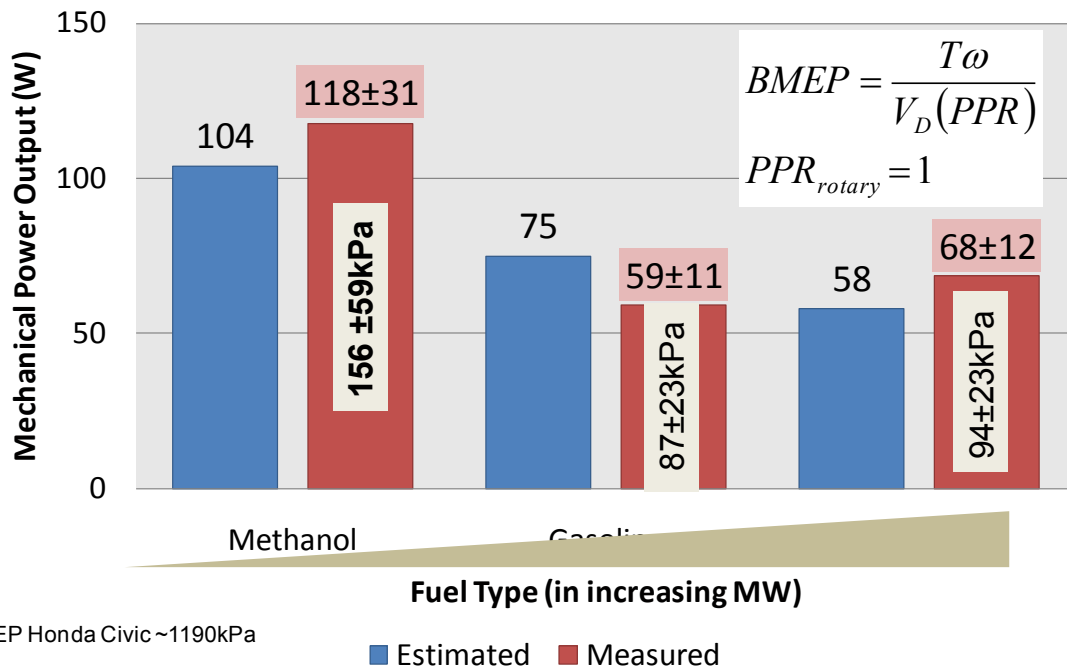


Figure 190: This plot compares the average power output across an engine speed achievable by the three fuels tested in this experiment (approx 9,000 RPM) and a rough estimate of the predicted power using measured efficiencies and energy density of the fuels. The Brake Mean Effective Pressure (BMEP) allows for the comparison of any motor regardless of its displacement. During this characterization, the dynamometer again lacked robust loading control, repeatable measurements for carburetor and poor measurement of fuel consumption (and therefore a lack of efficiency measurements).

Additionally, the predictions required an estimate of the engine efficiency under the operation of each fuel. Considering most fuels have much higher fuel to air ratios and elevated auto ignition points, it was assumed that less heat would be extracted by these heavier fuels as compared to methanol.

Additional characterization data from 2012

Output power curves for methanol

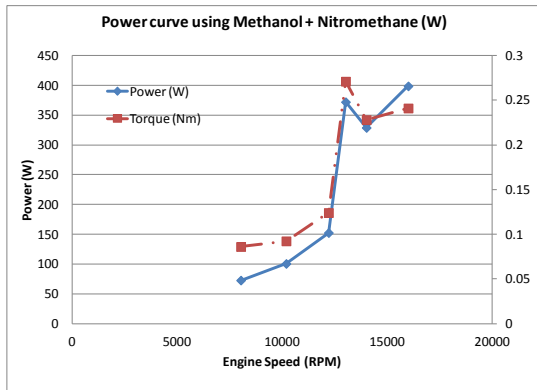


Figure 191: This is one of the first few power curves generated from the small-scale engine dynamometer. The strangeness of the curves comes from the method by which the engine was operated. Given the fragility of the engine, on top of the desire to preserve its functionality, the engine was not ran at full load. However, most dynamometers oscillate back and forth between fully opening the throttle and loading the motor such that it does not over run or over rev the engine. In this case, the motor was operated at various engine speeds by varying the throttle, hence the atypical performance curves (120703-engine-test-methanol-02).

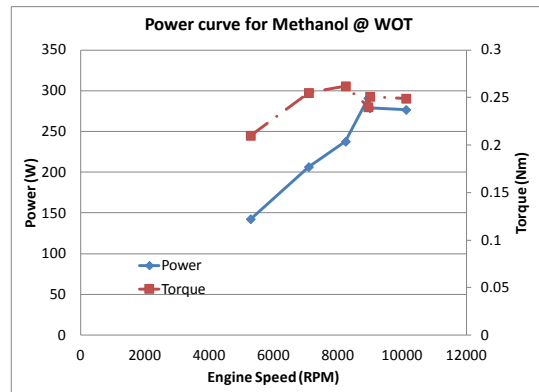


Figure 192: This figure was generated by the standard method of opening the throttle and increasing the load in order to manage the engine speed. Via this method, the maximum power and torque values should be measurable and easily attained. However the interesting fact remains that via this method, the maximum power of the motor was not realized nor did the engine speed reach the manufacturer’s specified maximum ratings (of nearly 1 horsepower) (120705-engine-test-methanol-04).

Output power from Diesel fuel

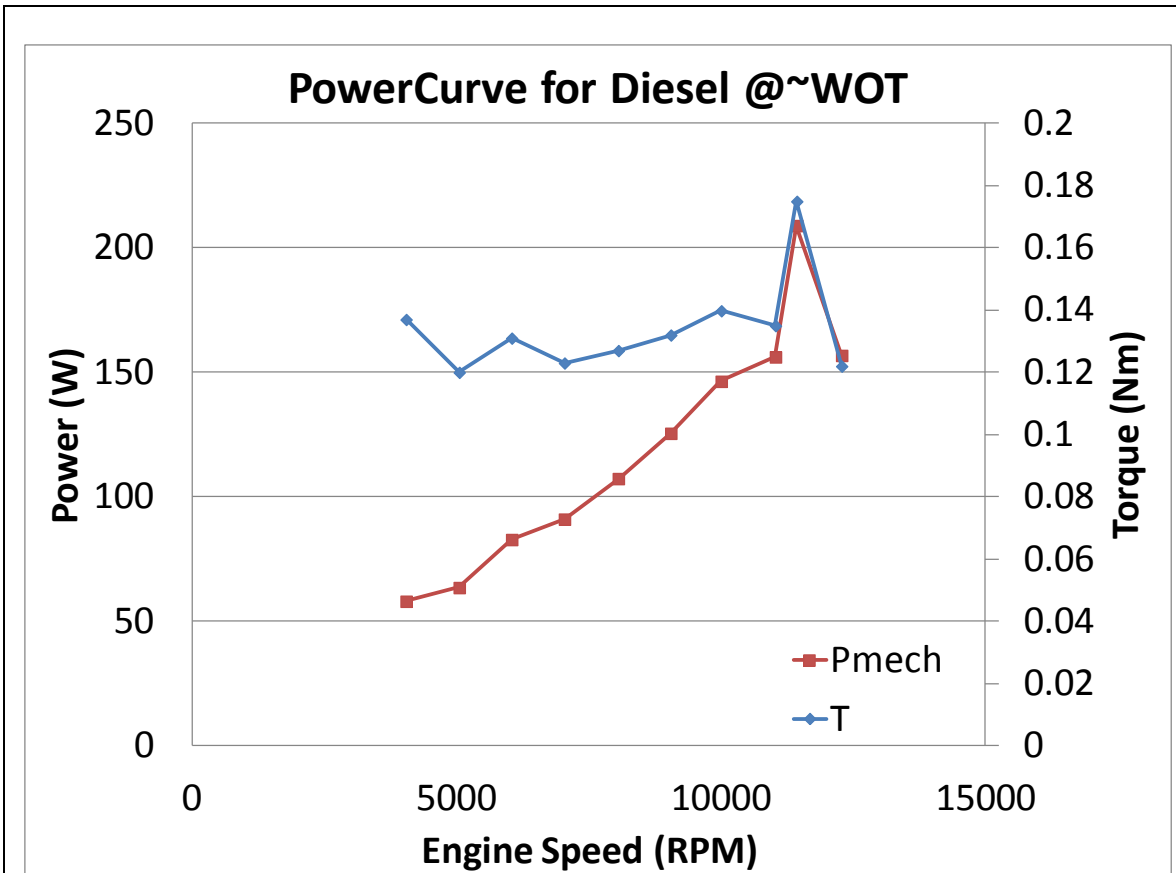


Figure 193: Mechanical power output of no. 2 diesel fuel while running at near 100% WOT (the motor failed to maintain reliable combustion at 100% wide open throttle). Current was constantly supplied to the glowplug during this test. This is No. 2 diesel fuel.

Stoichiometry Value (LVP)	$-233 \leq \phi \leq -593$
Max Power	239.2W @12940 RPM
External Engine Temp.	112.7°C
External Exhaust Temp	146.2 °C
Cooling fan speed (see Appendix C)	Level 3 - 850 m ³ /h
Mass Fuel Flow Rate	n/a
Maximum Efficiency Recorded	n/a

APPENDIX E: Relevant Fuel Properties

Table. 2. Flammability limits (in %vol) for premixed fuel/air gaseous mixtures at 25 °C, minimum quenching diameter at 25 °C, and autoignition temperature, all at 100 kPa.

Fuel	Lower Flammability Limit, LFL	Stoichiometric mixture	Upper Flammability Limit, UFL	Minimum quenching distance [mm]	Autoignition temperature [K]
CO, carbon monoxide	14	29.5	70		900
H ₂ , hydrogen	3.9	29.5	75	0.61	850
CH ₄ , methane	4.9	9.47	14	2.0	850
C ₂ H ₆ , ethane	3.0	5.64	13	1.8	800
C ₃ H ₈ , propane	2.0	4.02	9.5	1.8	750
C ₄ H ₁₀ , n-butane	1.5	3.13	8.5		700
C ₇ H ₁₆ , n-heptane	1.1	1.87	6.7		560
C ₈ H ₁₈ , n-octane	1.0	1.65	6		500
C ₈ H ₁₈ , iso-octane	0.95	1.65	6		690
C ₁₀ H ₂₂ , n-decane	0.80	1.34	5.4	2.1	480
C ₁₂ H ₂₆ , n-dodecane	0.60	1.12			480
C ₂ H ₂ , acetylene	2.5	7.75	80	2.3	600
CH ₃ O, methanol	6.7	12.3	36	1.5	680
C ₂ H ₅ O, ethanol	3.3	6.54	19		630
C ₂ H ₅ O, ether	1.8	3.13	37		440

Figure 194: Flammability limits, stoichiometry, autoignition temperatures and quenching distances of various fuels [199].

APPENDIX F: Mechanical Design Considerations

WOOD 6 MIL/COES DETAILS TO MAKE CLEAR

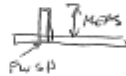
TR BASE → * 8 HOLES HAVE A TIGHT SLIP FIT FOR SHOULDER BOLT.

+ CHANNEL SLOT FOR A 10mm SQ. HEAD.

DAMPING PAD * MATERIAL'S RESISTANCE TO FUEL

TR MM BASE → * BETTER TO PRESS INTO THE BASE PLATES. B/C WE CAN BE SURE WE SIT

FLAT W/ THE DOWEL PIN



SOLE THAT DEPTH + 1/8" INTO MOUNTS W/ SLIP FIT. + 200#

LT EMM MOUNT * PRESS FIT OF

1/8" EMM BEARING

* SLIP FIT ON 1/4" DOWEL PINS

* TAP FOR M6

TR REM FACE * SLIP FIT FOR 1/4" DOWEL PINS

PEEK OS INSULATOR

* DOUBLE CHECK BOLT CIRCLE

* DOUBLE CHECK CLEARANCE FITS

FOR THESE BOLT/TAP ~~HOLE~~

HOLE DIMS

* PEEK RESISTANT TO HEAT, OTHER

CHEMICALS? MAYBE WOOD?

EM BASE

* PRECISION, SHOULDER BOLT HOLES

* PRESS FIT 1/4" DOWELS

APPENDIX G: O.S. Graupner Rotary Engine Considerations

4.97 cc O.S. Graupner Rotary Engine Break In Procedure

- BREAK IN PROCEDURE
- ① GET GP RED HOT
 - ② CLOSE NEEDLE VALVE
2-TURNS TO "START"
SETTING
 - ③ GET FUEL TO CARS
 - ④ SET TO 1/3 THROTTLE
 - ⑤ POWER GLOW PLUG
 - ⑥ SPIN MOTOR
 - ⑦ START ENGINE
 - ⑧ SLOWLY RAMP UP TO
WOT. 5-6 SECS
 - ⑨ REMOVE GP LEADS
- ① OPEN THROTTLE UNDER
RICH CONDITIONS
 - ② RUN FOR 1-2 MINUTES
~ 3/4 THROTTLE
 - ③ LEAN OUT → RUN FOR
EG 2 TIMES

4.97 cc O.S. Graupner Rotary Engine Dismantle or Break-down Procedure

- ENGINE BREAKDOWN
- ① REMOVE FROM ENGINE STAND / AIRPLANE
 - ② REMOVE SERVO & LINKAGE
 - ③ ~~REMOVE BOTTOM 4mm (NO!)~~
~~ALLEN~~ FHS
 - ④ LOOSEN 3 RING MOUNT
SCREWS THAT HOLD ON
ENGINE (2.5mm)
- | TOOLS NEEDED |
|--|
| PHILLIPS SCREW |
| PAPER TOWELS |
| ALLEN WRENCHES
2.5mm 4mm
2mm 3mm |
| VICE GRIPS PLAS# |

- ③ LOOSEN SHAFT NUT USING VICE GRIPS
3.1 REMOVE NUT & 3 PLASTIC SPACER WASHERS & STEEL SPACER
REMOVE CW + ~~KEY~~ WOODRUFF KEY
- ④ REMOVE FRONT COVER USING STAIN PATTERNS, PLACE BOLT + NUT COMBOS (2X) SOMEWHERE ELSE (ALL SAME SIZE SCREW)
- ⑤ REMOVE 6 SCREWS ON BACK (2mm)

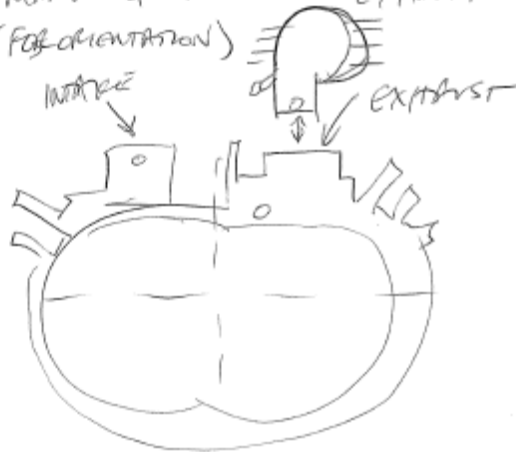
136

- ⑥ CAREFUL WITH 400 REMOVE-FACE, THERE ARE TWO HOLLOW DOWELS APERT SEAMS

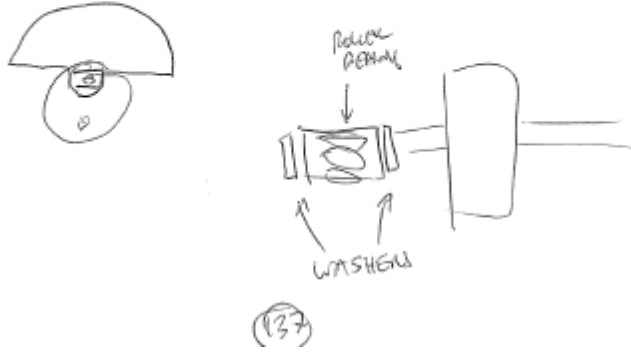


2X SEAMS

- ⑦ MARK & REMOVE EXHAUST & CAMB (FOR ORIENTATION)



REAR CENTERWEIGHT ^{FUCS} ① IS REVERSE
 THREADED. CW IS ALSO ORIENTED OPPOSITE
 THE E.L.



SAVE FOR REMAINDER
 OF BREAKDOWN GUIDE.

③ CAREFUL NOT TO LOSE THIN WASHERS THAT
 GO ON EITHER SIDE OF THE ROLLER
 BEARING

④ ~~FEEL~~ REAR WEAR PLATE W/ GEAR ~~IS~~
 HAS 4 SCREWS. IT APPEARS THAT IT HOLDS
 THE GEAR BUT THEY LOOK FUSED TOGETHER

4.97 cc O.S. Graupner Wankel Rotary Engine Assembly Procedure

- ASSEMBLY
- ① SHAFT ON ROTOR, OIL
 - ② F.W. → R.B. → F.W. → GEAR SIDE W.P.
 - ③ INSTALL C.W. & R.T. F.I.C.S (C.W. POINTS IN DIR. OF
 WOODRUFF KEY)
 - ④ INSTALL DOWELS
-
- ① C.S. W.P., 2 DOWELS, TROCHOID

- ④ INSTALL SPRINGS & SEALS
- ⑤ INSTALL WEAR PLATE + SCREWS & NUTS, INSTALL USING SPIDER PATTERN
- ⑥ INSTALL BACK PLATE (6X)
- ⑦ INSTALL CARB & EXTRACT. (CW COMP. VALVE PTS TO CARB)

Key operating conditions for model airplane engines

DVID

FUEL AIR IGNITION

180-200° F MAX TEMP

AIR LEAKS CARBURETOR

ORING NEEDLE VALVE

LET SOUND BE YOUR GUIDE

ENGINE WILL LEAN OUT AS IT RUNS HOT

RAW HARREYS - LOW PWG DIAPHS

TUNED PIPE ⇒ BIG ~~PIPE~~ HP GAIN

LENGTH

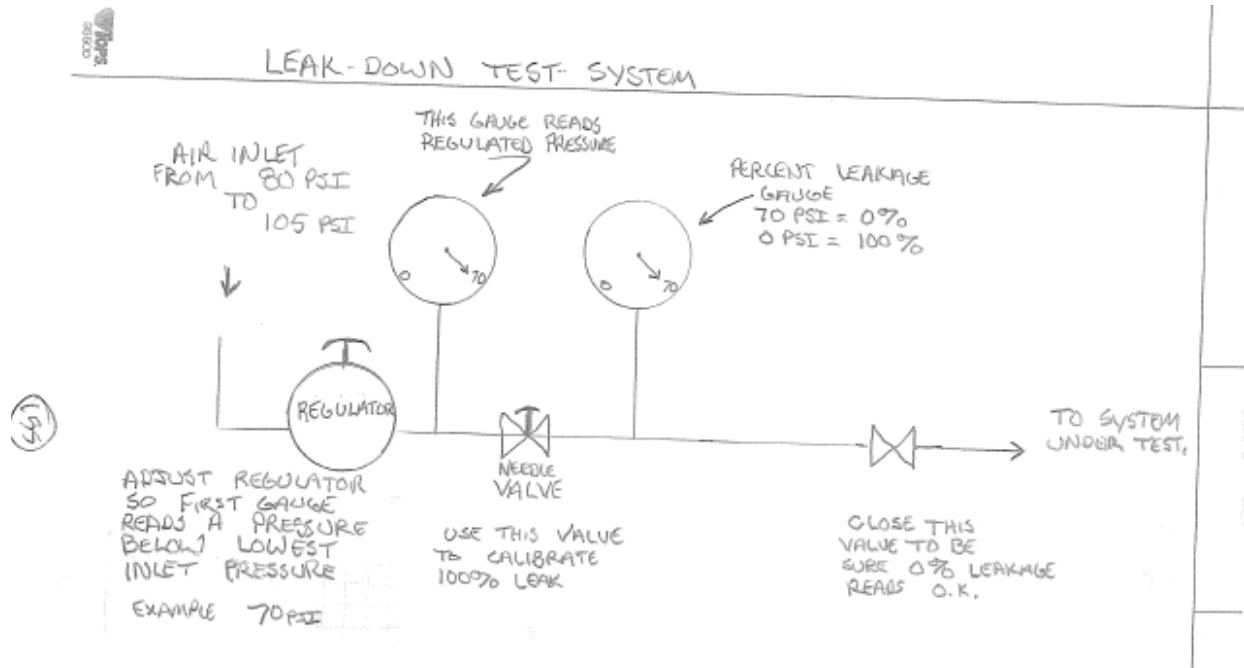
LONG - BUT GND AREA

SHORT = TOP END

DIAMETER ALLOW TO CLEAN

150

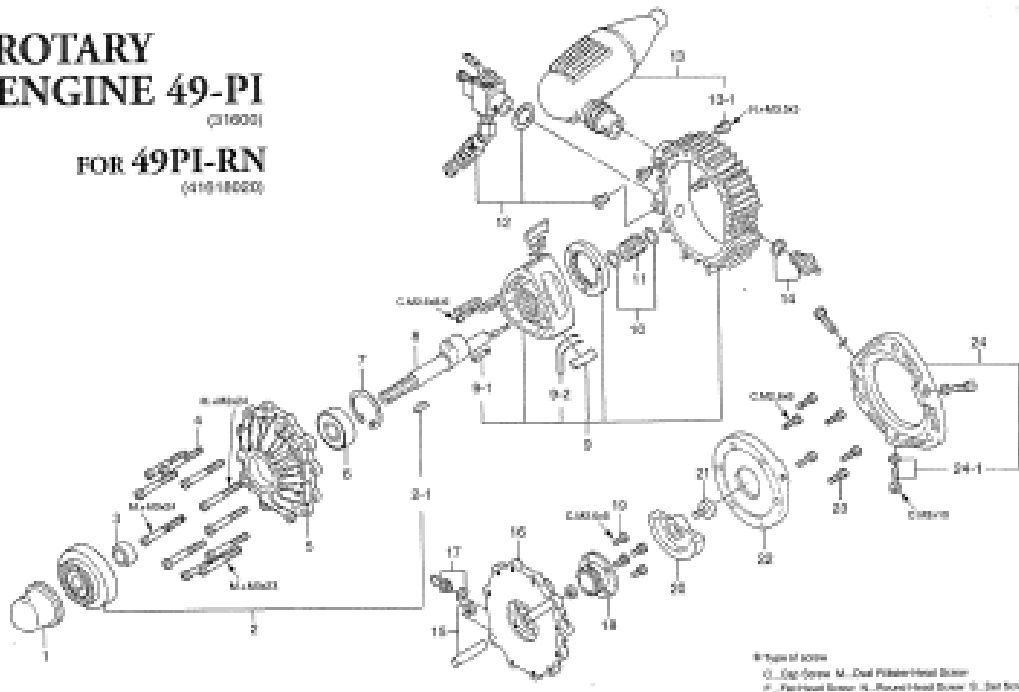
Leak down testing



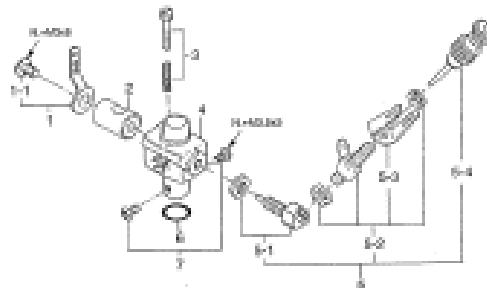
Rotary Engine Exploded View

OS ENGINE

**ROTARY
ENGINE 49-PI**
(218000)
FOR 49PI-RN
(41818000)



No.	Code No.	Description
1	23204000	Spinner Nut
2	41812000	Drive Hub
2-1	41829000	Woodruff Key
3	41829000	Shaft Spacer
4	41823000	Housing Assembly Screw Set
5	41801000	Front Housing
6	41814000	Camshaft Ball Bearing (F)
7	41814000	Front Bearing Retainer
8	41804000	Eccentric Shaft
9	41802010	Motor Housing Assembly
9-1	41802001	Motor Case Retaining Screw
9-2	41807004	Steel Spring (2pcs.)
10	41827000	Thrust Washer (2pcs.)
11	41815000	Rear Bearing
12	41818000	Carburetor Complete (Type 49PI-RN)
13	41838010	Silencer 49-PI Assembly
13-1	23201708	Silence Retaining Screw
14	71814001	Glove Plug Type REC
15	41830000	Housing Assembly Tabular Dovetail (2x2)
16	41803000	Rear Housing
17	23201953	Nipple No.1
18	41806000	Fixed Gear
19	41822000	Fixed Gear Retaining Screw (200)
20	41811000	Rear Counter Weight
21	45007319	Rear Counter Weight Retaining Screw
22	41816000	Rear Cover
23	41824000	Rear Cover Retaining Screw (2pcs.)
24	41833000	Engine Mount
24-1	41824000	Engine Retaining Screw (2pcs.)



No.	Code no.	Description
1	41814400	Throttle Lever
1-1	23201313	Throttle Lever Retaining Screw
2	23201200	Carburetor Motor
3	23201811	Throttle Stop Screw
4	41818110	Carburetor Body
5	41818800	Needle Valve Assembly
5-1	41818910	Needle Assembly
5-2	41818920	Needle Valve Holder Assembly
5-3	232011308	Ratchet Spring
5-4	23201977	Needle
6	41818030	Carburetor Hybrid Gasket
7	23201708	Carburetor Retaining Screw

O.S. GENUINE PARTS & ACCESSORIES

Code No.	Description
23204000	1/4"-28 (L) Spinner Nut
73101000	Long Projector Nut Set
73101020	1/4"-28 Projector Nut Set For Tru-Lum Spinner
41821010	Exhaust Pipe Assembly
71821000	Non-Adjustable Weight
72423050	Super Filter (L)
73871010	M2 Pan Cap Screw Set (18pcs.)
71821000	Long Socket Wrench With Plug Grip

The specifications are subject to alteration for improvement without notice.

References

- [197] Monarch Tachometer ACT 3A Datasheet - <http://www.monarchserver.com/Manuals/ACT-2-3%20Eng.pdf> accessed on 9 June 2011.
- [198] S. McAllister, J-Y. Chen, A.C. Fernandez-Pello, Fundamentals of Combustion Processes. Mechanical Engineering Series. Springer, NY, 2011.
- [199] Martinez, Isidoro, “Combustion Kinetics.” Course notes. <http://webserver.dmt.upm.es/~isidoro/bk3/c15/Combustion.pdf> accessed on 9 December 2012.
- [200] R. Seiser, K. Seshadri, “Chemical kinetic characterization of model fuels used for describing combustion of diesel.” Fischer-Tropsch conference proceeding. Diesel Engine Emission Reduction. 1997. Pg 275